



City Research Online

City, University of London Institutional Repository

Citation: Mhach, H.K. (1991). An experimental study of hydraulic fracture and erosion. (Unpublished Doctoral thesis, City University London)

This is the accepted version of the paper.

This version of the publication may differ from the final published version.

Permanent repository link: <https://openaccess.city.ac.uk/id/eprint/7765/>

Link to published version:

Copyright: City Research Online aims to make research outputs of City, University of London available to a wider audience. Copyright and Moral Rights remain with the author(s) and/or copyright holders. URLs from City Research Online may be freely distributed and linked to.

Reuse: Copies of full items can be used for personal research or study, educational, or not-for-profit purposes without prior permission or charge. Provided that the authors, title and full bibliographic details are credited, a hyperlink and/or URL is given for the original metadata page and the content is not changed in any way.

**AN EXPERIMENTAL STUDY OF HYDRAULIC
FRACTURE AND EROSION**

BY

HARI KRISHAN MHACH

A Thesis Submitted for the Degree of

DOCTOR OF PHILOSOPHY

CITY UNIVERSITY

CIVIL ENGINEERING DEPARTMENT

MARCH 1991

CONTENTS

		Page No.
	Contents	vii
	List of Tables	ix
	List of Figures	xiii
	List of Plates	xiv
	Acknowledgements	xv
	Declaration	xvi
	Abstract	xvii
	Glossary of Symbols	xvii
CHAPTER	1 INTRODUCTION	
	1.1 Embankment Dam Failures	1
	1.2 Statement of the Problem	2
	1.3 Objective and Method of Research	3
	1.4 British Embankment Dams with Puddle Clay Cores	4
CHAPTER	2 BASIC THEORY	
	2.1 Introduction	6
	2.2 Stress and Strain	6
	2.3 Isotropic Compression and Swelling Lines	7
	2.4 The Ultimate States	7
	2.5 State Boundary Surface	8
	2.6 Idealised Behaviour of Soils in Undrained Tests	9
	2.7 Excess Pore Pressure Response during Undrained Loading	10
	2.8 Undrained Shear Strength	11
	2.9 Mechanism of Internal Erosion	13
	2.10 Cylinder Dispersion Test	15
CHAPTER	3 PREVIOUSLY PROPOSED CRITERIA FOR HYDRAULIC FRACTURING IN EMBANKMENT DAMS AND BOREHOLES	
	3.1 Introduction	16
	3.2 Embankment Dams	16
	3.2.1 Kjaernsli and Torblaa	16
	3.2.2 Vaughan	17
	3.2.3 Sherard	17
	3.2.4 "Saturation Settlement" Mechanism	18
	3.3 Boreholes	18
	3.3.1 Morgenstern and Vaughan	18
	3.3.2 Haimson	19
	3.3.3 Kennard	20
	3.3.4 Bjerrum, Nash, Kennard and Gibson	22

	3.3.5	Massarsch	23
	3.3.6	Nobari, Lee and Duncan	24
	3.3.7	Jaworksi, Duncan and Seed	25
	3.3.8	Savvidou	28
	3.4	Discussion on Previously Proposed Criteria for Hydraulic Fracturing in Embankment Dams and Boreholes	29
CHAPTER	4	HYDRAULIC FRACTURE - LITERATURE REVIEW	
	4.1	Introduction	34
	4.2	Case Histories of Embankment Dams which have Experienced Problems Attributed to Hydraulic Fracture	35
	4.2.1	Dale Dyke Dam	35
	4.2.2	Oklahoma and Mississippi Failures	36
	4.2.3	Wister Dam	38
	4.2.4	Stockton Creek Dam	39
	4.2.5	Hyttejuvet Dam	40
	4.2.6	Balderhead Dam	41
	4.6.7	Yard's Creek Upper Reservoir Dam	43
	4.6.8	Teton Dam	44
	4.3	Conclusion from Evidence of Hydraulic Fracturing in Embankment Dam Studied	46
	4.4	Fluid Losses from Boreholes in Embankment Dams	48
	4.5	Comparison of Hydraulic Fracturing in Embankment Dam Cores and Boreholes	49
CHAPTER	5	INTERNAL EROSION OF CLAY IN CORES OF EMBANKMENT DAMS - LITERATURE REVIEW	
	5.1	Introduction	52
	5.2	Dispersive Clays	53
	5.3	Postulated Mechanism of Internal Erosion in Dispersive Clays	53
	5.4	Laboratory Tests for Identifying Dispersive Soils	54
	5.4.1	The Soil Conservation Service (SCS) Dispersion Test	55
	5.4.2	Chemical Tests	55
	5.4.3	Pinhole Erosion Test	56
	5.4.4	Crumb Test	57
	5.4.5	Rotating Cylinder Test	57
	5.4.6	Soil Security (Water Retention Test)	58
	5.5	Discussion	59

CHAPTER	6	THEORETICAL ANALYSIS OF HYDRAULIC FRACTURE IN CYLINDRICAL CAVITY EXPANSION TESTS	
	6.1	Introduction	61
	6.2	The Idealised Model	61
	6.3	Fracture Criteria	64
		6.3.1 Theoretical Analysis in Total Stress Conditions	65
		6.3.2 Theoretical Analysis in Effective Stress Conditions	68
	6.4	The Effect of Partial Penetration	75
	6.5	Justification of Rapid Laboratory Tests	76
	6.6	Summary	77
CHAPTER	7	APPARATUS	
	7.1	Introduction	79
	7.2	Objective of Experiment and Choice of Tests	79
	7.3	Sample Presses	80
	7.4	The Triaxial Stress Path Apparatus for 38 mm Diameter Samples	80
		7.4.1 General Description	80
		7.4.2 Semi Automatic Triaxial Cell	81
		7.4.3 Microcomputer Controlled Triaxial Cell	82
	7.5	Instrumentation	83
	7.6	Apparatus Calibration and Accuracy	83
	7.7	Pinhole Apparatus	84
	7.8	The Triaxial Apparatus for Fracture Tests	85
	7.9	Equipment Used for the Preparation of Samples for the Hydraulic Fracturing Tests	86
		7.9.1 Introduction	86
		7.9.2 Samples' Top Cap and the Probe	86
		a) 38 mm Samples	
		b) 100 mm Samples	
		7.9.3 Sample Borers	87
		a) 38 mm Samples	
		b) 100 mm Samples	
		7.9.4 The Base Plate and the "Guide" for 38 mm Samples	88
		7.9.5 38 mm Samples Top Cap "Holder"	88
CHAPTER	8	TEST PROCEDURES	
	8.1	Introduction	90
	8.2	Preparation of Reconstituted Samples	90
	8.3	Nomenclature of Laboratory Tests	91

	8.3.1	Introduction	91
	8.3.2	Triaxial Tests	91
		a) Semi automatic Triaxial Cell	
		b) Automatic Triaxial Cell	
	8.3.3	Erosion Tests	92
		a) Pinhole tests	
		b) Cylinder Dispersion Tests	
	8.3.4	Fracture Tests	93
8.4		Procedures for Triaxial Tests	93
	8.4.1	Setting up the Specimen	93
	8.4.2	Conduct of Triaxial Tests	94
	8.4.3	Ending Triaxial Tests	96
8.5		Procedures for Erosion Tests	96
	8.5.1	Pinhole Tests	96
	8.5.2	Cylinder Dispersion Tests	97
8.6		Procedures for Hydraulic Fracture Tests	98
	8.6.1	Installation of the Sand Pocket and the Probe in the Specimen	98
		a) 38 mm Diameter Samples	
		b) 100 mm Diameter Samples	
	8.6.2	Setting up the Specimen	99
	8.6.3	Conduct of Fracture Tests	100
	8.6.4	Ending Fracturing Tests	102
CHAPTER	9	TEST RESULTS	
	9.1	Introduction	104
	9.2	Fracture Tests	104
	9.3	Pinhole Tests	105
	9.4	Cylinder Dispersion Tests	105
CHAPTER	10	DISCUSSION OF RESULTS	
	10.1	Hydraulic Fracturing Tests	106
	10.1.1	Initial Fracturing Tests	108
		i) Influence of Type of Cavity Fluid	109
		ii) Influence of Sample and Cavity Size	111
		iii) Effect of Overconsolidation Ratio	112
		iv) Effect of Rate of Loading	113
		v) Effect of Stress Ratio σ'_1/σ'_3	115

		10.1.2 Closure Pressure Test	116
		10.1.3 "Immediate" Hydraulic Fracturing Tests	117
		10.1.4 "Delayed" Hydraulic Fracturing Tests	117
		10.1.5 Effect of Penetrating Fluid	118
		10.1.6 Comparison of Experimental Fracturing Results with the Proposed Theories.	118
		10.1.7 Comparison of Experimental Results with Theories Proposed by others	120
		10.1.8 Results of Complementary Studies	121
	10.2	Pinhole Tests	122
	10.3	Cylinder Dispersion Tests	123
		10.3.1 Cwmernderi Dam	123
		10.3.2 Gorpley Dam	124
		10.3.3 Ramsden Dam	125
		10.3.4 Various other Soils	125
		10.3.5 Index Properties of Soils Studied	126
CHAPTER	11	CONCLUSIONS	127
APPENDIX	A	Reasons for the Methods Adopted for Inducing Hydraulic Fracture in Triaxial Samples	131
APPENDIX	B	Basic Results of Soil Properties and Triaxial Tests on Puddle Clay	133
		B.1 Introduction	133
		B.2 Classification and Index Properties	133
		B.3 Isotropic Compression and Swelling Characteristics	133
		B.4 Undrained Compression and Extension Tests	133
		B.5 Relationship of Axial Stress, Pore Pressure and Deviatoric Stress with Shear Strain	134
		B.6 Discussion of Basic Test Results	134
		B.7 Summary of Laboratory Test Results	137
APPENDIX	C	Complementary Numerical Studies	138
REFERENCES			

LIST OF TABLES

TABLE	DESCRIPTION
3.1	Effect of Compactive Effort on Measured Values of u_r (after Jaworski et al 1981)
7.1	Accuracy and Measurements
8.1	Classification of Triaxial Tests
8.2	Classification of Pinhole Tests
8.3.	Classification of Cylinder Dispersion Tests
8.4	Classification of Fracturing Tests
9.1	Initial and Fracturing States for Fracturing Tests on Groups F1-A
9.2	Initial and Fracturing States for Fracturing Tests on Groups F1-B
9.3	"Delayed" (1-day) Fracturing Tests on Group F1-B
9.4	Initial and Fracturing States for Fracturing Tests on Groups F-2
9.5	Initial and Fracturing States for Fracturing Tests on Groups F-3
9.6	Initial and Fracturing States for Fracturing Tests on Groups F-4
9.7	Initial and Fracturing States for Fracturing Tests on Groups F-5
9.8	Initial and Fracturing States at Various Rates on Group F-6
9.9	Initial and Fracturing States for Initial Fracturing Tests on Groups F-7 and F-8.
9.10	"Delayed" Fracturing Tests on Group F-7 and F-8
9.11	Initial and Fracturing States for Fracturing Tests on Group F-9
9.12	Index Properties of Soil Tested for Dispersion/Erosion Tests
9.13	pH Values of Water used for Dispersion/Erosion Tests
9.14	Pinhole Tests on Puddle Clay from Cwmernderi Dam
9.15	Summary of Cylinder Dispersion Tests on Puddle Clay - Cwmernderi Dam
9.16	Summary of Cylinder Dispersion Tests on Puddle Clay - Gorphey Dam
9.17	Summary of Cylinder Dispersion Tests on Puddle Clay - Ramsden Dam
9.18	Summary of Cylinder Dispersion Tests on Various Soils
10.1	Analysis of Fracturing Tests on Group F1-A
10.2	Analysis of Initial Fracturing Tests on Group F1-B
10.3	Analysis of Fracturing Tests on Group F-2
10.4	Analysis of Fracturing Tests on Group F-3
10.5	Analysis of Fracturing Tests on Group F-4
10.6	Analysis of Fracturing Tests on Groups F-7 and F-8
10.7	Effect of Ratio of the Hole Size to the Sample Size (%) on Hydraulic Fracturing Pressures
10.8	Analysis of Hydraulic Fracturing Tests on Group F-5
10.9	Analysis of Time to Failure on Fracturing Tests on Group F-3
10.10	Analysis of Fracturing States at Various Rates of Group F-6
10.11	Analysis of Fracturing Tests on Group F-9
10.12	Analysis of "Delayed" Fracturing Tests on F1-B
10.13	Analysis of "Delayed" Fracturing Tests on Group F-7 and F-8
10.14	Effect of Fluid Penetration on the Analysis of Initial Fracturing Tests on Group F1-B

- 10.15 Effect of Fluid Penetration on the Analysis of Fracturing Tests on Groups F-3 and F-4
- 10.16 Effect of Fluid Penetration on the Analysis of Fracturing Tests on Groups F-7 and F-8
- 10.17 Comparison of the Experimental Fracturing Results with the Proposed Effective Stress Analysis and Kennard's Criterion for Normally Consolidated Samples
- 10.18 Comparison of Experimental Fracturing Results with the Theoretical Effective Stress Analysis - Group F-5
- 10.19 Comparison of Experimental Fracturing Results with the Plane Strain Finite Element Method - Overconsolidated Samples

- B-1 Summary of Index and Classification Tests of Puddle Clay - Cwmernderi Dam
- B-2 Initial and Ultimate States for Reconstituted Normally Consolidated Samples
- B-3 Initial and Ultimate States for Reconstituted Overconsolidated Samples
- B-4 Summary of Reconstituted Samples
- B-5 Variation of s_v/p'_o at various rates

LIST OF FIGURES

FIGURE	DESCRIPTION
1.1	Typical Cross-Section of an Old Embankment Dam with a Puddle Core (Charles and Watts 1987)
2.1	Isotropic Compression and Swelling Lines
2.2	The complete State Boundary Surface in $q':p':v$ Space (from Atkinson and Bransby 1978)
2.3	Idealised Behaviour of Soils in Undrained Tests
2.4	Cylinder Dispersion Test
3.1	Outline of the Hypothesis used to Explain the Development of Cracks in the Core (After Kjaernsli and Torblaa 1968)
3.2	Stress Changes Leading to Drained Hydraulic Fracture (After Vaughan 1976)
3.3	Apparatus for Hydraulic Fracturing Experiments (After Nobari et al 1973)
3.4	Axial Extension in Relation to the Axial Negative Load in Type 1 Test
3.5	Calculated Permeabilities in Type 1 Test (Fig. 3.4 and 3.5 after Nobari et al 1973)
3.6	Results of Borehole Hydraulic Fracturing Tests on Undisturbed Block Samples
3.7	Hydraulic Fracturing Tests on Recompacted Samples of Teton Dam Soil (Groups I and II)
3.8	Hydraulic Fracturing Tests on Recompacted Samples of Teton Dam Soil (Groups III, IV, V)
3.9	Effect of Duration of Tests (Fig. 3.6, 3.7, 3.8 and 3.9 from Jaworski et al 1981)
3.10	Criteria for Cracking (from Savvidou 1981)
3.11	Region of Cracking Stresses (After Savvidou 1981)
4.1	Cross-Section of Old Dale Dyke Embankment Dam (after Binnie 1978)
4.2	Wister Dam Section Showing Probable Location of Major Leaks (from Sherard 1973)
4.3	Wister Dam Showing Location and Direction of Major Leaks (from Sherard 1973)
4.4	Wister Dam Longitudinal Section Showing Thickness of Foundation Alluvium over Bedrock and Probable Location of Major Leaks (from Sherard 1973)
4.5	Stockton Creek Dam (a) Cross-Section (b) Longitudinal Section Looking Down Stream (after Sherard 1973)
4.6	Hyttejuvet Dam : Cross-Section (after Kjaernsli and Torblaa 1968)
4.7	Hyttejuvet Dam : Variation of Leakage and Water Level in Reservoir with Time (after Kjaernsli and Torblaa 1968)
4.8	Balderhead Dam Cross-Section (after Vaughan et al 1970)
4.9	Balderhead Dam : Reservoir Level, Seepage Flow and Upstream Piezometers (after Vaughan et al 1970)
4.10	Yard's Creek Upper Reservoir Dam (after Sherard 1973)
4.11	Teton Dam : Cross-Section Through Centre Portion of Embankment Founded on Alluvium (after Seed and Duncan 1981)

- 4.12 Teton Dam : Typical Cross-Section over Abutment Section Founded on Jointed Rhyolite (after Seed and Duncan 1981)
- 5.1 Relationship Between Dispersibility (susceptibility to Colloidal Erosion) and Dissolved Pore-Water Salts Based on Pin-hole Tests and Experience with Erosion in nature (after Sherard et al 1976)
- 5.2 Definition of Critical Shear Stress, Rate of Change of Erosion Rate and Rate of Erosion (after Arulanandan and Perry 1983)
- 5.3 Cross-Section View of Rotating Cylinder Test Apparatus (after Arulanandan et al 1975)
- 6.1 The Idealised Model
- 6.2 Stress Path During Hydraulic Fracturing Tests on Ideal Elastic-Plastic Soil
- 6.3 Distribution of Stresses Away from the Borehole
- 6.4 Plane Strain Analysis of a Thick Hollow Cylinder
- 6.5 Possible Behaviour of Overconsolidated Samples during Fracturing Tests
- 6.6 Possible Stress Changes in a Soil Element Adjacent to the Cavity during Hydraulic Fracturing Test
- 6.7 Pore Pressure at Failure in a Fracturing Test
- 6.8 The Effect of Penetrating Fluid
- 6.9 Isochrones during 1 - D Consolidation
- 7.1 Sample Press
- 7.2 Loading for a Hydraulic Cell for Triaxial Stress Controlled and Strain Controlled Tests and for Stress Path Tests
- 7.3 Apparatus for Pinhole Tests : a) General Arrangement, b) Details of Nipple
- 7.4 Laboratory Hydraulic Fracture Apparatus
- 7.5 Samples Top Cap and the Probe
- 7.6 100 mm Samples Top Cap and the Probe
- 7.7 Sample Borer
- 7.8 100 mm Sample Borer
- 7.9 "Final" Set up
- 7.10 Sample's Top Cap Holder
- 8.1 Sample Set Up
- 10.1 Plot of $\sigma_r\sigma_{\infty}$ against s_u : Group F1-A and F1-B (initial fracturing tests)
- 10.1A Plot of $(\sigma_r\sigma_{\infty})/s_u$ against $(1-a^2/b^2)$: Groups F-1B, F-3, F-4, F-7 and F-8
- 10.1B Plot of $(\sigma_r\sigma_{\infty})/2s_u$ against $\ln b/a$: Groups F-1B, F-3, F-4, F-7 and F-8
- 10.2 Plot of $\sigma_r\sigma_{\infty}$ against $\sigma_{\infty} [(1-a^2/b^2)/(1+a^2/b^2)]$: Group F1-B (initial fracturing tests)
- 10.3 Plot of $\sigma_r u_o$ against σ'_{∞} : Group F1-A (initial fracturing tests)
- 10.4 Plot of $\sigma_r u_o$ against σ'_{∞} : Group F1-B (initial fracturing tests)
- 10.4A Plot of $(\sigma_r u_o)/\sigma'_{\infty}$ against $(1-a^2/b^2)$
- 10.5 Plot of $\sigma_r\sigma_{\infty}$ against $s_u(1 - a^2/b^2)$: Group F1-B (initial fracturing tests)
- 10.6 Plot of $\sigma_r u_o$ against σ'_{∞} : Group F-2
- 10.7 Plot of $\sigma_r\sigma_{\infty}$ against $s_u(1 - a^2/b^2)$: Group F-2
- 10.8 Plot of $\sigma_r u_o$ against σ'_{∞} : Groups F-3 and F-4
- 10.9 Plot of $\sigma_r\sigma_{\infty}$ against $s_u(1 - a^2/b^2)$: Groups F-3 and F-4
- 10.10 Plot of $\sigma_r u_o$ against σ'_{∞} : Groups F-7 and F-8 (initial fracturing tests)

- 10.11 Plot of $\sigma_r\sigma_\infty$ against $s_u(1 - a^2/b^2)$: Groups F-7 and F-8 (initial fracturing tests)
- 10.12 Effect of Ratio of Hole Size to the Sample Size of $\sigma_r u_o/\sigma'_\infty$
- 10.13 Effect of Ratio of Hole Size to the Sample Size on $\sigma_r u_o/s_u(1 - a^2/b^2)$
- 10.14 Plot of $\sigma_r u_o$ against $\ln R_o$: Group F-5
- 10.15 Plot of $\sigma_r\sigma_\infty$ against $\ln R_o$: Group F-5
- 10.16 Plot of $(\sigma_r u_o)/\sigma'_\infty$ against $\ln R_o$: Group F-5
- 10.17 Plot of $(\sigma_r\sigma_\infty)/\sigma'_\infty$ against $\ln R_o$: Group F-5
- 10.18 Plot of $\sigma_r\sigma_\infty/s_u(1 - a^2/b^2)$ against $\ln R_o$: Group F-5
- 10.19 Effect of Time to Failure on $\sigma_r u_o$: Group F-3
- 10.20 Effect of Time to Failure on $\sigma_r\sigma_r$: Group F-3
- 10.21 Effect of Rate of Loading on $\sigma_r u_o$: Group F-6
- 10.22 Effect of Rate of Loading on $\sigma_r\sigma_\infty$: Group F-6
- 10.23 Effect of Rate of Loading on $\sigma_r u_o/\sigma'_\infty$: Group F-6
- 10.24 Effect of Time to Failure on $\sigma_r u_o$: Group F-6
- 10.25 Effect of Time to Failure on $\sigma_r\sigma_\infty$: Group F-6
- 10.26 Effect of Time to Failure on $\sigma_r u_o/\sigma'_\infty$: Group F-6
- 10.27 "Apparent" Stress Path during Fracturing Test on Sample F6-6
- 10.28 "Apparent" Stress Path during Fracturing Test on Sample F6-7
- 10.29 Effect of Stress Ratio σ'_r/σ'_a on $\sigma_r u_o$: Group F-9
- 10.30 Effect of Stress Ratio σ'_r/σ'_a on $\sigma_r\sigma_\infty$: Group F-9
- 10.31 Effect of Undrained Shear Strength on $\sigma_r\sigma_\infty$: Group F-9
- 10.32 Effect of Stress Ratio σ'_r/σ'_a on $\sigma_r\sigma_\infty/s_u(1 - a^2/b^2)$: Group F-9
- 10.33 Plot of σ_c against σ_∞
- 10.34 Plot of σ_θ against σ_∞
- 10.35 Plot of $\sigma_r u_o$ against σ'_∞ : Group F1-B (delayed fracturing tests)
- 10.36 Plot of $\sigma_r\sigma_\infty$ against $s_u(1 - a^2/b^2)$: Group F1-B (delayed fracturing tests)
- 10.37 Plot of $\sigma_r u_o$ against σ'_∞ : Groups F-7 and F-8 (delayed fracturing tests)
- 10.38 Plot of $\sigma_r\sigma_\infty$ against $s_u(1 - a^2/b^2)$: Groups F-7 and F-8 (delayed fracturing tests)
- 10.39 Plot of $\sigma_r\sigma_\infty$ against $s_u[1-(\frac{a+a1}{b})^2]$: Group F1-B (after fluid penetration)
- 10.40 Plot of $\sigma_r\sigma_\infty$ against $s_u[1-(\frac{a+a1}{b})^2]$: Group F-3 and F-4 (after fluid penetration)
- 10.41 Plot of $\sigma_r\sigma_\infty$ against $s_u[1-(\frac{a+a1}{b})^2]$: Group F-7 and F-8 (after fluid penetration)
- 10.42 Variation in Stresses with Cavity Water Pressure
- 10.43 Radial Variation in Pore Pressure at Fracture
- 10.44 Influence of Rate on Fracturing Pressure for Plane Strain Analyses
- 10.45 Variation of Fracturing Pressure with Confining Pressure: Rate 50 kPa/min.
Figs. 10.42 to 10.45: after Tam, Mhach & Woods (1988)
- 10.46 Activity Plot of P1(%) Versus Clay Content (%) - Group B-1
- B-1 Isotropic Compression and Swelling Results
- B-2 "Corrected" Isotropic Compression and Swelling Results
- B-3 Ultimate States
- B-4 Plot of σ_a and u_o against $\epsilon_i\%$ - Normally Consolidated Samples (automatic series)
- B-5 Plot of σ_a and u_o against $\epsilon_i\%$ - Overconsolidated Samples
- B-6 Stress-Strain Behaviour of Normally Consolidated samples - Compression Tests (semi-automatic series)

- B-7 Stress-Strain Behaviour of Normally Consolidated Samples - Extension Tests (semi-automatic series)
- B-8 Stress-Strain Behaviour of Normally Consolidated Samples (automatic series)
- B-9 Stress-Strain Behaviour of Overconsolidated Samples
- B-10 Undrained Effective Stress Paths (semi-automatic series)
- B-11 Undrained Effective Stress Paths - Extension Tests (semi-automatic series)
- B-12 Undrained Effective Stress Paths (automatic series)
- B-13 Stress Ratio-Shear Strain Relationship - Normally Consolidated Samples (semi-automatic series)
- B-14 Stress Ratio - Shear Strain Relationship
- B-15 Ultimate States
- B-16 Plot of Undrained Shear Strength Against Initial Effective Confining Pressure
- B-17 Plot of Specific Volume at Failure against Undrained Shear Strength
- B-18 Plot of q'/p'_0 against shear strength at various rates
- B-19 Variation of s_v/p'_0 with time

LIST OF PLATES

PLATE	DESCRIPTION
I	Laboratory Hydraulic Fracture Apparatus
II	Fractured Samples - Group F1
III	Fractured Samples - Group F2
IV	Fractured Samples - Group F3
V	Fractured Samples - Group F-7
VI	Fractured Samples - F6-7 Sample
VII	Dispersive - Type D
VIII	Non-Dispersive - Type N
IX	Non-Dispersive - Type C

ACKNOWLEDGEMENTS

I am indebted to the Building Research Establishment for contributing towards my research and grant by supporting the SERC-CASE award. In addition, they provided samples of puddle clay from a number of British dams and made arrangements for me to assist with their field work. I am grateful to Dr J.A. Charles and Dr P. Tedd for their helpful discussions and advice on the conduct of the research. I also wish to thank Dr Pugh of A.G. Weeks and Partners Ltd and Thames Water for providing some samples for the erosion tests.

My thanks and appreciation are due to Professor John Atkinson for his guidance and encouragement through out my research and whilst writing up this thesis. I would also like to thank staff and students in the Geotechnical Engineering Research Centre in particular Dr N Taylor, Dr P. Lewin and Mr H. Tam for the contribution they have made. In addition, the laboratory testing would not have been possible without Mr Keith Osborne and his team of technicians. My thanks also goes to Mrs Dawn Seymour for her neat and expert typing.

Finally, I would like to thank my wife Christine, without whose patience and encouragement this research, especially the writing up of this thesis, would not have been accomplished.

DECLARATION

I grant powers of discretion to those University Librarian to allow this thesis to be copies in whole or in part without reference to the author. This permission covers only single copies for study purposes, subject to normal contribution of acknowledgement.

ABSTRACT

This thesis concerns an experimental investigation of hydraulic fracturing when the water pressure is increased rapidly in a borehole and development of a possible simple method for identifying erodible clayey soils.

Case histories of hydraulic fracturing in embankment dams and boreholes are reviewed. It is found that hydraulic fracturing in dams is often associated with rapid reservoir filling and zones of low stresses. Previously proposed criteria for hydraulic fracturing are outlined. It is found that no existing theory adequately explains fracturing observed in laboratory tests. Characteristics of dispersive clays and the methods of identifying them are reviewed. It is found that no single test provides results that have a satisfactory level of reliability.

Hydraulic fracture was examined in the laboratory on samples of puddle clay from the core of Cwmernderi Dam in modified Bishop and Wesley triaxial cells. Various sets of tests examined the effects of sample geometry, loading rate and overconsolidation on the initial fracturing pressure and examined the effects of subsequent reconsolidation time on refracturing pressures. For the analysis of these tests results, simple criteria for hydraulic fracturing are proposed. The test results suggest that hydraulic fracturing for undrained conditions occurs when the drained strength of the soil element at the edge of a borehole is reached. For fully drained conditions, fracturing occurs when the soil element at the edge of the borehole reaches the no-tension cut-off.

A new test, the cylinder dispersion test, was developed and a series of tests were carried on samples of puddle clay from several British dams and on various other soils. The results of these tests demonstrate the major influence of pore water chemistry on the true cohesion and dispersion properties of the soils.

GLOSSARY OF SYMBOLS

A	Activity
A,B	Skempton's pore pressure parameters
A,B	(subscript) internal and external
E	Young's modulus
G_s	Specific gravity of soil grains
H	(subscript) horizontal
LL	liquid limit
PL	plastic limit
R_o	overconsolidation ratio
a	internal radius of the cavity
a	(subscript) axial
b	external radius of the cavity
c'	cohesion
c_v	coefficient of consolidation
e	voids ratios
f	(subscript) failure
ln	natural logarithm
o	(subscript) initial
p	(subscript) peak
p	$\frac{1}{3} (\sigma_a + 2\sigma_r)$ } stress parameters
q	$(\sigma_a - \sigma_r)$ } for $\sigma_r = \sigma_a$
r	(subscript) radial
s_u	undrained shear strength
t	time
u	pore pressure

v	(subscript) vertical
v	specific volume
v_v	specific volume of isotropically overconsolidated soil swelled up $p' = 1.0 \text{ kN/m}^2$
w	water content
σ'	effective stress (e.g. σ')
Γ	specific volume of soil at critical state with $p'=1.0 \text{ kN/m}^2$
Δ	large increment of
M	slope of critical state line when it is projected on to a constant volume plane
M_c	value of M for triaxial compression tests
M_e	value of M for triaxial extension tests
N	specific volume of isotropically normally consolidated soil at $p'=1.0 \text{ kN/m}^2$
δ	small increment of ...
e	strain
θ	(subscript) circumferential
k	slope of overconsolidation line (negative)
λ	slope of normal consolidation line (negative)
ν'	Poisson's ratio
σ	normal stress
ϕ'	angle of internal friction
ϕ'_e, ϕ'_c	angle of internal friction for triaxial extension and compression tests respectively

CHAPTER 1

INTRODUCTION

1.1 Embankment Dam Failures

The broad definition of failure is the conditions in which an embankment dam fails to fulfil its function for which it has been constructed namely to impound safely a reservoir of water. Failures of dams can result in a greater loss of human life and property than failure of most other man-made structures. In reviewing dam practice in the U.S.A., Middlebrooks (1953) listed unsatisfactory performance of about 200 dams. According to him the causes of partial or complete failures were: Overtopping, seepage, conduit leakage, slides and other factors. Seepage and conduit leakage accounted for 38%, overtopping accounted for 30%, slides accounted for 15% and other factors accounted for 17% of inadequacies of earth dams. In the U.K., Charles and Boden (1985) compiled a list of nearly 100 cases of unsatisfactory performance of U.K. embankment dams. They found that 24% were associated with external erosion caused by overtopping, 14% were due to shear failure involving slips and slides, 55% resulted from internal erosion and leakage and the remaining 7% resulted from other causes including mining subsidence. They concluded that this clearly suggests that the most serious hazard to old earth dams as they age in service is associated with internal erosion.

Internal erosion occurs when water flowing through a crack removes material from the walls of the crack and transports it from the downstream of the dam. This type of hazard had received relatively little attention in the past and yet may be the most important hazard to the safety of puddle clay core dams. This is mainly due to the mechanisms involved which are not as well understood as those connected with shear instability. Some of the old embankment dams that suffered from internal erosion were: Woodhead Dam in 1850, Dale Dyke Dam in 1864, Warmwithens in 1970 and Lluest Wen in 1969/1970, (Charles, 1984). In assessing the possibility of internal erosion there are two factors:

- 1) The conditions which lead to the development of cracking
- 2) Removal of material

For internal erosion to occur both must happen but they are different issues and should be treated separately. Hydraulic fracture of a narrow puddle clay core could be a mechanism which initiates erosion. Hydraulic fracture, under drained conditions, occurs if, at any time during impounding or operation of a dam, the minimum effective stress on any plane in the soil falls to zero. Cracks can also be formed by other mechanisms such as differential settlement within a core, and shrinkage of the clay due to drying out during a long period in which the reservoir is drawn down. Study of the mechanism of hydraulic fracturing and erosion from the surfaces of cracks into water is considered in this thesis. If hydraulic fracture of a core took place, the seriousness of this could depend on the erodibility of the clay.

1.2 Statement of the Problem

There are about 500 large dams (dams greater than 15 m height) in the U.K. About 40% of these dams were built before the beginning of this century. Almost all of these dams are of an embankment type, generally with a puddle clay core. Of the total stock of large dams in the U.K., about 60% are earth embankments built before 1950 and which consequently were designed and built without the full knowledge of soil mechanics, (Charles and Watts, 1987). Some British dams are located in river valleys upstream of densely populated regions. Due to the large volumes of water that they impound and their potential to inflict damage, the structural stability and safety of these dams is a major concern. Thus reservoir safety in the U.K. is mainly concerned with the behaviour and long term performance of these dams and the current implementation of the 1975 Reservoir Act (Reservoir Act, 1975) has focused attention on this subject. While the main focus of attention has been placed on efforts to ensure adequate spillway capacity, relatively little attention has been given to the investigation of the problems of internal erosion initiated probably by hydraulic fracturing of the cores. A study of the mechanism of hydraulic fracturing and internal erosion is urgently required.

Most of the embankment dam failures due to hydraulic fracturing, as discussed in chapter 4, have been associated with a rapid rise of reservoir water level which may suggest an "undrained" condition. Previous research, as discussed in chapter 3, has concentrated on drained failure mechanisms. This research sets out to study fracturing due to rapid rise of reservoir level.

Most of the research in erosion of clay cores has been directed towards dispersive clays found in countries like Australia and the U.S.A. As yet, there has been no mention in the literature of such highly dispersive clays in the U.K. Puddle clays used in the old embankment dams in the U.K. would be expected to erode slowly over relatively long periods of exposure to seepage. The common tests may not be sufficiently sensitive to examine the potential for long term resistance to erosion of puddle clays. Part of the research is concerned with the mechanism of erosion and development of a simple method to study the erosion properties of puddle clay.

1.3 Objectives and Method of Research

Although the phenomena of hydraulic fracturing and erosion are important in the Engineering of earth dams, the mechanics, however, need to be investigated further in order to understand fully these phenomena. The objectives and method of research are summarised as follows:

- a) To examine the evidence of hydraulic fracturing in earth dams.
- b) To outline and compare the mechanisms of hydraulic fracturing that have been postulated for each dams and boreholes.
- c) To study experimentally the mechanism of hydraulic fracturing under rapid application of water pressure in a discontinuity.
- d) To study the mechanism of erosion and the effect of long term exposure of puddle clay samples and other clay samples to water.

Hydraulic fracturing tests were performed in the laboratory by injecting a fluid rapidly through a hypodermic needle placed in a pocket of sand column in the middle of a sample. These tests were conducted in a Bishop and Wesley triaxial cell on both normally consolidated and overconsolidated reconstituted samples. By conducting tests in such a cell both total and effective stresses could be monitored and controlled to examine the stress conditions pressures required to initiate hydraulic fracturing. Most of the tests were conducted on 38mm diameter samples having an internal cavity of 6mm diameter. The effect of the size of the sample and the cavity on fracture were studied by conducting tests on 100mm diameter samples and by varying the size of the cavity both in 38mm and 100mm diameter samples. Tests were also conducted to study the effect of rate of increase

of water pressure on fracturing. Undrained triaxial tests were conducted on both normally consolidated and overconsolidated 38mm diameter samples to determine the values of shear strengths and changes in pore pressures due to shearing in order to interpret the fracture tests.

The effect of long term exposure of puddle clay to water was examined by immersing 38mm reconstituted samples of puddle clay obtained from the cores of various old dams and other common clays in a beaker of water of varying chemistry and observing their behaviour with time. Classification tests were conducted to determine the Activity of these clays.

1.4 British Embankment Dams with Puddle Clay Cores

The majority of embankment dams built in Britain during the last 150 years have central narrow cores of puddle clay, often taken down below the dam in a trench to a natural stratum of low permeability. Puddle clay is not a description of a particular type of clay, but refers to the way that the clay was placed at a high moisture content by puddling. A typical cross-section is shown in Fig 1.1 (Charles and Watts, 1987). Failures and problems with these early embankments led to important changes in design as described below.

Clay filled cut-off trenches below ground level to connect the cores to a stratum of low permeability were abandoned in favour of concrete filled trenches. In modern embankment dams grout curtains are often used instead of deep cut-off trenches, often in conjunction with shallow cut-off walls. The practice of taking outlet pipes or culverts through the embankment dam was argued to be unsafe since water could be released into the embankment. It was thought to be safer to place the pipes or culverts in the natural strata on which the embankment was built, either by tunnelling or trenching. The other important change in design of these dams was to place selected fill next to the puddle clay core. This selected fill was more cohesive than the general embankment fill and was conceived as providing a transition between the puddle clay and the shell coarse material. This change in design probably was the first introduction of a graded filter and this may be the reason for the success of old British puddle clay core embankment dams.

Despite the theoretical principles, the experiences gained from these dams led early dam engineers to a number of widely accepted code of practices in design and construction. The hazard and prevention of internal erosion was fully appreciated by these engineers.

CHAPTER 2

BASIC THEORY

2.1 Introduction

This chapter covers the fundamental concepts of soil mechanics related to this research. Behaviour of soil has been examined within the framework provided by Critical Soil Mechanics (Atkinson and Bransby, 1978). The basic theory relating to the mechanism of cracking is covered in chapter 6.

2.2 Stress and Strains

Soil Behaviour is governed by effective stresses defined as

$$\sigma' = \sigma - u \quad (2.1)$$

The state of soil may be described fully by the stresses acting on it and by its specific volume v . The critical state model was formulated in terms of the stress invariants p' and q' . In the triaxial apparatus where axial and radial directions are axes of principal stress, p' and q' are defined as follows:

$$p' = \frac{1}{3} (\sigma'_s + 2\sigma'_r) \quad (2.2)$$

$$q' = \sigma'_s - \sigma'_r \quad (2.3)$$

The corresponding strain invariants are:

$$\epsilon_v = (\epsilon_s + 2\epsilon_r) \quad (2.4)$$

$$\epsilon_s = \frac{2}{3} (\epsilon_s - \epsilon_r) \quad (2.5)$$

The most suitable parameter to describe the volumetric state of soil is the specific volume defined as:

$$v = 1 + e = 1 + wG_s \quad (2.6)$$

2.3 Isotropic Compression and Swelling Lines

Most soil samples tested in the triaxial apparatus are isotropically consolidated, i.e. consolidated under all round hydrostatic pressure before the commencement of the shearing part of the test. Other forms of consolidation are also possible, e.g. K_0 consolidation, but these forms will not be considered here.

It is convenient to record the results of an isotropic compression test by plotting specific volume v against p' for each loading or unloading increment. Fig 2.1 illustrates idealised shape of the isotropic consolidation of a saturated cohesive soil.

An equation for the isotropic compression line is given by:

$$v = N - \lambda \ln p' \quad (2.7)$$

where λ is the slope of the compression line in $v - \ln p'$ space, and N is the intercept of the line at $p' = 1.0 \text{ kN/m}^2$.

similarly, an equation for the isotropic swelling line is given by:

$$v = v_{\kappa} - \kappa \ln p' \quad (2.8)$$

where κ is the slope of the swelling line in $v - \ln p'$ space, and v_{κ} is the intercept of this line at $p' = 1.0 \text{ kN/m}^2$. λ , N and κ are soil constants.

2.4 The Ultimate States

In the critical state model, ultimate failure occurs when the state of soil reaches the critical state line. At this condition there can be continued deformation of the soil without change of state.

The locus of critical states for soil is found to project to a straight line in $q': p'$ space defined as follows:

$$q' = Mp' \quad (2.9)$$

The projection of the critical line is assumed to be parallel to the isotropic normal consolidation line in $v: \ln p'$ space, and is given by:

$$v = \Gamma - \lambda \ln p' \quad (2.10)$$

Assuming that the soil fails on the critical state line, the relationship between the frictional parameter M and the effective friction angle ϕ' for the soil is given as below (Atkinson and Bransby, 1978).

For the triaxial compression tests, the frictional parameter M is defined as:

$$M_c = \frac{6 \sin \phi'_c}{3 - \sin \phi'_c} \quad (2.11)$$

hence
$$\sin \phi'_c = \frac{3 M_c}{(6 + M_c)} \quad (2.12)$$

and for triaxial extension tests

$$M_c = \frac{6 \sin \phi'_c}{3 + \sin \phi'_c} \quad (2.13)$$

$$\sin \phi'_c = \frac{3 M_c}{(6 - M_c)} \quad (2.14)$$

2.5 State Boundary Surface

The main feature of the critical state model is the state boundary surface, which represents a limit to all possible states for the soil. The soil is assumed to behave elastically if its

states lie beneath the state boundary surface. Plastic flow occurs when the soil state lies on the state boundary surface.

The shape of the complete state boundary surface is represented graphically in $q':p':v$ space, as shown in Fig. 2.2. For normally consolidated soils the state boundary surface is curved and is called the Roscoe surface whilst the Hvorslev surface is the state boundary surface for overconsolidated samples. The critical state line forms a ridge separating the Roscoe and Hvorslev surfaces, and its height and gradient increase as the mean normal effective pressure increases. There is also a planer surface with a gradient of 3 corresponding the condition that the soil cannot sustain tension.

2.6 Idealised Behaviour of Soils in Undrained Tests

Fig. 2.3 illustrates idealised behaviour of samples of normally consolidated and overconsolidated soil with the same water content during undrained compression tests.

The normally consolidated sample follows the paths and the stress-strain curves AF from an initial isotropic state at A to an ultimate failure state of F on the critical state line where the deviatoric stress is q'_r and the stress ratio is $(q'/p')_r = M$. The overconsolidated sample follows the paths and stress-strain curves BRF from an initial isotropic state at B to F which is the same failure state as the normally consolidated sample but passing through a point R where the stress-ratio $(q'/p')_p$ is a peak as shown in Fig. 2.3 d. This peak is not well defined in Figs. 2.3 a, b or c. The two ultimate points coincide at F because both samples have the same specific volume and water content at failure and both ultimately reach the same critical state point.

In heavily overconsolidated soils there may be small changes in specific volume due to local drainage in rupture zones and hence it may not reach the point corresponding to ultimate failure of the truly undrained test (Atkinson and Richardson, 1987). Rupture zones would tend to form after the peak stress ratio $(q'/p')_p$ has been reached. The soil near the rupture zone would then dilate, suck in water from the neighbouring soil and soften. Hence the sample will fail at a higher specific volume and at a lower undrained shear strength. The amount of softening would evidently depend upon the rate of loading.

Expressions for p'_r and q'_r can easily be obtained since $v_o = v_r$, hence:

$$p'_r = \exp \left[\frac{\Gamma - v_o}{\lambda} \right] \quad (2.15)$$

$$q'_r = Mp'_r \quad (2.16)$$

2.7 Excess pore pressure response during undrained loading

In conventional undrained triaxial tests in which the total stress path is a straight line of gradient 3, the observed magnitude of excess pore pressure is made up of two components: the first component due to response of the clay to the shearing process represented by Δq and the second component due to the change in mean total stress Δp applied to the specimen. By varying the gradient of the total stress path and hence the values of Δp different observed magnitudes of the excess pore pressure can be achieved. Thus the magnitude of the excess pore pressure measured in a shear test is not a unique property of the soil behaviour but also depends on the changes in total stress applied externally to the specimen.

The pore pressures in an undrained triaxial test are conventionally defined by the equation:

$$\Delta u = B [\sigma_3 + A (\Delta \sigma_1 - \Delta \sigma_3)] \quad (2.17)$$

in which Δu is the total change in pore pressure from the start of the test, σ_1 and σ_3 are the changes in the total principal stresses and A and B are the Skempton's pore pressure parameters (1954). For a saturated clay in a triaxial compression test, ($B=1$), A is defined by the expression:

$$A = \frac{\Delta u - \Delta \sigma_3}{\Delta \sigma_1 - \Delta \sigma_3} \quad (2.18)$$

In chapter 6 of this thesis, where hydraulic fracture theories have been proposed, pore pressure at failure is fracturing tests have been estimated using the concepts of critical state soil mechanics.

2.8 Undrained Shear Strength

Undrained shear strength is often assumed to be a fundamental soil property which depends on the nature of soil and its water content. Both Bishop (1966) and Wroth (1984), in their Rankine Lectures, have shown that s_u not only depends on the current water content but also on the types of tests, e.g., triaxial compression or extensions, simple shear, plane strain, cone and vane.

The definition of s_u under triaxial compression conditions is somewhat controversial. Some consider s_u value should be taken as the peak deviator stress, while other consider it ought to be the value at maximum stress ratio, i.e., q'/p' . In normally consolidated soils $(q'/p')_f$ and the maximum q' usually occur nearly at the same point but it is not so for overconsolidated soils. In the critical state model, s_u corresponds to the end point of a test, i.e., at ultimate state. The basic definition of s_u is:

$$s_u = \frac{1}{2} (\sigma'_1 - \sigma'_3) = \frac{1}{2} q'_f \quad (2.21)$$

i.e., half the difference between the major and minor principal stresses, or the radius of Mohr's circle at failure and is equal to the maximum shear stress. Although widely used, this is an unsatisfactory definition as it neither takes account of the intermediate principle stress σ'_2 nor distinguishes between the types of test.

Theoretically, samples at different overconsolidation ratio but all at the same specific volume will all fail on the critical state line at their maximum similar value of q' . For undrained tests, $v = v_o$, and hence s_u is:

$$s_u = \frac{qf}{2} = \frac{1}{2} M p'_f = \frac{M}{2} \exp \left[\frac{\Gamma - v_o}{\lambda} \right] \quad (2.22)$$

The above expression is mostly true for normally and lightly overconsolidated samples but becomes progressively less reliable as the overconsolidation ratio increases. This is mainly due to local volume changes as discussed in section 2.6.

One of the factors that affect the value of s_u is the value of the intermediate principal stress σ'_2 at failure. Henkel and Wade (1966) found for K_0 - consolidated specimens of Weald Clay that the undrained shear strengths in plane strain were approximately 8% higher than those tested under conditions of axial symmetry. Henkel and Wade (1966) also conducted tests on hydrostatically consolidated samples and found that these samples gave about 12% higher strengths than those under plane strain conditions. Berre (1985) also found that the undrained shear strength for the plane strain test with lowest strength was about 5% higher than the ordinary triaxial test conducted under K_0 condition. On the other hand, Wu et al (1963) found that the shear strength parameters for the clay specimens tested were essentially independent of the magnitude of the intermediate principal stress.

It is now well established that the undrained shear strength of cohesive soils is greatly influenced by rate of loading; see for example Bjerrum et al (1958), Bishop and Henkel (1973), Richardson and Whitman (1963), Berre and Bjerrum (1973), Graham et al (1983) and O'Reilly et al (1989). Graham et al (1983) found that the undrained strength increased by 10- 20% with a tenfold increase in strain rate. Richardson and Whitman (1963) showed that in normally consolidated samples, the peak shear resistance increased about 10% in passing from the slow (1% strain in 500 minutes) to the fast (1% strain in 1 minute) strain rate and at small strains ($< \frac{1}{2} \%$) the resistance increased as much as 100%. They also found that the strain-rate effect upon strength was greater for overconsolidated specimens than the normally consolidated specimens. Atkinson and Richardson (1987) also demonstrated the variation of undrained shear strength with the rate of testing. They found that the sample which failed in 100 seconds had a strength about 14% higher than the sample which failed in about 50 hours and this strength increased by 38% for the sample which failed in 5 seconds. Wroth (1984) drew attention to the effect of strain rate on the value of the undrained shear strength of the soil during rapid pressuremeter tests.

In chapter 6, one of the proposed hydraulic fracture theories is related to the undrained shear strength in compression. It has been shown that some factors, as discussed above, can greatly affect the strength; although the precise increase may depend on the type of soil, hence it was decided to carry out a series of tests to investigate the effect of increase rate of testing on the clay used for the present studies.

2.9 Mechanism of Internal Erosion

The shearing strength of the soil may be attributed to a combination of physical and physico-chemical factors (Seed, Mitchell and Chan, 1960). The physical component of shear strength in soils is mainly due to frictional resistance, i.e. the resistance to sliding of one surface on another. The second component of soil strength is due to physico-chemical conditions in the soil and is often referred to as "cohesion". Thus cohesion in a soil is that part of the soil strength that is present independently of any effective normal stress, either mechanical or capillary, and would remain, though not necessarily permanently, if all effective normal stresses were removed. Cohesion present in a soil is due to interparticle forces that resist relative displacements of clay particles. It is only significant for clay particles since it is only for such particles that interparticle forces become significant with respect to particle weights.

The properties of clay are determined by its structure. Structure means the arrangement of soil particles and forces between adjacent particles (Lambe and Whitman, 1969). The two extremes in soil structure are flocculated structure and dispersed structure. In the flocculated state the soil particles are edge to face and attract each other. A dispersed structure, on the other hand has parallel particles which tend to repel each other. Between the two extremes there is an infinite number of intermediate stages. Besides the electrostatic attraction between negative clay surfaces and positive clay edges, attractive forces between clay particles are also due to Van-der Waal's forces. Chemical cementation between particles by various compounds generally present in soils can be a further source of particle adhesion (This is unlikely in compacted or reconstituted samples). These forces play an important part in erosion studies.

When clay particles are placed in an aqueous environment, the cations held at the surface of the dry clay, in order to balance in negative surface charge, tend to spread out into the

so called "diffuse double layer" surrounding the clay particles (Seed, Mitchell and Chan, 1960). If the water content is increased the double layer surrounding individual clay particles will expand and hence decrease the attractive forces between the particles. This will lead to loss of strength and individual particles will be progressively detached from the surface and go into suspension. If the water is flowing, the dispersed clay particles are carried away thus leading to rapid erosions. Thus the mechanism of soil erosion is basically a complex phenomenon involving the structure of the soil and the nature of the interaction between the pore and eroding fluids at the surface.

If a water-filled crack occurs, soil adjacent to the crack will swell in the presence of free water and effective stresses will approach (and reach) zero. Under these conditions, and neglecting shearing tractions due to flowing water, the behaviour of the soil will depend primarily on the true cohesion (i.e. on the component of shear strength available at zero effective stress). Qualitatively there are three possibilities; the true cohesion may be positive (i.e. interparticle forces are attractive), zero or negative (i.e. interparticle forces are repulsive). These forces need only be very small to have a major effect on the stability of the crack. They give rise to strengths which may be less than 1 kN/m^2 which in some circumstances could be sufficient to prevent erosion but which is far too small to be measured in routine soil tests.

If a crack forms in a soil with zero cohesion then, as pore pressures come into equilibrium and effective stresses become zero, grains will fall from the sides of the crack and will gather at the bottom so that the crack will gradually migrate upwards to the phreatic surface where pore pressures are zero. Soil grains will only be washed from the crack if the flow velocities are relatively large. If a crack forms in a soil with positive true cohesion soil grains remain attached to the surface of the crack, unless flow velocities are relatively very large. However, if the true cohesion is negative soil grains will move away from the surface of a crack when the effective stresses approach zero as pore pressures in the soil adjacent to the crack rise. In this case soil grains will disperse into the water in the crack and they may be carried through the dam by only small seepage velocities.

The magnitude of the true cohesion in soil, and particularly its sign will depend on the physico-chemical properties of the soil grains and of the pore water and the free water.

2.10 Cylinder Dispersion Test

A new test was developed to examine erosion and dispersion of soils from the surfaces of cracks into water. The test is an extension of the crumb test, (see section 5.4.4), and it was designed to examine the behaviour of soils at zero effective stresses by submerging a saturated sample in water. The soil will swell as water enters the sample which will ultimately reach a fully softened state. The time required for the complete sample to reach equilibrium is approximately equal to the time for triaxial consolidation with all round drainage. It is necessary to perform the test using a saturated sample as air or gas bubbles present in unsaturated soils may prevent pore pressures becoming equal to the external water pressures so leaving positive effective stresses even in the long term. In order to ensure that the samples are fully saturated, reconstituted samples (described in section 8.2) were used. The procedure for carrying out this test is explained in section 8.5.2.

When saturated soil samples are submerged in water one of three basic characteristics types of behaviour will be observed and these are illustrated in Fig. 2.4. Type N will be seen in soils for which the true cohesion is zero. The sample will slump to a cone as the effective stresses reduce to zero and the angle of the cone will approach the critical state friction angle. Type C will be seen in non-dispersive soils for which the true cohesion is positive. The sample will remain a cylinder although it may deform plastically by bulging near the bottom. Plastic failure will occur in a sample 80mm high if c' is less than about 0.4kN/m^2 . In both types, N and C, the water will remain clear. Type D behaviour will be observed in dispersive soils, for which the cohesion is negative and any interparticle forces are repulsive. In this case grains will leave the surface of the sample, when the stresses due to the repulsive forces, exceed the pore water suctions and the water will become cloudy and opaque. With time the grains may sediment to form a horizontal deposit at the base and the sample will gradually reduce in size while remaining approximately cylindrical.

CHAPTER 3

PREVIOUSLY PROPOSED CRITERIA FOR HYDRAULIC FRACTURING IN EMBANKMENT DAMS AND BOREHOLES

3.1 Introduction

Chapter 4 will indicate that the recognition of hydraulic fracturing in embankment dams is recent. Lofquist (1953) was probably the first to predict the phenomenon of arching of the impervious core giving rise to a risk of horizontal cracks. He gave examples of two dams where the measured vertical pressures in the cores were as low as half the overburden pressure due to arching. It was nearly 15 years after Lofquist's statement that Engineers started proposing criteria for hydraulic fracturing in embankment dams. Hydraulic fracturing in boreholes had been studied much earlier especially by the petroleum industry.

Fractures in embankment dams usually involve a stress redistribution in the core due to a general increase in seepage pressure due to impounding, whilst fractures in boreholes only involve local seepage pressure. However, it will be shown in Chapter 4, that a direct comparison can be made between them. For this chapter, criteria for hydraulic fracturing in embankment dams and boreholes which have been proposed by various engineers and research workers are reviewed. Details of these criteria are presented elsewhere; only the key features of their conclusions are presented here. Finally, these criteria are discussed.

3.2 Embankment Dams

3.2.1 Kjaernsli and Torblaa

After the cracking of the Hyttejuvet Dam (see Section 4.2.5), Kjaernsli and Torblaa (1968) postulated a mechanism of hydraulic fracturing in embankment dams. They suggested that at the start of impounding, compressive stresses exist throughout the core and hence there are no open cracks. However, during impounding horizontal cracks can suddenly be formed as a result of hydraulic fracturing in areas where the total vertical stress in the core is much lower than the overburden pressure because of arching between the core and the

less compressible shell. During impounding, the reservoir pressure acting in the upstream boundary of the core can exceed the total stress acting on some plane through the core as shown in Fig. 3.1.

3.2.2 Vaughan

Vaughan (1976) defined cracks formed during or after reservoir filling as wet cracks. If the seepage pressure is applied rapidly within some initial crack or imperfection then tensile failure may occur by undrained failure. This, according to Vaughan, is unlikely as the rate of impounding in relation to the permeability of the core will almost always ensure that there is a general increase in seepage pressure in the core before cracking can occur.

In drained fracturing, according to Vaughan, the tensile strength to be overcome is small and generally tensile failure must be preceded by shear failure. The stress changes leading to drained hydraulic fracturing at a point X within a core are shown in Fig. 3.2 in terms of total and effective stress. Points A', B', C' and D' are the effective stress states corresponding to points A, B, C and D respectively. Shear failure will occur at point C'. Cracking cannot occur until point D' is reached and this implies major shearing of the soil and stress redistribution. This may modify the total stress and this increase (from C to D) may prevent tensile fracturing. Vaughan concluded that cracking is only likely if there is a local and restricted zone of low stress which will shear and crack before shear occurs elsewhere in the core with the consequent stress transfer and increase in stress in the potential cracking zone.

3.2.3 Sherard

Sherard (1973) indicated that under certain conditions the reservoir pressure acting on the upstream face of a dam can cause existing closed cracks to open or can create new cracks. Sherard's postulate was more or less an extension of Kjaernsli and Torblaa's (1968) criterion as explained earlier. Sherard suggested that hydraulic fracturing in a core can occur whenever total minor principal stresses at a certain elevation in the core are sufficiently low with respect to the reservoir water pressure at the same elevation. The internal stress conditions necessary for hydraulic fracturing can be present on the first reservoir filling or they can develop later as the result of continuing differential settlement.

Non-uniform deformability would increase the probability of low total minor principal stresses occurring locally.

3.2.4 Saturation Settlement Mechanism

Several researchers have postulated saturation settlement as an alternative mechanism for cracking of cores by hydraulic fracturing (Paterson and Inverson, 1953; Ingles, 1972; Leonards and Davidson, 1984 and Mesri and Ali, 1988).

Saturation settlement develops during the filling of a reservoir when the poorly compacted soil or previous zones and layers of dry and loose material becomes saturated and consolidates under its own weight before the dry or denser soil arching over it has a chance to become saturated and collapse. A discontinuity or a crack is therefore developed along the position of the phreatic line and any subsequent increase in water level allows the entry of water into this crack enabling erosion to occur. According to Ingles (1972) such collapse can be either sudden or gradual.

3.3 Boreholes

3.3.1 Morgenstern and Vaughan

Morgenstern and Vaughan (1963) proposed a theory of hydraulic fracture for predicting allowable grouting pressures. According to their theory, as the pore pressure increases in the potential fracturing zone, the effective stress circle translates laterally to the left and fracture occurs when it becomes tangent to the effective stress Mohr-Coulomb failure envelope. Neglecting friction losses in the piping, the water pressure required to cause hydraulic fracturing, in terms of principal stresses, is given by

$$\sigma_f = \frac{\sigma_1 + \sigma_3}{2} - \frac{\sigma_1 - \sigma_3}{2 \sin \phi'} + c' \cot \phi' \quad (3.1)$$

where

- σ_1 and σ_3 are the major and minor principal total stresses respectively.
- ϕ' is the angle of shearing resistance
- c' is the cohesion intercept.

Vaughan (1971) indicated that for cracking to occur the minor principal effective stress, σ'_3 , must be zero or tensile and that the shear failure would cause stress redistribution on the core.

3.3.2 Haimson

Haimson (1968) developed a criterion for hydraulic fracturing around a borehole in rock and gave the following relationship for the borehole fluid pressure to cause vertical hydraulic fracture:

a) For permeable rock

$$\sigma_f = \frac{\sigma'_t + 2\sigma'_h}{2 - \alpha \left(\frac{1 - 2\nu'}{1 - \nu'} \right)} + u_o \quad (3.2)$$

b) For impermeable rock

$$\sigma_f = \sigma'_t + 2\sigma'_h + u_o \quad (3.3)$$

where

- σ'_t = the effective tensile strength
- ν' = Poisson's ratio

- $\alpha =$ the porous elastic parameter $= (1 - C_r/C_b)$
- $C_r =$ material matrix compressibility
- $C_b =$ material bulk compressibility

Haimson carried out tests on both cylindrical and cubical specimens of porous and nonporous rock. Tests were conducted by increasing the fluid pressure in the borehole until fractures were initiated, which were determined by a sudden drop in the internal pressure.

Haimson, from his experimental results, concluded the following : 1) In all samples, whether they were permeable or not, the resulting hydraulic fractures were always tensile ruptures originating at the wall of the borehole. 2) The direction of all fractures were either vertical or horizontal, depending on the loading conditions. All vertical fractures were perpendicular to the smaller horizontal compressive load. 3) The critical pressure required to initiate a vertical hydraulic fracture in permeable rock was lower than the critical pressure in an impermeable rock. 4) The "apparent tensile strength" of rock and hence critical pressure varied considerably with changes in rate of pressurizing, diameter of the hole, length of the hole and in some rock with the amount of external load applied.

3.3.3 Kennard

Kennard (1970) during his research in predicting safe pressures for conducting constant head permeability tests produced the following relationships for the excess pressures (Δu_c):-

- a) For the fully drained conditions in an infinite soil mass

$$\frac{\Delta u_c}{P_o} = \frac{2K}{1+\nu'} \quad \text{or} \quad 1 \tag{3.4}$$

whichever is the least since the horizontal fracture will become dominant at higher values of K.

- b) For the undrained conditions the excess pressure in the tip of the idealized piezometer in an infinite soil mass lies in the interval.

$$1 + \frac{1}{2A} < \frac{\Delta u_c}{Kp'_o} < \infty \quad (3.5)$$

For finite soil mass with no restraint on its boundary, the excess pressure is given by

$$\frac{\Delta u_c}{Kp'_o} = 1 + \frac{(1-a^2/b^2)}{2A} \quad (3.6)$$

where

Δu_c = increase in fluid pressure in borehole above initial pore pressure

p'_o = initial vertical effective stress

K = $\frac{\text{initial horizontal effective stress}}{\text{initial vertical effective stress}}$

ν' = Poisson's ratio

A = Skempton's pore pressure coefficient

a = radius of the borehole (piezometer)

b = radius of the outer boundary

In his theoretical analysis based on plane stress conditions, the soil was assumed to behave elastically up to a point of fracture. Fracturing was assumed to occur when the effective stress within the soil at the walls of the borehole was reduced to zero.

Kennard conducted laboratory tests in a scale model of a field piezometer installed in a large seepage tank and in a specially constructed tank which incorporated facilities for loading samples uniaxially or triaxially and for measuring effective stresses. Briefly, the

tests were conducted by applying an excess head in increments until, above a critical pressure, the flow rate showed a fundamental change, i.e, the sample had hydraulically fractured.

Kennard in his laboratory tests found that the fracturing pressure was in general greater than that predicted from his theory and varied quite widely. He concluded that it was wrong to assume that hydraulic fracture occurred during the head increment when the flow-rate increased by many orders of magnitude and cracks were seen through the side of the tank. It was more likely that this was the final stage of a fracture which had been initiated at a lower head increment. His tests also showed that the fracture pressures in fully drained conditions were less than that in undrained conditions.

3.3.4 Bjerrum, Nash, Kennard and Gibson (1972)

Bjerrum et al (1972) presented a theory for predicting the excess pressure at which hydraulic fracturing will occur in field permeability tests. From the field permeability tests Bjerrum et al (1972) concluded that hydraulic fracturing can take place at excess water pressures smaller than effective overburden pressure at the point of measurement. Model laboratory tests were carried out using equipment and test procedures similar to those of Kennard's (1970) which confirmed the field observations.

For radial cracks to develop in the soil the hydraulic pressure must exceed the effective circumferential stress and the excess head is given by

$$\Delta u_c = \left(\frac{1}{\nu} - 1 \right) [(1 - \alpha) \kappa p'_o + p'_t] \quad (3.7)$$

where p'_t is the maximum tensile effective stress which the soil skeleton is capable of sustaining.

- p_o' = the vertical effective pressure
- K = $\frac{\text{initial horizontal effectiveness}}{\text{initial vertical effective stress}}$
- α = empirical disturbance factor defining the change in circumferential stress due to installation of piezometer (α ranges between 0.4 and 1 for stiff clays)

The above condition applies when the soil cracks before moving away from the piezometer. If the soil moves away from the piezometer, then a blow off occurs and the excess head need for cracking is defined as

$$\Delta u_c = (1-\nu) [(2 + \beta - \alpha) K p_o' + p_i'] \quad (3.8)$$

where β = empirical disturbance factor for the change in radial stress due to installation. ($0.5 < \beta < 4$ for stiff clays)

3.3.5 Massarsch

Massarsch (1978) presented a theoretical approach to the mechanism of soil fracturing using the concept of expanding cylindrical cavities. His approach initially derived for soil fracturing due to driven piles was extended to hydraulic fracturing under undrained conditions.

The excess pressure, P_u , required to cause the expansion of the cavity can be calculated from

$$\frac{P_u}{s_u} = \ln \left[\frac{1.36 E_u}{s_u (1+\nu_u)} \right] \quad (3.9)$$

where

P_u = the expansion pressure

s_u = the undrained shear strength ($\phi_u = 0$)

$E_u =$ the young's modulus

$\nu_u =$ the Poisson's ratio ($= 1/2$)

The change in pore pressure within the soil mass due to the applied pressure at the walls of the borehole can be calculated by taking into account the change in mean normal stress $\Delta\sigma$ and mean shear stress $\Delta\tau$, using Skempton pore pressure parameter, A_r . Neglecting the tensile strength of cohesive soils, the critical conditions at which fracturing would occur in the plastic zone around the borehole is given by:

$$\frac{k_o \sigma'_v}{s_u} < 1.73 A_r + 0.43 \quad (3.10)$$

According to Massarsch (1978), equation 3.9 gives the stress conditions for which a plastic zone is generated around the expanding cavity and equation 3.10 gives the soil conditions at which fracturing can occur. Substituting equation 3.10 into equation 3.9 and taking $\nu_u = 0.5$, a simplified solution for soil fracturing in a drilled borehole is given by

$$\frac{P_u}{\sigma'_v} < \frac{k_o \ln\left(\frac{0.9 E_u}{s_u}\right)}{1.73 A_r + 0.43} \quad (3.11)$$

3.3.6 Nobari, Lee and Duncan

Nobari, Lee and Duncan (1973) used a modified triaxial apparatus, as shown in Fig. 3.3, to investigate fracturing in a compacted sandy clay. In this apparatus, different water pressures could be applied at the inner and outer surface of a hollow core sample during tests. In addition, the deviator stress and the chamber pressure could be controlled independently of the water pressures. Fracturing tests were carried out by combination of varying water pressures at the inner and outer surfaces of the hollow sample and axial stress.

From this experimental study, Nobari et al made the following conclusions: 1) The mechanism of hydraulic fracture was a tension failure with formation of a fracture on the plane of maximum tensile stress. Shear failure was not observed. 2) Under conditions of non-uniform stress, hydraulic fracturing was likely to begin at a point of low effective stress and then gradually propagate through a dam core, rather than occur suddenly through the core. Initiation of hydraulic fracturing at the upstream face of the core in a dam does not, therefore, necessarily mean that the fracture will propagate entirely across the core but, under conditions of uniform stress, the fracture will propagate suddenly. 3) The tensile strengths of most core materials are of the order to 10 to 20 kN/m² and hence can be ignored for the purpose of investigating the likelihood of hydraulic fracturing in dams.

Evidence that the fracture lengths did increase progressively in some of the tests was indicated by two types of observations made during the tests: progressive changes in apparent permeability and progressive jumps in axial deformation observed during the tests as shown in Figs. 3.4. and 3.5.

3.3.7 Jaworski, Duncan and Seed

Jaworski et al (1981) carried out a number of borehole fracturing tests in the laboratory to study the development of fracture under conditions where the stresses could be controlled accurately. The material used in their study was derived from the core of Teton Dam.

Tests were conducted in a 203mm cubical stress apparatus where three independent perpendicular stress could be applied to the faces. The stresses applied to the samples were such that the major principal stress, σ_1 , was equal to the twice the minor principal stress, σ_3 . For most of the tests the intermediate stress, σ_2 , was equal to σ_3 . Tests were performed in a 4.8 mm diameter uncased borehole, 51mm long, drilled in the centre of the sample. As the water pressure in the borehole was raised incrementally at a constant rate the flow rate from the borehole increased. As the fracturing pressure was approached the flow rate increased very rapidly with little or no increase in pressure.

The results of the various hydraulic fracturing test are shown in Figs. 3.6, 3.7 and 3.8. Fig. 3.6 shows the results of three tests on undisturbed samples, which despite being tested under similar conditions gave very different fracturing pressures. Fig. 3.7 shows the results of tests on recompacted samples, divided in two groups. (I and II) in which both the densities and moisture contents were controlled. Group I samples were compacted dry of optimum whilst Group II samples were compacted wet of optimum. The test results gave considerable scatter as shown in Fig. 3.7. Jaworski et al (1981) concluded tentatively that variations in soil composition had a more important effect on hydraulic fracturing than variation in density or water content. Additional tests were carried out on recompacted samples divided into three groups in which a stricter control of density and moisture content was observed. Initial pore water suction for these groups were between 25 and 50 kN/m². The effects of these suctions on the tests were considered to be negligible. The results of these tests are shown in Fig. 3.8. For each group of tests the measured values of hydraulic fracturing pressure varied consistently with the horizontal stress and increased as the lateral confining pressure increased. The effect of compactive effort on the hydraulic fracturing pressure was also investigated and the results are summarised in Table 3.1. From these tests, Jaworski et al (1981) concluded that higher compactive effort led to higher fracturing pressures. The results of the effect of duration of tests are summarised in Fig. 3.9. which shows that the pressures required to cause hydraulic fracture was greater in the long term tests. Jaworski et al (1979) suggested that these may be due to small increase in strength due to thixotropy and the soil may be more ductile and hence less brittle under slower loading. They also studied the effect of a pre-existing fracture or a crack on the hydraulic fracturing pressures. Refracture tests were conducted 24 hours from initial fracture tests. They found that the presence of an existing crack in a soil substantially reduced the fracturing pressure. But if the stresses were increased after a crack had been formed, the crack may heal to some extent over a period of time.

Jaworski et al (1981) suggested that hydraulic fracturing can occur only if there is some discontinuity, within which the water pressure can act to develop tension in the soil by wedging action. This means that hydraulic fracturing should not occur where water pressure impinges on a flat face of homogenous soil, no matter how high the water pressure might become. Tests were conducted to simulate this condition but were unsuccessful and hence the hypothesis could neither be proved or disproved.

Jaworski et al (1979) developed a theory to predict hydraulic fracturing around a borehole in soil. They assumed that the soil behaved as an impermeable linear elastic material and the strength of the soil was given by the Mohr-Coulomb failure criterion. Hydraulic fracturing was assumed to occur when the maximum tangential effective stress became tensile by an amount equal to the tensile strength of the soil. Their theory predicted that hydraulic fracturing would occur around a borehole when the borehole water pressure was equal to the sum of the total internal horizontal stress and one half of the tensile strength of the soil, i.e,

$$\sigma_r = \sigma_h + \sigma_{t/2} \quad (3.12)$$

They also performed finite element analyses which indicated that hydraulic fracture was always slightly greater than the initial horizontal stress (with $\sigma_r = 0$) and was independent of soil properties with the exception of the tensile strength.

Since fracturing pressures obtained in the experimental work could not be predicted by the theory (equation 3.12), they modified their theoretical equation to an empirical of the form.

$$\sigma_r = m\sigma_h + \sigma_u \quad (3.13)$$

where σ_u = the apparent tensile strength of the soil available to resist cracking at the fracture pressures; m = the slope of the linear function of fracture pressure with the horizontal stress. Values of σ_u determined from the borehole hydraulic fracturing tests were much higher than those determined from the Brazilian tensile tests. It was suggested that besides the actual tensile strength of the soil, the values of σ_u also reflected the special conditions inherent in a borehole fracturing tests and the effect of stress distribution. σ_u could vary between zero and the pressure required for cavity expansion. Jaworski et al summarised their experimental investigation by concluding that hydraulic fracturing in a borehole was highly variable and difficult to predict and was influenced by pressure redistribution around the borehole. They suggested that hydraulic fracturing was a "weak link" phenomenon in the sense that fracturing would develop at the point of least resistance.

3.3.8 Savvidou (1981)

Savvidou (1981) described two types of tests carried out on compacted samples of soil from the core of Teton Dam to study changes of air and water permeabilities when tensile cracks open at low effective stresses.

Air permeability was measured in an axial direction on partly saturated samples of 100 mm diameter and 159 mm long compacted at moisture content below optimum, while subjected to loading between flat plates across the diameter. The samples were enclosed in a sheath and immersed in oil. Loading on the flat plates was increased until air flow showed a sudden and marked increase indicating the formation of a crack. The development of a diametrical crack was seen on the face of each sample after the end of the test. Tensile strain at cracking was estimated to be the order of 0.5×10^{-3} .

Water permeability tests were conducted on fully saturated samples, having moisture content higher than the optimum, in the conventional triaxial apparatus. The samples were consolidated under anisotropic loading with $q' = 15$ kPa and p' varying between 200 and 450 kPa. Pore pressures in the 100 mm diameter samples were increased in stages via the 19 mm diameter central hole drilled in the sample filled with sand, thereby reducing the effective stresses in the samples. The drainage in 38 mm diameter samples was vertical. After equilibrium was established at each stage, a measurement of permeability was made by applying a small hydraulic gradient across the specimen. One test was conducted in which no permeability measurements were made in order to observe the influence of hydraulic gradient on cracking. Fracturing was indicated by a sudden increase in permeability and intake water at low effective stresses. After the end of each test vertical cracks propagating from the outer edge to the middle of the sample were visible and were also detected by x-ray pictures.

In the analysis of the test results Savvidou adopted a critical state soil mechanics concept of a no-tension criterion at low effective stresses. The no-tension limits were represented as $q'/p' = 3$ in compression and 1.5 in extension when one or more principle effective stress components ($\sigma_1', \sigma_2', \sigma_3'$) becomes zero. Consequently in this region, tension cracks could occur. Besides a tensile criterion, Savvidou also considered other criteria of tensile cracking such as $p'/p'_u = 0.1$, $p' = 0$ and a tensile strain criterion as shown in Fig. 3.10.

(p'_u is the critical effective pressure above which Coulomb rupture planes are not observed).

From her experimental work Savvidou concluded that the onset of cracking occurred in the region to the right of the three failure criteria - no tension, limiting tensile strain, and $p'/p'_u = 0.1$. All the tests on fully saturated samples showed cracking at effective stresses greater than those corresponding to the $q' = 3p'$ fracture failure surface as shown in Fig. 3.11. The results on partly saturated specimens showed that indications of cracking appeared on the near approach to the tensile strain criterion. Sensitive dial gauge measurement of sample axial compression gave no indication of crack formation which led Savvidou to suggest that large settlement need not appear for crack formation in dams. One test in which no permeability measurements were made also gave similar radial cracks which, according to Savvidou, suggested that cracks can be formed by means other than hydraulic fracture.

3.4 Discussion on Previously Proposed Criteria for Hydraulic Fracturing in Embankment Dams and Boreholes

A direct comparison of the proposed criteria presented here is difficult since the differences in the analyses result from different considerations involved in evaluating the effective stresses necessary for fracturing. Also for direct comparison it is essential to know the properties of the soil and the changes of pore pressure. Many assumptions have to be made in order for a direct comparison which may be misleading. In evaluating experimental work, each of the analyses assumed that the effective stresses necessary for fracturing must be tensile. Most of the analyses have studied fracturing under "drained" conditions.

Massarsch suggested that the fracturing pressure was given by the pressure required to expand a cavity plastically. However, a cavity during its expansion by water pressure may not reach its complete plastic state since penetration of water in the surrounding soil will alter the stress conditions. Massarsch and Broms (1977) drew attention to the effect of soil fracturing due to pile driving in cohesive soils. During driving piles, cracks may be

formed before the ultimate expansion occurs. Such cracks are difficult to observe or may close due to the remolding of cohesive soils by a pile, and also such cracks would not propagate due to the absence of sufficient free water.

One of the most extensive programmes of experimental work on the mechanism of hydraulic fracturing in earth dams was done by Jaworski et al and they presented very interesting experimental results. Unfortunately, they overlooked or did not report certain important factors that can influence fracturing results such as rate of pressurising the borehole and pore pressure changes during a test. These factors may help to explain to a certain extent the scatter of their test results. Initial pore pressures and its changes during a test can greatly influence the fracturing pressures. Jaworski et al (1979) gave suction values of the order of 50 kPa independent of compaction density and water content. They believed that since the values of pore water suction measured were small, their effect will be negligible and, moreover, when water is added to the borehole the pore water suction in the soil around the borehole would be reduced to zero. Small variations of initial water content and compactive effort can cause relatively large changes of pore pressure at failure and effect the final strength considerably (Seed, Mitchel and Chan, 1960). This may explain why the drier samples, as shown in Fig. 3.6 gave higher fracturing pressures than the wetter samples. Initial moisture content effects the fracture pressure much more than compactive effort. This can be examined by studying the tests LHF-7 and LHF-10 (Table 3.1). Both these tests were compacted to nearly the same high densities but at different moisture content. The drier sample gave a much higher fracturing pressure. Drier samples would be expected to have a higher suction than wetter samples.

Jaworski et al's elaborate theory failed to match their experimental results and they had to adopt an empirical relationship. In their theory they assumed that the soil behaved as an impermeable linear elastic material but the tests were conducted under almost drained conditions (typical tests lasted between 3 to 4 hours). The empirical factor m probably allowed for seepage in their analysis. Jaworski et al interpreted and plotted their test results in terms of total stresses. Behaviour of soil is controlled by effective stresses and had they known the changes of pore pressure during a test, their results might have given a better fit.

Jaworski et al suggested that the maximum value of apparent tensile strength which could be anticipated will be equal to the pressure required for cavity expansion. But according to Vaughan (1976) in drained hydraulic fracturing tests, the tensile strength to be overcome will be negligibly small in most cases. Jaworski et al postulated that a uniform increase in the pore water pressure in a continuous and homogenous soil mass will not result in tensile stresses and will therefore not lead to hydraulic fracturing. Savvidou, however, showed that under certain conditions (at low deviator stress) a uniform increase in the pore pressure can produce cracks. In hydraulic fracturing under undrained conditions, a necessary condition is the presence of a crack or imperfection. Savvidou's tests showed that it was possible for cracking to occur before reaching a tensile stress criterion. This finding of Savvidou raised questions on the assumption that hydraulic fracturing of earth dams will not occur as long as the minor principal stresses are always positive. It would appear to be safer to ensure that values of p' and q' in the core are within the boundaries of the no-tension ($q' = 3p'$) and Coulomb rupture criterion. Savvidou's simple analysis using the concept of the critical state soil mechanics has given valuable insight to the mechanism of cracking in earth dams. Her tests were essentially drained where the pore pressures were raised gradually and, at low stresses, the onset of cracking was observed by a sudden increase in permeability which may imply propagation of cracks under undrained conditions. Savvidou's tests showed similarity to tests conducted by Nobari et al (1973), who suggested that under conditions of non-uniform stress, hydraulic fracturing will gradually propagate through a dam core, but, under conditions of uniform stress, the fracture will propagate suddenly. Most of their tests results, showed a sudden increase of permeability similar to that of Savvidou's tests (Fig. 3.5). Hydraulic fracturing is most likely when the initial stresses in the core are non-uniform, and low stresses are local. Then fracture will occur locally, before general shear failure and the stress redistribution accompanying it are induced (Vaughan, 1976). As described in Chapter 4 most of the embankments which suffered from hydraulic fracturing did so during initial rapid filling of the reservoirs and the initial concentrated leaks appeared within a few days or even a few hours. These cases imply sudden propagation of cracks probably under undrained conditions. It may be possible that tests conducted by Nobari et al imposed certain restrictions to rapid propagation such as very small heads of water applied very gradually. Vaughan (1976) believed that shear failure precedes hydraulic fracturing while Nobari et al assumed the Mohr envelope was of a special type where the effective minor principal stress can be reduced to a tensile value without shear failure. Propagation

of a fracture across the dam core would depend on the characteristics of the core material and how quickly stress redistribution take place.

Most of the experimental work carried out to study the mechanism of hydraulic fracturing in embankments has been conducted in boreholes in the samples. The differences in mechanism of hydraulic fracturing in boreholes and embankment dams are discussed in Chapter 4. One of the differences that needs stressing is that the laboratory work carried out so far has not been able to simulate stress redistribution that takes place in the core due to increase in seepage pressure during impounding. The experimental studies, inspite of being qualitative, do explain the mechanism of cracking of dams, i.e., fracturing will occur at low stresses or when the stress becomes tensile under drained conditions. But one aspect of cracking which has not been studied in these proposed criteria is cracking related to rapid increase of reservoir water level which may be the cause of initiating and propagating cracks in earth dams. This phenomenon has been the key feature of the present research. Kennard studied fracturing in boreholes under undrained conditions and his theoretical analyses agree very well with the experimental results on normally consolidated samples conducted in the present research. One of the experimental features of tests conducted in stress boxes that needs more careful study is the restraint imposed by the outer boundary on fracturing pressures. Also in the tests conducted with piezometers, the piezometers may not be able to provide sufficient water to propagate the fractures rapidly at their earliest formations. For the flow rate to increase by many orders of magnitude much higher pressures would be required, as in the case of Kennard's tests. Kennard's theoretical expressions for predicting fracturing pressures would not work for overconsolidated soil (i.e. when $A < 0$). Haimson's theory is not applicable to soils, since for practical purposes, tensile strength of soils can be ignored. However, the findings of his experimental work is equally applicable to soils.

The most comprehensive study of mechanism of hydraulic fracturing in earth dams has been outlined by Vaughan (1976). He described cracks formed by either drained or undrained failure on reservoir filling. According to Vaughan, the formation of tensile cracks by undrained failure is unlikely, as the rate of impounding in relation to the permeability of the core will ensure that there is a general increase in seepage pressure in the core before cracking can occur. However, a crack formed by drained hydraulic fracturing may well propagate rapidly by undrained fracture. According to Vaughan,

drained fracture is only possible if the average total stress before impounding is less than the eventual seepage pressure. The effects of water load and of swelling are likely to increase the average total stress and so prevent cracking. At a slow rate of raising the reservoir level, the water entering any initial cracks may cause the cracks to close by swelling or collapse and self healing of the soil in the crack walls. According to Vaughan, hydraulic fracturing is much more likely if low stresses exist in a zone of small extent.

To conclude it may be said that no existing theory adequately explains cracking and hydraulic fracture observed in laboratory test. In many of the laboratory tests water pressures were applied slowly, or at some unspecified rate, so that the soil was at least partly drained. In some of the laboratory tests the boundary conditions on the samples were not precisely defined and insufficient water was available to propagate and maintain a newly formed crack. Many of the proposed theories depend on major assumptions and some do not distinguish between drained and undrained soil parameters.

CHAPTER 4

HYDRAULIC FRACTURE - LITERATURE REVIEW

4.1 Introduction

Hydraulic fracturing may be described as the conditions leading to the fracture and its propagation in a soil or rock mass when the fluid pressures are higher than the stresses within the soil or rock mass.

Although the effect of hydraulic fracturing was recognised and appreciated in many other fields, (e.g. petroleum industry), its importance for geotechnical problems especially in the area of earth dam design has only gained recognition in the last 20 years, particularly after the Hyttejuvet Dam disaster. Löfquist (1957) was probably the first to predict hydraulic fracturing in embankment dams. Since about 1970 it has been appreciated that during drilling, equipment that uses water can produce high water pressures at the bottom of the borehole, thus causing fracture of the adjacent soil mass. There have been numerous examples of water loss when drilling in the impervious cores of dams (Sherard 1973).

It is thus, only about 20 years ago that the dam engineers started speculating that in addition to the open cracks which appear on the dam crest, leaks may develop through the impervious earth dam by the process of hydraulic fracturing. However, the possibility of cracks formed in earth dams due to hydraulic fracturing is a controversial issue. The main point of the controversy is that it is difficult to prove or disprove conclusively that it has been the single main cause of failure. Cracks formed due to hydraulic fracturing are difficult to verify by visual inspection since they are inside the dam and are only open as long as the water pressure acts along them and also erosion and breaching usually destroys any evidence that might have existed.

This chapter deals with case histories of selected earth dams which have been suspected to have suffered erosion problems as a result of hydraulic fracture. The dams discussed here are both old and recent, homogeneous and zoned. Details of these dams and the events leading to their collapse are given elsewhere; only the key features and key

observations relevant to the present work is presented here. An assessment has been made on the evidence of hydraulic fracturing in these dams. Hydraulic fracturing in boreholes is also dealt in this chapter and compared with that in embankment dams.

4.2 Case Histories of Embankment Dams Which Have Experienced Problems Attributed to Hydraulic Fracture.

4.2.1 Dale Dyke Dam

Details of the original Dale Dyke Dam and its collapse have been reported and discussed by Binnie (1978 and 1981). The cross-section of the dam is shown in Fig. 4.1. Above the ground, the narrow vertical core of the puddle clay was supported by a fill consisting of poorly compacted and highly permeable stony shale. The dam was founded on relatively incompressible rock. Reservoir filling commenced in June 1863 and proceeded intermittently. There is no information regarding the rate of filling, however, in the final stages, the reservoir could have filled rapidly following a fortnight of heavy rainfall. On March 1864, the day before the collapse, the water level was 0.7m below the crest of the weir. The only detectable damage noticed just before the sudden collapse was a horizontal crack along the downstream slope near the crest.

In the reassessment of the failure, Binnie (1978) uncovered evidence, not mentioned at any inquiry, of a large spring of water issuing from the foot of the embankment where the breach and occurred and suggested that erosion had probably been going on a long time without being noticed. He also uncovered evidence, not mentioned at the inquest, of a depression in the pitching inside the bank and a whirlpool seen several weeks before the failure about the place where the hole was first blown through. The surface of the water was about 3 or 3.7m below the level of the weir. In 1981, Binnie found evidence of a powerful spring having been encountered during excavation of the cut-off trench and presence of two near vertical steps which had been left in the longitudinal section of the cut-off trench. Binnie (1981) concluded that both the presence of this powerful spring and these near vertical steps were the basic cause of the accident. Differential settlement of the puddle clay across these discontinuities could have produced sufficient reduction of total stress to permit hydraulic fracture.

Binnie postulated that hydraulic fracturing may have been the main contributing factor resulting in the collapse of the dam seems to be the most plausible mechanism. However, another mechanism not considered by Binnie or during discussion to his paper of 1978, is the settlement of the upstream shell when it became wetted for the first time. The upstream stony shale founded on relatively incompressible foundation was poorly compacted and therefore liable to settlement during impounding. The core being wetter probably did not follow the downward movement of the upstream fill at the same time thus leading to a horizontal crack along the upstream face through which some of the reservoir water could pour down. This may explain the depression in the pitching inside the bank and a whirlpool seen several weeks before the failure. No visible sign of any sinking of the crest of the dam was observed prior to the collapse, which may explain its separation from the upstream fill. Water flowing through this crack could have undermined the puddle clay core which combined with a fracture in the core initiated probably by hydraulic fracturing could have enabled the water to flow through the downstream shell. On wetting up with this flow of water and also from the heavy rainfall, the downstream shell also being poorly compacted, could have settled. This downward movement combined with the still upright core could have resulted in the downstream horizontal crack seen prior to the failure. The sequence of failure of the dam, after the above initial mechanism had taken place, probably followed that described by Binnie (1978). Such initial upstream settlement and movement during initial impounding leading to horizontal cracks have been noticed at other dams, for example, at Portland Dam in the U.S.A. (Leonards and Narain, 1963) and at El Isiro Dam in Venezuela (Sherard, 1973).

Finally, it is inconceivable that the powerful spring encountered during the excavation of the cut off trench, which according to Binnie (1981) was one of the main factors attributing to the collapse of the dam, would have been left unattended or unplugged. If it had been so, then the dam would have failed much earlier as more water from the reservoir at a higher pressure would have been available to the spring through a series of cracks or fissures in the bedrock.

4.2.2 Oklahoma and Mississippi Failures

Between 1950's and 1960's, about 1500 and 400 embankment dams were built in Oklahoma and Mississippi respectively. These were all low homogenous clay dams without vertical

chimney drains and were well constructed. Of these, eleven of the Oklahoma and three of the Mississippi dams failed by internal erosion. These dams and their failures have been described by Sherard et al (1972, a).

In the analysis of the cause of the failures, it was observed that essentially all the failures, occurred immediately after the initial rapid reservoir filling, and the initial leak appeared downstream within a few hours or a day or two after the reservoir filled. In almost all the cases the breach occurred at a point along the dam length where the maximum differential settlement was expected. Sherard et al (1972, a) suggested that it was probably that the leaks developed as a result of hydraulic fracturing. While differential settlement was frequently suspected as a cause of failure, in not one of the cases were any differential settlement cracks observed in the dams, either prior to or after failure. The low internal embankment stresses were caused as a result of differential settlement of the foundation or drying and shrinkage of the embankment during or after construction or combination of both. Sherard et al (1972, b) used the results of finite element analyses to support their hydraulic fracturing hypothesis. The main difference between the failed and other similar dams which did not fail was the fact that the failed dams were constructed in areas of highly dispersive clays.

The low dams of Oklahoma and Mississippi are excellent examples of internal erosion of dams constructed of dispersive clays. As discussed in Chapter 5, these clays go spontaneously in suspension leading to a catastrophic failure in relatively short time. The key observations common to these dams were the initial rapid rise of the reservoir, the sudden appearance of the initial leak and were constructed of dispersive clays. Besides the mechanism of hydraulic fracturing as suggested by Sherard et al (1972), failures due to saturation collapse have been suggested by others (Ingles, 1972, a; Mesri and Ali, 1988). However, Sherard et al (1972, a) argued that such a theory was not probably in the Oklahoma and Mississippi dams since they were well constructed. Such a collapse mechanism probably is the main contributing factor in the failure of dams compacted dry of optimum. There are numerous examples of such dams suffering from internal erosion (Patterson and Iverson, 1953; Aitchison and Wood, 1965). However, it is possible for various reasons for a drier region to exist in a well constructed dam in which a

saturation collapse may create the initial crack and then be extended by hydraulic fracturing through the core. Thus, hydraulic fracture or saturation collapse mechanism acting separately or even together may be responsible for the failure of these dams.

4.2.3 Wister Dam

Wister Dam, in Oklahoma, was essentially a homogenous dam consisting of silty clay as shown in Fig 4.2. It was a well constructed dam with the average compaction water content close to standard Proctor Optimum. The river was allowed to flow in its original channel, which cut diagonally across the dam axis, until the majority of the dam was completed and then a closure section was built as shown in Fig 4.3. The details of the dam have been described by Sherard (1973).

In January 1949, a heavy rainstorm caused the reservoir to rise rapidly for the first time. Seepage carrying eroded material was observed on the downstream slope. When the reservoir level had dropped about 4m., several erosion tunnels of about 0.6m in diameter, as shown in Fig. 4.4, were observed entering the upstream slope. Studies with dyes showed that the average leakage water travelled a distance of about 225 m through the dam in about 30 minutes. The leak had travelled through the closure section.

Studies carried after the failure were inconclusive, although it was generally agreed that the initial leak must have been travelling in a different settlement crack, even though the measured foundation settlement was the order of 25 cm, and no cracks were seen. Sherard (1986) strongly believed that "there can be no reasonable doubt that a concentrated leak developed by hydraulic fracturing completely through the dam". He suggested that this must have been caused by arching of the portion of the dam built last in the closure section between the two previously completed embankment sections on both sides of the river.

At Wister Dam, studies with dyes clearly demonstrated the presence of a crack through which the erosion of the dam took place. The crack could have been formed either due to hydraulic fracturing of the "closure section " as suggested by Sherard or by the alternative mechanism discussed in the failure of Oklahoma and Mississippi Dams. The cracks could also be initiated as a consequence of differential settlement even though

insignificant settlement was observed. It must be remembered that the dam was constructed of dispersive silty clay which may behave differently to a non-dispersive soil subjected to similar order of settlement. The experience of the Wister Dam also showed that only a small "excess-pressure" can be responsible for initiating cracks in a dam.

4.2.4 Stockton Creek Dam

Stockton Creek Dam, in central California, was a homogenous dam constructed essentially of clayey sand. The average abutment slopes were not excessively steep but there was a near vertical "step" in the right abutment at about midheight. The cross-section and the longitudinal section looking downstream are shown in Fig 4.5. The dam was well constructed, however, studies made after the failure showed that the average water content of the fill was about 2 to 4% below standard optimum value. It was also found that the material became appreciably more rigid and brittle when compacted dry. The material, however, was not highly erodible. The details of the dam and its problem have been described by Sherard (1973).

The failure occurred when the reservoir filled rapidly for the first time. A last inspection of the dam was made at 8pm and no sign of any distress was noted. But the next morning the dam was found to have breached where it was 12m high near the right abutment at the location of the near vertical "step". The embankment on both sides of the breach were left standing on near vertical slopes.

Sherard (1973) suggested that the most probable cause of failure was internal erosion through a differential settlement crack adjacent to the near vertical "step" in the abutment rock surface, even though no cracks were ever seen. The internal stress transfer caused by differential settlement of the dam, which was very small, must have led the opening of a crack by hydraulic fracturing.

Stockton Creek Dam failed within 12 hours of the last visual inspection when no sign of any distress was noticed. As usual with the most of the failed dams or problem dams experiencing internal erosion, the reservoir rose rapidly. The failure breach was located at a point where there was a near vertical step in the foundation enabling stress transfer and hydraulic fracturing. However, the dam with a low placement moisture content

allowing it to behave more rigid and brittle could be most susceptible to a saturation of collapse mechanism. The experience of the Stockton Creek Dam also showed that the dam does not have to be constructed of highly erodible material to suffer from internal erosion.

4.2.5 Hyttejuvet Dam

Hyttejuvet Dam was an earth core, rockfill dam completed in 1965 in Norway having a cross-section as shown in Fig. 4.6. The details of the dam and the experience with the leak through it have been described by Kjaernsli and Torblaa (1968). The narrow, approximately vertical core was constructed of gravelly, clayey sand (Morainic material) and was placed at water content which generally ranged between 1.0% below and 2.0% above optimum. After the first construction period, the width of the core was considerably reduced in order to enable a more rapid dissipation of pore pressure.

The reservoir was filled rapidly for the first time. Initially only negligible leakage appeared at the downstream toe but a rise in the reservoir level of 2 m produced a dramatic increase in the leakage as shown in Fig. 4.7. The leakage water was observed to be dirty indicating the removal of fines from the core.

Kjaernsli and Torblaa (1968) suggested that the arching between the core and the less compressible gravel fill led to a reduction in total vertical pressure in the core. In areas where the total vertical pressure was smaller than the water pressure exerted by the impounded water, horizontal cracks were opened as a result of hydraulic fracturing of the core.

The leakage of the Hyttejuvet Dam was the first embankment leakage associated with the phenomenon of hydraulic fracturing in embankment dams. The leakage was concentrated in the upper section of the core which was relatively thin. It seems most probable that the most important factor contributing to the cracking was the narrow width and vertical walls of the core which led to arching between the core and the gravel fill. According to Kjaernsli and Torblaa (1968), cracks were initiated by hydraulic fracture which probably did not exist before the reservoir reached the elevation of the low vertical stress. The dam had a markedly asymmetrical longitudinal section. Even though not excessive settlements

were recorded, any settlement along such a section could result in vertical transverse cracks which could be further propagated by reservoir water pressure or indeed eroded by seeping water. The leakage may as well be explained by the normal action of water seeping through the voids in the core. The core was constructed of gravelly clayey sand having a wide grain size distribution. Such a soil is not self filtering and hence susceptible to erosion in which the fines are carried away in the leakage water, leaving behind the coarser particles. From the cross-section of the dam (Fig. 4.6) it can be noticed that the sandy gravel filter provided in the lower section of the core was not provided along its upper half. It is possible that the problem may still have existed even if the filter was extended up to the height of the narrow core. A conventional filter would be inadequate to stop the loss of fines from the core. Although hydraulic fracture is assumed by other dam experts (Vaughan et al 1970 and Sherard, 1973), as the most plausible mechanism of the failure, erosion failure as discussed above should not be discounted. The relatively rapid rate of reservoir filling was probably another significant contributing factor.

4.2.6 Balderhead Dam

Balderhead Dam was a rockfill dam completed in 1965 in England having a cross-section as shown in Fig. 4.8. The details of the dam and the problems associated with internal erosion have been described by Vaughan et al (1970). The narrow vertical core was constructed of boulder clay and was placed at an average moisture content near optimum. The foundation was mainly shale except on the lower slopes of the main valley where substantial thickness of boulder clay was left in place over the shale. The vertical drain at the downstream edge of the core was constructed of crushed rock and had a fairly wide range of gradation.

The reservoir was filled slowly but just before the reservoir became full the seepage flow suddenly increased and then followed on erratic pattern as shown in Fig. 4.9. In the course of investigation depression and sinkholes were discovered. It was found that the settlements had occurred above the sides of the deepest part of the valley where there was a discontinuity in the longitudinal foundation profile. Sink holes and three of the settlements occurred where there was a substantial thickness of boulder clay in the

foundation. No seepage or settlements occurred in the section lying over the shale foundation. Lowering the reservoir showed that there was a critical level below which leakage was greatly reduced.

It was suggested that both arching of the core and longitudinal strains due to differential settlement across foundation discontinuities may have reduced the stresses in the core sufficiently for the reservoir pressure to cause hydraulic fracture. Loss of material was due to the segregation of the coarse part of the eroded material. The downstream filter was apparently not effective in preventing loss of fines through the core.

At Balderhead Dam, much of the erosion damage was found to be near the bottom of the vertical section of the core where the maximum arching would be expected. The presence of a discontinuity and substantial thickness of boulder clay would promote regions of low stress thus making hydraulic fracturing as the most likely mechanism for initiating fractures in the core. Hydraulic fracture is usually enhanced by a rapid reservoir filling since there is a less opportunity for stress redistribution to occur. At Balderhead dam, the reservoir was raised slowly and erosion took place over a period of several months. The fill generally had a high resistance to erosion (Vaughan and Soares, 1982), however, stones in excess of 0.15 m were encountered during remedial works which could have created non-uniform zones susceptible to erosion. The fill was of much higher permeability than the clay core thus allowing the full reservoir pressure to act on the core which could have allowed the seeping water to generate sufficient erosive forces to remove the fines from the core creating and enlarging a channel or channels. Vaughan et al (1970) did not consider that the boulders in the core contributed to the risk of cracking by causing a local stress variation since, according to them, this may not imply fracture right across the core. However, a local crack may enable reservoir water to widen the crack or undermine the fill around the crack by removing the fines. The filter failed to retain the finer particles that reached it thus allowing the internal erosion of the core. From the investigation after the disaster it was not clear why the problem developed. However, it can be suggested that the circumstances which may have contributed to the problem were: the narrow almost vertical core, the presence of a discontinuity and clay in the foundation, the nature of the core material and the ineffectiveness of the filter.

4.2.7 Yard's Creek Upper Reservoir Dam

Yard's Creed Upper Reservoir Dam was a long rockfill dam completed in 1965 in New Jersey having a cross-section as shown in Fig.4.10. The details of the dam and the problem associated with internal erosion has been described in detail by Sherard (1973). The central narrow vertical core was constructed of gravelly clayey sand (glacial marine) and was founded on hard quartzite bedrock.

During the first rapid reservoir filling very dirty leakage emerged abruptly at the downstream toe of the dam. The surface of the rock foundation under the core over this length of the dam was irregular with 1 to 2 m high near vertical steps running transversely across the core. Over most of the rest of the length of the dam, the bedrock surface under the core was more uniform and smooth. The leakage alternately ran dirty and clear.

During the investigation "wet seams" were observed in test pits put down in the core down to the bedrock foundation in locations where there was no leakage emerging at the toe of the dam. The core exposed in the walls of the test pits generally appeared uniformly well compacted, homogenous and highly impervious. However, there were occasionally thin horizontal layers, 1-2 m apart, which were much softer with water content much higher than the compaction water content. These layers were similar in appearance to the rest of the embankment except for soft and wet consistency and appeared impervious with no evidence of any erosion having passed through. The walls of a test pit put down at the location where loss of drilling water (during exploratory boring) was observed, there was a thin horizontal layer containing small "pipes" which showed evidence of a concentrated leak having passed through. Directly above and below this layer the core material was dense and impervious.

At the time of the failure, no definite conclusion was reached regarding the cause of the erosion. Sherard (1973) suggested the problem was caused by one or both of the following:

- i) the difficulty of obtaining a satisfactory seal between the narrow core and the irregular rock surface;

- ii) arching of the core between the upstream and downstream filters or from differential settlement adjacent to steps in the rock surface which caused horizontal cracks in the core, which may have been opened partially by hydraulic fracturing.

Investigators at that time could not explain the existence of the "wet-seams" but Sherard (1986) believes that they were caused by hydraulic fracturing. Finally, Sherard (1973) suggested the inability of the fine filter to retain individual clay-sized particles in suspension in water.

Yard's Creek Upper Reservoir Dam is another example of an embankment dam with a central vertical narrow core constructed of widely graded material similar to those at Hyttejuvet and Balderhead Dams which suffered from internal erosion. The presence of the narrow core and the irregular rock surface enhance hydraulic fracturing and therefore Sherard's (1973) suggestion to the cause of the fracture seems very probable. The leakage problem of this dam could also be explained due to the action of the seeping water eroding the fines from the widely graded core material similar to those discussed in the cause of failures of both Hyttejuvet and Balderhead Dams. The main conclusion reached in this case history is that which ever mechanism may have been the cause of the problem, it was the characteristic of the core and the inadequacy of the filter to retain clay-size particles that enabled piping to occur.

4.2.8 Teton Dam

Teton Dam was a central core zoned earth fill dam completed in 1975 in Texas having a cross-section as shown in Fig. 4.11. The details of the dam and its failure has been reported and discussed by Independent Panel (1976), Penman (1977), and Seed and Duncan (1981). The wide core was constructed of fine, wind blown silt and placed at about 1.3% dry of optimum. The main features which probably had a major influence on the events leading to its failure were: the foundation rock of volcanic origin which contained numerous interconnecting open joints and voids, the provision of key trenches, in the upper part of the abutments and the lack of adequate protection of the fill material against internal erosion. The key trenches with its sides, made as steep as possible to minimise excavation, were backfilled with the core material as shown in Fig 4.12. Despite

of being a modern dam, no instrumentation other than settlement monuments were provided to monitor the dam's performance.

Initially it was intended to fill the reservoir at a slower rate but in the final stages the reservoir was filling at much higher rate. An inspection made a day prior to the failure showed no unusual conditions. On the day of the failure, a small trickle of muddy water was observed in the morning which, within 4 hours began to increase rapidly emerging from an eroded tunnel. The tunnel became an erosion gully developing headward up the embankment, and within the next hour, a complete failure occurred. It took only 5 hours from the time of the first observed seepage in the immediate proximity of the dam until the dam failed.

Following the failure the Independent Panel (1976) after an intense study in the cause of the failure suggested two possible failure mechanisms: one was the flow of water against the highly erodible and key trench filling, through joints in the unsealed rock beneath the grout cap and the consequent development of an erosion tunnel across the base of the key trench fill. The second was erosion through cracks caused by the differential settlement or hydraulic fracturing of the material used in the key trench. The rigidity of the rock walls in the key trench combined with their steep slopes, caused arching over the key trench with a corresponding reduction in stresses on the key trench fill. A finite element analysis was carried out which confirmed the possibility of this arching and hence likelihood of hydraulic fracturing.

The recent spectacular failure of Teton Dam - a modern dam designed and constructed by competent engineers have been extensively investigated, reported and discussed (for example, Independent Panel, 1976). No instruments, other than settlement monuments, were provided and therefore the assessment of the behaviour of the dam during impounding and during the erosion leading to the failure depended solely on the visual inspection. The leakage may have started much earlier than reported and was not or could not be observed due to very permeable bedrock. Tests on aeolian silt had showed that the material was brittle and highly erodible. Such soils, especially when compacted dry of optimum as in the case of Teton Dam, have a tendency to collapse on wetting up. Such a collapse may have initiated the initial crack enabling the reservoir water to penetrate and further the crack by hydraulic fracture. The relatively rapid rate of reservoir filling

probably accelerated this collapse mechanism. However, the Independent Panel (1976), concluded that the increased rate of filling had no demonstrable influence on the failure. In spite of the detailed investigation carried during design showing the open joint system in the rock and the erodibility nature of the core material, no transition filters were provided to protect the silt. This probably was the major factor contributing to the failure. Had transition filters been provided between the core and the sand and gravel and between the key trench fill and the abutment rock walls, the failure could have been avoided by the filter trapping any silt removed by water. The steep vertical walls of the key trench most certainly was responsible for low stresses leading to hydraulic fracture. From the various investigations conducted to study the failure including the saturation collapse mechanism, it is apparent that a number of possible mechanism are possible. No single mechanism can prove the failure with any certainty and hence it may be concluded that a combination of these mechanism may have attributed to the failure of the Teton Dam. One of the most important observations made during the collapse was the speed at which the dam failed. It took only 5 hours from the time of the first observed seepage in the immediate proximity of the dam until the dam failed. This implies that the initial crack, produced by any one of the mechanism, was propagated through the dam at a very rapid rate.

4.3 Conclusion from Evidence of Hydraulic Fracturing in Embankment Dams Studied

In the case histories studied here, or in any embankment dam associated with hydraulic fracturing, it is difficult to know whether a narrow crack existed before the reservoir was filled or whether the pressure of the reservoir had an important part in the crack development. The possibility of low stresses due to, for example, either geometry of the core or the foundation is feasible. Steps or irregularities in the rock foundations can also allow low stresses to develop locally. In such cases, the possibility of low stresses makes it much more probable that the cracks were initiated by the pressure of the reservoir water. Cracks can also be formed in dams with narrow vertical central cores of compressible impervious material or even formed during construction shut down. These cracks, which may be very narrow, could easily be opened and propagated further by the reservoir water pressure. Besides hydraulic fracture other mechanisms, as discussed earlier, can also be responsible for concentrated leaks in embankment dams. Thus it can be difficult to prove or disprove conclusively that any single mechanism had been the main

cause of failure and moreover any evidence that might have existed is usually destroyed by the breach and the erosion. Although the case histories provide various hypotheses for the failures but not any conclusive evidence in support of hydraulic fracturing, a number of observations can be made from them. In all cases except that at Balderhead Dam, the reservoir level rose rapidly. One of the most important observations made here is the sudden failure of the embankment dam, for example, as the case of Teton and Stockton Creek Dams. These dams failed within hours of the last inspection when no sign of any concern of distress was noted. This action suggests cracking under "undrained" conditions. Hence it is relevant to consider fracturing as an undrained loading phenomenon in many instances. The cores of most of the dams were compacted at water contents close to optimum except at Stockton Creek and Teton Dams where the cores were compacted dry of optimum. Thus there does not appear to be any clear indication from the case histories studies that cores compacted on the wet side of the optimum are much less susceptible to cracking and therefore less likely to erosion. Cracking and internal erosion can develop in embankment dams constructed of almost all types of soils. Fracturing leading to internal erosion can be initiated by only small heads of reservoir water. Presence of a local discontinuity in foundation, vertical steps or irregular rock surface are detrimental since they may not be subjected to a general stress redistribution and hence can create regions of low stresses thus allowing cracking. Four case histories have shown that the troubled dams had narrow vertical cores. Though there should be no reason for not adopting such cores, the possible problem associated with such cores could be difficulty of obtaining a good seal between the core and the rock foundation, and the nature of the core material. Such materials may be susceptible to erosion accompanied by segregation of the eroded material within the crack and hence are not self filtering. Homogenous dams without internal drains or filters to control erosion are not safe. Hydraulic fracturing can occur in dams not experiencing large settlements and can occur in dams of all sizes, ranging from low to high central core dams.

Small leaks would be expected to develop fairly commonly through embankment dams for various reasons and the reasons why there are not many cases of erosion failures is the presence of effective filters into which the leaks discharge. Cracking is not itself dangerous. If progressive erosion does not develop too quickly, the crack may seal itself or the effective filter may deter loss of fines. Thus it seems that the main emphasis should be directed towards the downstream filter as being the main line of the defense.

To summarise, it can be said that although internal cracks due to hydraulic fracturing are theoretically possible, it is difficult to prove the process. Open cracks observed after the drawdown (for example, Wister Dam), grout filled cracks or dirty leaks do show the presence of cracks but it does not mean that they were initiated by hydraulic fracturing.

4.4 Fluid Losses from Boreholes in Embankment Dams

As mentioned in the introduction (4.1) drilling equipment that uses water can produce high water pressure at the bottom of the borehole which may exceed the earth pressure adjacent to the borehole and may cause a fracture of the adjacent soil mass. Total or partial loss of drilling fluid has occurred in boreholes indicating that the fluid has escaped into the embankment through a crack.

During investigation into the leakage of Hyttejuvet and Balderhead Dams, boreholes put down into the cores from the crest of the dams were found to lose their water when they reached a certain depth. Kjaernsli and Torblaa (1968) were aware that the fractures could be caused by high water pressures in the boreholes and hence did not take these tests as evidence of cracks by reservoir water in the core of Hyttejuvet Dam. Vaughan (1971), during the exploratory work at the Balderhead Dam, found that water losses occurred in the areas where cracking was deduced to have taken place from the results of cored holes and from the settlement observations. Water losses were also observed in boreholes adjacent to damaged areas where other evidence suggested that the holes were in intact and undamaged fill. The water pressures during drilling were approximately 2.4 m greater than those which could have been applied to the core by the full reservoir. From this, Vaughan concluded that water losses were occurring due to hydraulic fracture around the boreholes.

At Shek Pik Dam (Carlyle, 1965), drilling water was lost in some of the grout holes put down through the cores to grout the in situ weathered rock beneath. On investigation with trial pits, cracks were found which had been filled with grout. The cause of the water losses in the boreholes and the grout filled cracks could not be explained at the time. Carlyle (1965) concluded that although the total settlements of the foundation and the embankment were not great, cracking resulted from foundation settlement which were locally severe during construction. Even though the rolled earth core was placed at about

2.5% wet of optimum, measured pore pressures in all zones during construction were very low or zero. This clearly suggests low total stresses in the core thus enhancing hydraulic fracturing during boring.

Sherard (1973) gave several examples where holes put down in the core of the dams experienced loss of drilling fluid. At El Isiro Dam, grout filled cracks were encountered in the walls of most of the exploratory test pits. At Djatiluhur Dam, in almost all of the borings drilling water was lost at one or more elevations. Water losses occurred only when the elevation of water in boreholes was above a certain value. Water pressures recorded in the standpipes installed in several of the boreholes where water losses were encountered showed a pressure head which was about 20 metres higher than the level of the reservoir at the time. From these studies it was concluded that the cracks were probably being opened in the core by the water pressure in the boreholes. These cracks could have been new fractures or cracks which were initially closed. At Yard's Creek Upper Reservoir Dam, water was lost nearly in all the exploratory borings put down through the core in the area of dirty leakage.

4.5 Comparison of Hydraulic Fracturing in Embankment Dam Cores and Boreholes

From the previous section it is apparent that fluid losses in borings not only indicate fractures by reservoir water but also can create new fractures even where there was no likelihood of fractures by reservoir water.

Fracturing pressures as deduced from borings can vary with the method of test (Vaughan, 1971). Vaughan found that hydraulic fracturing occurred at higher pressure when the holes were made by mud circulation drilling than those observed in the water flush tests. He also observed higher fracturing pressure on tests conducted on borehole piezometers with sand pockets placed in holes bored dry with a clay cutter. From his field tests, Vaughan concluded that hydraulic fracturing was occurring around the water flush holes at pressures comparable to the reservoir pressure which it was thought caused the original cracking of the core. Relatively low fracturing pressure in the water flush tests were probably due to very irregular walls and imperfections in the walls which may enable the cracks to propagate at low pressure.

Sherard (1986) reported that there is some speculation among the dam engineers, that the upstream face of the impervious embankment section can be considered as a smooth, uniformly impervious wall, in which there is no opportunity for water to penetrate. However, this is not strictly a correct assumption. In an embankment, a discontinuity can be due to many factors such as a poorly compacted layer, zones between layers of different rigidity or material properties and shear planes caused by heavy earth moving plant and compaction machinery. Thus, in order to evaluate fracturing pressures in embankment dams from borehole tests, fracturing tests need to be carried out in boreholes which have very irregular walls similar to those used in Vaughan's field tests. In the present research, imperfections to the walls of the holes bored in samples to be fractured were created by compacting a pocket of sand in it (see Appendix A). It has been suggested that the seepage pressures developed around a borehole are only local and they will not induce stress redistribution in a core in the same way as a general increase in seepage pressure due to impounding (Vaughan, 1976). Although this statement is correct, in a discontinuity low stresses may still prevail and the seepage pressure may as well be local which may reduce one of the effective stresses around it to zero thus creating a fracture. This fracture which initially may have started under drained conditions (due to small water penetration) could be propagated rapidly under undrained conditions. This phenomenon may explain the speed and the rate at which some of the dams studied here failed. Furthermore, as seen in Section 4.2, hydraulic fracturing is a localised phenomenon initiated in regions of low stresses. However, relying fully upon the evidence of cracks during borings can be misleading. Loss of water from a borehole indicates lower total stresses with respect to the reservoir water pressure applied at that instant and point and such loss before impounding should be inferred as the potential for fracturing and not the likelihood of it. Stress redistribution during impounding may increase the stresses around a discontinuity and prevent fracturing occurring. The other main difference, according to Vaughan (1976), is swelling of the core during impounding which would increase the average total stress and hence inhibit fracturing. This difference will not apply to soils which have a low swelling characteristics and hence may be prone to greater risk of hydraulic fracture.

In order to use the results from borehole fracture tests for evaluating the possibility of hydraulic fracture due to reservoir water, due considerations should be given to the difference in boundary conditions and the method of testing. Tests should be carried out

before, during and after impounding which would give indications of stress changes due to impounding. Close-up pressure (the pressure at which there is a sudden reduction in flow after fracturing or at which the crack closes) may furnish a more simple and practical way of monitoring stress changes in dam cores than fracture tests (Vaughan, 1971).

CHAPTER 5

INTERNAL EROSION OF CLAY IN CORES OF EMBANKMENT DAMS

LITERATURE REVIEW

5.1 Introduction

Recent studies of embankment dams failures have shown that a large number had problems due to seepage, conduit leakage, internal erosion and hydraulic fracture (Middlebrooks, 1953; Penman, 1980 and 1986). Failure by internal erosion is much more dangerous because it can occur suddenly, with a full reservoir. It is the most serious current geotechnical problem relating to embankment dams (Penman, 1986). Numerous cases of near failure and total failure of dams, as a result of internal erosion, have been investigated and reported in detail in the literature (for example, Sherard, 1973 and Vaughan et al, 1970); some of these have been discussed in Chapter 4.

Internal erosion in dams may be classified into two types: one that occurs in granular soils and the other that occurs in clayey soils. Erosion in granular soils may be termed as "mechanical erosion" to distinguish from "chemical erosion" in clayey soils. Mechanical erosion implies erosion of granular material under a critical hydraulic gradient. In chemical erosion (here the word "chemical" is used in a broad sense) the erosion is controlled by variables such as the mineralogy and chemistry of the clay and the dissolved salts in the soil pore water and in the eroding water. Most of the research and studies involving internal erosion of dams have been directed towards erosion of clayey soils called dispersive soils. The terms "dispersive" was defined in chapter 2 and will be further elaborated here. Erosion of a crack involves both the loss of material from its sides and the transport of eroded material through it. This chapter deals with the recognition of dispersive clays and to the tests used to identify them. An assessment has been made on the reliability of these tests. Transport of the eroded material is not considered here.

5.2 Dispersive Clays

Although clays are generally considered to have a fairly high resistance to erosion, it has long been noticed that there is a great difference between erodibility of different clays in nature. These erodible clays which cannot be differentiated from ordinary resistant clays by routine civil engineering tests erode rapidly in slow moving or even quiet water (Sherard et al, 1972, b). Existence of such clays used in earth dams was first generally recognised by the Australian engineers after investigations of eroded clay dams in the early 1960's. These dams were mostly homogenous, without filters or internal drains, and in many cases were built without moisture control and compacted only by the hauling plant. Because of the climatic conditions they were usually constructed dry of the optimum, (Aitchison and Wood, 1965). Earth dams constructed according to good engineering practice, but without such erodible soils, also showed similar internal erosion problems, as shown by the failure of Flagstaff Gully Dam in Tasmania (Phillips, 1976). Sherard et al (1972,a) also reported erosion problems of some of the earth dams built in Oklahoma and Mississippi, (see Chapter 4). Similar problems with embankment dams have been observed in other parts of the world; for example, in Israel (Kassiff and Henkin, 1967) and in Thailand (Cole et al, 1976) etc. Such clays have been called "dispersive" because of their ability to pass spontaneously into suspension ("disperse") in water.

Deposits of dispersive clays have been found in so many parts of the world that it could be suspected that they could be found anywhere. Embankment dams experiencing internal erosion have been reported in Western Canada (Patterson and Iverson, 1953), in New Zealand (Matahina Dam; Sherard, 1973), in England (Balderhead Dam; Vaughan et al, 1970) and in Norway (Hyttejuvet Dam; Kjaernsli and Torblaa, 1968). But this does not imply that these dams were constructed of dispersive soils.

5.3 Postulated Mechanism of Internal Erosion in Dispersive Clays

Aitchison et al (1963) were one of the first to suggest that the cause of internal erosion in earth dams could involve dispersion of clay. Sherard et al (1972,b), summarising the Australian research reported that "dispersive" or "deflocculation" occurs when the repulsive forces (electrical surface forces) between the individual clay particles exceed the attractive (Van der Waals) forces so that when the clay mass is in contact with water, individual clay

particles are progressively detached from the surface and go into suspension. If the water is flowing, the dispersed clay particles are carried away. They reported that the main property of the clay governing the susceptibility to erosion is the ratio of dissolved sodium cations in the pore water to the other main basic cations, calcium and magnesium. Sodium acts to increase the thickness of the diffused double layer surrounding individual clay particles and hence to decrease the attractive forces between the particles, making it easier for individual particles to be detached from the mass. They also reported that a second main factor in the susceptibility of the clay mass to erosion is the total content of dissolved salts in the eroding water. The lower the content of dissolved salts in the water, the greater is the susceptibility of clay to erosion. They also concluded that there was no good relationship between the piping potential and the results of ordinary index properties tests for clay. Soils with high contents of exchangeable sodium range from cohesionless silts to clays of high plasticity. The role of sodium in the process of dispersion and flocculation of soils has been studied and verified by several other researches (for example, presented in ASTM 623, 1976; Heede, 1971; Arulanandan et al, 1975).

It has been reported that besides the role of exchangeable sodium percentage and salt concentration of the eroding fluid, pH, initial moisture content and type of clay particles can effect the spontaneous dispersion of the soil (Holmgren and Flanagan, 1976). Certain anions, such as bicarbonate have been known to have increased the dispersive behaviour of a soil (Ingles, 1972; McDonald et al, 1981). The role of the total contents of dissolved salts in the reservoir water on the dispersion of clay soils was substantiated by case histories presented by Aitchison and Wood (1965).

5.4 Laboratory Tests for Identifying Dispersive Soils

Due to the potential loss to life and property resulting from erosion failure of embankment dams constructed of dispersive and erodible soils there has been a great interest in developing reliable tests to identify such soils. The various methods used to identify dispersive soils can be categorised as: (a) indirect or physico-chemical tests where the clay mineralogy and its role on influencing dispersability is analysed and compared to selected parameters, (b) direct or physical tests where the physical performance of a sample with water is observed and compared to selected parameters.

These selected parameters have been derived from the observations of case histories. Indirect or physico-chemical tests include the soil conservation service dispersion and the chemical tests. Direct or physical tests include the pinhole tests, the crumb test, the rotating cylinder test and the soil security test. These tests are described below:

5.4.1 The Soil Conservation Service (SCS) Dispersion Test

In this test, the content of 5 micron size particles is measured in two ways; firstly using the standard hydrometer test in which dispersant and mechanical stirring are used. Secondly a parallel test is made in which dispersant and mechanical stirring are omitted. The percent dispersion is defined as follows:

$$\text{Percent Dispersion} = \frac{\% \text{ finer than } 0.005 \text{ mm without dispersant} \times 100}{\% \text{ finer than } 0.005 \text{ mm with dispersant}}$$

According to SCS, percent dispersion greater than 50% indicates a highly dispersive soil. over 30% indicates a moderately dispersive soil and less than 15% indicates non-dispersive soil. Decker and Dunnigan (1976) stated that 85% of soils which show 30% or more dispersion are subject to dispersive erosion.

The SCS dispersion test is the oldest test that has been used for identifying dispersive soils. However, it does not always give a consistently good measure of the dispersibility and is not always reproducible in the same laboratory. Minor differences in the quality of water and air drying of the sample can affect the results, (Decker and Dunnigan, 1976). The test was found to be less reliable when low values of dispersion were indicated (Forsythe, 1976). The test does not take into consideration the interaction of the pore and eroding fluid composition. This may be improved to a certain extent by carrying out an additional hydrometer test using soil-reservoir water suspension which is not stirred. Such studies were carried out by Coumoulos (1976).

5.4.2 Chemical Tests

These tests have been described in greater details by Sherard et al (1972,b). Briefly, they described two types of test, one on the pore water and the other on the clay itself to determine the relative amount of sodium cations present in the clay. They suggested that

for the purposes of evaluating dispersive clay it was sufficient to test the pore water extract.

The saturation extract is analysed to determine the amounts of the four main metallic cations in solutions (calcium, magnesium, sodium and potassium). Both the total dissolved salts and the percentage sodium in saturation extract are defined below:

$$\text{Total dissolved salts in saturation extract} = \text{Ca} + \text{Mg} + \text{Na} + \text{K} \quad (5.1)$$

$$\text{Percentage Sodium in saturation extract} = \frac{\text{Na}}{\text{Ca} + \text{Mg} + \text{Na} + \text{K}} \times 100 \quad (5.2)$$

The sodium absorption ration (SAR) is defined by:

$$\text{SAR} = \frac{\text{Na}}{\frac{\sqrt{\text{Ca} + \text{Mg}}}{2}} \quad (5.3)$$

Sherard et al (1976,b) produced a relationship between these parameters and dispersibility based on pinhole tests and experience with erosion, as shown in Fig 5.1.

The chemical tests can fail to identify certain types of clay which may be susceptible to erosion in the core of an embankment dam. These tests exhibited poor overall correlation with the pinhole test from a dam site in Oklahoma (Craft and Acciardi, 1984). Craft and Acciardi believed that one of the reasons for this lack of agreement may be that the saturation extract does not contain all the ions responsible for dispersion. Air drying can also affect the test results by reducing sodium percent (Francq and Post, 1976). The chemical test results on samples from Washington Country, Stockton Creek, Balderhead, Hyttejuvet and Hill's Creek Dams failed to classify them as erodible or dispersive soils, (Sherard et al, 1972 b). All these dams had erosion problems.

5.4.3 Pinhole Erosion Test

Essentially the test consists of punching a 1.00 mm diameter hole through a compacted sample and passing a flow of distilled water through the hole under controlled head

conditions. The rate of flow of water is measured and its colour and sediment noted. For dispersive clays, the water becomes coloured and the hole rapidly erodes. For non-dispersive clays, the water is clear and there is no erosion (Sherard et al, 1976 a).

The Pinhole test is the most widely used test for identifying dispersive clays. However, factors such as the initial state of the sample (e.g. drying and rewetting) can affect the test results (Sherard et al, 1976 a; Schaffer, 1977; Francq and Post, 1976). The test can also fail to identify high sodium clays as dispersive (Francq and Post, 1976; Coumoulos, 1976). One of the drawbacks of the test may be the remoulded and disturbed conditions of the soil around the hole during its formation. Pore pressures may be increased around the hole thereby weakening the surrounding soil and the hole may be not very smooth thus enabling the soil to be removed by the flowing water. The test may not be sensitive to swelling soils since the hole dimensions may be much reduced leading to an erodible soil being classified as non-erodible.

5.4.4 Crumb Test

This test is performed by dropping a small, moist (at natural moisture content) crumb of soil into a beaker of distilled water or 0.001N sodium hydroxide and observing visually the behaviour. If soils are dispersed, a colloidal cloud develops around the periphery of the crumb. Sherard et al (1976, b) developed a dispersibility rating system ranging from 1 to 4 for this test with 1 designating non-dispersive and 4, severely dispersive.

The Crumb test has been widely used as a quick field identification of dispersion potential. However, the test can fail to correctly identify dispersive clays (Forsythe, 1976). Factors such as initial moisture content can also affect the test results (Holmgren and Flanagan, 1976). It is worth pointing out that the comparison is usually made with the results of the pinhole tests. This comparison may not be a realistic approach since no single test gives a definite and correct identification.

5.4.5. Rotating Cylinder

The Rotating Cylinder test presents an attempt to use external erosion test results for predicating internal erosion in clay cores (Maschi et al, 1965; Sargunam et al, 1973;

Arulanandan et al, 1975; Arulanandan and Perry, 1983). Arulanandan and Perry (1983) stated that the critical shear stress, τ_c - a measure of erosion resistance, may be defined as the value of the stress for zero sediment discharge that would be obtained by extrapolating a graph of observed erosion rate versus shear stress as shown in Fig. 5.2. According to them, τ_c is dependent on the factors involved in the mechanism of soil erosion and hence can be used as a fundamental parameter to classify erodibility characteristics. Values of critical shear stress on soil samples can be measured directly using a rotating cylinder, briefly described below.

The apparatus is shown diagrammatically in Fig. 5.3 and the test has been described in a greater detail by Arulanandan et al (1975). Essentially, the test consists of imparting a shear stress to the surface of a saturated soil sample by the rotation of the fluid. The erosion loss is measured at each rpm, and the cumulative losses at each rpm are determined as a function of time. The intercept of the applied shear stress axis gives the critical shear stress. Arulanandan and Perry (1983) tentatively proposed three categories for the classification of core material with respect to their erosion resistance. Using this concept and method they correctly classified the core materials from Washington County, Stockton Creek, Balderhead, Hyttejuvet and Hill's Creek Dam as dispersive or erodible soils (as mentioned earlier, all these dams had erosion problems and could not be identified as such by the chemical tests).

The Rotating Cylinder method considered by Arulanandan and Perry to be an improvement over the existing tests, is an attempt to use external erosion results for predicting internal erosion in clay cores. This may not be a realistic approach since internal erosion may be influenced by internal swelling of the clay which may close the cracks and reduce permeability thereby avoid loss of colloidal particles. In open channels there is a threshold water velocity below which no erosion occurs. Whether such a threshold operates in a crack is unknown (Vaughan, 1983).

5.4.6 Soil Security (Water Retention) Test

The test described by Tadanier and Ingles (1985) is based on water retention properties under given compaction conditions. The test involves filling a central hole in a compacted soil cylinder with water and measuring the time taken to fail. Failure is defined when

there is significant water loss from the cylinder. If no failure occurs within 420 minutes, then the test is terminated and "no-failure" recorded. According to Tadanier and Ingles, this time interval is equivalent to a soil permeability of 10^{-4} cm/sec for the cylinder, corresponding to the threshold below which dispersive soil tunnelling is thought not to occur.

Tadanier and Ingles admitted that the test has similar reliability as the SCS dispersion and chemical tests; and the major problem with the test is the difficulty of defining any precise acceptance - rejection boundary.

5.5 Discussion

In this chapter the mechanism relating to internal erosion in dispersive soils and the tests to identify such soils have been reviewed. It has been pointed out the erodibility of a soil depends on many factors such as the chemistry of the soil and the composition of pore and eroding fluid which can be difficult to separate for identification tests. As shown by the cases of earth dam failures in Mississippi and Oklahoma, the potentially troublesome soil can be very localised and difficult to distinguish from other sound soils within the same geographic area. The chemistry and dispersibility of clay can vary greatly within short distances in apparently uniform deposits and may vary greatly from stratum to stratum. Obtaining representative samples is very important and can be very difficult and this may account for the variations in results obtained from the same dam or an area. It would be necessary to carry out extensive tests which can be very time consuming and expensive. During construction of an embankment, soils are taken from an environment of equilibrium and placed in an environment of disequilibrium where they may be dried, rewetted, compacted etc., which may have some effect on its erosion resistance characteristics.

The clay mineralogy aspect should be studied in more detail in conjunction with the electrolyte concentration and its chemical composition. A soil material may produce a large amount of dissolved salts which flocculate the clay particles and make them resistant to erosion, but a reservoir of water with low electrolyte concentration will dilute the salt concentration through both ion migration and mass flow. Ion migration may take considerable time. With long term reduction in the amount of dissolved salts the erosion properties of the soil may be modified and hence monitoring and laboratory studies may

be continuously required. Dams constructed of high sodium content soils can continue to perform satisfactorily if the salt content of the reservoir is high. (Coumoulos, 1976).

It may be concluded that even though a number of tests have been proposed to identify dispersive soils, no single test provides results that have a satisfactory level of reliability and define a simple or consistent boundary between dispersive and non-dispersive soils. In some tests, such as pinhole and crumb test, there is not guarantee that the samples are saturated and so the tests may be influenced by suctions in the samples, even after exposure to free water, which can give rise to substantial effective stresses. There is a need for further research to improve understanding of dispersive or erodible soils and to develop tests and criteria to evaluate this problem. It is important to note that all the laboratory tests described here do not adequately predict or examine the potential for long term resistance to erosion of clays. The soils in an embankment dam may take many years before reaching an equilibrium state with the impounded water, and also changes in the soil chemistry can take place if the reservoir is emptied for a long period. So far the research has been directed towards dispersive clays used in earth dam construction in and or semi-arid areas. In the literature, there is no mention of such clays being present in U.K but that does not imply that the problem cannot exist. Clays in the puddle clay core of dams would be expected to be in a fully saturated condition and may erode slowly over relatively long periods of exposure to seepage and hence the above tests may not be sufficiently sensitive.

CHAPTER 6

Theoretical Analysis of Hydraulic Fracture in Cylindrical Cavity Expansion Tests

6.1 Introduction

It is often assumed that hydraulic fracturing in both embankment dams and boreholes occurs when one of the effective stresses is tensile and equal in magnitude to the effective tensile strength of the soil, or ignoring the effective tensile strength of the soil when one of the effective stresses is zero. However, it is also possible that hydraulic fracturing occurs when the undrained or drained shear strength of the soil is reached due to the rapid application of water pressure in a discontinuity. In this chapter theoretical analyses of hydraulic fracture in a cylindrical cavity are proposed and they will be compared with the experimental results in chapter 10. Study of hydraulic fracture is complex and involves many unknown factors and the simple analyses as proposed below should be sufficient for practical purposes. A discontinuity in a soil mass is necessary for hydraulic fracture to occur under rapid application of water pressure. This condition in the present experimental work was provided by a sand column placed in the sample. During placing some sand would penetrate the excavated soft clay walls of the borehole thus creating an irregular surface. A simple theory is also presented here to take account of penetration of water in the soil during slow fracture tests and its consequence on fracture pressures.

6.2 The Idealized Model

Due to the complexity of the problem regarding the mechanisms of hydraulic fracture several simplifying assumptions have been made. Some of the factors that can be significant during the test are: i) effect of installation of the sand pocket and the probe on the stresses around the cavity, ii) initial stress conditions and changes of stresses due to increase of cavity pressure and due to fracturing pressure, iii) in-homogenities of stresses around the borehole. Borehole is defined here as the excavated hole in the sample.

The sand pocket is assumed to be rigid and to have a high permeability compared with that of the soil. The length is great compared with the diameter thus giving a condition of a cylindrical cavity. Due to lack of information, it is assumed that the effect of the sand

pocket and the probe on the stresses in the soil adjacent to the borehole is negligible after the sample has been consolidated to relatively higher effective stress. The stresses occurring in a soil element near the borehole are shown in Fig 6.1.

It is assumed that the soil is a homogenous, isotropic and ideal elastic-plastic solid with an undrained shear strength equal to s_u . As described in Chapter 2, the failure at ultimate state can be described by the following equations:

$$q' = Mp' \quad (6.1)$$

$$v = \Gamma + \lambda \ln p' \quad (6.2)$$

During a cavity expansion test in this ideal material, the total and effective mean stresses remain constant until yield occurs. In Fig. 6.2, this path is represented by A → 0. The corresponding effective stress path followed will be vertical until yield. Yield occurs at an undrained shear strength s_u . The effective stress followed by lightly overconsolidated soil is B → 0 and by heavily overconsolidated soil is C → 0, as shown in Fig. 6.2. In Fig. 6.2 yield, ie the end of elastic behaviour, occurs at point Y and ultimate failure occurs at point 0. (After yield, total stresses may change so that point 0 (total) may move to the right). If the soil fractures at the effective stress state 0, it could be said to be fracturing in shear. (The effective stress path followed by a soil fracturing at no-tension cut-off is shown in Fig 6.7a).

Before the test, the total stresses in the soil are $\sigma_r = \sigma_\theta = \sigma_A = \sigma_B = p_0$ and the pore pressure is u_0 . σ_A and σ_B are the internal and external total pressures respectively acting on the soil sample. During the test the water pressure tends to expand the borehole so that the radial strain is compressive, the circumferential strain is tensile and the axial strain is zero. The ordering of the stresses is therefore;

$$\sigma_r > \sigma_\theta > \sigma_z \quad (6.3)$$

This causes an increase in σ_r and a decrease in σ_θ as shown in Fig. 6.3.

Expressions describing the state of stress in a thick walled linear elastic cylinder subjected to the action of uniformly distributed internal and external pressures as shown in Fig 6.4 have been given by Jaeger and Cook (1971). The equation of equilibrium in axially symmetric plane polar co-ordinates is:

$$\frac{d\sigma_r}{dr} + \frac{1}{r} (\sigma_r - \sigma_\theta) = 0 \quad (6.4)$$

and the total stresses in an element at a radius r are;

$$\sigma_r = \frac{\sigma_B b^2 - \sigma_A a^2}{b^2 - a^2} - \frac{(\sigma_B - \sigma_A) a^2 b^2}{r^2 (b^2 - a^2)} \quad (6.5)$$

$$\sigma_\theta = \frac{\sigma_B b^2 - \sigma_A a^2}{b^2 - a^2} + \frac{(\sigma_B - \sigma_A) a^2 b^2}{r^2 (b^2 - a^2)} \quad (6.6)$$

here σ_A and σ_B are the internal and external pressure respectively, a and b are the internal and external radii respectively. The changes in these total stresses resulting from an increase $\delta\sigma_A$ in the internal borehole pressures with the external pressure σ_B held constant can be written as follows:-

$$\delta\sigma_r = \frac{-\delta\sigma_A a^2}{b^2 - a^2} + \frac{\delta\sigma_A a^2 b^2}{r^2 (b^2 - a^2)} \quad (6.7)$$

$$\delta\sigma_\theta = \frac{-\delta\sigma_A a^2}{b^2 - a^2} - \frac{\delta\sigma_A a^2 b^2}{r^2 (b^2 - a^2)} \quad (6.8)$$

At $r = a$

$$\delta\sigma_r = \delta\sigma_A \quad (6.9)$$

$$\delta\sigma_\theta = -\delta\sigma_A \frac{(1+x)}{(1-x)} \quad (6.10)$$

where $x = a^2/b^2$

The above analysis assumes that the soil remains in the elastic range during the changes in total stresses. Hence, using the principle of superposition, the following expression is obtained.

$$\sigma_r - \sigma_\theta = \delta\sigma_r - \delta\sigma_\theta = \frac{2(\sigma_A - \sigma_B)}{(1-x)} \quad (6.11)$$

6.3 Fracture Criteria

Fracturing in a cylindrical cavity may be analysed either in total or effective stresses conditions using either the undrained shear strength or the drained shear strength or some other criterion to define the initiation of fracture.

As discussed in Section 2.6, heavily overconsolidated samples dilate locally in shear zones during shear even in nominally undrained tests and may not reach the same ultimate state points as reached by normally consolidated samples having the same water content. Values of s_u were determined from undrained compression triaxial tests on normally consolidated samples and these were related to both the water contents and to p'_o of the samples. The values of s_u for normally consolidated samples were determined from the relationship $s_u/p'_o = 0.38$ (see Fig B.16). During a hydraulic fracture test the dilating element not only has access to water from the surrounding soil element but also from the free water in the borehole. Thus the specific volume of such an element will increase and the element may

fail on the critical state line much earlier as indicated in Fig. 6.5 at E rather than at F. Hence, for heavily over-consolidated samples it may be appropriate to take the value of undrained shear strength at the maximum stress ratio (q'/p') at the point R (Fig. 6.5) for interpreting fracture tests.

6.3.1 Theoretical Analysis in Total Stress Conditions

Condition 1) The undrained shear strength is mobilised at the surface of the borehole (i.e. at $r = a$)

It is assumed that the soil behaves elastically until the onset of yielding which is determined by the Tresca criterion, when the stresses satisfy the following equation: (Yield and failure both occur together at $q=2s_u$)

$$\sigma_r - \sigma_\theta = 2s_u \quad (6.12)$$

Plastic yielding and failure first occur at the surface of the borehole, i.e. at $r = a$, when the stresses satisfy equation 6.12. From equation 6.11 and 6.12, the borehole water pressure required to cause hydraulic fracturing is:

$$\sigma_A - \sigma_B = s_u(1 - a^2/b^2) \quad (6.13)$$

At fracturing $\sigma_A = \sigma_r$ where σ_r is the borehole water pressure required to cause hydraulic fracturing, σ_B is the cell pressure and is equal to σ_∞ . Equation 6.13 may be rewritten as:

$$\sigma_r - \sigma_\infty = s_u(1 - a^2/b^2) \quad (6.14)$$

If cracks were formed the stress state in the soil adjacent to the cavity could become unstable and shear fractures may propagate from the inner surface of the borehole. It is thought that initially there may be more than one such crack around the borehole, but if fluid enters one of these cracks then the stress is raised to a higher level due to stress concentration caused by the fluid pressure giving rise to a rapid failure through the sample.

The penetration of fluid in a crack would depend on the rate of pressurising the cavity. The likelihood of a stress concentration would be higher in a cavity having an irregular face than in one having a smooth face. Equation 6.14 indicates that from this analysis hydraulic fracture in a borehole depends on the total confining pressure σ_{ro} , the undrained shear strength s_u and on the geometry of the borehole and the intact sample. The above analysis assumes that fracture takes place under undrained conditions, i.e., the fluid has not penetrated into the soil. If the fluid penetrates into the soil, the specific volume of the soil adjacent to the borehole will increase and hence decrease the undrained shear strength. This effect can be taken into account by considering a higher value of a in equation 6.14. This effect of partial penetration is discussed in Section 6.5.

Condition 2) The undrained shear strength is mobilised throughout the sample.

If full plasticity is allowed, then from equations, 6.4 and 6.12 the borehole water pressure required to cause hydraulic fracturing is:

$$\sigma_f - \sigma_{ro} = 2s_u \ln \left(\frac{b}{a} \right) \quad (6.15)$$

Comparing equations 6.14 and 6.15 it is found that the pressure required to expand a cylindrical cavity under undrained conditions when full plasticity is allowed for is much greater than the pressure calculated by the elastic-plastic theory in condition (1) above.

Condition 3) Limiting value of $\sigma_\theta = 0$ at $r = a$.

At failure

$$\sigma_\alpha = \sigma_{\alpha 0} + \delta \sigma_\theta \quad (6.16)$$

$\sigma_{\alpha 0} = \sigma_B$ and from equation 6.10,

$$\delta \sigma_{\theta} = - \delta \sigma_{\lambda} \left(\frac{1 + \lambda}{1 - \lambda} \right)$$

therefore equation 6.16 becomes:

$$\sigma_{\theta, r} = \sigma_B - \delta \sigma_{\lambda} \left(\frac{1 + \lambda}{1 - \lambda} \right) \quad (6.17)$$

At failure $\delta \sigma_{\lambda} = \sigma_r - \sigma_{\lambda} = \sigma_r - \sigma_B = \sigma_r - \sigma_{ro}$

substituting these values in equation 6.17, the following expression for fracturing pressure σ_r is obtained:

$$\sigma_r = \frac{1}{(1 + a^2 / b^2)} [2\sigma_{ro} - \sigma_{\theta, r} (1 - a^2 / b^2)] \quad (6.18)$$

The limiting value of σ_{θ} investigated is when $\sigma_{\theta} = 0$

Hence from equation 6.18

$$\sigma_r = \frac{2\sigma_{ro}}{(1 + a^2 / b^2)} \quad (6.19)$$

Equation 6.19 can be written in the form of:

$$\sigma_r - \sigma_{ro} = \sigma_{ro} \left\{ \frac{1 - a^2 / b^2}{1 + a^2 / b^2} \right\} \quad (6.20)$$

Equation 6.20 indicates that fracturing pressure in a borehole depends on the total confining pressure σ_{ro} and on the geometry of the borehole and the intact sample but is independent of the undrained shear strength s_u . It should be noted that equations 6.19 and 6.20 are valid provided $\sigma_{ro} \leq (1+a^2/b^2)s_u$.

6.3.2 Theoretical Analysis in Effective Stress Conditions

Fracture tests were commenced by bringing the probe (cavity) pressure to the value of the confining pressure before opening the external valve of the probe (for details see Section 8.6.3). As soon as the valve is opened the pore pressure (u_o) in the sand pocket will rise to the value of the applied cavity pressure resulting in zero effective stress in the sand. All the water pressure will then be taken by the clay adjacent to the borehole. At $t > 0$ a further increase in the cavity pressure will result in changes in total stresses. There will be an increase in the total radial stress which will be equal to the cavity pressure σ_A and a decrease in circumferential stress as shown in Fig. 6.6.

The change in total stresses resulting from an increase from the borehole cavity pressure is given by equations 6.7 and 6.8 as before and hydraulic fracturing may be analysed in terms of effective stresses. It is assumed that the reconstituted samples have zero effective tensile strength.

At failure, as before (see equation 6.17)

$$\sigma_{\theta_f} = \sigma_B - \delta\sigma_A \left(\frac{1+x}{1-x} \right) \quad (6.21)$$

Also at failure $\delta\sigma_A = \sigma_r - \sigma_A = \sigma_r - \sigma_B = \sigma_r - \sigma_{ro}$, and $\sigma'_{\alpha} = \sigma_{\alpha} - u_f$

substituting these values in equation 6.21, an expression for σ'_{α} is obtained as:

$$\sigma'_{\theta_f} = \frac{1}{(1-x)} [2\sigma_{ro} - \sigma_f (1+x)] - u_f \quad (6.22)$$

From equation 6.22, there are two possibilities of fracture as described below:

- i) Fracture occurs when $\sigma'_{\alpha} = 0$ at $r = a$.
- ii) Fracture occurs when $(\sigma'_{\alpha}/\sigma'_{\alpha})_t = K_{\alpha}$ at $r = a$ where $K_{\alpha} = (1 - \sin \phi')/(1 + \sin \phi')$.

This is the Mohr-Coulomb criterion for ultimate failure with $c' = 0$.

For the above possibilities, i.e., if failure occurs on the no-tension line or on the critical state line, there will have been plastic deformation and hence the basic assumption of elasticity used to obtain equation 6.22 are no longer strictly valid. However, the error is likely to be not large provided the plastically deforming zone is small.

Possibility (i) when $\sigma'_{\alpha} = 0$, then from equation 6.22

$$\sigma_r = \frac{1}{(1 + x)} [2\sigma_{ro} - u_r (1 - x)] \quad (6.23)$$

The effective stress path followed by a non-elastic soil element at the edge of the borehole is shown in Fig 6.7a. Fracture occurs when, at low effective stresses, the soil element at $r = a$ reaches the no-tension line cut-off represented by $q' = 3p'$.

At failure:

$$u_t = p_o - \frac{1}{3} q'_t = p_o - \frac{1}{3} (\sigma'_r - \sigma'_\theta)_t \quad (6.24)$$

For $\sigma'_{\alpha} = 0$

$$u_t = p_o - \frac{1}{3} \sigma'_r \quad (6.25)$$

At fracture $\sigma'_{\alpha} = \sigma'_t$ and hence:

$$u_t = p_o - \frac{1}{3} \sigma'_t \quad (6.26)$$

Since fracturing tests were conducted under nearly isotropic conditions it can be assumed that $\sigma_{\infty} = p_o$, then equation 6.26 can be re-written as:

$$u_r = \sigma_{\infty} - \frac{1}{2}(\sigma_r - u_r) \quad (6.27)$$

or

$$u_r = \frac{3}{2} \sigma_{\infty} - \frac{1}{2} \sigma_r \quad (6.28)$$

Substituting this value in equation 6.23, fracturing at $r = a$ occurs (assuming $b \gg a$) when:

$$\sigma_r = \sigma_{\infty} \quad (6.29)$$

or

$$(\sigma_r - u_o) / \sigma'_{\infty} = 1 \quad (6.30)$$

Equation 6.30 indicates that fracturing will take place when $\sigma_r - u_o$ reaches the effective confining pressure and is independent of the geometry of the sample. The assumption $b \gg a$ has been made which is reasonable for the tests undertaken.

Possibility (ii)

when $(\sigma'_r / \sigma'_t)_r = K_a$ at $r=a$, where $K_a = (1 - \sin \phi') / (1 + \sin \phi')$. At fracture $\sigma'_{\alpha} = \sigma'_t$ and hence $\sigma'_{\alpha} = K_a (\sigma_r - u_r)$. Substituting this value of σ'_{α} in equation 6.22, the following expression for σ_r is obtained:

$$\sigma_r = \frac{1}{(K_a - K_a x + 1 + x)} [2\sigma_{\infty} - u_r (1 - x - K_a + K_a x)] \quad (6.31)$$

or

$$\sigma_f - u_o = \frac{1}{(K_a - K_a x + 1 + x)} [2\sigma_{ro} - u_f (1 - x - K_a + K_a x)] - u_o \quad (6.32)$$

u_f can be estimated by the following expressions:

$$v_o = N - \lambda \ln p'_o \quad (6.33)$$

$$p'_f = \exp \left[\frac{\Gamma - v_o}{\lambda} \right] \quad (6.34)$$

$$u_f = p_o - p'_f \quad (6.35)$$

It should be noted that equation 6.33 applies, strictly speaking, to isotropically normally consolidated soils only. Also, it has been assumed that p_o remains constant as the shear stress increases (Fig. 6.7b and equation 6.35) which may not be the case, particularly as a normally consolidated soil will yield prior to reaching the maximum shear stress.

The pore pressure, just before failure, can either increase or decrease as shown in Figs. 6.6 and 6.7c, but for a purely elastic soil, it will remain unchanged (Figs 6.6 and 6.7b). The value of K_a will depend on ϕ' mobilised at failure. For a normally consolidated soil ϕ' mobilised is either equal to ϕ'_c at critical state or ϕ'_y at yield, and similarly for a heavily overconsolidated soil ϕ' mobilised could be at ϕ'_c at critical state or ϕ'_y at yield (peak stress ratio q'/p'). For normally consolidated soils, ϕ'_y mobilised at yield could be lower than ϕ'_c at critical state. An estimate of ϕ'_y mobilised for such soils can be assessed as follows:

$$M = \frac{q'}{p'} = \frac{q'}{p'_o} = \frac{2s_v}{p'_o} \quad (6.36)$$

(provided p'_o does not change during shearing which may be the case for some soils in an overconsolidated state).

From Section B-6, $s_u = 0.38 p'_o$ (for normally consolidated soils) which would imply $M = 0.76$, ϕ' , mobilised = 19.7° and $K_s = 0.496$. However, as can be seen from Figures B.10 and B12, p'_o is not constant during the test and this value of M will then differ from the critical state M .

Equations 6.30 and 6.32 were used to calculate the theoretical values of $\sigma_r - u_o$ at various confining pressures and initial pore pressure, ie., σ'_{ro} . Since $\sigma_r - u_o$ depends on σ'_{ro} , the theoretical values were normalised with σ'_{ro} in order to compare with the experimental values of $(\sigma_r - u_o)/\sigma'_{ro}$. The steps for determining the theoretical values of $(\sigma_r - u_o)/\sigma'_{ro}$ for the above possibilities are illustrated by the following example:

Initial stress conditions:

$$\begin{aligned} \sigma_{ro} &= 500 \text{ kPa}, & u_o &= 100 \text{ kPa} & \sigma'_{ro} &= 400 \text{ kPa} \\ \text{Sample geometry:} & & a &= 3 \text{ mm}, & b &= 19 \text{ mm} \end{aligned}$$

Possibility (i) Fracture occur when $\sigma'_\alpha = 0$ at $r = a$ (when the soil element at $r = a$ reaches the no-tension cut-off).

From equation 6.30

$$(\sigma_r - u_o)/\sigma'_{ro} = 1$$

Possibility (ii) Fracture occurs when $(\sigma'_\theta/\sigma'_r)_l = K_s$ at $r = a$

case (a) For an elastic soil failure occurs at yield (Fig 6.7b) then $u_o = u_r$ and ϕ' , mobilised might be taken as 19.7° as suggested earlier. Equation 6.32 for this case can be written as:

$$\sigma_r - u_o = 0.663 [2\sigma_{ro} - 0.491u_o] - u_o$$

$$\sigma_f - u_o = 0.663 [2 \times 500 - 0.491 \times 100] - 100$$

or

$$(\sigma_f - u_o)/\sigma'_{vo} = 1.33$$

case b) Failure occurs on the critical state line (Fig 6.7c)

The soil properties of the soil studied here are:

$\lambda = 0.120$, $N = 2.390$ and $\Gamma = 2.338$ (see Section B-6 and Table B-4). Initial stresses of the sample studied are:

$$p'_o = \sigma'_{vo} = 400 \text{ kPa}, p_o = \sigma_{vo} = 500 \text{ kPa and } u_o = 100 \text{ kPa}, \phi'_c = 30^\circ.$$

From equations 6.33, 6.34 and 6.35; $v_o = 1.671$ and $u_f = 241 \text{ kPa}$. Hence from equation 6.32.

$$\sigma_f - u_o = 0.741 [2 \times 500 - (0.65 \times 241)] - 100$$

$$(\sigma_f - u_o)/\sigma'_{vo} = 1.31$$

The above modes of failure can also be applied to heavily overconsolidated samples. As discussed earlier, there are certain problems associated with testing of such samples. Undrained triaxial compression tests were conducted on samples having stresses and values of R_o similar to the overconsolidated samples tested for fracturing tests. The pore pressure changes observed in the triaxial tests (assessed under a constant p_o conditions) were used to determine $\sigma_f - u_o$ as described below:

Initial stress conditions (Test No. F5-7): $\sigma_{vo} = 346 \text{ kPa}$, $\sigma'_{vo} = 45 \text{ kPa}$, $u_o = 301 \text{ kPa}$ and $R_o = 12$.

Sample geometry: $a = 3$ mm and $b = 19$ mm.

From the undrained triaxial compression test u_r at the ultimate state is 179 kPa.

Possibility (i) Fracture occurs when $\sigma'_{\alpha} = 0$ at $r = a$ (when the soil element at $r = a$ reaches the no-tension cut-off).

From equation 6.30

$$(\sigma_r - u_o)/\sigma'_{\infty} = 1$$

Possibility (ii) Fracture occurs when $(\sigma'_o/\sigma'_r)_r = K_s$ at $r = a$.

case (a) Fracture occurs at yield, then $u_o = u_r$ and ϕ'_y mobilised at (q'/p') peak = 38° and $K_s = 0.238$. From equation 6.32.

$$\sigma_r - u_o = 0.976 [2 \times 346 - (0.743 \times 301)] - 301$$

$$(\sigma_r - u_o)/\sigma'_{\infty} = 1.60$$

case (b) Fracture occurs at the critical state.

ϕ' mobilised = $\phi'_c = 30^\circ$. From equation 6.32:

$$\sigma_r - u_o = 0.741 [2 \times 346 - (0.65 \times 179)] - 301$$

$$(\sigma_r - u_o)/\sigma'_{\infty} = 2.79$$

6.4 The Effect of Partial Penetration

It is well established that the fluid penetration into the soil mass adjacent to the borehole being pressurized has a significant effect on the magnitude of the fracturing pressure, (for example, Kennard, 1970). A simple theory is presented here which takes account of fluid penetration and its effect on the magnitude of the fracturing pressure.

With reference to Fig. 6.8, for non-penetrating fluid (undrained) the stress path followed by the soil element adjacent to the borehole is AB. If the fluid penetrates the soil element the stress path would then deviate along AC. The initial specific volume would increase and hence pore pressure and s_u at failure would be higher and lower respectively than that observed during the undrained test. The change in specific volume can be determined by the following relationship:

$$\delta_v = G_s \delta_w \quad (6.37)$$

where

δ_v = change in specific volume

G_s = specific gravity

δ_w = change in moisture content

substituting equation 6.37 into equation 6.34, gives:-

$$p_f = \exp \frac{[\Gamma - (v_o + \delta_v)]}{\lambda} \quad (6.38)$$

Thus p'_f would decrease leading to a higher pore pressure which will consequently lower the fracture pressure. At very low pressure, $q'/p' = 3$ would be the limiting value corresponding to no-effective tension limit.

The depth of water penetration into the sample during fracturing tests may be evaluated by an approximate solution for one-dimensional consolidation by parabolic isochrones

(Atkinson and Bransby, 1978). The analysis is used only to give an estimate of water penetration since it is recognised that the axisymmetric conditions in the experiments differ from the conditions of one-dimensional flow used in the analysis. Fig. 6.9 shows a family of parabolic isochrones for one-dimensionally consolidating clay. For the clay layer in Fig. 6.9 at $t = 0$, no water has been squeezed from the clay (or no water has penetrated in the fracturing test) and so there is no volume change and no change of effective stress. With time the isochrones will move into the sample. At time t_1 an isochrone will intersect the line ED at a point L. Below L there has been no consolidation and no change in volume and hence there is no flow of pore water. The distance $l (=EL)$ is given by the equation.

$$l = \sqrt{(12 c_v t)} \quad (6.39)$$

where c_v = the coefficient of consolidation. It is assumed that while pore pressure change to the full length l the mean change of pore pressure is equivalent to a depth of penetration $\frac{1}{3}l$ from the properties of a parabola. In the fracturing tests, it may be assumed that with time water may penetrate a distance $\frac{1}{3}l$ into the sample. Thus knowing c_v and time to fracture t can be determined. This partial penetration of water into the sample can be taken into account by considering that the internal radius of the borehole is increased by $\frac{1}{3}l$. Thus the new radius of the cavity is:

$$a_1 = a + \frac{l}{3} = a + \sqrt{\frac{4}{3} c_v t} \quad (6.40)$$

6.5 Justification of Rapid Laboratory Tests

Case histories of hydraulic fracturing of dams have shown that most of the dams suffered from hydraulic fracturing during initial rapid filling of reservoirs and that concentrated leaks appeared within a few days and even a few hours. The relative rate of loading during reservoir filling may be considered by comparing a 20 mm thick laboratory sample with a 2 m thick core in the field as described below. From consolidation theory:

$$\left(\frac{t}{L^2}\right)_{\text{laboratory}} = \left(\frac{t}{L^2}\right)_{\text{field}} \quad (6.41)$$

From equation 6.41 it is found that a 3 minute fracturing test in the laboratory is equivalent to nearly 21 days in the field. Hence it is relevant to consider fracturing as an undrained loading phenomenon in many instances.

6.6 Summary

In this chapter a number of conditions which might govern hydraulic fracturing in a cylindrical cavity have been considered each involving different assumptions and approximations stated during their derivation. These conditions gave a number of different expressions relating the fracturing pressure to the geometry of the sample and the cavity and the soil properties. Briefly, these expressions are as below:

i) Total stress conditions

Condition 1: When s_u is mobilised at $r = a$

$$\sigma_f - \sigma_{ro} = s_u (1 - a^2/b^2) \quad (6.42)$$

Condition 2: When s_u is mobilised everywhere

$$\sigma_f - \sigma_{ro} = 2s_u \ln (b/a) \quad (6.43)$$

Condition 3: Limiting value of $\sigma_\theta = 0$ at $r = a$

$$\sigma_f - \sigma_{ro} = \sigma_{ro} \left[\frac{1 - a^2/b^2}{1 + a^2/b^2} \right] \quad (6.44)$$

ii) Effective stress conditions

Condition 1 : When $\sigma'_\theta = 0$ at $r = a$

$$\sigma_r = \sigma_r \quad (6.45)$$

or

$$(\sigma_r - u_o)/\sigma'_\infty = 1 \quad (6.46)$$

Condition 2 : When $(\sigma'_\theta/\sigma'_r)_r = K_a$ at $r = a$

$$\sigma_r - u_o = \frac{1}{(K_a - K_a x + 1 + x)} [2\sigma_{r0} - u_f (1 - x - K_a + K_a x)] - u_o \quad (6.47)$$

where $x = a^2/b^2$

Values of u_f would depend whether failure occurs at yield or on the critical state line.

In Chapter 10 these expressions will be compared with the results of laboratory tests in which hydraulic fracture was caused in hollow samples of clay by undrained and partially drained cavity expansions.

CHAPTER 7

APPARATUS

7.1 Introduction

This section describes the equipment used in preparing reconstituted samples, the Bishop and Wesley stress path cells, erosion apparatus, laboratory hydraulic fracture apparatus and details of equipment used to prepare samples for fracture tests and mount them in the hydraulic fracture apparatus.

The Bishop and Wesley stress path cells and their control system and the equipment for preparation of triaxial samples were part of the general facilities in Geotechnical Engineering Research Centre (GERC) at the City University. The probe inserted into triaxial samples for fracture tests, the pressure supply and the equipment for inserting the probe was designed by the writer and manufactured in the G.E.R.C. workshop.

7.2 Objectives of Experiment and Choice of Tests

One of the aims of this research is to study fracturing experimentally in the laboratory. Hydraulic fracturing is a result of changes in stress conditions in a dam and therefore the ideal equipment to study these conditions is a stress path triaxial cell. In the Bishop and Wesley triaxial cell, samples of clay can be consolidated to required conditions and both total and effective stress can be monitored and controlled. Samples can be made with a desired stress history and hence influence of overconsolidation ratio on fracturing can be studied. In order to simulate the conditions of imperfection to the face of a core, it was decided to apply water pressure in a borehole drilled in the middle of a sample to a depth just exceeding half the length of the sample. This hole was not extended to the full depth of the sample for two reasons: firstly to avoid loss of water pressure or water between the bottom of the sample and the porous stone and secondly to confine the application of water pressure in space that will behave as a discontinuity in a dam. Use of reconstituted samples was preferred since such samples would be similar.

Many factors can effect fracturing pressures in the field and hence tests were required to examine the effects of sample geometry, loading rate, initial effective stresses, and

overconsolidation on the initial fracturing pressure and also the effects of subsequent reconsolidation time on refracturing pressures.

7.3 Samples Press

Reconstituted 38mm diameter samples were made in the sample press illustrated in Fig. 7.1. This comprised a 200mm long and 38mm internal diameter, thick walled, perspex tube equipped with two close fitting hollow pistons with porous stones on their internal faces. A hanger loaded with suitable weights supplied the load for consolidation via a ball bearing on the top piston. This arrangement in effect produced a long oedometer. Reconstituted 100mm diameter samples were prepared in a sample press which consisted of a 400mm long steel tube of 100mm internal diameter. A loading frame with suitable weights supplied the load via a ball bearing on the top of the top cap. *The top cap, which had vents for drainage, was placed on the porous stone with a filter paper placed on top of the slurry.*

7.4 The Triaxial Stress Path Apparatus for 38mm Diameter Samples

7.4.1 General Description

The principles of the design of the conventional triaxial apparatus were described fully by Bishop and Henkel (1962). A more versatile hydraulically operated cell was introduced by Bishop and Wesley (1975). The triaxial apparatus used for the triaxial tests on 38mm diameter samples was similar in principle to the Bishop and Wesley Cell.

The cell pressure was monitored by a pressure transducer at the base of the cell, and the deviator load was measured through a load cell within the pressure vessel. A second pressure transducer was mounted in a block on the base plate and measured the pore pressure at the base of the sample, connected by a short lead to the pedestal. Drainage from the sample was through a second lead from the pedestal to a volume gauge adjacent to the cell. The axial deformation of the sample was measured by monitoring the upward movement of the axial ram piston using a displacement transducer. Pore pressure, cell pressure and axial ram pressure were supplied by electromanostats.

Electrical instrumentation was used to measure the pressures on the sample and resulting strains. In the semi-automatically operated triaxial cell outputs from the instruments were read on a Digital Voltmeter and then converted manually into stresses and strains. In the fully automatic system the electrical signals were converted to digital form in a interface unit and transmitted to a microcomputer which converted these to stresses and strains.

7.4.2. Semi-Automatic Triaxial Cell

This cell was initially used for triaxial tests (Tests Nos. S-1, S-2, S-3, S-4, S-5 and S-6) and later adapted for fracturing tests on 38mm diameter samples. This cell was also used for special tests (ST-1, ST-2 and ST-3).

Simple pressure control equipment built at the City University (Atkinson, 1985) controlled the Bishop and Wesley hydraulic stress path cell for 38mm diameter sample with instrumentation monitored by a simple transducer reading device. The arrangement is illustrated in Fig. 7.2.

The pressure supplies required in this type of cell are cell and pore pressures and the axial pressure for the loading ram. The axial pressure was supplied by water in the lower ram, the cell pressure was supplied by water and the back pressure by air. In case of both the axial and the cell pressure, air water interfaces were used to generate the fluid pressure from the compressed air supply. The air pressure required to generate all these pressures was supplied from a standard air compressor. The air from the compressor was cleaned and dried before passing through a manostat valve which allowed a pressure of about 800 kN/m² to be supplied to the equipment. The purpose of this valve was to ensure a smooth pressure supply to the cell unaffected by the varying output of the compressor. The air supply then passed through the electromanostats. These electromanostats, which operated in the range of 10 - 1000 kPa, were obtained from John Watson-Smith Ltd. They were housed in the control box which also contained all the necessary wiring and plumbing connections. The Bourdon gauges mounted on the control box indicated the mains air supply pressure and the manostat delivery pressures. They were not used to record sample stresses.

In this hydraulic triaxial the axial stress was supplied from an electromanostat for stress controlled loading and axial strains were controlled using a Bishop ram as illustrated in Fig. 7.2. With the valve opened the axial loading was controlled by an electromanostat for stress-controlled loading. With the valve closed, the Bishop ram displaced fluid into the lower chamber of the hydraulic cell at a controlled rate for strain-controlled loading. With this apparatus it was possible to change from stress control to strain control during a test.

Stepper motors which controlled the electromanostats and the Bishop ram were operated simply by opening and closing switches; opening and closing a switch turned the motor through discrete steps and a second switch controlled the direction of turn. Switches were opened and closed by variable speed cyclic relays. These relays were obtained from RS Components Ltd. They had periods in the range of 0.5 - 400 seconds per step which gave loading rates in the range from about 50 kPa/minute to about 4 kPa/hour with Watson-Smith electromanostats. Alternatively, the switches may be opened or closed by operating push-button switches by hand.

7.4.3 Microcomputer Controlled Triaxial Cell

Microcomputer controlled stress path testing equipment developed at the City University, called the spectra system, was used for tests C1 to C7 (Definition of these tests is given in Section 8.3). The stress path testing system for 38mm diameter samples was described by Atkinson, Evans and Scott (1985). Full details of the control program was described by Clinton (1986). A brief description of this system is given here.

The control system for this type of apparatus was similar to that described in Section 7.4.2 except that the electromanostats were operated by small DC stepper motors acting through gears. The motors were controlled by the microcomputer. Logging and test control was carried out by a spectra microcomputer with a spectra xb interface unit manufactured by Intercole System Ltd. The basic function of the microcomputer was to receive digital output from the transducers, convert these to stresses and strains and to command the pressure sources to supply the required loading pressure. With this central microcomputer driving a number of tests it was necessary to have a second microcomputer for analysis of data. This was achieved by an Epsom QX 10.

The main function of the control program was to take instrument readings and control the test. The values were stored in the sideways RAM every hour. A full print out of the stored records could be obtained and the records could be dumped to a disc for analysis. The control loop of the program could also be interrupted for starting and stopping tests, calibrating the transducers and setting zero readings of stress and strain. Correction for the current area as the sample deformed during a test was also incorporated in the program.

7.5 Instrumentation

The instrumentation provided in Bishop and Wesley cell comprised standard triaxial instruments measuring the axial force, cell pressure, pore pressure, axial displacements and change of volume of the sample. All instruments used were of resistive type, that is, measurements of distortions of the sample and changes of stresses were sensed by changes in resistance of the device.

Axial forces on 38mm diameter samples were measured using a standard 450 kgf Imperial College load cell whilst on 100mm diameter samples (for hydraulic fracture tests) were measured using a 10kN Wykenham Farrance Load Cell. Both cell and pore pressures were recorded using a Druck pressure transducers with a range of 0-1000 kN/m². Axial displacements were measured externally as the relative displacements of the top of the cell and the cross head below the sample on a linear displacement transducer type HS-25B manufactured by MPE Transducers Ltd. Volume changes of 38 and 100mm diameter samples were measured using the Imperial College 50 and 100 c.c. capacity volume gauges respectively.

7.6 Apparatus Calibration and Accuracy

Each instrument was calibrated by applying a known displacement, load or pressure to the device as appropriate. On the semi-automatic system, measurement and recording of each transducer outputs in mV was made with a Digital Voltmeter (DVM). On the fully automatic system, calibration measurements were made using the main control program. Each instrument was calibrated by applying a known displacement, load or pressure to the device as appropriate, such that a known stress or strain was displayed on the screen. The

recordings and control program incorporated linear calibration factors for all measurements. This was found to be adequate for all control purposes. Fine adjustments to the calibration constants could be made by repeating the tests. Full details of the calibration procedures are given by Lau (1988).

Test data were analyzed using standard procedures described by Bishop and Henkel (1962). Corrections were made to the area of the sample and to the axial stress to take account of the stiffness of the side drains. Because the triaxial tests were not concerned with stiffness no corrections were made to measurement of strain to account for bedding, seating and apparatus compliance.

The triaxial cells and their instruments were frequently calibrated and were checked for errors due to noise and drift. The estimated accuracy of the measurements are summarised in Table 7.1.

7.7 Pinhole Apparatus

The pinhole apparatus, shown in Fig 7.3 (a), was designed and manufactured in the Geotechnical Engineering Research Centre at the City University. The basic features are the same as those described by Sherard et al (1976).

The apparatus consisted of 110mm long perspex cylindrical body of 38mm internal diameter in which a sample to be tested was placed. The perspex cylinder had caps at each ends fitted with 'O' - rings seals in order to give a water tight fit to the body. The top and base and caps were fitted with water inlet and outlet connections respectively. The top cap was also connected to a standpipe which measured the head of water applied to the specimen. Further water tight fit was achieved by clamping the end caps to the body by two long screws. The whole arrangement was then clamped onto a wooden stand which also carried the standpipe.

A hole through the sample was made by a 50mm long hypodermic needle of 1.1mm outside diameter. The needle was guided into the sample by a metal nipple. The truncated cone shaped metal nipple as shown in Fig 7.3 (b) was 12mm long with a 1.5mm hole.

Pea gravel and a wire mesh disc was placed on the top end of the specimen while the other end had two wire mesh discs and pea gravel. The wire mesh discs had an aperture of 1.5mm and were of 37.5mm in diameter.

Compaction was carried by a specially designed compaction hammer which weighed 775 gms. Compaction to 95% of standard Proctor could be achieved with this hammer by using 13 blows per layer from a free falling height of 50mm.

7.8 The Triaxial Apparatus for Fracture Tests

Laboratory hydraulic fracture tests were conducted on reconstituted samples each having a sand pocket in a cylindrical cavity in which a probe was inserted. Cavity pressure was measured by a pressure transducer and flow of fluid into the cavity was measured by a volume gauge.

The tests on 38mm diameter samples were conducted in a standard Bishop and Wesley triaxial cell. The tests on 100mm diameter samples were conducted in a larger Wykeham Farrance triaxial apparatus. The Bishop and Wesley Cell arrangement as described in Section 7.4 was extended to accommodate the above mentioned pressure transducer and its volume gauge. The arrangement used for hydraulic fracture tests is shown diagrammatically in Fig 7.4 and Plate I.

The volume gauge of the probe was connected to one end of a block by a short lead. The block which was placed outside the cell had a pressure transducer and a de-airing bleed valve. The other end of the block was connected to a probe by a lead via the sample's top cap after passing through the base of the cell. The sample top cap is described in Section 7.9.2. The lead connecting the block to the sample had a valve outside the cell body. This valve served two main functions, firstly, when closed, it stopped flow of water from the sample into the probe's volume gauge during the consolidation stage and, secondly, it was used to cut off the supply of injecting fluid into the sample once hydraulic fracture had taken place.

Cavity pressure was applied by air pressure at one end of the volume gauge causing equal pressure in the fluid system at the other end. The stepper motor controlling the probe

pressure electromanostat was operated using a variable speed relay of the type described in Section 7.4.2. The use of this relay ensured a steady rate of supply of probe pressure.

The volume gauge of the probe and the external pressure transducer were connected to two separate digital voltmeters (DVM) which enabled both the instruments to be monitored at the same time. The instrumentation and their calibration procedures were the same as described in Sections 7.5 and 7.6. The larger triaxial apparatus used for fracture tests on 100mm diameter samples had a 10kN Wykeham Farrance load cell.

7.9 Equipment Used for the Preparation of Samples for the Hydraulic Fracturing Tests

7.9.1 Introduction

This section describes the top cap with its probe for both 38mm and 100mm diameter samples and other various components of the equipment used to excavate cylindrical cavities in the samples and to place the probe in the cavity.

7.9.2 Samples' Top Cap and the Probe

a) 38mm Samples

The perspex top cap used for 38mm samples was 30mm deep and had an external diameter of 38mm. It had a side inlet which was joined to a vertical probe placed in the middle of the top cap as shown in Fig. 7.5. The steel probe of 1.6mm external diameter and of 1.2mm internal diameter had an outer length of 38mm from the base of the top cap. The length 38mm was adopted in order to place the end of the probe in the centre of the sample. 25mm of the outer length of the probe from the base of the top cap had a knurled brass sleeve of the shape shown in Fig. 7.5. The purpose of this brass sleeve was to fill the excavated borehole above the sand pocket. During consolidation stage, the walls of the borehole will fit around the sleeve tightly thus preventing the escape of the injecting fluid out of the sample. Two types of top caps having the same size and length of probes but with 6mm and 16mm external diameter brass sleeves were used for two distinct tests. The open ends of the steel probes were filed to form two slits. The function of these slits

were to prevent blockage of the probe by a sand grain. If a grain of sand were to be pushed against the outlet of the probe, the slits would ensure the flow of water into the sample.

b) 100mm Samples

The brass top cap, used for 100mm samples, was 30mm deep and had an external diameter of 100mm. It had an inlet drilled on one side of its top surface which joined to a vertical probe screwed in the middle of the top cap as shown in Fig 7.6. Cavity pressure was applied through this inlet.

Two types of probes were used for two distinct tests. The first probe had a 14mm external diameter and 70mm long knurled brass sleeve as shown in Fig. 7.6. The second probe had a 6mm external diameter and 87mm long knurled brass sleeve. Both the probes were 100mm long with 1.2mm and 1.6mm internal and external diameters respectively. The open ends of the steel probes were filed in the similar to those used for 38mm samples.

On its upper face, the top cap had a ball locator which enabled it to be joined to the Wykenham Farrance load cell.

7.9.3 Sample Borers

a) 38mm Samples

It consisted of a thin walled brass tube 50mm long embedded in the middle of a perspex cap of 38mm external diameter and 20mm deep as shown in Fig 7.7.

Two types of the sample borers having the same length of the brass tubes but with external diameters of 6mm and 16mm were used for two distinct tests. The ends of the brass tubes were filed to provide a cutting edge. The middle of the top of the perspex cap had a threaded recess in which a perspex rod for 250mm length could be screwed. The function of this rod was to enable the sample borer to be lowered into the "guide" (see Section 7.9.4) and into the sample. The diameter of the rod was chosen to give a slight "loose" fit in the "guide".

b) 100mm Samples

Two types of sample borers were used to excavate cavities in the samples for two distinct tests. Both the borers consisted of thin walled brass tubes embedded in the middle of a perspex cap of 100mm diameter and 30mm deep as shown in Fig. 7.8. Each perspex cap had two holes drilled through it to act as vents for the air during excavation. The ends of the brass borers were filed to provide a cutting edge.

The first borer was 128mm long and had an external diameter of 14mm, while the second borer was 113mm long and had an external diameter of 6mm.

7.9.4 The Base Plate and the "Guide" for 38mm Samples

The circular base plate was 250mm in diameter and 10mm deep. It had a solid rod of 110mm length in its middle as shown in Fig. 7.9. The solid rod accepted the sample press which would have a reconstituted sample in it.

The "guide" consisted of a 400mm long perspex tube which had an internal diameter of a dimension which gave a good fit around the sample press. The purpose of this "guide" was to enable the sample borer to excavate a cylindrical cavity in the middle of the sample and to place the probe in the centre of the cavity. In the case of 100mm diameter samples, the press, described in Section 7.3, also acted as a guide.

7.9.5 38mm Samples' Top Cap 'Holder'

The lead which connects the probe's volume gauge to the probe can only be pushed into the inlet of the samples' top cap once the rubber membrane has been placed around the sample and sealed top and bottom with "O" rings. This operation of pushing the lead into the top cap can easily damage the sample and hence it was necessary to hold the sample in its upright position. This requirement led to the simple design of a sample's top cap "holder".

The top cap "holder" consisted of two steel legs which could be fixed to the base of the triaxial cell and a light aluminium adjustable cross arm as shown in Fig 7.10. This

adjustable cross arm had two split circumferential securing collars in its middle. The internal diameters of the securing collars was of a dimension which gave a slight "loose" fit around the samples' top cap. During setting of a sample in the triaxial cell, the samples top cap "holder" was placed over the top cap of the sample in such a way as to expose the inlet of the top cap through the split circumferential securing collars. The lead for connecting the volume gauge to the probe was then pushed into the cap.

CHAPTER 8

TEST PROCEDURES

8.1 Introduction

This chapter describes the procedures followed in preparation of reconstituted samples, conduct of triaxial tests, erosion tests and fracture tests. Index and classification tests were carried out according to B.S. 1377: 1975.

8.2 Preparation of Reconstituted Samples

Reconstituted samples 38mm diameter for both triaxial and fracture tests were prepared from air-dried puddle clay which was ground and passed through a 0.425mm sieve. In order to prepare a slurry a known weight of the air dried sample was mixed with distilled, de-aired water to a water content of 70% (approximately one and three quarters time the liquid limit). The mixing was done slowly and carefully in order to avoid air being trapped into the slurry. The slurry was then carefully poured into the press described in Section 7.2. The slurry was tapped gently in order to remove any air-bubbles trapped in the slurry. The slurry was compressed in the sample press under a maximum load of 8kg. The weights were added in increments of 1,1,2,2 and 2 kg via a vertical piston. The slurry was then left for complete consolidation. Filter papers were used between the slurry and the porous discs in order to avoid clogging of the porous discs. In order to reduce friction during consolidation of the sample, about 15-20 mm section of the lower piston was pulled out of the cylinder thus allowing the tube to 'float' on the lower piston. Friction was also reduced by cleaning any portion of slurry if trapped between the cylinder and the pistons. After a couple of trials exact amounts of soil and water were chosen to produce about 76mm long samples.

Similar procedures were followed for the preparation of 100mm diameter reconstituted samples for fracture tests. The final weight for the compression of the sample was 54kg.

8.3 Nomenclature of Laboratory Tests

8.3.1 Introduction

This section describes the various symbols and groups used to identify all tests conducted in the present work. The present work consisted of three distinct types of tests: triaxial, erosion and fracture tests.

8.3.2 Triaxial Tests

The main function of the triaxial tests were to obtain soils constants (e.g. λ , κ , M , N , Γ), pore pressure response of normally consolidated and overconsolidated samples, relationships between undrained shear strength and moisture content and to study the effect of rate of undrained loading on the undrained shear strength. These tests were conducted in semi-automatic and micro-computer controlled triaxial cells and the results were used to evaluate and interpret fracture tests. Triaxial tests have been given symbols for their identifications and are listed in Table 8.1. A brief explanation of the classification, with respect to the equipment used, is given below.

a) Semi-Automatic Triaxial Cell

Three undrained compression (S-1, S-2 and S-3) and three undrained extension (S-4, S-5 and S-6) tests were carried out with constant p stress paths. These tests were carried out in the initial stages of the research and the main purpose of following the particular stress path was to evaluate the equipment.

Three special tests (ST-1, ST-2 and ST-3) were carried out in the final stages of the research. Since most of the fracture tests were conducted rapidly, it was necessary to study the influence of rate of loading on the values of undrained shear strength. Samples were normally consolidated at $p' = 100$ kPa and were loaded at different strain rates. The duration of these tests were 3 minutes, 30 minutes and about 300minutes. One slow test (C-1) at $p' = 100$ kPa was carried out in the microcomputer controlled triaxial cell.

b) Automatic Triaxial Cell

Three tests on normally consolidated (C-1, C-2 and C-3) and four overconsolidated (C-4, C-5, C-6 and C-7) samples were carried in this type of cell. The fully automatic triaxial cell allowed slower loading rates. The three normally consolidated samples were carried out to supplement tests S-1, S-2 and S-3.

8.3.3 Erosion Tests

Two types of erosion tests were conducted in the present research, namely, Pinhole and Cylinder Dispersion tests.

a) Pinhole Tests

Pinhole tests were conducted only on puddle clay samples from the core of Cwmernderi Dam. They were divided into groups described in Table 8.2. separated by their initial water content and water content history.

b) Cylinder Dispersion Tests

Cylinder Dispersion tests conducted on various clays were divided in various groups separated by the water used to make reconstituted samples and by water used for the conducting the tests. All samples were reconstituted samples unless otherwise stated. The various groups are described in Table 8.3. Groups B-9 and B-10 were conducted on natural samples from the core of King George V reservoir. Samples tested were Kaolin, Cowden Till, London clay, Oxford clay, Laterite soil from Kenya and puddle clay from the cores of Cwmernderi, Ramsden, Gorpley, Lambieathan and King George V reservoir.

8.3.4 Fracture Tests

Hydraulic fracture tests conducted on both 38mm diameter and 100mm diameter reconstituted samples were divided in various groups as described in Table 8.4. Groups were separated by the size of the sample, size of the sand pocket, initial p'_0 and u_w , R_u , type of injecting fluid used and rate of testing. Group F-9 were conducted at two different values of σ'_1/σ'_3 to compare with tests from group F-1. It should be noted the samples of Group F-9 were not consolidated under K_u conditions. All fracture tests were conducted using water as the injecting fluid unless otherwise stated.

8.4 Procedures for Triaxial Tests

8.4.1 Setting up the Specimen

The soil sample was extruded from the press. Its height and weight were determined before mounting in the triaxial cell.

The sample was mounted on a saturated, de-aired stone on the lower pedestal of the triaxial cell, with a soaked filter paper between the sample and the porous stone to prevent clogging. A similar filter paper was placed on top of the specimen and the top cap was then placed on top of the sample. Moistened filter paper side drains were then placed around the sample to overlap the porous stone at the bottom. For compression tests strip filter paper side drains to the pattern of Bishop and Henkel (1962) were used. "Fish-net" type filter paper side drains were used for extension tests in order to minimize the apparent strength contribution by the strip filter papers. In order to minimize leakage during the test the sides of the top cap and bottom pedestal were lightly greased with vacuum grease. The membrane surrounding the sample was sealed top and bottom with two "O" rings each. A top cap with a rubber suction cap was then screwed into the top cap. The cell body was then placed over the sample, screwed down and filled with de-aired water. Usually the sample was left for a period, usually overnight, to check for any leakage.

In the spectra controlled triaxial cell the top cap was connected to the load cell before the start of the test. This was achieved by adjusting the pressure in the lower bellofram until it just balanced the cell pressure and the axial loading ram could be moved by light pressure of the hand. The load cell was screwed down to a suitable position. A Bishop ram was then used to draw water from the load cell connector. This brought the top platen into firm contact with the connector with the suction cap. On contact no further movement of the axial loading ram was noticed. The Bishop ram was then disconnected and the lead was left vented to the atmosphere. This procedure could not be carried out in the semi-automatic triaxial cell before the commencement of the isotropic consolidation. In the semi-automatic triaxial cell, the pressure in the lower Bellofram chamber could not be altered by stepper motor controlled by variable speed relay to respond precisely to the changes in the cell pressure during isotropic consolidation. The load cell was connected to the top platen at the end of a loading stage.

8.4.2 Conduct of Triaxial Tests

In the semi-automatic triaxial cell, samples S-1 to S-6 were isotropically consolidated against a back pressure equal to the pore pressure response at cell pressure equal to 200 kPa. Samples were consolidated by increasing the cell pressure continuously in the range of about 4-10 kPa per hour. With this system, readings had to be taken down manually. The loading speed was selected in order to register the end of a loading stage during working hours. In the Spectra controlled triaxial cell samples were compressed and swelled at a rate of about 4 kPa per hour. This procedure was used rather than following the usual procedure of undrained compression followed by consolidation to avoid non-uniform water contents and effective stresses in samples with radial drainage (Atkinson, Evans and Ho, 1985).

Samples in the semi-automatic triaxial cell were connected to the load cell at the end of their loading stages and then were allowed to consolidate further. It should be noted that before the top cap was connected to the load cell all strains had to be calculated on the basis that the samples behaved isotropically, that is $\Delta \epsilon_v = 3\Delta \epsilon_r$; this is not necessarily true. The initial states of these samples are given in Table B-2 of Appendix B.

Samples S-1 to S-6 (in the semi-automatic triaxial cell) were tested undrained at a constant p stress path. In order to achieve a constant p stress path it was necessary to maintain $\dot{\sigma}_v/\dot{\sigma}_r = -2$ condition. The dot signifies stress rate. During a test, values of p were calculated at ten minute intervals, and adjusted if required by adjusting either the variable speed relay controlling the loading ram or the one controlling the radial stress.

All compression tests (S-1, S-2 and S-3) were loaded at a nominal rate of deviator stress rate of $q = 30$ kPa per hour. This rate was selected in order to finish a test in one working day. Sample S-4 was also loaded similarly. Due to the problems encountered while testing sample S-4, as described below, the other two extension tests were loaded at $q = -30$ kPa per hour to an axial strain of about 2% and thereafter loaded initially under slower strain rate and then progressively at higher strain rates to failure. In stress control tests the failure is usually very abrupt. This problem is more apparent at an early stage of an extension test. Sample S-4, after 2% of axial strain started "running away". During an extension test, the sample tends to form a neck (having a smaller area) and therefore an increase in deformation will make it weaker and unstable. The advantage of stress control is that the initial portion of stress strain behaviour can be determined precisely.

In the spectra controlled triaxial cell the test was straight forward. The sample dimensions were entered through the keyboard together with the parameters for the required stress path. Control of the tests and all measurements were then carried out automatically. Sample C-1, C-2 and C-3 (normally consolidated) were slowly compressed at rate of about 4 kPa per hour to the states given in Table B-2 of appendix B with constant pore pressure $u = 200$ kPa. Sample C-4, C-5, C-6 and C-7 (overconsolidated) were also compressed at a rate of about 4 kPa per hour with a high back pressure (varying from 100 - 200 kPa) and then swelled by first decreasing p and then increasing u at a rate of about 4 kPa per hour to the states given in Table B-3 of Appendix B.

Samples C-1, C-2, C-3 and C-4 were loaded undrained with stress control initially, but at a suitable time and interval were changed to strain control. The loading rate for undrained loading was about 4 kPa per hour. Samples C-5, C-6 and C-7 were loaded undrained at a constant strain rate of about $\epsilon_v = 0.5\%$ per hour.

Special tests (ST series) were conducted in a semi-automatic triaxial cell. There were compressed at a rate of about 4 kPa per hour. A pre-set timer was used to switch off the variable speed cyclic relay and hence switching off the stepper motors controlling the electromanostats. Samples were connected to the load cell at the end of their loading stages and then allowed to consolidate further. In these tests only the initial and final volume readings were noted. The samples were loaded undrained at a constant strain rate and brought to failure in 3 minutes, 30 minutes and about 300 minutes. A constant strain rate was supplied by a Bishop ram connected to the lower bellofram chamber of the cell. The initial states and time for failure used are given in Table B-5 of Appendix B.

8.4.3 Ending Triaxial Tests

After a triaxial test had been completed, the sample was disconnected from the load cell by pumping water in the suction cap with a Bishop ram and reducing the ram pressure. Both the cell and the ram pressures were brought to zero values. The sample was quickly removed from the cell, weighed and dried in the oven to obtain the final water content. The whole sample was used to determine the final water content.

8.5 Procedures for Erosion Tests

8.5.1 Pinhole Tests

Testing procedures of pinhole tests have been described in greater detail by Sherard et al (1976). A brief outline of the testing procedures is given here.

Representative samples of puddle clay of Cwmernderi Dam were divided in the groups described in Table 8.2 separated by their initial water content and water content history. Recompaction of the samples were carried as follows:

Pea gravel was placed to a depth of 53mm in the cylinder with its lower end closed by the base plate. The cylinder was tapped gently in order to allow pea gravel to settle. Two wire mesh discs were placed on top of the gravel. The weight of the cylinder with its contents were then measured. The sample to be tested was compacted using the compacting hammer described in Section 7.6 to a depth of 38mm in 5 layers with 13 blows

per layer. The cylinder, with its compacted sample, was weighed. The nipple was pushed into the middle of the top of the sample with finger pressure and a hole was then punched through the nipple with the hypodermic needle. A wire mesh disc was placed on top of the sample followed by pea gravel to the top of the cylinder. The top base plate was then placed in position.

The cylinder containing the sample to be tested was mounted and secured in the pinhole apparatus. The cylinder was then connected to the standpipe which measured the head applied to the specimen and to the reservoir mounted on a bracket above the specimen. The position of the reservoir could be altered by a pulley system so that any desired head of water could be achieved.

A constant supply of distilled water of 50mm head measured from the centre line of the cylinder with its axis supported horizontally was applied. After a steady flow had been reached, the colour and the rate of flow of the outflow were recorded. If the colour of the outflow was clear and the rate of flow was small, the inlet head was raised to 180mm, then 380mm and finally to 1020mm and in each case the colour and the rate of outflow were recorded. *At the end of a test, the apparatus was dismantled and the soil sample extruded from the cylinder and broken up to examine the condition and the size of the hole, which was measured approximately by comparing with the hypodermic needle. The final moisture content of the sample was then determined by oven drying the whole sample.*

8.5.2 Cylinder Dispersion Tests

Erosion properties of clay samples were studied by cylinder dispersion tests. This simple test was carried out by immersing 38mm diameter samples in a beaker of water and observing visually the behaviour. Types of samples, and water have been described in Section 8.3.3. The beakers containing the samples were covered with "cling-film" to avoid loss of water due to evaporation for long term observations.

It is important that the samples during the test should not suffer any physical disturbance and hence tests were carried out in a quieter area which was not subjected to any physical disturbance. Index and classification tests were carried out according to B.S. 1377:1975 on soils tested in "Beaker tests".

8.6 Procedures for Hydraulic Fracture Tests

8.6.1 Installation of the Sand Pocket and the Probe in the Specimen

a) 38mm Diameter Samples

The sample press containing the sample was placed around the solid rod of the circular base plate which had been described in Section 7.8.4. The sample was pushed up by the rod to a depth of about 12mm below the top of the press. This enabled the excavation of the borehole and placing of the sand pocket. The "guide" also described in Section 7.8.4 was then located around the cylinder. The sample borer was then lowered on to the middle of the sample with the help of the perspex rod. The soil was excavated slowly in stages to a depth of 50mm, (except for Group F-4, where the depth of excavation was 60mm). After achieving the right depth of the borehole, the sample borer and the guide were removed. A moistened filter paper with a central hole of borehole diameter was placed on top of the sample. The purpose of this moistened filter paper was to minimise loss of moisture from the sample during the placing of a sand pocket. Leighton Buzzard sand (100% passing 2mm sieve and retained on 425 μ m sieve) previously wetted with de-aired water was placed in the borehole bit by bit with the help of an especially designed thin spatula and tapped with a smooth circular rod to a depth of 25mm (except for Group F-4, where the depth was 35mm). After removing the moistened filter paper, the probe was lowered into the sample with the help of the perspex rod.

b) 100mm Diameter Samples

The procedures for installing sand pocket and the probe in the sample were more or less similar to those described above.

The sample in the press was pushed up to a required depth below the top of the press. The borehole was excavated in stages to a required depth using the appropriate sample borer. Wetted Leighton Buzzard sand was then placed in the borehole bit by bit and tapped with a circular rod to the required depth. The probe was lowered into the sample with a long screw screwed into the top cap of the probe.

8.6.2 Setting up the Specimen

The procedures for setting up both 38 and 100mm diameter samples were nearly the same. The main difference was in the connections of the tubings to the top cap through which probe pressure was applied. This difference is explained here.

The extruded sample, after determining its height, was mounted in the triaxial cell with a bottom saturated de-aired porous stone, a lower moistened filter paper and a moistened filter side drains which were wrapped around the lower middle section of the sample. Use of nearly three quarter length of normal strip filter side drains were used in order to avoid any hinderence to the formation of cracks. The sides of the top cap and bottom pedestal were lightly greased with vacuum grease to minimise leakage during the test. A rubber membrane was then stretched over the sample and sealed top and bottom with two "O" rings each. Care was taken not to stretch the rubber membrane over the inlet of the 38mm diameter top cap.

For 38mm diameter samples, the top cap "holder" described in Section 7.8.5 was placed over the top cap and the plastic tube was then firmly pushed into the inlet of the top cap. A water tight seal was achieved by about 20mm long rubber sleeve wrapped around the end of the plastic tube, and pushed together into the inlet of the top cap. A top cap with a rubber suction cap was screwed into the top cap. The final sample set up is shown in Fig. 8.1. In 100mm diameter samples, the tubing was connected to the upper part of the top cap using nut and olive connections (compression fittings). The top cap was firmly held while tightening the connections.

Air trapped in the probe had to be expelled. Initially, air was expelled by flushing fluid through the probe and the sand pocket by increasing the probe pressure above cell pressure. It was felt that this method could initiate premature fracture into which some sand grains may be forced. Although this crack may close during consolidation of the sample, it could be re-opened during the test. The new technique employed was to increase the cavity pressure slightly above the cell pressure and pushing a known volume of fluid (pre-determined using the DVM) that would only fill the probe. All the air in the probe would then be pushed into the sand pocket and finally go into the solution during consolidation of the sample. This operation was done taking great care and when the

required reading in mV (corresponding to the volume change of the volume gauge connected to the probe) on the DVM was obtained the external valve connecting the probe to its reservoir (volume gauge) was quickly closed. The cell body was then placed over the sample screwed down and filled with de-aired water. Usually the sample was left for a period, usually overnight, to check for any leakage.

8.6.3 Conduct of Fracture Tests

Samples were compressed at a rate of about 4 kPa per hour to the required stress states. Overconsolidated samples were also compressed at a rate of about 4kPa per hour and then swelled using the same rate to the required stress states. The final stress states are summarised in Chapter 9. A pre-set timer was used to switch off the variable speed cyclic relay which stopped any further increase of cell pressure. Samples were connected to the load cell at the end of their loading stages and then allowed to consolidate further. The Wykeham Farrance cell used for 100mm diameter samples did not have the same facilities as the Bishop and Wesley cell for connecting the top cap to the load cell. 100mm diameter samples were brought into contact with the load cell by locating the ball connection of the load cell to the ball locator of the top cap. At the end of consolidation stage, samples were loaded under drained conditions by increasing q' at a rate of about 10 kPa per hour for two hours thus giving a deviator stress of about 20 kPa. The samples were then left to consolidate further before carrying out undrained fracture tests. Samples of group F-9 were consolidated isotropically initially and then loaded at rate of about 10 kPa per hour to the required value of q' .

Most of the fracturing tests were conducted by increasing the probe pressure at a rate of about 50 kPa per minute using a variable speed relay. Taking considerations of the size of the probe's bore and the size of the sample, this rate was considered to be fast for the tests. Much higher rates will give a higher fracturing pressure but the increase may be within acceptable order. Nevertheless, the influence of rate on fracturing was investigated. Fast rates (>50 kPa/minute) were achieved by operating the push button switches (clicker box) manually. Initially, some of the test of Group 1 were conducted by increasing the probe pressure at a rate of about 15 kPa/minute but were found to be slow. From pilot studies it was established that fractures occurred at pressures greater than confining pressures. This observation enabled the tests to be conducted in a shorter time interval

by adopting the following procedures: before the start of a test, the probe (cavity) pressure was brought to the value of confining pressure (cell pressure). This was achieved by firstly closing the external valve of the probe and increasing the pressure manually in the volume gauge connected to the probe. On achieving the required pressure the external valve was opened and the test commenced.

During the test, readings of the probe's pressure and the volume of the injecting fluid were monitored. Whenever possible, readings of the load cell, pore pressure and axial strain were also monitored. A sudden increase in the volume gauge monitoring the flow of the injecting fluid and an expansion in the rubber membrane indicated that the injecting fluid was passing through the sample and pushing the membrane outwards. At this instant the supply of the injecting fluid was cut off, relay switched off and the fracturing pressure σ_f noted down. Readings of the load cell and the axial strains were also noted down. These fractures have been termed as "initial" fractures to distinguish from subsequent fractures on the same sample. The drainage valve of the drainage lead was opened and the excess water surrounding the sample allowed to drain off. After a few minutes when most of the extra water had drained off the drainage valve was closed and the supply of the injecting fluid opened again. The probe pressure was reduced very quickly by operating the relay manually. Initially the volume gauge of the injecting fluid showed further increase but soon started slowing down until no further increase was noticed. This implied that the fluid was not longer passing through the sample indicating that the crack had closed thus giving closure pressure σ_c . A similar procedure was used to determine closure pressure for samples in which paraffin oil was used as the injecting fluid except that after initial fracture the extra paraffin surrounding the samples was not allowed to drain off as not to foul the samples' volume gauge.

A few "immediate" refracture tests were conducted on samples of Groups F-1 and F-3. "Immediate" refracturing refers to refracturing of samples soon after conducting "initial" fracturing and closure pressure tests. These tests were conducted in the manner as described below. After conducting closure pressure tests, the drainage valve to the base of the sample was opened in order to drain off the excess water. The valve was then closed and the probe pressure increased again. Cracking of the samples was established

in a similar way as explained earlier. This operation took place in relatively short time (on average about 10 to 20 seconds) and the refracturing pressures were always slightly greater than closure pressures. Closure pressures were again established by following the same procedures as described earlier.

A few "delayed" fracture tests were also conducted on Groups F-1B, F-7 & F-8. "Delayed" fracturing refers to fracture of samples which had been fractured initially and then were allowed to consolidate for a certain time. "Delayed" fracture tests were conducted in the same manner as the "immediate" fracture tests.

8.6.4 Ending Fracturing Tests

After conducting fracture tests the samples were removed from the cell. The periphery of these samples were always wet and soft. Muddy water could be seen around the pedestal of the cell and the rubber membrane and side filter papers were "coated" with soil. Soil also got stuck to the fingers while removing the samples from the pedestal of the cell. Since soil was lost, final moisture contents could not be determined accurately and hence were not determined. The top cap with its probe had to be pulled out of the sample which was invariably difficult. This signified that there had been a close contact between the brass sleeve of the probe and the walls of the borehole. The tops of the samples were also observed for any sign of wetness or water but were always found to be "dry" which further confirmed that the fluid had not escaped between the top cap and the tops of the samples. A few tests were rejected in which the fluid had escaped out of the sample and the top cap. Samples were checked visually for cracks. Tests conducted on samples with water as the injecting fluid had no visible cracks but they had a pipe formed through which water had escaped. In the case of the narrow diameter probe, the pipe was usually at about the mid height of the probe, whereas in the case of larger diameter probe the pipe formed just above the point where the brass sleeve was rounded to meet the probe. Very minute and small vertical cracks seem to be originating from these pipes. Various dyes were tried to observe the cracks but were not successful. Fluorecein was also tried and sliced discs of the samples were studied under ultraviolet light but it was impossible to detect a clear line of the crack. Looking down the borehole wall, two vertical cracks facing each other could be detected. Fractured samples were left to dry in air to check for any growth of cracks. On drying no cracks were observed in the case of

smaller diameter probe samples. In the case of larger diameter probe dried samples a near vertical crack extended from the hole upwards to the top of the sample and the same crack extended from the hole diagonally downward to the base of the sample. In contrast to the above observations, tests conducted on samples with paraffin always had visible vertical and radial cracks extending from the middle of the samples upwards. (These observations will be discussed in greater details in Chapter 10). Some samples were also broken up in the middle to observe the sand pocket. The walls of the borehole containing the sand pocket had a very irregular shape. The widest width across this irregular hole in the case of small diameter borehole was about 9-10mm and in the case of larger diameter borehole was about 19-20mm. Very fine cracks originating from the sand pockets were noticed. It was very difficult to check and measure the zone of wetness around the borehole but there was a zone which seemed to be wetter than the rest of the sample. The wetness of the zone would be different for different tests depending upon the duration of a test.

CHAPTER 9

TEST RESULTS

9.1 Introduction

This chapter describes the tests results of erosion and fracture tests. Basic classification and triaxial tests of puddle clay investigated are summarised in Appendix B.

9.2 Fracture Tests

The results of hydraulic fracturing tests carried out on various groups described in Table 8.4 are presented in a tabular form (Table 9.1 to 9.11) which give both the initial and fracturing states of these tests and the closure pressures.

Hydraulic fracturing tests carried out on 38mm diameter samples with a 6mm diameter sand pocket divided in Groups F1-A and F1-B at a rate of about 15 to 50 kN/m²/min respectively are summarised in Tables 9.1 and 9.2. The effect of the type of pressurising fluid on fracturing pressures was studied by Group F-2, in which paraffin oil was used instead of water on samples having the dimensions similar to Group F1-A. The results of these tests are summarised in Table 9.4. The effect of the size of the sand pocket in a 38mm diameter samples on the hydraulic fracturing pressures were studied by Groups F-3 and F-4 and the results are presented in Tables 9.5 and 9.6 respectively. One test from Group F-3 was conducted using paraffin oil as the pressurising fluid and the result is also presented in Table 9.5. A few "immediate" tests carried out on Groups F-1 and F-3 are summarised in Tables 9.1, 9.2 and 9.4. The effect of the overconsolidation ratio on the fracturing pressures was studied by Group F-5 and the results are presented in Table 9.7. The role of the rate effect on the fracturing pressures was investigated by some tests in Group F-3 and by tests in Group F-6 and the results are given in Table 9.5 and 9.8 respectively. The effect of the geometry of both the sample and the cavity on the fracturing pressures was investigated by Groups F-7 and F-8. In these groups, the samples had a diameter of 100mm but the cavity diameter in Group F-7 was similar to that of Groups F-3 and F-4, that is, of 16mm, whilst in Group F-8 was similar to Group F-1, that is of 6mm. The results of these groups are summarised in Table 9.9. A few "delayed" fracturing tests carried out on samples from Groups F1-B, F-7 and F-8 are presented in

Tables 9.3 and 9.10. The effect of stress ratio, σ'_v/σ'_h , on the fracturing pressures were studied by Group F-9 and the results are summarised in Table 9.11.

9.3 Pinhole Tests

Results of six pinhole tests on recompacted puddle clay from Cwmernderi Dam carried out at various initial water contents and water content history are summarised in Table 9.4.

9.4 Cylinder Dispersion Tests

The basic index properties for the different soils used for the cylinder dispersion tests are summarised in Table 9.12. Table 9.13 gives the pH values of different types of water used for these tests. The results of the cylinder dispersion tests carried out on samples of puddle clay and on various other soils, classified in various groups as described in Table 8.3, are presented in tabular form which describes both the type of pore and cylinder water used and the type of behaviour observed.

Tables 9.15 and 9.16 summarise the results of the tests carried out on puddle clay from the cores of the Cwmernderi and Gorpley Dams respectively. These tests were carried out using pore and cylinder water of distilled water, brine solution and reservoir water. Table 9.17 summarises the results of tests carried out on puddle clay from the core of Ramsden Dam. These tests were conducted using both distilled and reservoir water. Table 9.18 presents the results of tests on puddle clay from the cores of two dams and on various other soils. All the samples in these groups were reconstituted samples except those from King George V Dam which were extruded from "U-100".

CHAPTER 10

DISCUSSION OF RESULTS

10.1 Hydraulic Fracturing Tests

Hydraulic fracturing tests conducted here investigated fracturing under rapid application of fluid in a cylindrical cavity. These tests, called the initial fracturing tests, examined the effects of both the sample and cavity dimensions, the type of pressurising fluid, the rate of loading and overconsolidation ratio on initial fracturing pressures. The effect of stress ratio, σ'_f/σ'_u , on the initial fracturing pressure was also investigated. Tests were also conducted to study immediate and delayed fracturing and closure pressures. In-order to compare with the proposed theories outlined in Chapter 6, the fracturing tests have been evaluated as follows:-

i) Total stress conditions:

Condition 1: When s_u is mobilised at $r = a$

$$\sigma_f - \sigma_{ro} = s_u (1 - a^2/b^2) \quad (10.1)$$

Condition 2: When s_u is mobilised everywhere in the sample

$$\sigma_f - \sigma_{ro} = 2 s_u \ln (b/a) \quad (10.2)$$

Condition 3: Limiting value of $\sigma_\theta = 0$ at $r = a$

$$\sigma_f - \sigma_{ro} = \sigma_{ro} \left[\frac{1 - a^2/b^2}{1 + a^2/b^2} \right] \quad (10.3)$$

ii) Effective stress conditions

Condition 1: When $\sigma'_\theta = 0$ at $r = a$

$$\sigma_f = \sigma_r \quad (10.4)$$

Equation 10.4 can be rewritten as:

$$(\sigma_f - u_o) / \sigma_{ro} = 1 \quad (10.5)$$

Condition 2: When $(\sigma'_\theta/\sigma'_r)_t = K_a$ at $r = a$

$$\sigma_f - u_o = \frac{1}{(K_a - K_a x + 1 + x)} [2\sigma_{ro} - u_f (1 - x - K_a + K_a x)] - u_o \quad (10.6)$$

where $x = a^2/b^2$

Values of u_t would depend whether fracture occurs at yield or on the critical state line.

The above proposed theories are firstly compared with the experimental results of group F-1. From this comparison the theories that give the best fit are then compared with the experimental results of other groups of normally consolidated samples. This is to avoid unnecessary repetition. The above theories will be examined separately for overconsolidated samples.

10.1.1 Initial Fracturing Tests.

The investigation in the study of hydraulic fracturing in the laboratory was initiated by tests of group F1. A number of tests were conducted to study the influence of initial pore pressures, initial total and effective stresses and also to check the repeatability of the test results. Analysis of initial fracturing tests of group F1 are summarised in Tables 10.1 and 10.2. Comparison of the experimental results with the theoretical predictions are discussed below.

Fig. 10.1 (a) and (b) show that $\sigma_r - \sigma_{\infty}$ increases linearly with increasing s_u . It is clear from these plots that the gradients depend principally on the rate of loading. It was realised at an early stage that the rate used in Group F1-A was slow and hence was increased for the Group F1-B. The gradients of the experimental results are 1.43 and 1.65 for Groups F1-A and F1-B respectively. The gradients predicted by conditions 1 and 2 under total stress conditions are 0.98 and 3.69 respectively. These results show that these conditions do not predict the fracturing pressures correctly.

Comparisons of the experimental results with the theoretical analyses based upon total stress conditions 1 and 2 for various cavity and sample sizes are shown in Fig 10.1A and 10.1B. (The experimental results plotted in these figures are the average values of the groups studied). The plots show that $(\sigma_r - \sigma_{\infty})/s_u$ and $(\sigma_r - \sigma_{\infty})/2s_u$ depend on the geometry of the samples and increase with increase in $(1 - a^2/b^2)$ and $\ln(b/a)$ respectively as predicted. However, these conditions do not predict the experimental results. Condition 1 (ie., when s_u is mobilised at $r = a$) underpredicts whilst condition 2 (ie., when s_u is mobilised throughout the sample) overpredicts the experimental results.

Fig 10.2 shows that $(\sigma_r - \sigma_{\infty})$ is not a linear function of σ_{∞} . Various experimental values of $(\sigma_r - \sigma_{\infty})$ are obtained at a particular value of σ_{∞} . However, σ_r is always greater than σ_{∞} . Hence total stress condition 3 is not satisfied.

Figs. 10.3 and 10.4 show that $(\sigma_r - u_e)$ increases linearly with increasing σ'_{∞} . Comparing these two figures, it is again evident that the gradients depend on the rate of loading. The gradients of these results are 1.56 and 1.65 for Groups F1-A and F1-B respectively. In Fig 10.4, the experimental results are compared with the theoretical effective stress models.

This comparison shows that these models do not accurately predict the fracturing pressures. However, the drained shear failure model gives a better prediction than when $\sigma'_0 = 0$ at $r = a$. Comparison of the experimental results for various cavity and sample sizes with the effective stress models is summarised in Fig 10.4A. This plot shows that the prediction by the drained shear failure becomes poorer with an increase in the value of $(1 - a^2/b^2)$. Comparison of the experimental fracturing results with the proposed theories will be discussed in detail in section 10.1.6.

Various theories based upon total and effective stress conditions have been proposed and compared with the experimental results of Group F-1. From these comparisons it is seen that fracturing depends on both s_u and σ'_{rc} . However, under undrained conditions fracturing is best predicted when the drained strength of the sample is reached at the edge of the borehole. Although the total stress condition represented by the condition when s_u is mobilised at the edge of the borehole underpredicts the fracturing pressure, it would be interesting and worthwhile to investigate this condition further. Hence, these two above conditions, one effective (drained shear) and the other total stress (undrained shear), will now be further examined by studying other test groups. The role of s_u on fracturing will also be investigated by the tests conducted on overconsolidated samples. At the end of these studies, with more results, a critical review of these two proposed models will be carried out and the reasons for any inadequacy of the model will be discussed. The results of fracturing pressures in terms of total stress condition will be examined by plotting the experimental values of $\sigma_r - \sigma_{rc}$ against $s_u (1 - a^2/b^2)$ (Condition I.1). Thus the fracturing results of group F1-A are replotted as shown by Fig. 10.5.

After completing Group F-1 series of tests, further investigation in various factors influencing hydraulic fracturing was carried out as described below:

i) **Influence of Type of Cavity Fluid**

Group F-2 tests were conducted using paraffin oil as the cavity fluid. The purpose of these tests were to check the validity of rapid tests in which water was used as the cavity fluid. Paraffin oil being immiscible with clay would not penetrate and create any softened zone around the cavity and hence affect the test results (ignoring the effect of strain rate). If water were to penetrate the soil mass, then under similar conditions fracturing pressures

lower than those of Group F-2 would be obtained. The fracturing tests of Group F-2 are analysed in Table 10.3 and the results plotted in Figs 10.6 and 10.7. These plots show similar pattern as shown by Group F-1 tests results. $\sigma_t - u_o$ increases linearly with increasing σ'_o and has a gradient of 1.59. Similarly $\sigma_t - \sigma_o$ increases linearly with increasing $s_o (1-a^2/b^2)$ and has a gradient of 1.57. Both these plots pass through the origin. Fracturing pressures obtained in this group were found to be slightly less than the corresponding pressures for similar tests of Group F1-B. This was an unexpected finding. One of the possible explanations could be that during de-airing (whilst setting up the specimen), fractures around the cavity *may have been initiated into which both the sand grains and paraffin oil may have been forced*. Since paraffin will not be absorbed by the clay mass, the crack will not close during consolidation and hence would require a lower fracturing pressure to re-open. This explanation seems possible after observing and studying the results of test F2-8. The sample of this test was prematurely fractured during de-airing. Paraffin oil was seen issuing out of the middle of the sample. Instead of rejecting it, the sample was consolidated to a high effective stress of 400 kN/m², hoping that the crack would close. On testing a lower fracturing pressure was obtained as shown in Figs. 10.6 and 10.7. A low fracturing pressure was also recorded in test F2-9. This sample fractured horizontally along its middle even though the axial stress was greater than the radial stress. It seems very probably that the sample had fractured prematurely during the de-airing process. This fracture must have been small since paraffin oil did not issue out of the sample. Such premature fractures are also possible in samples tested with water, but these fractures would tend to close during consolidation since water would be absorbed by the surrounding soil mass. The fact that the paraffin oil would not penetrate and soften the soil mass around the cavity resulting in a lower fracturing pressure, may be confirmed by test F2-3. The time for fracturing for this test was comparatively greater than the other tests and yet its result lies to the average gradient of the other tests as shown in Figs. 10.6 and 10.7.

The other difference between this group and Group F-1 (and other groups in which water was used as the cavity fluid) was in the formation of cracks. Samples fractured using water had very short cracks and approximated to a circular pipe extending from the cavity radially to the outer face of the sample. These pipes were usually at about the mid height of the probe, but very occasionally also occurred close to the top of the sample just below the top cap. The fractured samples of Group F1 are shown in Plate II. The fractured samples of

Group F-2 had two discernable vertical and radial cracks in its middle (about 180° apart) often 10 to 30 mm along the length of the sample as shown in Plate III. This difference could be due to the dispersive nature of this clay in water (see Section 10.3). Initially a fine crack may be formed but water at high pressures would erode this clay to form a concentrated leak. Flow of water out of the sample will be restricted through this channel giving rise to a pipe. Furthermore, a crack formed in this sample would easily disappear due to water entering the clay matrix and also due to the smearing produced during the removal of the rubber membrane whilst dismantling the sample at the end of a test. This clay was not dispersive in paraffin oil. This was confirmed by immersing a slice of reconstituted sample of the clay in paraffin oil. The slice remained intact without any loss of fines and remained thus for a couple of days. Hence, this oil will not create a concentrated leak in the sample. The oil in the crack will not enter the clay mass and hence the crack will not close.

ii) **Influence of sample and cavity size**

The influence of sample and cavity size on the initial fracturing pressures was investigated by tests of Groups F-3, F-4, F-7 and F-8. Groups F-3 and F-4 tests were conducted on 38 mm diameter samples with a cavity of 16 mm diameter but with a cavity length of 25 mm in Group F-3 and of 35 mm in Group F-4. Analysis of the groups are summarised in Tables 10.4 and 10.5 and the results plotted in Figs. 10.8 and 10.9. These plots show a similar form of results to that of Group F-1 but with lower fracturing pressures at corresponding pressures. $\sigma_r - u_0$ increases linearly with increasing σ'_0 and has a gradient of 1.39. Similarly, $\sigma_r - \sigma_{r0}$ increases linearly with increasing of $s_v (1 - a^2/b^2)$ and has a gradient of 1.20. No significant difference is apparent from Figs. 10.8 and 10.9 between the test results of Group F-3 and F-4. The fractured samples of these groups initially had a pipe like crack similar to those from Group F-1, but on drying single large near vertical cracks were formed as shown in Plate IV.

Groups F-7 and F-8 tests were conducted on 100 mm diameter samples. The cavity in Group F-7 samples had a diameter of 16 mm and a length of 66 mm whilst Group F-8 samples had a diameter of 6 mm and a length of 25 mm. Analysis of these groups are summarised in Table 10.6 and the results plotted in Figs 10.10 and 10.11. $\sigma_r - u_0$ of Groups F-7 and F-8, as before, increases linearly with increasing σ'_0 and have gradients of 1.65 and

1.77 respectively. Similarly, $\sigma_t - \sigma_{ro}$ of Groups F-7 and F-8 increases linearly with increasing $s_v(1-a^2/b^2)$ and have gradients of 1.98 and 1.69. These samples had similar pipe-like cracks as those of Groups F-1. The vertical crack observed inside the cavity of a samples of Group F-7 is shown in Plate V.

The above tests clearly demonstrate that hydraulic fracturing pressure is dependent on the size of the sample and the cavity, but is not dependent on them if they (the dimensions) are considered separately but on the ratio of a/b (radius of cavity/radius of the sample). These results are summarised in Table 10.7 and plotted in Fig. 10.12 and 10.13. Both Groups F1-B and F-8 had a cavity radius of 3 mm and yet the average value of $\sigma_t - u_o$ obtained in Group F-8 was about 7% higher than those obtained in Group F1-B. Similarly, the average value of $\sigma_t - \sigma_{ro}$ obtained in Group F-8 was about 16% greater than that obtained in Group F1-B. The fracturing pressures obtained in Group F-7 were much higher than those obtained in Groups F-3 and F-4, even though these groups had a similar cavity radius of 8 mm. The increase was about 19% in the values of $\sigma_t - u_o$ and about 41% in the values of $\sigma_t - \sigma_{ro}$. The dependency of fracturing pressures on the ratio of a/b is demonstrated by the results of groups F1-A and F-7. The samples and the cavities of these groups had very different dimensions to each other but had the same a/b ratio (0.16). The results of these groups were similar. The relationships of fracturing pressures to the ratio of a/b are shown in Fig 10.12 and 10.13. These plots show a linear relationship with fracturing pressure increasing with decreasing a/b ratio. These plots show the behaviour as suggested by the proposed theories, that is, the fracturing pressure depends on the geometry of the borehole and the sample. (But not suggested by $\sigma'_o = 0$ model).

iii) Effect of overconsolidation ratio

The effect of overconsolidation ratio on the fracturing pressures was investigated by the tests of Group F-5. The analysis of these tests is summarised in Table 10.8 and the results plotted in Figs. 10.14 to 10.18. The results plotted in Fig. 10.14 and 10.15 show that both $\sigma_t - u_o$ and $\sigma_t - \sigma_{ro}$ decrease with an increase of overconsolidation ratio R_o . These plots, however, can not be used to compare fracturing pressures of these samples, because these samples, although have similar v_o have very different initial states and stress histories. For comparison these results have been normalised by σ'_{ro} as shown in Figs. 10.16 and 10.17. These plots show that both $(\sigma_t - u_o)/\sigma'_{ro}$ and $(\sigma_t - \sigma_{ro})/\sigma'_{ro}$ increase linearly with $\ln R_o$.

These plots also show that the samples with similar R_o and $p'_{o,}$ but having different $u_o,$ have similar normalised fracturing pressures. These samples also had a similar time to failure, $t_f,$ as shown in Table 9.7. The increase in the above normalised fracturing pressures with an increase in R_o is due to different pore water changes during the tests. Normally consolidated samples will fail with a large positive pore pressures whilst the heavily overconsolidated samples will fail with negative or decreased pore water pressures. The reduction in pore water pressure will increase with increasing $R_o.$ Examination of Fig. 6.6 indicates that the greater the decrease in pore water changes the greater the cavity pressure will be withstood by the sample. Lightly overconsolidated samples will behave as an elastic soil with no change in its pore pressure.

Fig. 10.18 shows that $\sigma_f - \sigma_{vo},$ normalised with the undrained shear strength values measured at peak and ultimate stress ratio (q'/p') decreases with an increase of $R_o.$ The decrease of $\sigma_f - \sigma_{vo}$ is much greater when normalised with the ultimate values of $s_u.$ These observations lead to a very different interpretation to the above discussion in which fracturing pressures were normalised by $\sigma'_{vo}.$ These plots (Fig. 10.18) do not take account of the initial conditions and stress history of the sample. Samples having similar v_o or s_u (mainly at the ultimate state) can have different fracturing pressures depending upon their stress history and on the pore water changes during the test. This finding suggests that fracturing of overconsolidated samples do not depend on s_u and can be better explained by effective stress theory.

iv) **Effect of rate of loading**

The influence of rate of loading on the initial fracturing pressure was investigated by certain tests of Group F-3 and by tests of Group F-6. The test results are analysed in Table 10.9 and 10.10 and the results plotted in Figs. 10.19 to 10.26 inclusive. These plots show that higher fracturing pressures are obtained at higher rates.

Group F-3 tests conducted to study the rate effect were conducted at similar $\sigma'_{vo} = 398$ kPa and at rates varying from 50 to 150 kPa/min. The results are plotted in Figs 10.19 and 10.20. A smooth curve is obtained showing a decrease in fracturing pressure with a decrease in the rate of loading which evidently increases the duration of the tests. The results indicate that a test conducted at a rate of 150 kPa/min which failed in about 1.3

minutes had $\sigma_t - u_o$ about 16% greater than a test conducted at 50 kPa/min which failed in about 11 minutes (this slow test was started with the probe pressure equal to u_o of the sample in order to increase the duration of the test and yet maintaining the rate commonly used in this research). The results also indicate that $\sigma_t - u_o$ obtained in the fast test was only about 3% greater than obtained in a test conducted at half the rate, i.e., at about 70 kPa/min which failed in about 2.3 minutes.

Group 6 tests were conducted at similar σ'_{vo} of about 245 kPa and u_o of 203 kPa with rates varying from 0.05 to 150 kPa/min. One test (F6-7) was conducted with probe (cavity) pressure maintained at the value of confining pressure. The results are plotted in Figs. 10.21 and 10.26. In all these plots smooth curves are obtained showing a decrease in both $\sigma_t - u_o$ and $\sigma_t - \sigma_{vo}$ with a decrease in rate of loading and with the increase of test duration. In these tests and those mentioned earlier, the reduced rates allowed partial drainage to occur so that the loading conditions were no longer fully undrained. This partial drainage resulting from the penetration of free water in the cavity creates softening of the soil mass adjacent to the cavity wall leading to decreased strength and increase in excess pore pressure generated during the test. On the other hand, in a faster test, due to strain rate effect there will be an increase in shear strength and a slower generation of excess pore water pressure. The results of test Group F-6 indicate that for a test duration in excess of about 4800 minutes ($\ln t_r = 8.48$) the tests were essentially fully drained, so that, at the cavity, total stresses and pore pressure were equal and effective stresses were zero.

"Stress-paths" followed by the slow tests F6-6 and F6-7 are plotted in Figs. 10.27 and 10.28 respectively. These effective "stress-paths" were determined using the pore pressure measured at the base of the sample. For these slow tests, these pore pressure readings can be assumed to be similar to that of the soil mass at the cavity wall. These paths, strictly speaking, are not exact but would not be far from expected paths. Moreover, they show the path followed by the soil mass at the edge of the cavity during the slow fracturing test. As mentioned earlier in Section 8.6.3 (Conduct of Fracture Tests) readings of the load cell and axial strain were also monitored during the fracture tests. Test F6-6 was carried out by increasing the cavity pressure at the rate of 0.05 kPa/min. and fractured in about 480 minutes, whilst test F6-7 was carried out by keeping the cavity pressure equal to the total radial stress of 451 kPa and allowing the pore pressure to increase. This sample failed in 4800 minutes (about 3.3 days). In both these tests, there was decrease of p' at almost

constant q' to the right of the critical state line. The apparent "stress-path" followed by the sample F6-6 during fracturing (that is, when the rubber membrane started bulging) is shown by the dotted line in Fig. 10.27, and fails when it reaches non-tension line, represented by $q'/p' = 3$. The onset of failure or fracture was fairly rapid. The "stress path" followed by sample F6-7 was easier to monitor (it was the slowest test) and again the failure occurred when an element of soil adjacent to the cavity reached the no-tension line. Since this failure was gradual it was possible to monitor the stress changes along the $q' = 3p'$ line as shown in Fig. 10.28. In this test, fracturing was initiated at a cavity pressure of 456 kPa. Fracturing took place gradually and the rubber membrane was observed bulging at various locations. The cracks observed in this sample were radial and vertical as shown in Plate VI. Fracture in form of a pipe (as observed in other tests in which water was used) were not observed in this sample. This could be due to very low values of $\sigma_t - \sigma_{\infty}$ in the cavity which was unable to erode the soil in form of a pipe.

The main conclusion provided by the above tests is that fracturing, under nearly fully drained conditions, occurs when $\sigma'_r = 0$ at $r = a$, ie., when the stress state of the sample reaches the no-tension cut-off, whilst fracturing under nearly fully undrained conditions, occurs when the drained strength of the soil is reached. The above observation and the results of the tests conducted under nearly fully drained conditions are different to those obtained by Savvidou (1981) in her experiments (section 3.3.8), where the onset of cracking was observed to occur to the right of the no-tension criterion.

v) **Effect of stress ratio σ'_r/σ'_a**

The effect of stress ratio σ'_r/σ'_a on the initial fracturing pressure have been investigated by tests of Group F-9. The analysis of these tests are summarised in Table 10.11 and the results plotted in Figs. 10.29 to 10.32 inclusive. All these tests had similar values of σ'_{∞} . Figs 10.29 and 10.30 show that $\sigma_t - u_o$ and $\sigma_t - \sigma_{\infty}$ increase with decreasing σ'_r/σ'_a values respectively. The tests results indicate that the sample with σ'_r/σ'_a of 0.4 had $\sigma_t - u_o$ about 16% greater than that of a sample with σ'_r/σ'_a of 0.8. This result was to be expected since the sample with a smaller ratio of σ'_r/σ'_a will have a higher value of p'_o and hence will

reach the critical state line at a point higher than that reached by the sample having a larger σ'_r/σ'_v , both the samples having similar values of σ'_{vo} . This observation should not be confused with K_o samples.

Fig. 10.31, as expected, shows that higher values of $\sigma_r - \sigma_{vo}$ are obtained for samples having higher values of s_u (s_u of samples F9-1 and F9-2 were determined using the plot of v_r against s_u as shown in Fig. B-17). However, if these values of $\sigma_r - \sigma_{vo}$ are normalised by their respective values of s_u , as shown in Fig. 10.32, it can be seen that the effect of s_u decreases with a decrease in σ'_r/σ'_v , and yet the sample with a lower σ'_r/σ'_v has a higher value $\sigma_r - u_o$ than the sample with a higher σ'_r/σ'_v . This observation suggests that s_u is not the controlling parameter of fracturing of samples having different stress history. Fracturing of such samples is controlled by effective stress.

10.1.2 Closure Pressure Tests

Closure pressure tests were carried out as explained in Section 8.6.3. The probe pressure was reduced until no more flow of fluid into the sample was observed. These tests were carried out on all the test groups and the results are included in Tables which give fracturing pressures for the various groups. The results for all the groups are summarised in Fig. 10.33.

From this plot, it can be seen that the closure pressure σ_c is nearly equal to the total confining or total radial stress. (Some closure pressures lower than total radial stresses were recorded in tests on 100 mm diameter samples). The results of these tests are supported by the tests conducted by Bjerrum and Anderson (1972) on laboratory triaxial samples. Vaughan (1971) conducted hydraulic fracture tests on the compacted clay cores of earth fill dams and concluded that for a crack in the vertical plan, the closure pressure was consistent with the likely minor principal stress in the core. Penman (1975) on the other hand, reported hydraulic fracture tests made near the total pressure cells embedded in the cores of two earth dams and concluded that the closure pressure was about 15% greater than the minor principal stress and about equal to the mean of the three principal stresses.

The closure pressure tests is now one of the methods used for measuring lateral stresses in soft clays. It offers a simple and practical way of monitoring stress changes in dam cores.

10.1.3 "Immediate" Hydraulic Fracturing Tests

"Immediate" fracturing tests were conducted soon after initial fracturing tests as described in Section 8.6.3. The results of these tests for Group F1-B and F-3 are summarised in Fig. 10.34. This plot shows that the "immediate" fracturing pressures were just above the initial total radial stresses. Once fracturing takes place the effective stresses in the soil adjacent to the crack become zero, the strength of the soil reaches a very low value and thus require very little pressure to re-open the crack. This phenomenon has a great implication in fracturing of dams. Any crack formed could be opened up further by a very small pressure applied by the reservoir water.

10.1.4 "Delayed" Hydraulic Fracturing Tests

"Delayed" fracturing tests were carried out as described in Section 8.6.3. The results of these tests on some tests of Group F1-B are analysed in Table 10.12 and plotted in Figs. 10.35 and 10.36 whilst those of Groups F-7 and F-8 are analysed in Table 10.13 and plotted in Figs. 10.37 and 10.38. These plots show a similar pattern as shown by the results of the initial fracturing tests on these groups, but with reduced fracturing pressures. These "delayed" tests gave values of $\sigma_t - u_o$ of about 3 to 8% lower than those registered during the initial fracturing tests and about 10 to 21% in the case of $\sigma_t - \sigma_m$. The fracturing pressures recorded during "delayed" tests of Group F1-B were much higher than those recorded during "immediate" tests of the same group. This demonstrates that if the stresses are increased after a crack has formed, a pre-existing crack can heal after a period of time. The healing effect may be attributed to reconsolidation as pore pressure changes generated during initial fracturing test dissipate. Healing of cracks due to increase in stresses has an important consideration for cracks formed during construction. Healing of such cracks formed in the laboratory will also depend upon the amount of erosion that may have taken place during initial fracturing tests.

10.1.5 Effect of Penetrating Fluid

Even though the tests were conducted at relatively fast rates, water will still penetrate the soil mass. This penetration, no matter how small it may be, will influence the stresses around the cavity. This effect can be examined by considering an increased radius of the borehole or the cavity as described in Section 6.5. The study was conducted on tests of Groups F1-B, F-3, F-4, F-7 and F-8. The results are summarised in Tables 10.14 to 10.16 and plotted in Figs. 10.39 to 10.41. [In the present study only the effect of fluid penetration on the values of $\sigma_r - \sigma_\infty$ was investigated. Similar procedures can be used to study this effect on the values of $(\sigma_r - u_o)$]. The gradient of the plots of test Groups F1-B, F-7 and F-8, after considering fluid penetrations was about 2 - 3% higher than the gradient of these groups where no effect of fluid penetration was considered. Similarly, the gradient of the plots of test Groups F-3 and F-4 was about 7% higher. This simple study shows that the effect of fluid penetration can be small in tests conducted rapidly in smaller boreholes but can be significant as the radius of the cavity with respect to sample size increases. As noticed from section 6.5 the depth of penetration will depend on the c_v values of the material.

10.1.6. Comparison of Experimental Fracturing results with the Proposed Theories

In Chapter 6, theoretical analysis regarding fracturing in boreholes based upon total and effective stresses were postulated. These theories were compared with the experimental results of Group F-1 in Section 10.1.1. From these comparisons it was concluded that fracturing was best predicted when the drained strength of the sample at $r = a$ was reached.

In Section 10.1.1 it was stated that out of all the fracturing conditions represented by total stress analysis, the condition in which s_u is mobilised at the edge of the cavity wall would be useful to investigate further. The availability of further fracturing results offers this opportunity. The test results of the present research show that for normally consolidated samples, $\sigma_r - \sigma_\infty$ increases linearly with increasing s_u ($1-a^2/b^2$) and depends principally on the geometry of the sample expressed as a/b . The values of $\sigma_r - \sigma_\infty$ were much higher than the prediction: the values varied from about 20% in Groups F-3 and F-4, 70% in Groups F-1B and F-7 and 98% in Group F-8. The predicted values of various test groups are

shown in Figs 10.5, 10.9 and 10.11. As mentioned earlier in Section 2.8, s_u is dependent on the rate of loading. From a series of tests carried out on this puddle clay to study the effect of strain rate of s_u , it was concluded in Section B.6 (Discussion of basic test results) that the undrained shear strength of a sample failed in hydraulic fracturing test in 1 minute would be about 31% higher than that under triaxial conditions. The strain rate effect does not offer a complete explanation of the theoretical observations. One of the reasons may be that the condition at which fracturing occurs may be somewhere between the condition at which s_u is mobilised at the edge of the borehole and the condition at which s_u is mobilised throughout the sample. This reason seems to offer the best explanation since some plastic annulus would develop around the edge of the borehole in which s_u would be much higher than that measured in the triaxial compression test. Thus, it can be said that these total stress models are not suitable in predicting fracturing pressures. Nevertheless, the first model (s_u mobilised at the edge of the borehole) gives a lower bound solution for normally consolidated samples. The role of s_u in overconsolidated samples is not straight forward and the present work suggests that the samples having similar values of s_u can have different $(\sigma_t - \sigma_\infty)$ values depending upon their stress history and initial stress conditions.

Comparisons of the experimental fracturing pressures of the normally consolidated samples with the results obtained using the proposed effective stress conditions are summarised in Table 10.17. The predicted values of various test groups by the drained strength failure model are shown in Figs 10.3, 10.8 and 10.10. Both these plots and the tabulated values (Table 10.17) show that the condition when the drained strength of the soil is reached at the edge of the borehole gives a better prediction than the condition when $\sigma'_e = 0$ at $r = a$. The prediction by the drained strength failure occurring at yield and at the critical state line (C.S.L.) are very similar. However, this model does not predict the experimental values accurately. One of the reasons may be that this model predicts the initiation of fracture at the edge of the cavity. The other reasons may be the inadequacy of the assumption made in the theoretical analysis. The theory does not take account of a plastic annulus around the cavity, where the stresses would be different to those given by the elastic theory. The strength of the rest of the intact sample may increase due to the rapid application of the water pressure in the cavity and hence would be able to withstand higher pressure before the crack can propagate throughout the sample. This explanation seems plausible when the experimental results of Groups F-3 and F-8 are compared with the predictions. In Group F-8 the ratio of a/b is much smaller than that of Group F-3 and the

difference in the experimental and the predicted values is much greater for Group F-8 than for Group F-3.

Comparison of the experimental fracturing pressures of the overconsolidated samples with the results obtained using the proposed effective stress conditions are summarised in Table 10.18 and plotted in Fig. 10.16. Pore pressures at failure (at C.S.L.) were assessed from the triaxial tests conducted on samples having similar stress history and initial conditions to that of the fractured samples. Both the plot and the tabulated values show that the condition when the drained strength of the soil is reached at the edge of the borehole gives a better prediction than the condition when $\sigma'_o = 0$ at $r = a$. The predictions by the drained strength failure at C.S.L. are closer to the experimental values than that by failure at yield. The predictions by the failure at C.S.L. gets better with an increase in R_r . One of the reasons for this may be that the increase in strength due to the rapid application of water pressure in the cavity gets less with an increase in R_r . This may be due to the rate of dilation which would increase with increase in R_r . The dilating element would suck in water from the surrounding soil elements and from the borehole and hence the conditions will no-longer be fully undrained.

From the comparison of experimental results with the proposed theories it is evident that hydraulic fracturing is an effective stress phenomenon. Under rapid application of water pressure, it occurs when the drained strength of the soil element at $r = a$ reaches the C.S.L. For fully drained conditions (ie., when the water pressure is applied at very slow rate) fracturing occurs when the soil element at $r = a$ reaches the no-tensions cut-off.

10.1.7 Comparison of Experimental Results with Theories proposed by others

The experiments carried out in this research were mainly concerned with the studies of hydraulic fracturing under a rapid application of water pressure, that is, when "undrained" conditions exist. In the review of the previous research in the study of experimental fracturing (see Chapter 3), mostly drained conditions were studied. Kennard (1970) also studied fracturing under undrained conditions. Comparison of the present experimental results with those derived using Kennard's criterion are tabulated in Table 10.17. This shows that Kennard's criterion agrees with the experimental results and gives better predictions than the proposed effective stress models. In Kennard's criterion, the soil was

assumed to behave elastically up to the point of fracture. Fracturing was assumed to occur when the circumferential effective stress was reduced to zero at $r = a$. The pore pressure changes in the soil element during the fracturing tests were estimated using Skempton's pore pressure parameter A_r . In the present research, σ'_θ reduces to zero only at the no-tension cut-off. Kennard's criterion, however, would not apply to heavily overconsolidated samples whose A_r would tend to have negative values.

In the analysis of drained tests, Savvidou (1981) also adopted a no-tension criterion at low effective stresses. However, her experimental results showed that the onset of cracking occurred in the region to the right of the no-tension criterion, whilst the present work suggests that cracking, under nearly fully drained conditions, occurs at about the no-tension failure line.

10.1.8. Results of Complementary Studies

The results of the finite element study (see Appendix C) are presented in Figs. 10.42 to 10.45. The results refer to plane strain sections only. Fig. 10.42 shows the variation of stresses with cavity water pressure increased at 50 kPa/min. It is clear from this figure that there are reductions in (effective) hoop, radial and mean stresses, and increases in total mean stress, pore pressure, deviator stress and stress ratio as the cavity water pressure was increased. The criterion which was satisfied was that of zero effective hoop stress; no peak is observed in the deviator stress and no elements reach critical state. Fig. 10.43 shows the radial variation in pore pressure response across the radius of the clay sample at the point of hydraulic fracturing (i.e., at $\sigma'_\theta = 0$). Fig. 10.44 shows the influence of rate on fracturing pressure. A smooth curve was obtained, asymptotic to the drained and undrained limits. This curve has a similar shape to the one obtained with the experimental results shown in Fig. 10.25. In Fig. 10.45, the plane strain and axisymmetric finite element analyses are shown together with the experimental results. It may be noticed from Fig. 10.44 that rates in excess of about 50 kPa/min (rate used in the laboratory tests) ensure that the fracturing pressure will be within 3% of the undrained value. Assuming the zero effective hoop stress criterion to be valid, the plane strain finite element results agree with the laboratory observations. It needs to be mentioned here that the soil parameters used in this study were based on the results of tests carried out in semi-automatic triaxial tests to which filter paper corrections were not applied, but it is thought that the difference would be minor.

Tam (1988) also carried out similar studies on the overconsolidated samples and the results summarised in Table 10-19 are compared with both the experimental results. Tam used the corrected soil parameters (as presented in this thesis) for the finite element studies. It can be seen from Table 10-19 that the plane strain finite element underestimates the fracturing pressures by 8 to 9% for samples having R_o from 2 to 6 and by 22% for sample having a R_o of 12.

The finite element studies generally give better predictions than the proposed models in this research. In the finite element studies, modified cam clay was used to model the clay behaviour. This model enables the soil to be modelled as an elasto-plastic material and enables both the stress and pore pressure changes due to cavity expansion to be determined. Fracture was assumed to occur at zero effective hoop stress which was not restricted to the no-tension cut-off as postulated in the proposed model (when $\sigma'_\alpha = 0$ at $r = a$).

10.2 Pinhole Tests

The results of dispersion tests on recompacted puddle clay samples from Cwmernderi Dam using the pinhole apparatus are summarised in Table 9.14. Test samples were manufactured in a number of ways including remoulding at natural water content and after drying and rewetting. Samples tested at natural water content and samples dried from natural water content to a moisture content equivalent to the plastic index were found to be non-dispersive under all heads. It took a couple of trials to punch a hole in the samples at natural water content of 40%. At this moisture content, the samples were very soft and hence the hole closed very quickly. Samples air dried, powdered and rewetted to moisture contents of 37 and 25% were found to be dispersive even under low heads. Distilled water was used for all these tests.

The difference in the erosion properties of the same soil with different types of water in its matrix could be due to the chemistry of the water. Clay samples classified as non-dispersive had reservoir water in its matrix while the dispersive samples were prepared with distilled water. However, it is known that the initial state of the sample can affect the test results (see Section 5.4.3). Due to the reasons discussed earlier in Section 5.5, further pinhole tests on other soils to be investigated were not attempted.

10.3 Cylinder Dispersion Tests

The results and types of erosion observed on samples of puddle clay from various dams and on various other soils are summarised in Tables 9.15 to 9.18 and discussed below. Each of the characteristic types of behaviour as described in Section 2.10 and illustrated in Fig. 2.4 was observed in these tests.

10.3.1. Cwmernderi Dam

Table 9.15 summarises the results of tests carried out on puddle clay from Cwmernderi Dam using different types of pore and cylinder water. It can be seen from this table that the clay was dispersive with distilled water in both pore water or free water. It was also dispersive with the appropriate reservoir water in both pore water and free water and also with the distilled water in pore water and reservoir water in free water. All these samples were classified dispersive of type D. In all these tests the characteristic *clouding of the water* started within less than 5 minutes from the start of the tests. The clouding started at the base of the sample and gradually the "dirty front" moved upwards. During this process, the sample was observed getting thinner as the particles were being detached from the sample. Within 30 minutes the water surrounding the sample had become completely dirty and the sample was no longer visible. The clay particles being dispersive were going into solution thus clouding the water. With clay particles no longer in the soil matrix, the non-clay particles fell to the bottom thus leading to the collapse of the sample. A test conducted on a sample with the distilled water in both pore water and free water and having an overconsolidation ratio of 3 (Test Group B-5, sample overconsolidated in the sample press) was also found to be dispersive with similar behaviour of dispersion as the other dispersive samples. It was thought that an overconsolidated sample might show a small true cohesion and hence may be erosion resistant. It is possible that the overconsolidation ratio was rather low. Much higher overconsolidation ratio could not be achieved with this type of sample press.

A completely different behaviour of this clay was observed when brine solution was used as either pore water or free water. Non-dispersive type C behaviour was observed when the samples made either with distilled water or brine solution were immersed into brine solution. The samples stayed intact without any sign of erosion and stayed thus even after

periods of several months. Non-dispersive type N behaviour was observed when a sample made in brine solution was immersed in distilled water. In this test some erosion was observed and the water at the base of the sample had become slightly dirty. However, the erosion which had been taking place very slowly stopped completely after a day. Most of the erosion was concentrated at the upper half of the sample. The sample collapsed in a month's time and the water had become clear. These tests clearly show the significance of the brine solution influencing the erosion resistance of this clay. It is apparent that the brine solution must have made the clay particles non-dispersive. In the tests which was classified as non-dispersive type N, there probably was not enough brine solution to make all the clay particles non-dispersive.

10.3.2 Gorpley Dam

Table 9.16 summarises the results of tests carried out on puddle clay from Gorpley Dam using different types of pore and cylinder water. Dispersive behaviour having elements of two types, N and D, was observed when a sample prepared using distilled water was immersed in distilled water. Characteristic clouding of the water, an indication of dispersive soils, was observed and in an hour the water surrounding the sample had become dirty and the sample obscured. After a month, when the water started getting clearer, the sample could be seen with about 60% of its original height intact with fines lying at the bottom and stayed thus even after periods of several months. This combined behaviour was possibly due to the grading of the soil containing dispersive clay together with non-clay grains. However, it is also possible that the free water had reached an equilibrium state with the clay and hence no longer making it dispersive. This could have been verified by changing the free water. Dispersive behaviour type D was observed when a sample prepared using appropriate reservoir water was immersed in distilled water. The behaviour was similar to that observed in other dispersive soils.

This clay was found to be non-dispersive type C when there was brine solution in either the pore water or free water. The sample stayed intact without any sign of erosion and stayed thus even after a period of several months. Non-dispersive type C behaviour was also observed when samples made in either distilled water or appropriate reservoir water was immersed in reservoir water. However, some particles were removed from the sample, but the free water did not acquire any dirty colour. These samples stayed intact even after a period of several months.

The above tests show the influence of both brine solution and reservoir water on the erosion resistance of the clay from Gorpley Dam. But a sample made with reservoir water and tested in distilled water was found to be dispersive possibly because the influence of the small quantity of reservoir water was masked by the larger quantity of distilled water.

10.3.3 Ramsden Dam

Table 9.17 summarises the results of tests conducted on puddle clay from Ramsden Dam. Dispersive behaviour having elements of two types, N and D, was observed when a sample prepared using distilled water was immersed in distilled water. Non-dispersive type N was observed when there was appropriate reservoir water in either the pore water or free water. Some erosion of the samples were observed and the sample eventually broke up but the free water was almost clear. The eroded or the detached particles and the broken part of the sample had settled at the bottom without dirtying the water. This clay was not dispersive but could be eroded or removed from a crack by the flowing water.

10.3.4. Various other Soils

Table 9.18 summarises the results of tests carried out on puddle clay from two dams and on various other soils. All these samples except those from King George V Dam, were prepared in distilled water and all of them were tested in distilled water. The samples of King George V Dam had reservoir water as pore water. Except the sample of Laterite, all samples were non-dispersive of types N and C. The characteristic clouding of the water, in the case of Laterite sample, was very distinct and occurred very rapidly. On the other hand, if there was no evidence of dispersion within a few hours or days then there was no evidence of dispersion after periods of several months and the samples were classified as non-dispersive type C. All these non-dispersive samples stayed intact in clear water. A sample of puddle clay from Lambeilethan Dam and a sample of Cowden Till were classified as non-dispersive type N. Some erosion of these samples were observed and they eventually broke up with water acquiring a very slight colour which soon disappeared. No erosion or dispersion of the broken sample was observed.

10.3.5 Index Properties of Soils Studied

Table 9.12 summarises the basic index properties of the different soil used in the present studies. An activity plot of PI(%) against clay content (%) is shown in Fig. 10.46. These results show that there is no obvious relationship between erosion resistance and index properties. However, a tentative observation may be drawn that the clays with Plastic Index greater than 30% are less likely to be susceptible to erosion or dispersion. Clays with Plastic Index less than 30% may either be dispersive or non-dispersive. However, these non-dispersive soils may experience "mechanical erosion" (see Section 5.1), that is, soil grains could be washed from the crack if the flow velocities are relatively large. pH values of water used for these tests is summarised in Table 9.13 and show that these values have no effect in influencing the dispersion or erosion resistance of the soil.

Typical examples of these three classes of behaviour are illustrated in Plate VII, VIII and IX. and IX.

CHAPTER 11

CONCLUSIONS

The research described in this thesis has investigated hydraulic fracturing and erosion of puddle clay in laboratory tests. The mechanism of hydraulic fracturing was examined in model tests on samples of puddle clay from the core of the Cwmernderi dam. Dispersion and erosion of soils in conditions similar to those in the walls of cracks was studied by a new tests called the cylinder dispersion tests.

For hydraulic fracturing tests, fluid pressures inside a cavity in a triaxial sample were raised relatively quickly so that fracture occurred under essentially undrained conditions. It was found that the hydraulic fracturing pressure ($\sigma_f - u_o$) in normally consolidated samples was a linear function of initial effective confining pressure (σ'_m) and passed through the origin. The gradient was found to depend on the geometry of the test samples. Fracturing pressure ($\sigma_f - u_o$) was found to increase with decreasing a/b ratio. Samples having different dimensions but with a similar ratio of a/b were found to have similar fracturing pressures. The fracturing tests also showed that in normally consolidated samples the fracturing pressure, ($\sigma_f - \sigma_m$), was a linear function of s_u of the sample and passed through the origin. The gradient, as before, was found to depend on the geometry of the test samples. Fracturing pressure, ($\sigma_f - \sigma_m$), was also found to increase with decreasing a/b ratio. The value of ($\sigma_f - \sigma_m$) could be up to twice the value of s_u as determined from conventional compression triaxial tests. The fracturing tests conducted here have showed that the fracturing pressure (σ_f) was not a linear function of the initial horizontal (confining) total pressure (σ_m) but was always greater than it. However, a linear relationship was found to exist when the results were plotted in terms of effective stresses. This observation underlies the importance of the initial pore pressure of the sample (in other words the effective stress).

Cracks formed in samples fractured using water were very short and approximated to a circular pipe. But the cracks formed in samples fractured using paraffin oil were vertical and radial, formed in the middle of the samples and were often 10 to 30 mm long. The differences in these two types of cracks were thought to be due to the dispersive nature of the clay in water. Tests conducted on samples with different R_o suggest that it was

necessary to take account of initial stress states and stress histories of the samples in order to interpret the fracturing results. This may be done by normalising fracturing pressures by the initial effective radial stress σ'_{r0} . It was found that the normalised fracturing pressures increase linearly with $\ln R_c$. Samples having similar v_o or s_u had different values of $\sigma_f - \sigma_{r0}$ depending on their stress history and on the pore pressure changes during the tests. These tests suggest that the fracturing pressure of overconsolidated samples under undrained conditions was best predicted by the drained strength for failure at the critical state line.

From the comparison of experimental results with the proposed effective stress models, it was found that the fracturing of the normally consolidated samples, under undrained conditions, was predicted by the drained strength for failure at either yield or at the critical state line. Fracturing of the overconsolidated samples, under undrained conditions, was best predicted by the drained strength for failure at the critical state line. The present research has shown that s_u is not the controlling parameter of fracturing of samples having different stress history. Fracturing is an effective stress phenomenon. The plane strain finite element studies (FES) which predicted fracturing when $\sigma'_o = 0$ at $r = a$ (but not necessarily at no tension cut-off) gave better predictions for both normally and overconsolidated samples than the effective stress models. FES predicted the fracturing pressure for normally consolidated samples within 3% but underestimated the fracture pressure for the overconsolidated samples by 8 to 22%. The difference increased with an increase of R_c .

Fracturing pressure was found to decrease with a decrease in rate of loading and with the increase in test duration. The reduced rates or increase of test duration allowed partial drainage to occur in the soil around the cavity wall so that the tests were no long fully undrained. This partial drainage resulting from the penetration of free water in the cavity leading to generation of high excess pore pressure will modify the stresses around the cavity thus lowering the soil strength and subsequently the fracturing pressures. Apparent "stress paths" followed by two slow tests (F6-6 and F6-7) suggested that fracturing under drained conditions occurs at the no-tension line represented by $q = 3p'$.

In all the fracturing tests, closure pressures were found to be equal to the total confining or radial stresses. Immediate hydraulic fracturing pressures were found to be slightly

greater than the initial total radial stresses. The delayed fracturing tests showed that the samples will heal to a greater extent depending upon the amount of soil eroded from the crack and also upon the extent of delay. This healing effect may be attributed to reconsolidation as pore pressure changes generated along the crack during the initial fracturing tests dissipate. A few tests conducted in the present investigation to study the effect of σ'_r/σ'_v on fracturing pressures suggest that fracturing pressures increase with decreasing values of the stress ratio σ'_r/σ'_v . The effect of penetrating fluid can be taken account of by considering an increased radius of the borehole. This increase radius is a function of both the duration of the test and the c_v of the soil. The theoretical studies carried here showed that the effect of the penetrating fluid can be minimal in tests conducted rapidly in smaller diameter boreholes.

Erosion tests were carried out using the cylinder dispersion method on a number of different soils including samples of puddle clay from British embankment dams. The results of these tests have demonstrated the major influence of pore water chemistry on the true cohesion and dispersion properties of the soils. This test, which has an advantage over the current tests for erosion determination (e.g. crumb, pin-hole etc) since it employs saturated samples, has the potential as a method for examining dispersion and erosion of soils. It has a sound theoretical basis and gives a qualitative measure of true cohesion.

The main objective of this research was to study hydraulic fracturing under rapid application of water pressure. This was prompted since many dams failures attributed to hydraulic fracturing were initiated by rapid filling of reservoirs. Whilst this objective seems to have been accomplished it has given rise to further questions that need investigation.

- i) It would be necessary to verify and check the validity of the proposed models for other soils. This would require carrying out similar tests.
- ii) All the tests were carried out where σ'_v was greater σ'_r . It would be interesting to carry out tests where σ'_v is less than σ'_r . These tests will also give an opportunity to check whether the direction of cracks is still perpendicular to the minimum principal stress, and also to check the applicability of the proposed model for such cases.

- iii) Hydraulic fracturing tests carried out in this research were essentially isotropic with q' value being around 20 kN/m^2 . For further understanding of hydraulic fracturing it would be necessary to carry out tests under K_0 conditions or with varying σ'_1/σ'_3 ratios.
- iv) The proposed theory or the experiments carried out here did not take account of arching, zones of low stresses and stress redistribution which will result from reservoir impoundment. These conditions may be difficult to model in the laboratory and probably will require use of some sort of numerical studies.

In all the cylinder dispersion tests performed here no provision was made to change the free water after some interval. There is a possibility that free water could reach an equilibrium state with the sample and hence stop any further change in its erosion characteristics. Such provision would be an improvement to the tests. It would be interesting to relate the cylinder dispersion tests with the mineralogy and chemistry of the soil and with soils from dams which have already suffered erosion. Another factor that may have some bearing on these laboratory tests is the effect of temperature. Temperatures in a dam will not be expected to be around 20°C - the temperature at which the laboratory tests are conducted. It would be worth while carrying out tests at the temperature range likely to be experienced in the field.

APPENDIX A

REASONS FOR THE METHOD ADOPTED FOR INDUCING HYDRAULIC FRACTURE IN TRIAXIAL SAMPLES

Before starting the programme of fracturing tests it was necessary to select a technique for inducing hydraulic fracture in triaxial samples. Hydraulic fracture would be initiated by high water pressures acting in the middle of a sample, and hence a probe was designed with which water pressure could be applied in a sample. This further required selection of a technique for placing the probe in the middle of a sample. The various techniques tried are listed below.

- a) The probe was simply pushed into the middle of the sample with the help of the equipment described in Section 7.9.4. Initially the soil travelled up the probe which was then removed. The process was repeated until no more soil blocked the probe. The sample was set up in the triaxial cell. Trapped air in the probe was expelled by pushing a small amount of water into the probe by slightly increasing the probe pressure above the cell pressure. The sample was then brought to a certain stress state and tested rapidly. In many cases samples could not be fractured. On removing the probe it was found to be blocked with a clay plug which must have travelled up into the probe during consolidation and application of cell pressure. This method clearly was not suitable.
- b) The above technique was repeated using a probe which was closed at the tip and which had two small holes punched in the circumference of the probe at about 180 degrees. The problem of blockage was again encountered. This method was also abandoned.
- c) Another technique tried was to attach a small cylindrical fine porous stone to the end of the probe. The porous stone was placed in the pre-drilled hole and back filled with a slurry. The flow of water through the stone was very small and not enough to create and propagate fracture and hence not suitable for rapid fracture tests.

In order to produce a relatively large flow to propagate a crack a much coarser porous stone would be required. It would be very difficult to manufacture such a stone for a 38 mm diameter samples.

At this stage of research it was felt that none of the above techniques would simulate the conditions required for hydraulic fracture in embankment dams. Except the porous stone, none of the above techniques would create a discontinuity in the sample. It is known that hydraulic fracture is initiated by water pressure acting in some discontinuities or pre-existing cracks in the core of an embankment dam. To simulate this condition in the laboratory a borehole is required. It is also necessary, in the writer's opinion, that the borehole should not be smooth faced but should have an irregular face. Such a borehole would then represent the true condition prevailing in dams. These conditions would be met by compacting a pocket of sand in the clay sample. Thus the method adopted for this research was to place the end of the probe in the middle of a sand pocket in the middle of a sample. This method also had a few problems, described below, which needed development.

Initially the procedure used was to excavate a borehole, place a sand pocket to the required depth and then back fill it with slurry of puddle clay. The probe was then pushed through the slurry into sand. Initially the slurry would fill the probe which was removed. This process was repeated until no more slurry entered the probe. This method was not suitable since the probe did get blocked occasionally. This problem was solved by providing a knurled brass sleeve of required length to the probe. The sleeve had a diameter similar to that of the probe hole. This brass sleeve would fill the hole above the sand pocket.

The material used was Leighton Buzzard Sand. Various types of sands from fine to coarse were tried but Leighton Buzzard sand was found to be the most suitable. It did not block the probe and allowed water to flow freely thus enabling pressure to be applied to the borewall.

Fracturing tests were conducted on reconstituted samples. Reconstituted samples were preferred since all such samples would initially be similar.

APPENDIX B

Basic Results Of Soil Properties And Triaxial Tests On Puddle Clay.

B.1 Introduction

This section describes the index and classification tests, undrained compression tests on both normally consolidated and overconsolidated samples, undrained extension tests on normally consolidated samples, and the effect of rate of loading on the undrained shear strength of puddle clay samples from Cwmernderi Dam.

B.2 Classification and Index Properties

Results of the classification and index properties carried out according to BS 1377 (1975) are summarised in Table B.1.

B.3 Isotropic Compression and Swelling Characteristics

Both the isotropic compression and swelling results of the puddle clay tested are shown in Fig B.1 plotted in $v - \ln p'$ space, and the characteristics are summarised in Table B.4.

B.4 Undrained Compression and Extension Tests

Ten undrained compression and three undrained extension tests to study the properties of puddle clay from the Cwmernderi Dam were carried out. Six of these tests were on normally consolidated samples failed in compression, four tests were carried out on overconsolidated samples failed in compression and three tests were on normally consolidated samples failed in extension. The classification and the rates of loading of these tests is described in Table 8.1 and the results are summarised in Tables B.2 to B.4. A correction for filter paper of $(\sigma_v - 10) \text{ kN/m}^2$ has been applied for the compression tests (Head, 1987). A series of tests were carried out to study the effect of rate of loading on the undrained shear strength and the results are presented in Table B.5.

B.5 Relationship of Axial Stress, Pore Pressure and Deviatoric Stress with Shear Strain

The behaviour of axial stress and pore pressure during compressing tests of both the normally consolidated and overconsolidated samples are plotted against shear strain in Figs B.4 and B.5. The deviatoric stress-strain characteristics of all the samples tested both in compression and extension tests are plotted in Figs B.6 to B.9.

B.6 Discussion of Basic Test Results

A detailed discussion of test results is not required here and only the essential features relevant to this research are discussed.

The sample was a dark grey brown clay having a particle size distribution of 34% clay, 56% silt and 10% sand. According to the unified soil classification system the sample was inorganic clay of intermediate plasticity (CL). The activity of the puddle clay was 0.71. From the plot of PI(%) against clay percentage, the puddle clay tested consisted mainly of illite minerals.

One of the fundamental features of the critical state soil mechanics is the normal consolidation line, and reconstituted samples having a similar history of production would be expected to have a similar normal consolidation line. For analyses the values of specific volumes at the start of shearing, v_o , were adjusted so that the starting state fell on same normal consolidation line as shown in Fig B.2. This adjustment of v was of the order of 0.02. The tests gave values for the compression and swelling parameters $\lambda=0.120$, $\kappa=0.030$ and $N=2.390$.

The plot of u_o against shear strain in Figs B.4 and B.5 show the typical behaviour of normally consolidated and overconsolidated samples during undrained shearing. Normally consolidated samples tested in compression gave on average value of A_r of 0.82. Stress strain characteristics of all normally consolidated samples are shown in Figs B.6 to B.8 and do not indicate well defined peaks thus corresponding to a behaviour commonly associated with such soils. The absence of well defined peaks is also supported by the relationship between stress ratio and shear strain in Figs B.13 and B.14 (a). Stress-strain characteristics

of overconsolidated samples are shown in Fig B.9 which also do not show well defined peaks. However, the peaks are defined in Fig B-14 (b) which shows the relationship between stress ratio and shear strain. The peaks are better defined in the case of samples having overconsolidation ratios of 6, 8 and 12 than the sample having an overconsolidated ratio of 2. In all the tests the deviator stress increases in the initial stages. About 65 - 70 % of the maximum deviator stress reach at ϵ_s of about 1% after which the ratio of the increase in the deviator stress with incremental strain is low and the stress-strain curves become more or less parallel to the strain axis. Comparing compression and extension results, it is noticeable that at ultimate state, q' reached in extension tests is lower than that reached in compression tests.

The effective stress paths followed by the samples during compression and extension tests are plotted in $q' - p'$ space and are shown in Figs B.10 to B.12. From these plots it can be seen that the positions of the effective stress path depends on the magnitude of the pre-shear consolidation pressure. The effective stress paths of normally consolidated samples are of similar shape and show a tendency to move up along the critical state line. This tendency is much more apparent in the stress paths of samples tested in semi-automatic triaxial cell. In this region both p' and q' increase, but the stress ratio, q'/p' (Figs B.13 and B.14a) reaches a constant value. A possible explanation, according to Atkinson and Little (1985), is that, although samples are tested at constant volume, there are local volume changes. These may occur due to non-uniform stresses arising from platen restraint. This process will decrease the specific volume and increase p' and hence this part of the sample, which may have thickness of few grains of the soil, will get stronger than its neighbour. The front will then move outwards resulting in a stronger sample than when it was first reaching critical state. The specific volume during an undrained test is assumed to be constant and hence a slight change in specific volume due to the above process is not registered. It is interesting to mention here that according to Atkinson and Little (1985) for a soil with a value of $\lambda=0.1$, a change of 1% in moisture content can theoretically lead to difference in p' between two points on the C.S.L in the order of 25%. Due to this phenomenon the critical state strength is not clearly defined and hence difficulties can arise in obtaining consistent values for undrained strength. The stress paths of samples tested in automatic triaxial cell, except of sample C1, have a hook at the end of their paths showing a slight decrease in q' at constant p' . The effective stress paths of the overconsolidated samples, tested at similar specific volume, show characteristic

behaviour according to their overconsolidation ratio, however, the paths end at a decreasing q' with an increasing overconsolidation ratio. This phenomenon was discussed in Section 2.6.

The ultimate state points of all the samples lie very close to the ultimate or critical state lines. In $q' - p'$ space as shown in Fig B.15, the critical state lines pass through the origin. The compression and extension frictional parameters $M_c=1.20$ and $M_e=0.89$; these correspond to friction angles $\phi'_c=30^\circ$ and $\phi'_e=31.5^\circ$ respectively. In $v_t - \ln p'_t$ plot, shown in Fig B.3, the ultimate state points for both compression and extension tests fall on an unique critical state line. This critical state line is straight and parallel to the isotropic consolidation line with $\Gamma=2.338$. A summary of the results at the ultimate states is given in Table B.4.

The undrained shear strength, s_u , is given as $\frac{1}{2}(\sigma'_s - \sigma'_t)$ at the ultimate state and the values for the samples tested are summarised in Tables B.2 and B.3. From these tables, it can be seen that for the overconsolidated samples tested at similar specific volume the undrained strengths are very close to each other and are also close to the strength of a normally consolidated sample at the similar specific volume. Figs B.16 and B.17 show the variation of undrained shear strength with consolidation pressure and specific volume of normally consolidated samples. These show characteristic relationship for clay soils. For normally consolidated samples, tested in compression, the ratio s_u/p'_o is 0.38, (This ratio is used in determining the strength of the samples in the fracturing tests). Table B.5 and Fig B.18 shows the variation of the ratio s_u/p'_o with time to failure for normally consolidated samples. This variation is a characteristic property of clay soils. It can be noticed that at 0.5% axial strain, the sample (ST-1) which finally failed in about 3 minutes had a strength about 77% higher than the sample (C-1) which failed in about 4 days at similar strain. But at the end of the test, the sample ST-1 had an undrained strength of only about 16% higher than the sample C-1 at that stage. Fig B.19 shows the value of s_u/p'_o at the ultimate state of a sample brought to failure 1 minute which is about 25% higher than brought to failure in about 96 hours. If, on average the shear strength under plane strain conditions is about 5% higher than that under triaxial conditions (see Section 2.8), then the undrained strength of a sample failed in a hydraulic fracturing test conducted in 1 minute would be about 31% higher than that under triaxial conditions.

B.7 Summary of Laboratory Test Results

The laboratory testing carried out has shown that the puddle clay of Cwmernderi Dam is an organic clay of intermediate plasticity. A set of critical state parameters for the reconstituted samples of this clay have been derived and these are summarised in Table B.4. Tests were also conducted to study the effect of rate of loading on the undrained shear strength in order to interpret hydraulic fracturing tests. From these tests it was found that the undrained strength of a sample brought to failure in 1 minute in a hydraulic fracturing tests could have strength about 31% higher than the sample tested in a triaxial cell in about 96 hours.

APPENDIX C

Complementary Numerical Studies

Laboratory fracturing tests described here were simulated with finite elements implementing Biot's consolidation theory together with an elasto-plastic strain hardening constitutive model. Both diametral (axisymmetric) and plan (plane strain) sections were modelled. This study was carried out at City University and the details were reported by Tam, Mhach and Woods (Innsbruck 1988). The computations were performed using the CRISP finite element method. Modified cam-clay was used to model the clay behaviour. An elastic perfectly plastic (Mohr-Coulomb) model was used for the sand in the cavity. In the numerical studies, fracturing was deemed to have occurred as soon as one of the following criteria was satisfied in the clay elements near the cavity: a) soil reaches critical state, b) shear stress achieves maximum value and c) effective hoop stress becomes zero. The results of these numerical studies and their comparisons with the experimental results are discussed in section 10.1.8.

REFERENCES

- Aitchison G. D., Ingles O. G. and Wood C. C. (1963) "Post-Construction Deflocculation as a Contributory Factor in the Failure of Earth Dams", 4th Australia-New Zealand conf on S.M. & F.E. pp 275-279.
- Aitchison G.D, and Wood C. C. (1965) "Some Interaction of Compaction, Permeability and Post-Construction Deflocculation Affecting the Probability of Piping Failure in Small Earth Dams" 6th Int. Conf. S.M. & F.E Vol 1.
- Arulanandan K, Loanathan P and Krone R.B. (1975) "Pore and Eroding Fluid Influences on Surface and Erosion in Soil" *Jnl. of Geot. Eng. Div., ASCE*, Vol 101, No. GT1 pp 51-66.
- Arulanandan K and Perry E.B. (1983) "Erosion in Relation to Filter Design Criteria in Earth Dams" *Jnl. Of Geot. Eng., ASCE*, Vol 109, No. 5 pp 682-698.
- Atkinson J.H. (1985) "Simple and Inexpensive Pressure Control Equipment for Conventional and Stress Path Testing of Soils" *Geotechnique* 35, No. 1, pp 61-63.
- Atkinson J.H. and Bransby P.L. (1978) "The Mechanics of Soils" McGraw - Hill, London.
- Atkinson J.H, Evans J.S. and Ho E.W.L (1985) "Non-uniformity of Triaxial Samples due to Consolidation with Radial Drainage" *Geotechnique* 35, No. 3 pp 353-355.
- Atkinson J.H., Evans J.S. and Scott C.R. (1985) "Developments in Microcomputer Controlled Stress Path Testing Equipment for Measurement of Soil Parameters" *Ground Engineering*, pp 15-22.
- Atkinson J.H. and Little J.A. (1985) "Undrained Triaxial Compressive Strength of Reconstituted and Undisturbed Samples of a Till from the Vale of St. Albans" *Geot. Eng. Res. Report GE/85/16* The City University, London.
- Atkinson J.H. and Richardson D (1987) "The Effect of Local Drainage in Shear Zone on the Undrained Strength of Overconsolidated Clay" *Geotechnique* 37, No. 3, pp 393-403.

- Binnie G.M. (1978) "The Collapse of the Dale Dyke Dam in Retrospect" *Quarterly Jnl. of Geology*, Vol 1, No. 4, pp 305-324.
- Binnie G.M. (1981) "Early Victorian Water Engineers" Thomas Telford, London.
- Berre T (1985) "Plane Strain and Ordinary Triaxial Tests on Plastic Clay from Drammen" *Int. Report NO. 50301-10, NGI*.
- Berre T and Bjerrum L (1973) "Shear Strength of Normally Consolidated Clays" *Proc. 8th Int. Conf. S.M. & F.E., Moscow, Vol. 1.1, pp 39-49*.
- Bishop A.W. (1966) "The Strength of Soils as Engineering Materials" *Rankine Lecture, Geotechnique 16, pp 91-128*.
- Bishop A.W. and Henkel D.J. (1962) "The Measurement of Soil Properties in the Triaxial Test". Edward Arnold Ltd, London.
- Bishop A.W. and Wesley L.D. (1975) "A Hydraulic Triaxial Apparatus for Controlled Stress Path Testing" *Geotechnique 25, No. 4, pp 657-670*.
- Bjerrum L and Anderson K.H. (1972) "In-situ Measurement of Lateral Pressures in Clay" *Proc. 5th European conf. S.M. & F.E., Vol 1, pp 29-38*.
- Bjerrum L, Nash J.K., Kennard R.M. and Gibson R.E. (1972) "Hydraulic Fracturing in Field Permeability Testing" *Geotechnique 22, No. 2, pp 319-332*.
- Bjerrum L, Simon N and Torblaa I (1958) "The Effect of Time on the Shear Strength of a Soft Marine Clay". *Proc. Brussels conf. on earth pressure problems, Vol 1, pp 148-158*.
- British Standards Institution. *Methods of Testing Soils for Civil Engineering Purposes BS1377:1975*.
- Carlyle W.J. (1965) "Shek Pik Dam". *Proc. ICE (London) Vol 30, pp 557-588*.

- Charles J.A. (1984) "Embankment Dams and Reservoir. Safety in Britain; Floods, Slides and Internal Erosion".. BNCOLD conf. on safety of dams, pp 51-68.
- Charles J.A. and Boden J.B. (1985) "The Failure of Embankment Dams in the U.K." Failures in earthworks Telford, London, pp 181-202.
- Charles J.A. and Watts K.S. (1987) "The Measurement and Significance of Horizontal Earth Pressures in the Puddle Clay Cores of Old Earth Dams" Pro. ICE (U.K.) Part 1, pp 123-152.
- Clinton D.B. (1986) "User Manual for Triax and Triax +" Geot. Eng. Res. Report GE/86/14. The City University, London.
- Cole B.A. and Liggins T.B. (1976) "Dispersive Clay in Irrigation Dams in Thailand" Dispersive clays, related piping and erosion in geotechnical projects. ASTM, Special Technical Publication, STP 623,pp 25-41.
- Coumoulos D.G. (1976) "Experience with the Studies of Clay Erodibility in Greece" Dispersive clays, related piping and erosion in geotechnical projects, ASTM, STP 623, pp 42-57.
- Craft C.D and Acciardi R.G (1984) "Failure of Pore Water Analysis for Dispersion" Jnl. of Geot. Eng. ASCE, Vol 110, pp 459-472.
- Decker R.S. and Dunnigan L.P. (1976) "Development and Use of the Soil Conversation Dispersion Test" Dispersive clays, related piping and erosion in geotechnical projects. ASTM, STP 623, pp 94-109.
- Forsythe P (1976) "Experiences in Identification and Treatment of Dispersive Clays in Mississippi Dams" Dispersive clays, related piping and erosion in geotechnical projects. ASTM, STP 623, pp 135-155.
- Francq J and Post G (1976) "Laboratory Testing on High Sodium Non-dispersive Clays are Related to the Repair of a Clay Dam in Algeria " Dispersive clays, related piping and erosion in geotechnical projects. ASTM, STP 623, pp 156-171.

- Graham J, Crooks J.H.A and Bell A.L. (1983) "Time Effects on the Stress-strain Behaviour of Natural Soft Clays". *Geotechnique* 33, No. 3, pp 327-340.
- Haimson B (1968) "Hydraulic Fracturing in Porous and Non-porous Rock and its Potential for Determining In-situ Stresses at Great Depths" Phd thesis, Univ. of Minnesota.
- Head K.H. (1987) "Manual of Soil Laboratory Testing" Vol. 3, Effective stress tests. Pentech Press, London.
- Heede B.H. (1971) "Characteristics and Process of Soil Piping in Gullies" Rocky Mountain Forest and Range Experiment Station, Forest Service, U.S. Dept. of Agriculture, paper RM-68 pp 1-15.
- Henkel D.J. and Wade N.H. (1966) "Plane Strain Tests on a Saturated Remoulded Clay" *Jnl. of S.M. & F.D. ASCE*, SM6 pp 67-81.
- Holmgren G.G.S. and Flangan C.P. (1976) "Factors Affecting Spontaneous Dispersion of Soil Materials as Evidenced by the Crumb Test" Dispersive clays, related piping and erosion in geotechnical projects. ASTM, STP 623 pp 218-239.
- Ingles O.G. (1972) "Discussion on Piping in Earth Dams of Dispersive clays" Proc. ASCE conf. Performance of earth and earth supported structures. S.M. & F.D., Vol 3, pp 105-130.
- Independent Panel (1976) "Failure of Teton Dam" Report to US Dept. of Int. and State of Idaho. US. Govt. Printing Office, Washington.
- Jaworski G.W., Duncan J.M and Seed H.B. (1979) "An Experimental Study of Hydraulic Fracturing" Univ. of California, Dept. of Civil Eng. Berkeley, California.
- Jaworski G.W, Duncan J.M and Seed H.B. (1981) "Laboratory Study of Hydraulic Fracturing" Proc. ASCE, Vol 107, No. GT6, pp 713-732.
- Jaeger J.C. and Cook N.G. (1971) "Fundamentals of Rock Mechanics" Chapman and Hall Ltd, London.

Kassiff G and Henkin E.N. (1967) "Engineering and Physicochemical Properties Affecting Piping Failure of Low Loess Dams in the Neger" Proc. 3rd Asian Regional conf. S.M & F.E, Vol 1, pp 13-16.

Kennard R.M. (1970) "The Measurement of Soil Permeability In-situ by Constant Head Test" Phd Thesis, Univ. of London.

Kjaernsli B and Torblaa I (1968) "Leakage through Horizontal Cracks in the Core of Hyttejuvet Dam" N.G.I. Publication No. 80.

Lambe T.W. and Whitman R.V. (1969) "Soil Mechanics" M.I.T., John Wiley and Sons, Inc.

Lau W.H.W, (1988) "The Behaviour of Clay in Simple Shear and Triaxial Test" Phd. Thesis, City University.

Leonard G.A. and Davidson L.W. (1980) "Reconsideration of Failure Initiating Mechanism for Teton Dam" *Int. Conf. on case histories in Geot. Eng.* Vol 3, St. Luis, pp 1103-1113.

Leonard G.A and Narain J (1963) "Flexibility of Clay and Cracking of Earth Dams" *Jnl. of S.M. & F.D., ASCE, S.M.2.* pp 47-98.

Lofquist B (1951) "Earth Pressure in Thin Impervious Core" *Trans. 4th Int. Congress on large dams, New Delhi, Vol 1,* pp 99-108.

Lofquist B (1957) "Discussion on Cracking in Earth Dams" *Proc. 4th Int. Conf. S.M. & F.E.* Vol 3, pp 261-262.

Maschi F.D., Espey W.H and Moore W.L. "Measurements of the Shear Resistance of Cohesive Sediments". *Federal Inter-Agency Sediments Conf. Proc. Agricultural Res. Service, Publications No. 970, Washington D.C.,* pp 151-155.

Massarsch K.R. (1978) "New Aspects of Soil Fracturing in Clay" *Jnl. Geot. Eng. Div., ASCE, GT8,* pp 1109-1123.

Massarsch K.R. and Broms B.B. (1977) "Fracturing of Soil Caused by Pile Driving in Clay" 9th Int. Conf. S.M & F.E., Vol 1/40, pp 197-200.

McDonald L.A., Stone P.C. and Ingles O.G. (1981) "Practical Treatments for Dams in Dispersive Soil" 10th Int. Conf. S.M. & F.E., Vol 2, pp 335-360.

Mesri G and Ali S (1988) "Discussion on Hydraulic Fracturing in Embankment Dams" Jnl. of Geo. Eng. ASCE, Vol 114, No. 6, pp 742-746.

Middlebrooks T.A. (1953) "Earth Dam Practice in the USA" Trans. AM. Soc. Civil. Eng. Centennial Volume, pp 697-722.

Morgenstern N.R. and Vaughan P.R. (1963) "Some Observations on Allowable Grouting Pressures" Grouts and Drilling Muds, I.C.E., London, pp 36-42.

Nobari E.S., Lee K.L. and Duncan J.M. "Hydraulic Fracturing in Zoned Earth and Rock Fill Dams" Report No. T.E. 73-1, University of California, Berkeley.

O'Reilly M.P., Brown S.F. and Overy R.F. (1989) "Viscous Effects Observed in Tests on Anisotropically Normally Consolidated Silty Clay" Geotechnique 39, Vol 1, pp 153-158.

Peterson R and Iverson N.L. (1953) "Study of Several Low Earth Dam Failures" Proc. 3rd Int. Conf. S.M. & F.E. Switzerland, pp 273-276.

Penman A.D.M. (1975) "Earth Pressures Measured with Hydraulic Piezometers" Proc. ASCE speciality conf. on in situ measurements of soil properties, North Carolina State University, Vol 2, pp 361-381.

Penman A.D.M. (1977) "The Failure of Teton Dam" Ground Engineering, U.K., pp 18-27.

Penman A.D.M. (1980) "Deterioration and Failure of Dams" BNCOLD, News and Views, Thomas Telford Ltd, London, pp 13-15.

Penman A.D.M. (1986) "On the Embankment Dam" Rankine Lecture, Geotechnique 36 No. 3, pp 303-348.

Philips J.T. (1976) "Case Histories of Repairs and Design for Dams Built with Dispersive Clay" Dispersive Clays, Related Piping and Erosion in Geotechnical Projects, ASTM, STP 623, pp 330-340.

Reservoir's Act (1975) Her Majesty's Stationary Office, London.

Richardson A.M. and Whitman R.V. (1963) "Effect of Strain Rate upon Undrained Shear Resistance of a Saturated Remoulded Fat Clay" Geotechnique, Vol 13, pp 310-324.

Sargunam A, Riley P, Arulanandan K and Krone R.B (1973) "Physico-chemical Factors in Erosion of Cohesive Soils" Jnl. of Hyd. Div. ASCE, Vol 99 No. HY3, pp 555-558.

Savidou C (1981) "Fracture and Permeability Changes in Soils" M Phil Dissertation, Cambridge University, U.K.

Schafer G (1978) "Pinhole test for Dispersive Soil - Suggested Change" Jnl. of Geot. Eng. Div. ASCE, Vol 104, No. GT6, pp 760-766.

Seed H.B. Mitchell J.K. and Chan C.K. (1960) "The Strength of Compacted Cohesive Soils" Res. Conf. on shear strength of cohesive soils, ASCE, Univ. of Colorado, Boulder, Colorado, pp 877-964.

Seed H.B. and Duncan J.M. (1981) "The Teton Dam" A retrospective review. Proc. 10th Int. Conf. S.M. & F.E., Vol 4, pp 219-238.

Sherard J.L. (1973) "Embankment Dam Cracking" Embankment Dam Engineering, Casgrande Volume, Wiley, New York, pp 271-353.

Sherard J.L. (1986) "Hydraulic Fracturing in Embankment Dams" Jnl. of Geot. Eng. Div. ASCE, Vol 112, No. 10, pp 905-927.

Sherard J.L., Decker R.S and Ryker N.L. (1972a) "Hydraulic Fracturing in Low Dams of Dispersive Clay" Proc. Conf. on the performance of earth and earth supported structures, ASCE, Vol1, pp 653-689.

Sherard J.L., Decker R.S and Ryker N.L. (1972b) "Piping in Earth Dams of Dispersive Clay" Proc. Conf. on the performance of earth and earth supported structures, ASCE, Vol 1, pp 589-626.

Sherard J.L., Dunningham L.P., Decker R.S. and Steel E.F. (1976a) "Pinhole Test for Identifying Dispersive Soils" Jnl. of Geot. Eng. Div. ASCE, Vol 102, GT1, pp 69-85.

Sherard J.L. Dunningham L.P., and Decker R.S. (1976b) "Identification and Nature of Dispersive Soils" Jnl. of Geot. Eng. Div. ASCE, Vol 102, GT4, pp 287-301.

Skempton A.W. (1954) "The Pore Pressure Coefficient A and B" Geotechnique 4, pp 143-147.

Tam H.K., Mhach H.K. and Woods R.I. (1988) "Numerical Investigation of Hydraulic Fracturing in Clays" Proc. 6th Int. Conf. on Numerical Methods in Geomechanics, Innsbruck, pp 563-570.

Tam H.K. (1988), Private Communication.

Tadenier R, and Ingles O.G. (1985) "Soil Security Test for Water Retaining Structure" Jnl. of Geot. Eng. ASCE, Vol III, No. 3, pp 289-301.

Vaughan P.R. (1971) "The Use of Hydraulic Fracturing Tests to Detect Crack Formation in Embankment Dam Cores" Interim Report, Dept. of Civil Eng. Imperial College, London.

Vaughan P.R. (1976) "Cracking of Embankment Dam Cores and the Design of Filters for their Protection" Lecture given in Madrid and published in the Bulletin of Sociedad Espanola de Mecanica del Suelo Y Cimentaciones, pp 23-34.

Vaughan P.R. (1983) "M.Sc Lecture Notes" Imperial College, London.

Vaughan P.R., Kluth D.J., Leonard M.W. and Pradowa H.H.M. (1970) "Cracking and Erosion of the Rolled Clay Core of Balderhead Dam and the Remedial Works Adopted for this Repairs" Trans. 10th Int. Conf. Large Dams Vol 1, pp 73-93.

Vaughan P.R. and Soares H.F. (1982) "Design of Filters for Clay Cores of Dams" Jnl. of Geot. Eng. Div. ASCE, Vol 108, NO. GT1, pp 17-31.

Wu T.H., Loh A.K. and Malvern L.E. (1963) "Study of Failure Envelope of Soils" Jnl. of S.M. & F.D, ASCE, Vol. 89, SM1, pp 145 - 181.

Wroth C.P. (1984) "The Interpretation of in situ Soil tests" Rankine Lecture, Geotechnique 34, No. 14, pp 449-489.

Test No.	Compactive Effort	γ_s kN/m ³	W %	u_t kg/cm ²
(1)	(2)	(3)	(4)	(5)
LHF-7	High	17.7	14.9	>6.9
LHF-10	High	17.0	17.1	4.5
LHF-12	Low	15.8	17.3	3.1
LHF-19	Low	15.6	16.2	3.3
LHF-22	Low	16.1	19.8	3.4

Note: $\sigma_v = \sigma_t = 4\text{kg/cm}^2$; $\sigma_H = \sigma_2 = \sigma_3 = 2\text{kg/cm}^2$ in all tests

Table 3.1 - Effect of compactive Effort on measured values of u_t (After Jaworski et al 1981)

Measurement	Instrument	Range kPa	Noise kPa	Drift kPa	Accuracy kPa
Axial load	Load cell	1000	± 0.5	± 2	± 3.5
Cell and pore pressure	Pressure Transducer	1000	± 0.5	± 1.0	± 1.0
Axial strain	Linear Transducer	40%	0.0	$\pm 0.01\%$	$\pm 0.01\%$
Volume strain	Linear Transducer	40%	0.0	$\pm 0.02\%$	$\pm 0.02\%$

Table 7.1 - Accuracy and Measurements

Test No.	Equipment Used	R _e	Type of Test
S-1, S-2 & S-3	Semi-automatic triaxial cell	1	Undrained compression tests at constant p - stress controlled
S-4, S-5 & S-6	Semi-automatic triaxial cell	1	Undrained compression tests at constant p. Test S-4: stress controlled. S-5 and S-6 loaded under hybrid conditions
ST-1, ST-2 & ST-3	Semi-automatic triaxial cell	1	Conventional undrained compression tests using different strain rates
C-1, C-2 & C-3	Automatic triaxial cell	1	Conventional undrained compression tests - under hybrid conditions
C-4	Automatic triaxial cell	2	Conventional undrained compression tests - under hybrid conditions
C-5, C-6 and C-7	Automatic triaxial cell	6,8 12 Resp	Conventional undrained compression test. Loaded at $\epsilon_v = 0.5\%$ per hour.

Table 8.1 - Classification of Triaxial Tests

Group No.	Initial Water Content %	Water Content History
P-1	40.0	Soil at "natural" water content (as received in the laboratory)
P-2	21.6	Soil air dried from "natural" water content of 40.0%.
P-3	36.8	Soil air dried, powdered, and rewetted. Tested after 1 day.
P-4	37.0	Soil air dried, powdered and rewetted. Tested after 1 day.
P-5	25.7	Soil air dried, powdered and rewetted. Tested after 1 day.
P-6	25.4	Soil air dried, powdered and rewetted. Tested after 1 day.

Table 8.2 - Classification of Pinhole Tests

Group No.	Test Conditions
B-1	Sample made with distilled water and tested in distilled water
B-2	Sample made with distilled water and tested in brine solution
B-3	Sample made with brine solution and tested in distilled water
B-4	Sample made with brine solution and tested in brine solution
B-5	Sample ($R_o = 3$) made with distilled water and tested in distilled water
B-6	Sample made with distilled water and tested in its reservoir water
B-7	Sample made with its reservoir water and tested in distilled water
B-8	Sample made with its reservoir water and tested in its reservoir water
B-9	Natural sample tested in distilled water
B-10	Natural sampled tested in its reservoir water

Table 8.3 - Classification of Cylinder Dispersion Tests

Group	Size of Sand Pocket and Sample	R_o	Test Conditions
F1 - A	a = 3.0 l = 25.0 b = 19.0	1	p'_o varying from 100-300 kN/m ² rate about 15 kN/m ² /min
F1 - B	a = 3.0 l = 25.0 b = 19.0	1	p'_o varying from 10-400 kN/m ² u_o varying from 10-400 kN/m ²
F2	a = 3.0 l = 25.0 b = 19.0	1	Test conducted with paraffin at different p'_o .
F3	a = 8.0 l = 25.0 b = 19.0	1	At different p'_o , also influence of rate of pressuring on fracturing pressure at $p'_o = 400$ kN/m ²
F4	a = 8.0 l = 35.0	1	At different p'_o .
F5	a = 8.0 l = 25.0 b = 19.0	-	Tests conducted with $R_o = 1, 2, 6,$ 8 and 12 and at nearly same v_o .
F6	a = 3.0 l = 25.0 b = 50.0	1	Tests conducted at various rates
F7	a = 8.0 l = 66.0 b = 50.0	1	At different p'_o .
F8	a = 3.0 l = 25.0 b = 50.0	1	At different p'_o .
F9	a = 3.0 l = 25.0 b = 19.0	1	Tests conducted at different σ'_1/σ'_3 .

All dimensions are in mm, a = radius of sand pocket, l = depth of the sand pocket, b = radius of the sample

Table 8.4 - Classification of Fracturing Tests

Test No.	σ_a kN/m ²	σ_r kN/m ²	u_o kN/m ²	v'_o kN/m ²	S_u kN/m ²	Approx t_f min	σ_f kN/m ²	σ_B kN/m ²	σ_c kN/m ²
F1-1A	421	400	302	105	40	4	449	403	402
F1-2A	421	400	203	204	78	8.5	516	414	406
F1-3A	520	500	203	304	116	11.5	666	505	504

Table 9.1 - Initial and Fracturing States for Fracturing Tests on Group F1-A.

Test No.	σ_a kN/m ²	σ_r kN/m ²	u_o kN/m ²	v'_o kN/m ²	S_u kN/m ²	Approx t_f min	σ_f kN/m ²	σ_B kN/m ²	σ_c kN/m ²
F1-1B	220	201	102	105	40	1.3	263	209	203
F1-2B	320	300	214	93	35	1.3	359	309	304
F1-3B	322	300	209	98	37	1.8	386	308	302
F1-4B	326	300	201	108	41	1.4	369	312	300
F1-5B	522	500	407	100	38	1.3	558		501
F1-6B	173	152	12	147	56	1.8	240		-
F1-7B	422	400	202	205	78	2.90	536		402
F1-8B	521	500	310	197	75	2.60	622	535	502
F1-9B	329	310	12	304	116	4.0	498		311
F-10B	420	397	103	302	115	4.0	587		399
F1-11B	517	498	209	295	112	4.0	666	515	505
F1-12B	533	499	203	307	117	4.0	688		500
F1-13B	472	449	102	355	135	5.0	679		449
F1-14B	430	409	14	402	153	5.20	665		409
F1-15B	523	500	100	408	155	5.40	752		503
F1-16B	522	500	108	399	152	5.40	751	522	501

Table 9.2 - Initial and Fracturing States for Initial Fracturing Tests on Group F1-B

Test No.	σ_a kN/m ²	σ_r kN/m ²	u_o kN/m ²	p'_o kN/m ²	s_a kN/m ²	σ_r kN/m ²	σ_c kN/m ²
F1-1B	219	201	103	104	40	242	204
F1-2B	321	300	209	98	37	348	303
F1-3B	322	300	227	80	30	328	302
F1-4B	323	299	203	104	40	348	300
F1-5B	518	499	404	101	38	550	500
F1-8B	520	500	317	190	72	610	506
F1-11B	513	499	275	229	87	604	-
F1-16B	517	499	146	359	136	696	-
F5-1	428	406	110	303	115	553	406

Table 9.3 - "Delayed" (1 - Day) Fracturing Tests on Group F1-B

Test No.	σ_a kN/m ²	σ_r kN/m ²	u_o kN/m ²	p'_o kN/m ²	Approx t_r min.	s_a kN/m ²	σ_r kN/m ²	σ_c kN/m ²
F2-1	225	212	102	114	1.70	43	295	209
F2-2	423	400	202	206	2.20	78	505	399
F2-3	469	449	204	252	8.20	96	588	447
F2-4	415	399	104	300	4.30	114	602	397
F2-5	468	450	102	354	4.20	135	642	450
F2-6	484	453	102	361	4.50	137	647	452
F2-7	529	506	107	407	4.80	155	724	505
F2-8	516	498	101	403	2.50	153	616	-
F2-9	466	449	53	402	4.10	153	640	449

Table 9.4 - Initial and Fracturing States of Group F-2

Note: Test F2-3 Started with probe pressure equal to u_o
Test F2-8 The sample was prematurely fractured during de-airing before the start of the test. Paraffin was seen coming out of the middle of the sample and pushing the rubber membrane outwards.
Test F2-9 The sample fractured with a horizontal fracture in its middle.

Test No.	σ_a kN/m ²	σ_r kN/m ²	u_o kN/m ²	P'_o kN/m ²	Approx t_f min	S_u kN/m ²	σ_f kN/m ²	σ_H kN/m ²	σ_c kN/m ²
F3-1	340	318	248	77	0.8	29	347	321	318
F3-2	272	252	101	158	1.4	60	314	258	251
F3-3	418	400	204	202	1.8	77	475	403	400
F3-4	420	399	202	204	1.6	78	476		400
F3-5	421	401	102	306	2.3	116	512	404	400
F3-6	521	500	102	405	3.1	154	645		499
F3-7	520	498	101	404	3.1	154	642		499
F3-8	522	500	102	405	1.5	154	719		502
F3-9	519	500	102	404	1.3	154	691	518	504
F3-10	520	498	103	402	2.3	153	675		505
F3-11	522	499	101	406	11.0	154	610	507	502

Table 9.5 - Initial and fracturing states for Hydraulic Fracturing Tests on Group F-3

Note: Test No. F3-7: Conducted using paraffin as the probe fluid

Tests F3-8 and F3-9 Rate: 150 kN/m²/min

Test F3-10 Rate: 70kN/m²/min

Tests F3-11: Started the test with probe pressure equal to u_o at a rate of 50 kN/m²/min.

Test No.	σ_a kN/m ²	σ_{ro} kN/m ²	u_o kN/m ²	P'_o kN/m ²	Approx t_f min	S_u kN/m ²	σ_f kN/m ²	σ_c kN/m ²
F4-1	424	401	201	208	1.9	79	484	402
F4-2	424	399	103	304	2.1	116	509	398

Table 9.6 - Initial and Fracturing states for Hydraulic Fracturing Tests on Group F-4

Test No.	σ_a kN/m ²	σ_c kN/m ²	u_o kN/m ²	p'_o kN/m ²	R_o	Approx t_f min	σ_f kN/m ²	σ_c kN/m ²
F5-1	430	407	102	313	1	4.1	606	408
F5-2	491	469	288	188	2	3.7	650	469
F5-3	402	375	297	87	6	2.7	506	375
F5-4	111	90	10	87	6	2.6	218	90
F5-5	390	365	300	73	8	2.2	473	366
F5-6	100	75	12	71	8	2.3	183	75
F5-7	368	346	301	52	12	1.8	433	343
F5-8	80	55	11	52	12	1.8	142	55

Table 9.7 - Initial and Fracturing states for Fracturing Tests on Group F-5

Test No.	σ_a kN/m ² min	σ_c kN/m ²	u_o kN/m ²	p'_o kN/m ²	Rate kPa/min	Approx t_f min	s_u kN/m ²	σ_f kN/m ²	σ_c kN/m ²
F6-1	472	449	204	253	150	1.3	96	631	449
F6-2	475	453	203	257	150	1.3	98	640	452
F6-3	471	449	203	253	50	3.4	96	602	447
F6-4	472	450	207	250	5	24.0	95	574	448
F6-5	472	450	205	252	0.5	117.0	96	513	449
F6-6	475	451	203	256	0.05	460.0	97	474	451
F6-7	475	451	203	256	0	4800.0	97	456	

Table 9.8 - Initial and Fracturing States at Various Rates of Group F-6

Test No.	σ_a kN/m ²	σ_r kN/m ²	u_o kN/m ²	p'_o kN/m ²	Approx t_f min	S_u kN/m ² min	σ_f kN/m ² min	σ_c kN/m ²
F7-1	320	300	202	105	1.3	40	368	290
F7-2	319	298	102	203	2.8	77	426	288
F7-3	471	447	103	352	4.0	134	641	452
F8-1	471	449	207	249	4.1	95	646	442
F8-2	465	446	101	351	5.9	133	703	450

Table 9.9 - Initial and Fracturing States for Initial Fracturing Tests on Groups F7 and F-8.

Test No.	σ_a kN/m ²	σ_r kN/m ²	u_o kN/m ²	p'_o kN/m ²	Interval Days	Approx t_f min	S_u kN/m ²	σ_f kN/m ²	σ_c kN/m ²
F7-1	317	300	202	104	10	1.0	40	348	290
F7-2	318	297	103	201	6	2.3	76	405	286
F7-3	469	445	105	348	7	3.6	132	624	434
F8-1	469	448	205	250	10	3.3	95	615	439
F8-2	462	445	101	350	8	5.3	133	694	439

Table 9.10 - "Delayed" Fracturing Tests on Groups F-7 and F-8

Test No.	σ_a kN/m ²	σ_r kN/m ²	u_o kN/m ²	σ'_f/σ'_a	p'_o kN/m ²	Approx t_f min	S_u kN/m ² min	σ_f kN/m ² min	σ_c kN/m ²
F9-1	444	301	204	0.4	145	1.9	67	396	303
F9-2	404	301	201	0.5	134	1.7	55	383	302
F1-4B	326	300	201	0.8	108	1.4	41	369	300

Table 9.11 - Initial and Fracturing States for Fracturing Tests on Group F-9

Soil	LL %	PL %	PI %	G _s	Clay %	Activity
Puddle Clay Cwmernderi Dam	42	18	24	2.69	34	0.71
Puddle Clay Gorpley Dam	51	26	25	2.74	46	0.54
Puddle Clay Ramsden Dam	50	26	24	2.74	36	0.67
Puddle Clay Lambeithan Dam	34	15	19	2.72	48	0.40
Puddle Clay King George V	63	22	41	2.77	56	0.73
Laterite	42	22	20	2.70	36	0.56
Oxford Clay	60	32	28	-	-	0.86*
London Clay	70	25	45	2.75	42	1.07
Kaolin	65	35	30	2.60	80	0.38
Cowden Till	34	16	18	2.66	33	0.55

* Skempton A.W (1953)

Table 9.12 - Index Properties of Soils Tested for Dispersion/Erosion Tests

Water Used	pH Value
Distilled Water	7.0 +
Brine Solution	7.1
Reservoir Water - Cwmernderi Dam	5.1
Reservoir Water - Gorpley Dam	7.8
Reservoir Water - Ramsden Dam	7.1
Reservoir Water - King George V	7.9

+ Assumed

Table 9.13 - pH Values of Water used for Dispersion/Erosion Test

Group No.	Initial m.c %	Water Content History	Curing after compaction	Appearance of effluent in test	Hole size after test (needle dia)	Classification
P-1	40	Soil at natural water content	Nil	At all heads-clear	1 No Erosion	ND-1
P-2	21.6	Soil air dried from natural water content	Nil	At small and medium heads-clear. At high heads - very slight colour	1	ND-1 non-Dispersive
P-3	36.8	Soil air dried, powdered and rewetted, tested after 1 day	Nil	At low heads - colloidal flow	3	D-1 Dispersive
P-4	37	Soil air dried, powdered and rewetted. Tested after 1 day	Nil	At low heads - colloidal flow	3	D-1 Dispersive
P-5	25.7	Soil air dried, powdered and rewetted, tested after 1 day	Nil	At low heads - colloidal flow	2	D-2 Dispersive
P-6	25.4	Soil air dried powdered and rewetted, tested after 1 day	Nil	At low heads - colloidal flow	2	D-2 Dispersive

Table 9.14 - Pin-hole tests on Puddle Clay from Cwmernderi Dam

Test Group	Pore Water	Beaker Water	Classification/Type
B-1	Distilled Water	Distilled Water	Dispersive Type D
B-2	Distilled Water	Brine Solution	Non-Dispersive Type D
B-3	Brine Solution	Distilled Water	Non-Dispersive Type N
B-4	Brine Solution	Brine Solution	Non-Dispersive Type C
B-5 ($R_o = 3$)	Distilled Water	Distilled Water	Dispersive Type D
B-6	Distilled Water	Reservoir Water	Dispersive D
B-8	Reservoir Water	Reservoir Water	Dispersive D

Table 9.15 - Summary of Cylinder Dispersion Tests on Puddle Clay - Cwmernderi Dam

Test Group	Pore Water	Beaker Water	Classification/Type
B-1	Distilled Water	Distilled Water	Dispersive Type N/D
B-2	Distilled Water	Brine Solution	Non-Dispersive Type C
B-3	Brine Solution	Distilled Water	Non-Dispersive Type C
B-6	Distilled Water	Reservoir Water	Non-Dispersive Type C
B-7	Reservoir Water	Distilled Water	Dispersive Type D
B-8	Reservoir Water	Reservoir Water	Non-Dispersive Type C

Table 9.16 - Summary of Cylinder Dispersion Tests on Puddle Clay - Gorpely Dam

Tests Group	Pore Water	Beaker Water	Classification/Type
B-1	Distilled Water	Distilled Water	Dispersive Type N/D
B-6	Distilled Water	Reservoir Water	Non-Dispersive Type N
B-8	Reservoir Water	Reservoir Water	Non-Dispersive Type N

Table 9.17 - Summary of Cylinder Dispersion Tests on Puddle Clay - Ramsden Dam

Soil	Test Group	Pore Water	Beaker Water	Classification/Type
Puddle Clay Lambeilethan Dam	B-1	Distilled Water	Distilled Water	Non-Dispersive Type N
Puddle Clay King George V	B-9	Reservoir Water (Natural State)	Distilled Water	Non-Dispersive Type C
Puddle Clay King George V	B-10	Reservoir Water (Natural State)	Reservoir Water	Non-Dispersive Type C
Laterite (from Kenya)	B-1	Distilled Water	Distilled Water	Dispersive Type D
Kaolin	B-1	Distilled Water	Distilled Water	Non-Dispersive Type C
Oxford Clay	B-1	Distilled Water	Distilled Water	Non-Dispersive Type C
London Clay	B-1	Distilled Water	Distilled Water	Non-Dispersive Type C
Cowden Till	B-1	Distilled Water	Distilled Water	Non-Dispersive Type N

Table 9.18 - Summary of Cylinder Dispersion Tests on Various Soils

Test No	σ'_{∞} kN/m ²	s_u kN/m ²	$s_u(1-a^2/b^2)$ kN/m ²	$\sigma_f - \sigma_{\infty}$ kN/m ²	$\sigma_f - u_o$ kN/m ²
F1-1A	98	40	39	49	147
F1-2A	197	78	76	116	313
F1-3A	297	116	113	166	463

Table 10.1 - Analysis of Fracturing Tests on Groups F1-A

Test No	σ'_m kN/m ²	s_u kN/m ²	$s_u(1-a^2/b^2)$ kN/m ²	$\sigma_t - \sigma_{ro}$ kN/m ²	$\sigma_t - \sigma_o$ kN/m ²
F1-1B	99	40	39	62	161
F1-2B	86	35	34	59	145
F1-3B	91	37	36	86	177
F1-4B	99	41	40	69	168
F1-5B	93	38	37	58	151
F1-6B	140	56	55	88	228
F1-7B	198	78	76	136	334
F1-8B	190	75	73	122	312
F1-9B	298	116	113	188	486
F1-10B	294	115	112	190	484
F1-11B	289	112	109	168	457
F1-12B	296	117	114	189	485
F1-13B	347	135	132	230	577
F1-14B	395	153	149	256	651
F1-15B	400	155	151	252	652
F1-16B	392	152	148	251	643

Table 10.2 - Analysis of Initial Fracturing Tests on Group F1-B

Test No	σ'_{∞} kN/m ²	$s_u(1-a^2/b^2)$ kN/m ²	$\sigma_t - \sigma_{\infty}$ kN/m ²	$\sigma_t - \sigma_o$ kN/m ²
F2-1	110	42	83	193
F2-2	198	76	105	303
F2-3	245	94	139	384
F2-4	295	111	203	498
F2-5	348	132	192	540
F2-6	351	134	194	545
F2-7	399	151	218	617
F2-8	397	149	118	515
F2-9	396	149	191	587

Table 10.3 - Analysis of Fracturing Tests on Group F2

Test No	σ'_{∞} kN/m ²	$s_u(1-a^2/b^2)$ kN/m ²	σ_s kN/m ²	σ_c kN/m ²	$\sigma_t - \sigma_{\infty}$ kN/m ²	$\sigma_t - \sigma_o$ kN/m ²
F3-1	70	24	321	318	29	99
F3-2	151	49	258	251	62	213
F3-3	196	63	403	400	75	271
F3-4	197	64	-	400	77	274
F3-5	299	95	404	400	111	410
F3-6	398	127	-	499	145	543
F3-7	397	127	-	499	144	541

Table 10.4 - Analysis of Fracturing Tests on Group F-3

Test No	σ'_{m0} kN/m ²	$s_a(1-a^2/b^2)$ kN/m ²	σ_c kN/m ²	$\sigma_t - \sigma_{m0}$ kN/m ²	$\sigma_t - u_0$ kN/m ²
F4-1	200	65	402	83	283
F4-2	296	95	398	110	406

Table 10.5 - Analysis of Fracturing Tests on Group F-4.

Test No	σ'_{m0} kN/m ²	$s_a(1-a^2/b^2)$ kN/m ²	σ_c kN/m ²	$\sigma_t - \sigma_{m0}$ kN/m ²	$\sigma_t - u_0$ kN/m ²
F7-1	98	39	290	68	166
F7-2	196	75	288	128	324
F7-3	344	131	434	194	538
F8-1	242	95	442	197	439
F8-2	345	133	450	257	602

Table 10.6 - Analysis of Initial Fracturing Tests on Groups F7 and F8

Test Group	a/b	$\frac{\sigma_t - u_0}{\sigma'_{m0}}$	$\frac{\sigma_t - \sigma_c}{s_a(1-a^2/b^2)}$
F1-B	3/19 = 0.16	1.65	1.70
F-3	8/19 = 0.42	1.39	1.20
F-7	8/50 = 0.16	1.65	1.69
F-8	3/50 = 0.06	1.77	1.98

Table 10.7 - Effect of Ratio of the Hole Size to the Sample Size (a/b) on Hydraulic Fracturing Pressures

Test No	R _o	ln R _o	σ' _{so}	σ _r -u _o	$\frac{qf-u_o}{\sigma'_{ro}}$	σ _r σ _{so}	$\frac{q_r \sigma_{so}}{\sigma'_r}$	s _w (1-a ² /b ²)		$\frac{q_r \sigma_{so}}{s_{wp}(1-a^2/b^2)}$	$\frac{q_r \sigma_{so}}{s_{wo}(1-a^2/b^2)}$
								Peak	UH		
F5-1	1	0	305	504	1.65	199	0.65	-	116	-	1.72
F5-2	2	0.693	181	362	2.0	181	1.0	-	111	-	1.63
F5-3	6	1.792	78	209	2.68	131	1.68	85	111	1.54	1.18
F5-4	6	1.792	80	208	2.60	128	1.60	85*	111*	1.51	1.15
F5-5	8	2.079	65	173	2.66	108	1.66	68	103	1.59	1.05
F5-6	8	2.079	63	171	2.71	108	1.71	68*	103*	1.59	1.05
F5-7	12	2.485	45	132	2.93	87	1.93	56	102	1.55	0.85
F5-8	12	2.485	44	131	2.98	87	1.98	56*	102*	1.55	0.85

Note: * Assessed from the triaxial tests.

s_{wp}(1-a²/b²) at peak stress ratio (q'/p') from the triaxial tests.

s_{wo}(1-a²/b²) at ultimate (end of test) stress ratio (q'/p') from the triaxial tests.

Table 10.8 - Analysis of Hydraulic Fracturing Tests on Group F5

Test No	σ' _{so} kN/m ²	s _w (1-a ² /b ²) kN/m ²	ln t _f min	σ _r σ _{so} kN/m ²	σ _r -u _o kN/m ²
F3-6	398	127	1.13	145	543
F3-8	398	127	0.41	219	617
F3-9	398	127	0.26	191	589
F3-10	396	126	0.83	177	573
F3-11	398	127	2.40	111	509

Table 10.9 - Analysis of Time to Failure on Fracturing Tests on Group F-3

Test No	σ'_{∞}	ln Rate kN/m ² /min	ln t_f min	$\sigma_r \sigma_{\infty}$ kN/m ²	$\sigma_r - \sigma_{\infty}$ kN/m ²	$\frac{\sigma_r \sigma_{\infty}}{\sigma'_{\infty}}$
F6-1	245	5.01	0.262	182	427	1.74
F6-2	250	5.01	0.262	187	437	1.75
F6-3	246	3.91	1.224	153	399	1.62
F6-4	243	1.61	3.178	124	367	1.51
F6-5	245	-0.69	4.762	63	308	1.26
F6-6	248	-3.00	6.131	23	271	1.09
F6-7	248	$-\infty$	8.476	5	253	1.02

Table 10.10 - Analysis of Fracturing States at Various Rates of Group F6.

Test No	$\sigma'_f / \sigma'_{\infty}$	σ'_{∞} kN/m ²	$S_w(1-a^2/b^2)$ kN/m ²	$\sigma_r \sigma_{\infty}$ kN/m ²	$\frac{\sigma_r \sigma_{\infty}}{\sigma'_{\infty}}$	$\sigma_r \sigma_{\infty}$ kN/m ²	$\frac{\sigma_r \sigma_{\infty}}{S_w(1-a^2/b^2)}$	$\frac{\sigma_r \sigma_{\infty}}{S_w(1-a^2/b^2)}$
F9-1	0.4	97	65	192	1.98	95	1.46	2.95
F9-2	0.5	100	54	182	1.82	82	1.52	3.37
F1-4B	0.8	99	40	168	1.70	69	1.73	4.20

Table 10.11 - Analysis of Fracturing Tests on Group F9

Test No	σ'_m kN/m ²	$s_a(1-a^2/b^2)$ kN/m ²	$\sigma_r\sigma_m$ kN/m ²	$\sigma_r u_o$ kN/m ²
F1-1B	98	39	41	139
F1-2B	91	36	48	139
F1-3B	73	29	28	101
F1-4B	96	39	49	145
F1-5B	95	37	51	146
F1-8B	183	70	110	293
F1-11B	224	85	105	329
F1-16B	353	133	197	550
F5-1	296	122	147	443

Table 10.12 - Analysis of "Delayed" Fracturing Tests on Group F1-B

Test No	σ'_m kN/m ²	$s_a(1-a^2/b^2)$ kN/m ²	σ_c kN/m ²	$\sigma_r\sigma_m$ kN/m ²	$\sigma_r u_o$ kN/m ²
F7-1	98	39	290	48	146
F7-2	194	74	286	108	302
F7-3	340	129	434	179	519
F7-4	243	95	439	167	410
F7-5	344	133	439	249	593

Table 10.13 - Analysis of "Delayed" Fracturing Tests on Groups F7 and F8

Test No	$a_1 = \frac{1}{2}l$ mm	$s_n = \frac{[1-(a+a_1)^2]}{b^2}$ kN/m ²	$\sigma_r \sigma_m$ kN/m ²
F1-1B	0.95	38	62
F1-2B	0.95	33	59
F1-3B	1.12	35	86
F1-4B	0.99	39	69
F1-5B	0.95	36	58
F1-6B	1.12	53	88
F1-7B	1.42	74	136
F1-8B	1.34	71	122
F1-9B	1.67	109	188
F1-10B	1.67	108	190
F1-11B	1.67	105	168
F1-12B	1.67	110	189
F1-13B	1.86	126	230
F1-14B	1.90	143	256
F1-15B	1.93	145	252
F1-16B	1.93	142	251

$$l = \sqrt{(12c_v t_f)}$$

$$c_v = 0.52 \text{ mm}^2/\text{min. (100 - 200 kN/m}^2)$$

Table 10.14 - Effect of Fluid Penetration on the Analysis of Initial Fracturing Tests on Group F1-B

Test No	$a_1 = \frac{y_3}{3}$ mm	$s_a = \frac{[1-(a+a_1)^2]}{b^2}$ kN/m ²	$\sigma_r \sigma_m$ kN/m ²
F3-1	0.74	23	29
F3-2	0.99	47	62
F3-3	1.12	59	75
F3-4	1.05	60	77
F3-5	1.26	88	111
F3-6	1.47	116	145
F3-7	1.47	116	144
F4-1	1.15	61	83
F4-2	1.21	89	110

Table 10.15 - Effect of Fluid Penetration on the Analysis of Fracturing Tests on Groups F3 and F4

Test No	$a_1 = \frac{y_3}{3}$ mm	$s_a = \frac{[1-(a+a_1)^2]}{b^2}$ kN/m ²	$\sigma_r \sigma_m$ kN/m ²
F7-1	0.95	39	68
F7-2	1.39	74	128
F7-3	1.67	129	194
F8-1	1.69	94	197
F8-2	2.02	132	257

Table 10.16 - Effect of Fluid Penetration on the Analysis of Fracturing Tests on Groups F7 and F8

Test No	Experimental $\frac{\sigma_r u_o}{\sigma'_{\infty}}$	Proposed Effective Stress Models			Kennard's (1970) $\Delta u / \sigma'_{\infty}$
		Condition 1 $(\sigma_r u_o) / \sigma'_{\infty}$	Condition 2 $(\sigma_r u_o) / \sigma'_{\infty}$		
		At no-tension cut-off	At Yield	At C.S.L	
F1-B	1.65	1.0	1.33	1.31	1.59
F-3	1.39	1.0	1.26	1.24	1.50
F-7	1.65	1.0	1.33	1.31	1.59
F-8	1.77	1.0	1.34	1.32	1.61

Condition 1: Fracture occurs when $\sigma'_u = 0$ at $r = a$

Condition 2: Fracture occurs when $(\sigma'_o / \sigma'_r)_r = k_o$ at $r = a$

Kennard's Criterion (1970) $\frac{\Delta u_o}{\sigma'_{\infty}} = 1 + \frac{(1-a^2/b^2)}{2 A_r}$

(A_r for the puddle clay tested = 0.82)

Table 10.17 - Comparison of the Experimental Fracturing Results with the Proposed Effective Stress Analysis and Kennard's Criterion for Normally Consolidated Samples.

Test No.	Experimental $\frac{(\sigma_r - u_o)}{\sigma'_{\infty}}$	u_o kPa	u_r (at C.S.L) kPa	Condition 1 $\frac{\sigma_r - u_o}{\sigma'_{\infty}}$		Condition 2 $\frac{\sigma_r - u_o}{\sigma'_{\infty}}$	
				At No-tension cut-off	At Yield	At C.S.L	
F5-1	1.65	102	210	1.0	1.33	1.31	
F5-2	2.0	288	270	1.0	1.48	1.53	
F5-3	2.68	297	192	1.0	1.53	2.13	
F5-4	2.60	10	-93*	1.0	1.52	2.10	
F5-5	2.66	300	185	1.0	1.53	2.34	
F5-6	2.71	12	-105*	1.0	1.52	2.38	
F5-7	2.93	301	179	1.0	1.60	2.79	
F5-8	2.98	11	-112*	1.0	1.59	2.83	

Condition 1: Fracture occurs when $\sigma'_{\alpha} = 0$ at $r = a$

Condition 2: Fracture occurs $(\sigma'_o / \sigma'_r)_l = k_o$ at $r = a$

Notes: * Assessed from the triaxial Tests
 ϕ'_c mobilised at peak = 33° for samples F5-3 to F5-6
= 38° for samples F5-7 and F5-8
 ϕ'_c mobilised at C.S.L. = 30°

Table 10.18 - Comparison of Experimental Fracturing Results with the Theoretical Effective Stress Analysis - Group F-5

Test No	R_o	Experimental $\frac{\sigma_{r u_o}}{\sigma'_m}$	Plane Strain Finite Element Method $(\sigma_{r u_o})/\sigma'_m$
F5-2	2	2.0	1.86
F5-3	6	2.68	2.45
F5-5	8	2.66	2.46
F5-7	12	2.93	2.40

Table 10.19 - Comparison of Experimental Fracturing Results with the Plane Strain Finite Element Method - Overconsolidated Samples

Atterberg Tests	
Liquid Limit	LL = 42%
Plastic Limit	PL = 18%
Plasticity Index	PI = 24%
Activity	A = 0.71
Specific Gravity	$G_s = 2.69$
Grain Size Distribution	
Sand	= 10%
Silt	= 56%
Clay	= 34%

Table B - 1 - Summary of Index and Classification Tests

Sample	p_o' kN/m ²	$v_r = v_o$	p_r' kN/m ²	q_r' kN/m ²	s_u kN/m ²
C-1	100	1.837	68	80	40
C-2	200	1.754	129	154	77
C-3	300	1.706	186	218	109
S-1	120	1.816	78	96	48
S-2	189	1.761	139	177	88
S-3	347	1.688	209	257	128
S-4	128	1.808	94	-99	50
S-5	199	1.755	130	-120	60
S-6	323	1.697	231	-197	99

Table B-2 - Initial and Ultimate States for Reconstituted Normally Consolidated Samples

Note: Correction for filter paper: $(\sigma_v - 10)$ kPa for compression tests.

Sample	p'_o kN/m ²	R_o	$v_r=v_o$	p'_r kN/m ²	q'_r kN/m ²	s_o kN/m ²
C-4	184	2	1.706	196	228	114
C-5	79	6	1.705	188	227	113.5
C-6	66	8	1.708	180	212	106
C-7	45	12	1.709	167	210	105

Table B-3 - Initial and Ultimate States for Reconstituted Overconsolidated Samples

λ	κ	N	r	M_c	ϕ'_o	M_o	ϕ'_o
0.120	0.03	2.390	2.338	1.20	30°	0.89	31.5°

Table B-4 - Summary of Reconstituted Samples

Sample	p'_o kN/m ²	v_r	t_r min (ultimate)	$\ln t_r$ min (ultimate)	s_v/p'_o at e_s			
					0.5 %	1.0 %	2.0 %	end of test
ST-1	100	1.837	3	1.1	0.39	0.45	0.50	0.52
ST-2	100	1.837	30	3.4	0.39	0.43	0.49	0.51
St-3	96	1.842	265	5.6	0.34	0.40	0.44	0.46
C-1	100	1.837	5781	8.7	0.22	0.30	0.38	0.45

Table B-5 - Variation of s_v/p'_o at various rates.

(Note : Correction of filter paper not applied).

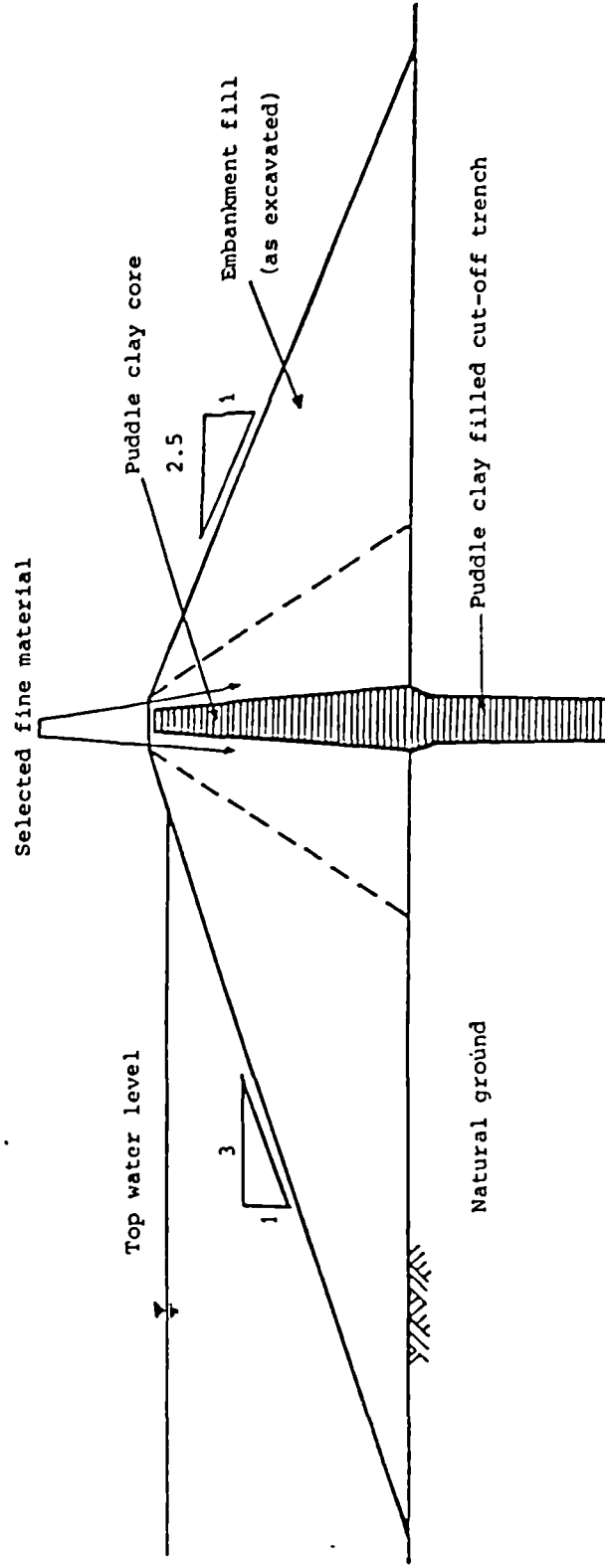


Fig 1.1 TYPICAL CROSS - SECTION OF AN OLD EMBANKMENT DAM WITH A PUDDLE CLAY CORE
 (Charles and Watts 1987)

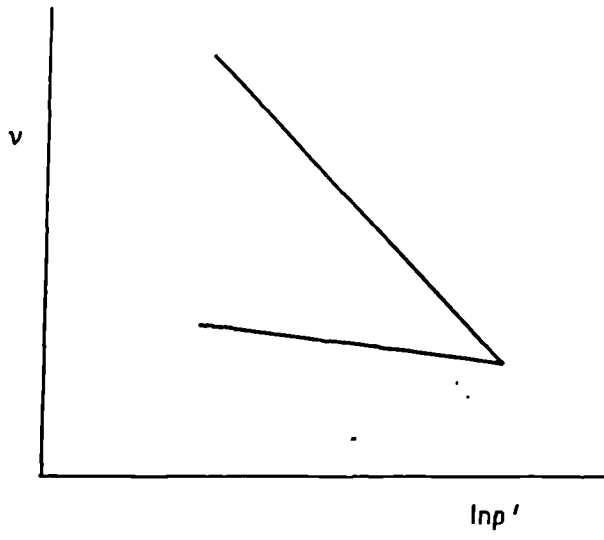


Fig 2.1 ISOTROPIC COMPRESSION AND SWELLING LINES

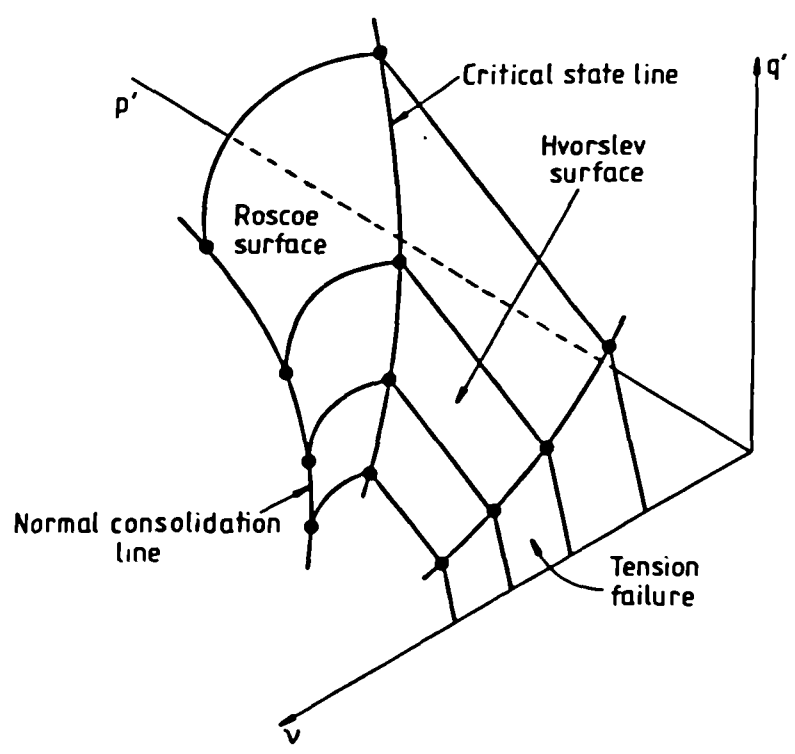
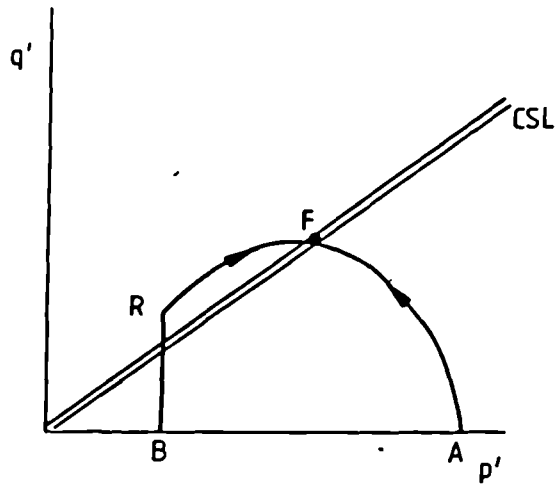
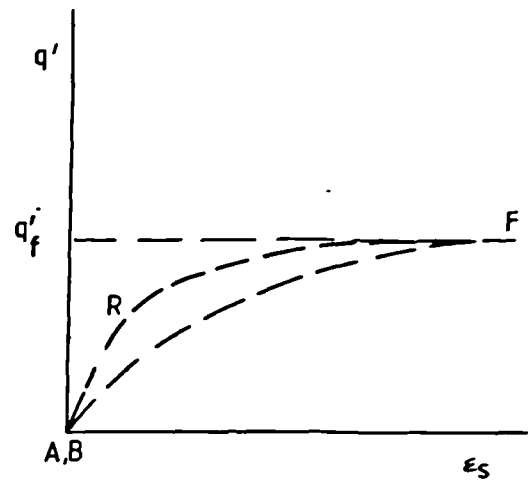


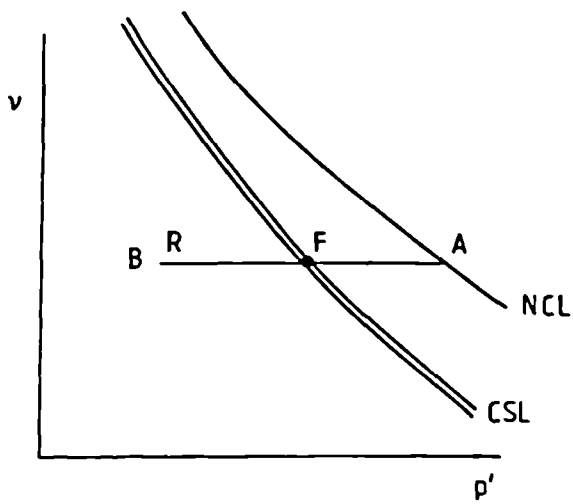
Fig 2.2 THE COMPLETE STATE BOUNDARY SURFACE IN $q':p':v$ SPACE (FROM ATKINSON AND BRANSBY, 1978)



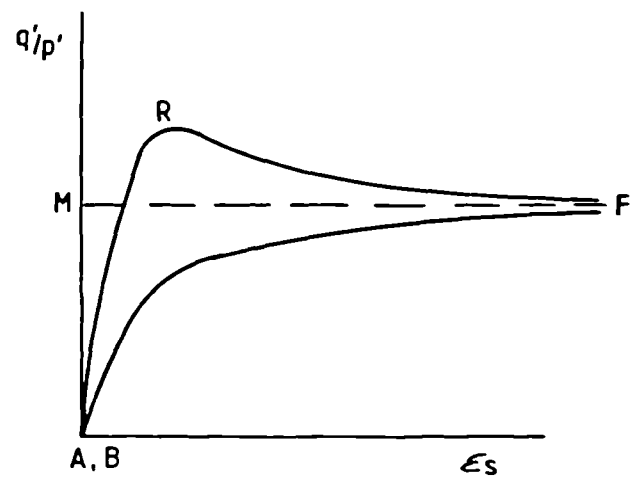
(a)



(b)

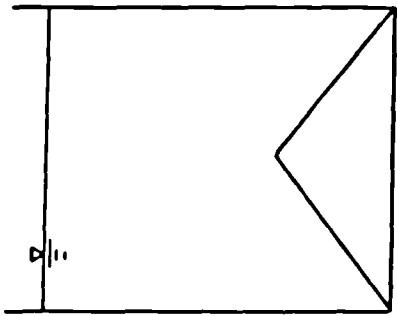


(c)

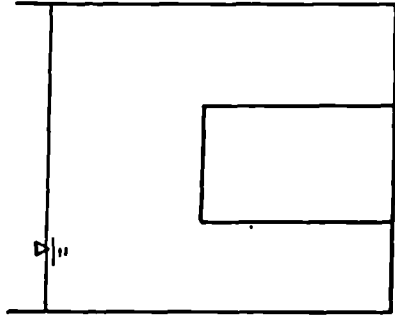


(d)

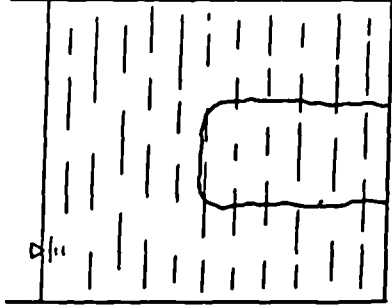
Fig 2.3 IDEALISED BEHAVIOUR OF SOILS IN UNDRAINED TESTS



Type N



Type C



Type D

Fig 2.4 CYLINDER DISPERSION TEST

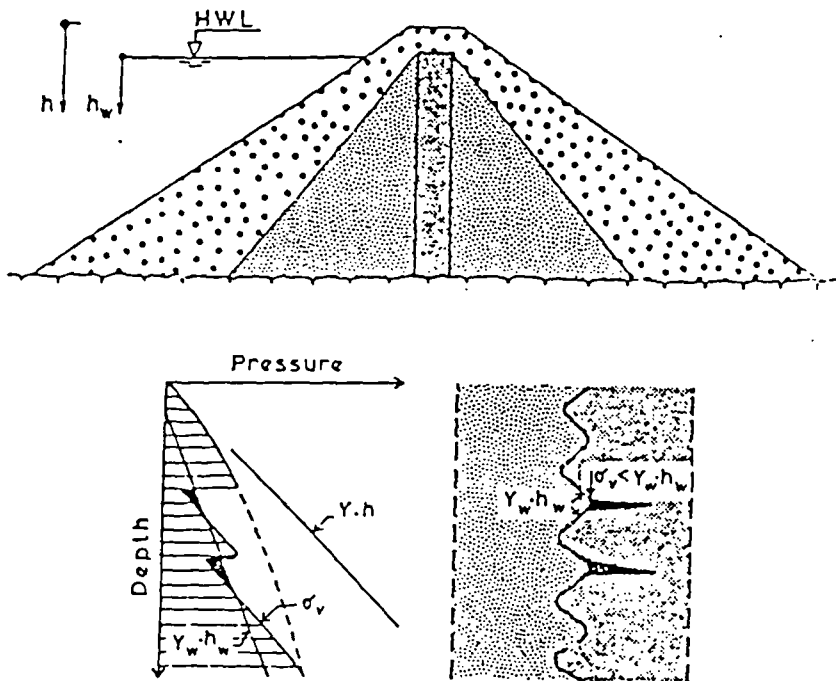


Fig 3-1 OUTLINE OF THE HYPOTHESIS USED TO EXPLAIN THE DEVELOPMENT OF CRACKS IN THE CORE (After Kjaernsli and Torblaa, 1968)

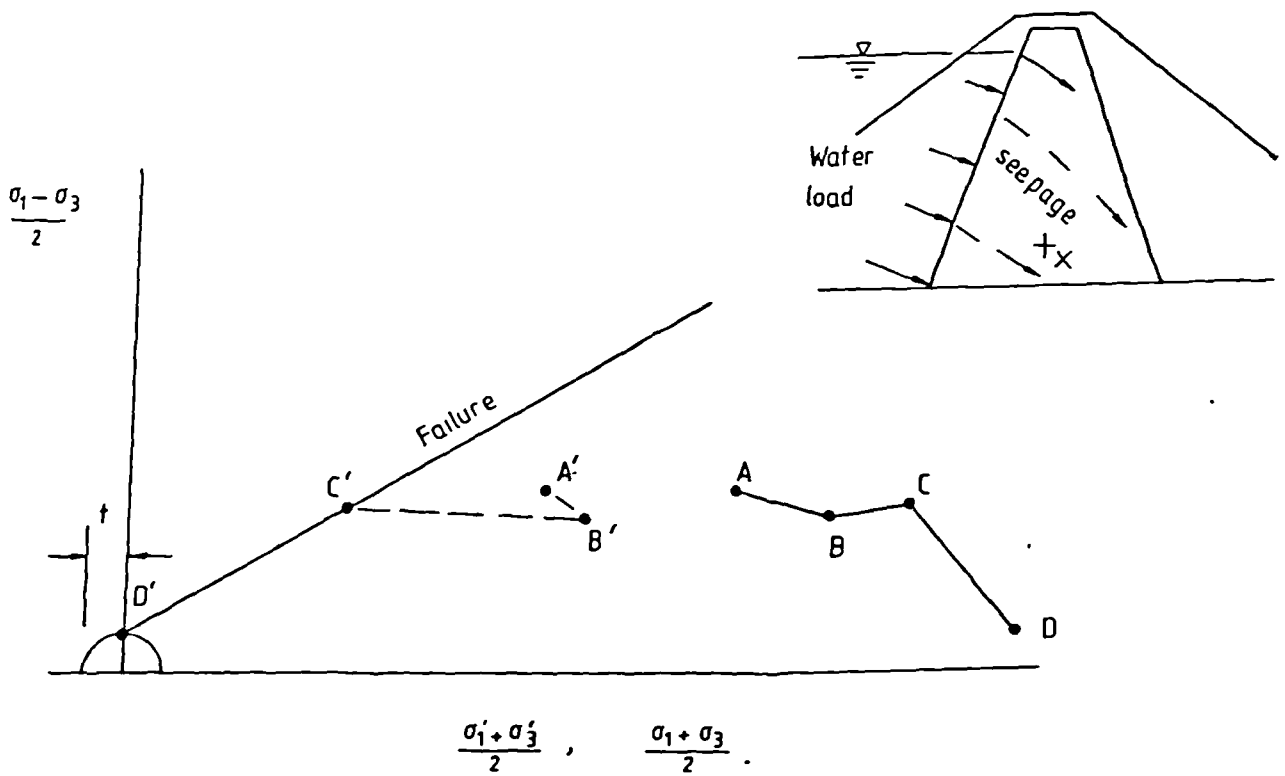


Fig 3.2 STRESS CHANGES LEADING TO DRAINED HYDRAULIC FRACTURE (After Vaughan, 1976)

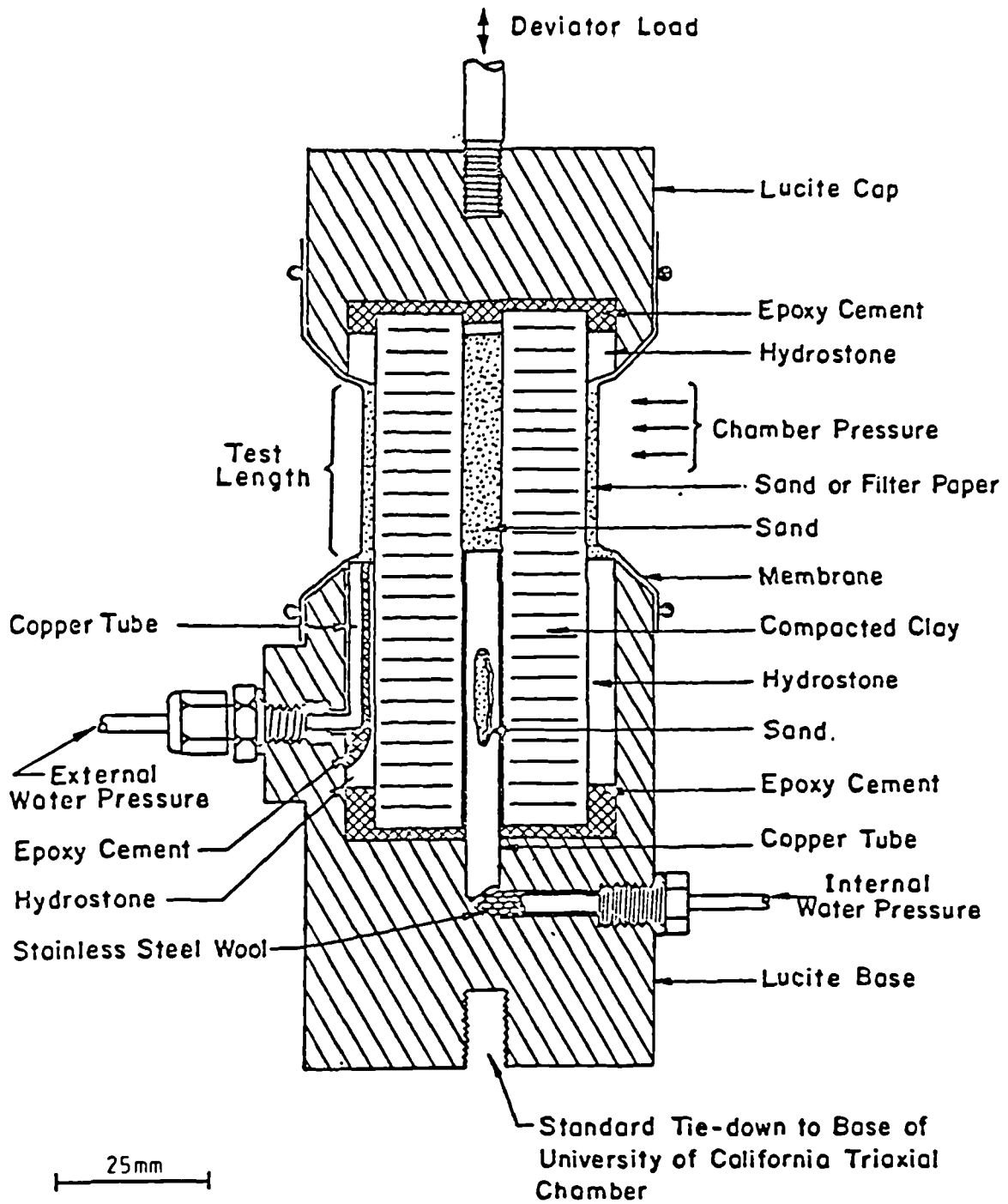


Fig 3.3 APPARATUS FOR HYDRAULIC FRACTURING EXPERIMENTS (After Nobari et al 1973)

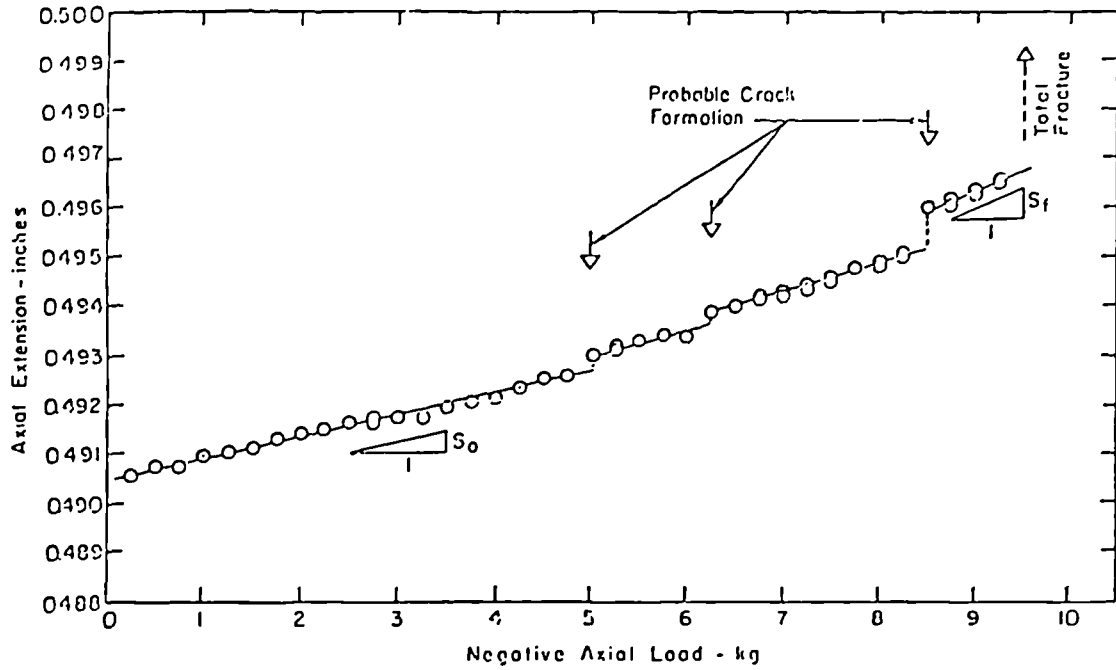


Fig 3.4 AXIAL EXTENSION IN RELATION TO THE AXIAL NEGATIVE LOAD IN TYPE 1 TEST

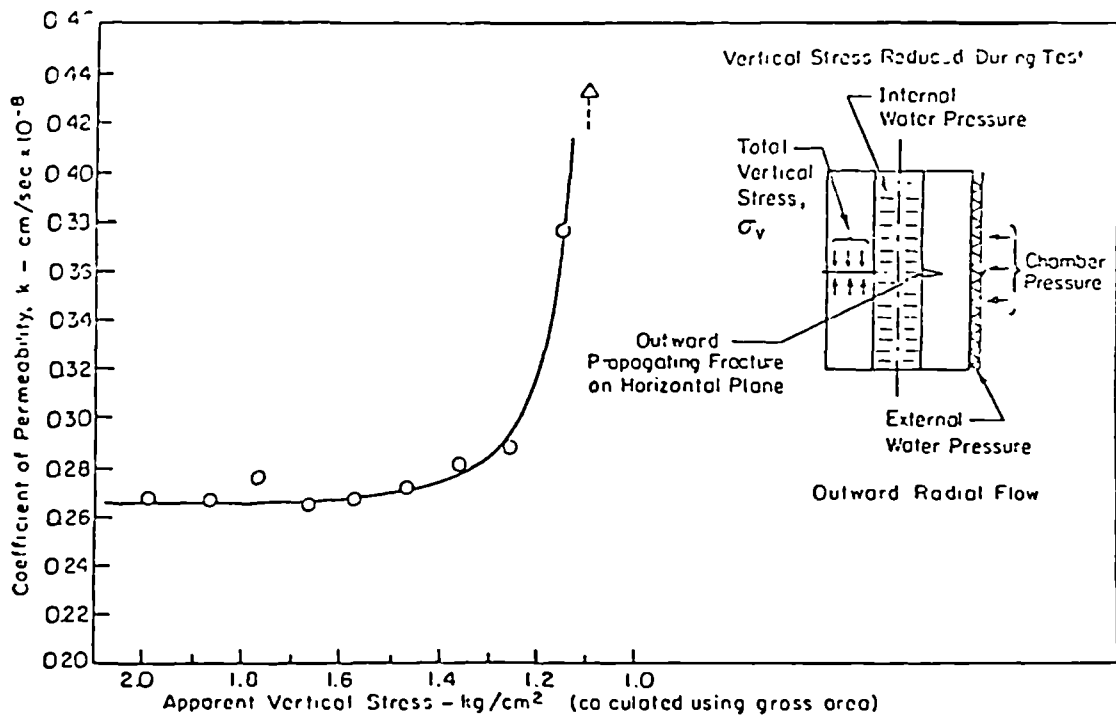


Fig 3.5 CALCULATED PERMEABILITIES IN TYPE 1 TEST (Fig 3.4 & 3.5 - After Nobari et al, 1973)

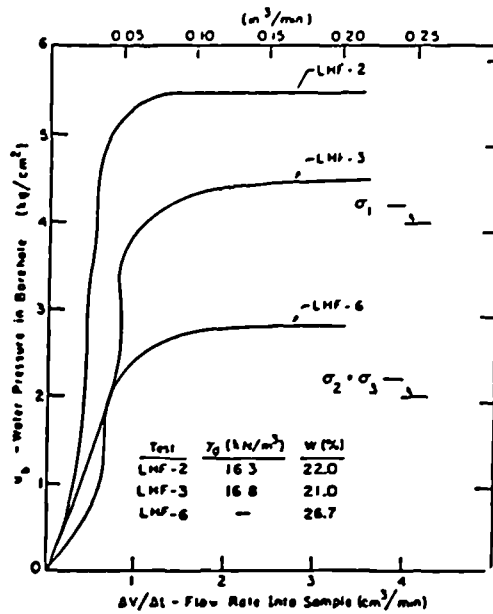


Fig 3.6 RESULTS OF BOREHOLE HYDRAULIC FRACTURING TESTS ON UNDISTURBED BLOCK SAMPLES

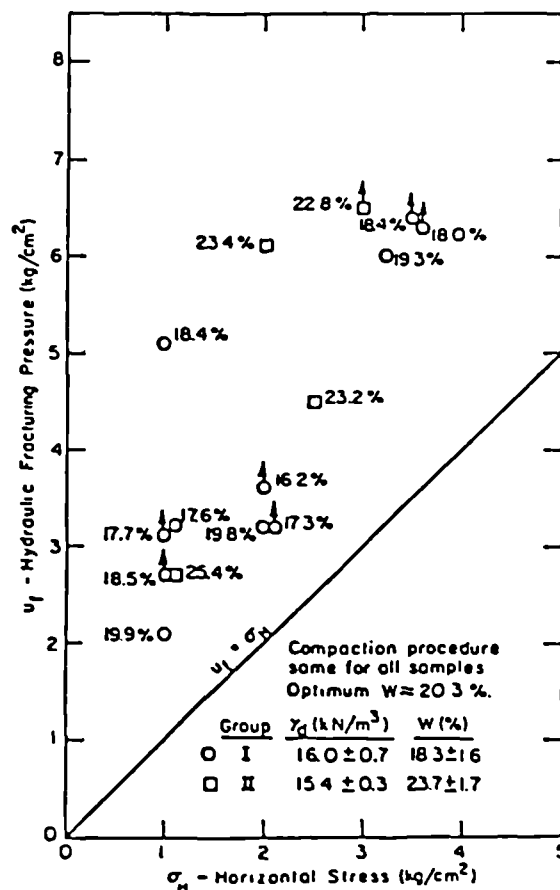


Fig 3.7 HYDRAULIC FRACTURING TESTS ON RECOMPACTED SAMPLES OF TETON DAM SOIL (GROUPS I AND II)

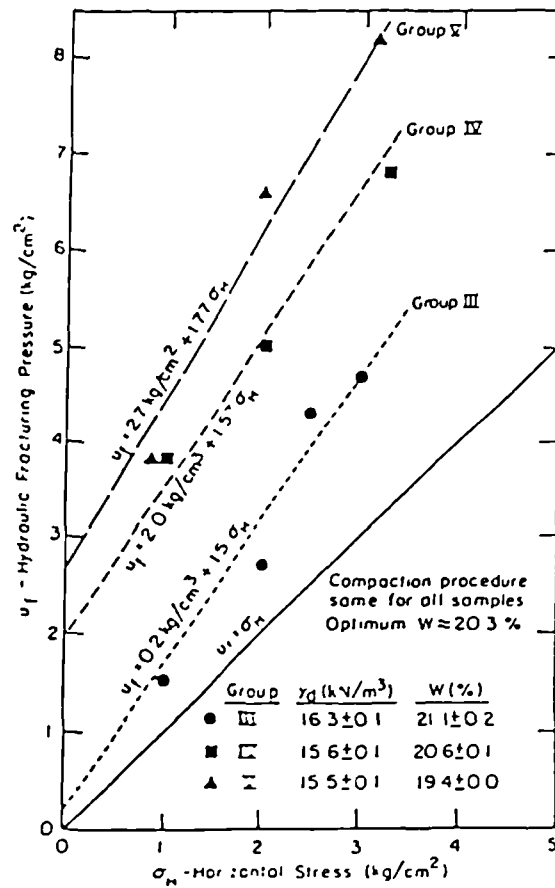


Fig 3.8 HYDRAULIC FRACTURING TESTS ON RECOMPACTED SAMPLES OF TETON DAM SOILS (GROUPS. III, IV, V)

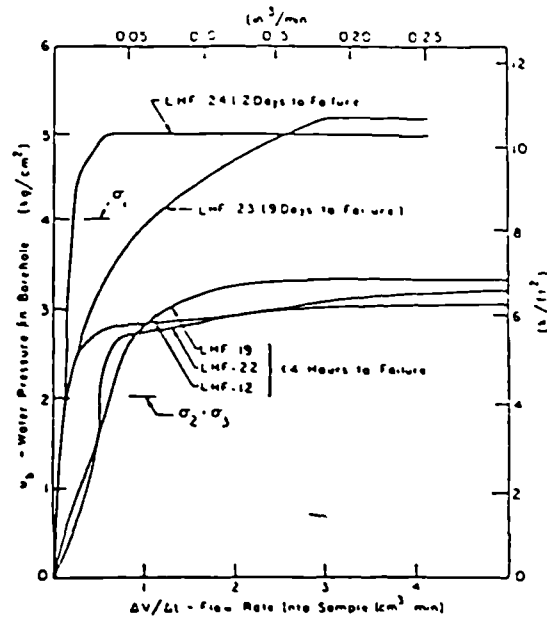


Fig 3.9 EFFECT OF DURATION ON TESTS

(Fig 3.6, 3.7, 3.8 and 3.9 - From Jaworski et al, 1981)

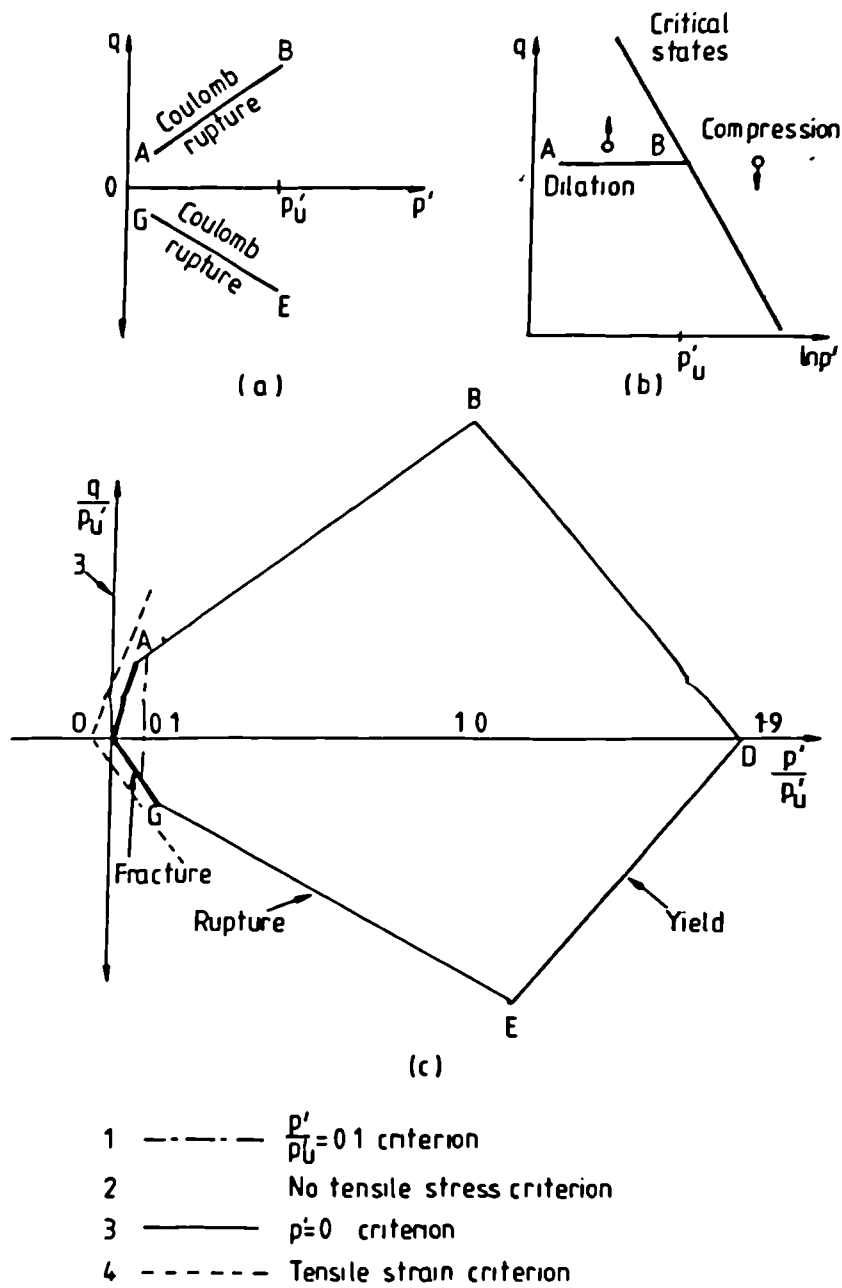


Fig 3.10 CRITERIA FOR CRACKING
(From Savvidou, 1981)

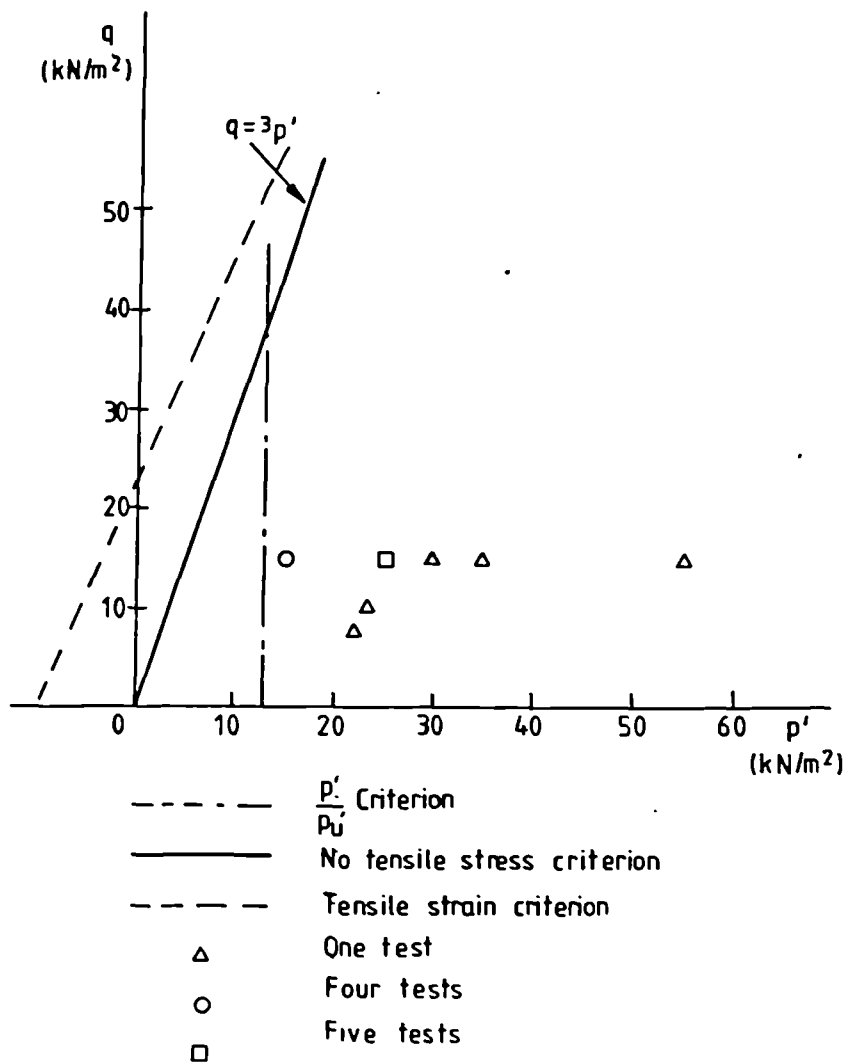


Fig 3.11 REGION OF CRACKING STRESSES
(After Savvidou, 1981)

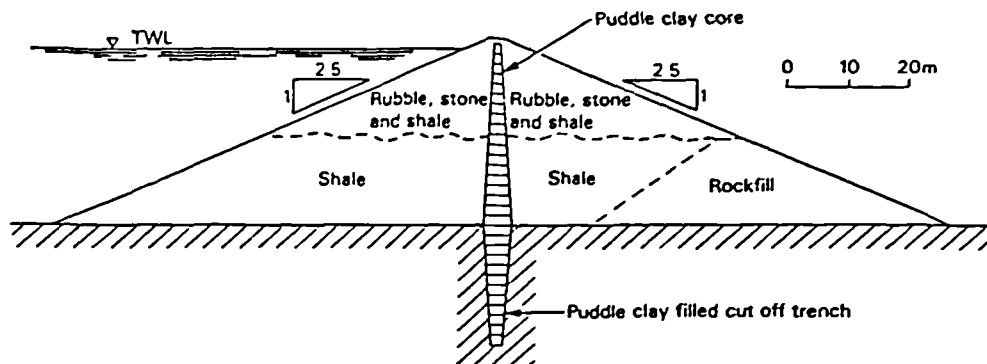


Fig 4.1 CROSS SECTION OF OLD DALE DYKE EMBANKMENT DAM (After Binnie 1978)

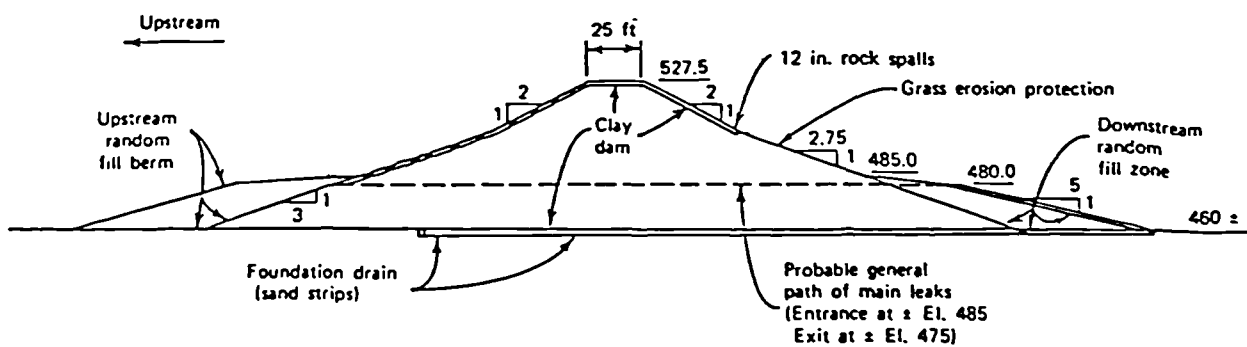


Fig 4.2 WISTER DAM SECTION SHOWING PROBABLE LOCATION OF MAJOR LEAKS (From Sherard 1973)

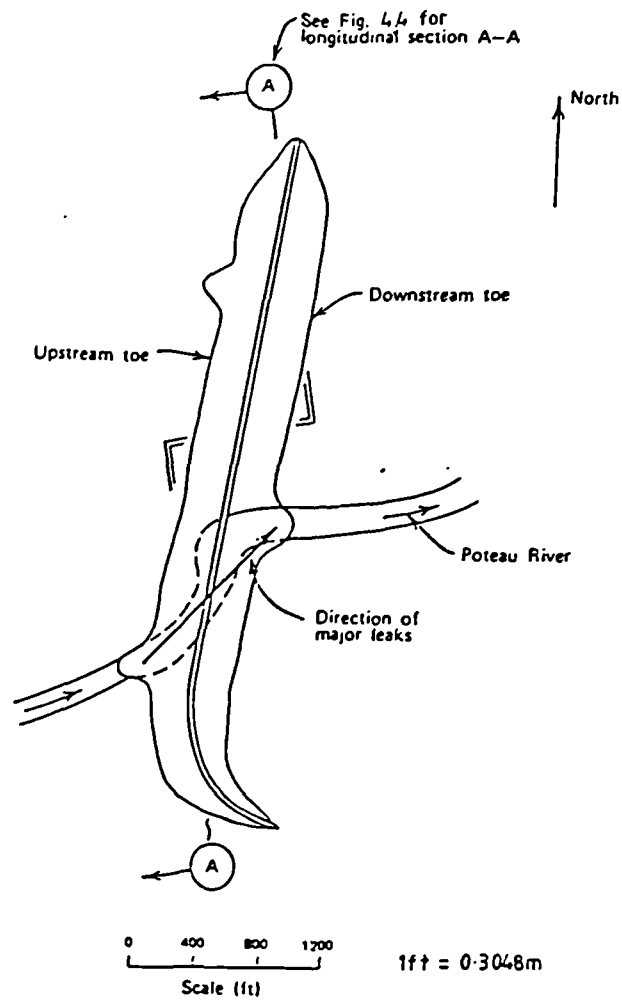


Fig 4.3 WISTER DAM SHOWING LOCATION AND DIRECTION OF MAJOR LEAKS (From Sherard 1973)

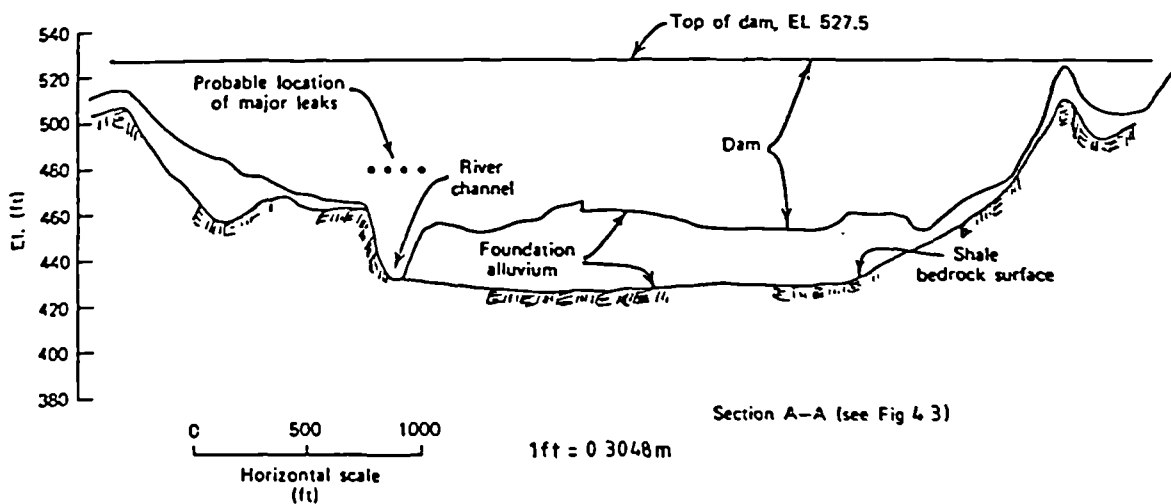


Fig 4.4 WISTER DAM LONGITUDINAL SECTION SHOWING THICKNESS OF FOUNDATION ALLUVIUM OVER BEDROCK AND PROBABLE LOCATION OF MAJOR LEAKS (From Sherard 1973)

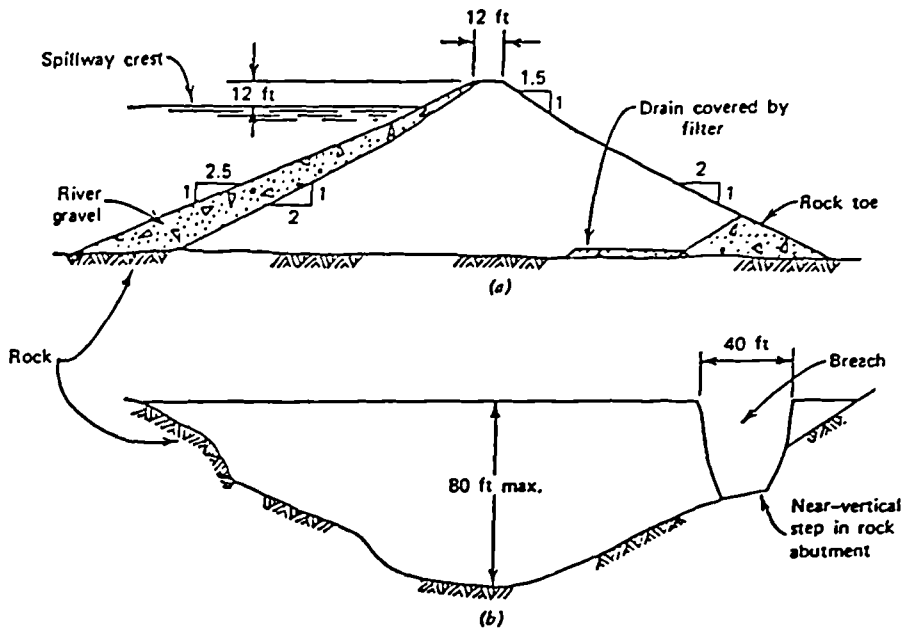


Fig 4.5 STOCKTON CREEK DAM (a) CROSS SECTION
 (b) LONGITUDINAL SECTION LOOKING DOWN STREAM
 (After Sherard 1973)

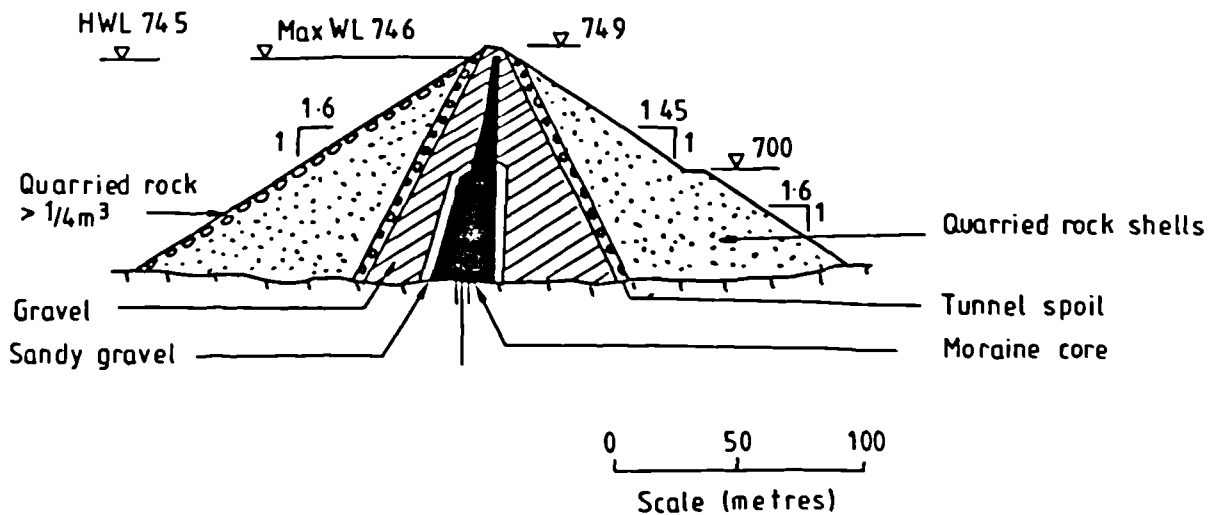


Fig 4.6 HYTTEJUVET DAM CROSS SECTION
 (After Kjaernsli and Torblaa 1968)

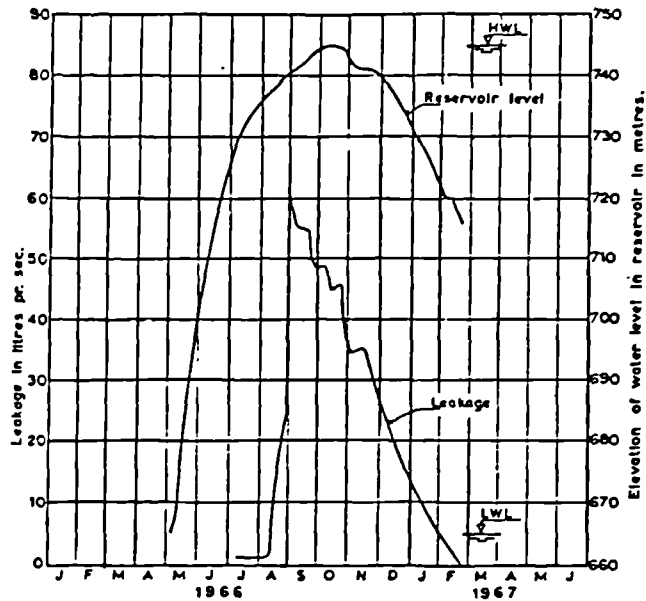
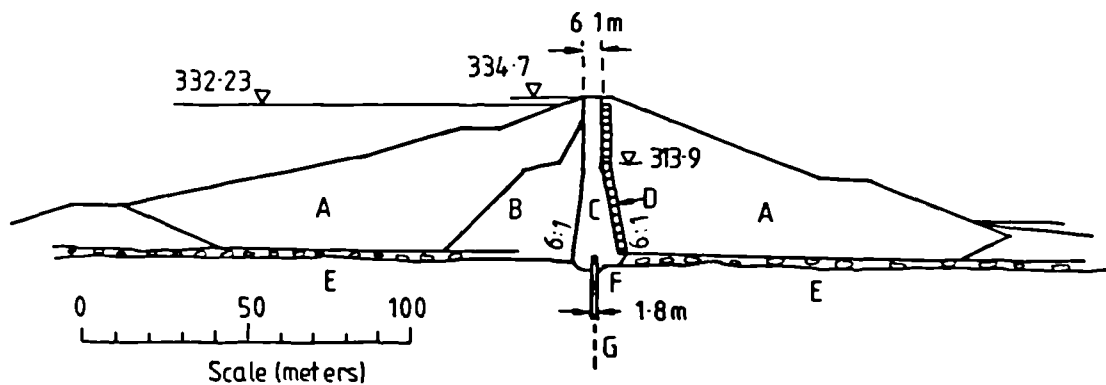


Fig 4.7 HYTTEJUVET DAM VARIATION OF LEAKAGE AND WATER LEVEL IN RESERVOIR WITH TIME (After Kjaernsli and Torblaa 1968)



- | | |
|------------------------------|----------------------|
| (A) Shale fill | (E) Shale foundation |
| (B) Fine shale fill | (F) Concrete cut-off |
| (C) Boulder clay core | (G) Grout curtain |
| (D) Crushed limestone filter | |

Fig 4.8 BALDERHEAD DAM CROSS SECTION (After Vaughan et al 1970)

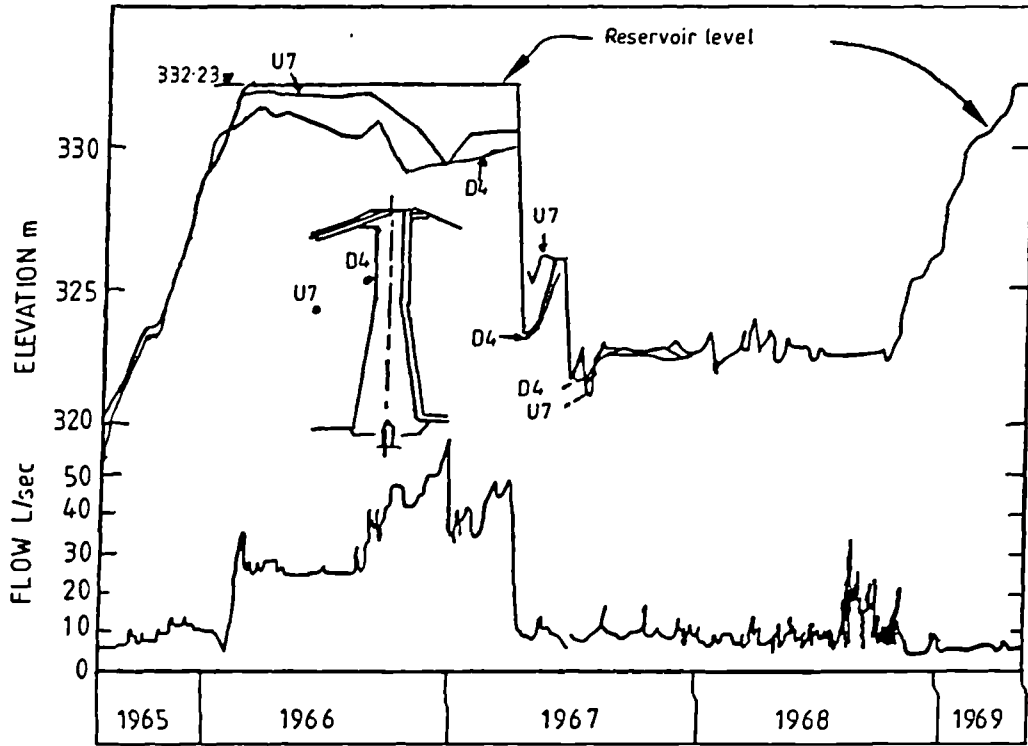


Fig 4.9 BALDERHEAD DAM RESERVOIR LEVEL, SEEPAGE FLOW AND UPSTREAM PIEZOMETERS (After Vaughan et al 1970)

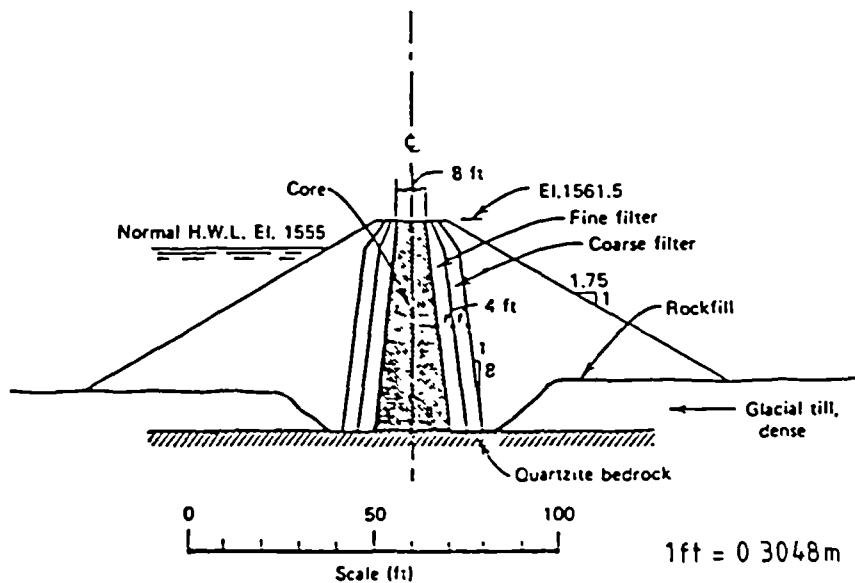


Fig 4.10 YARD'S CREEK UPPER RESERVOIR DAM CROSS SECTION (After Sherard 1973)

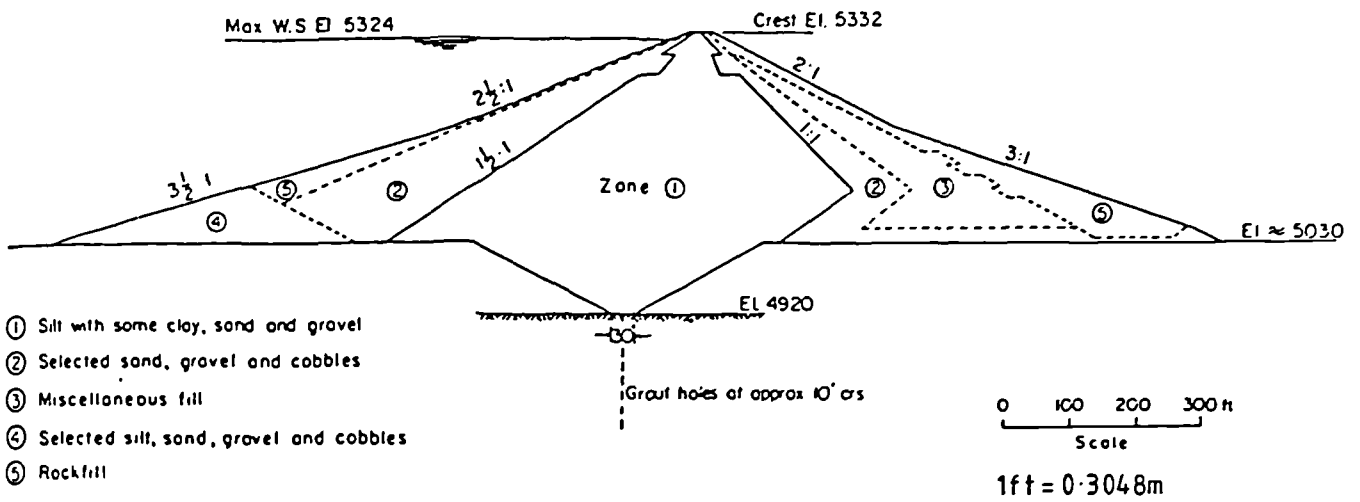


Fig 4.11 TETON DAM : CROSS SECTION THROUGH CENTRE PORTION OF EMBANKMENT FOUNDED ON ALLUVIUM (After Seed and Duncan 1981)

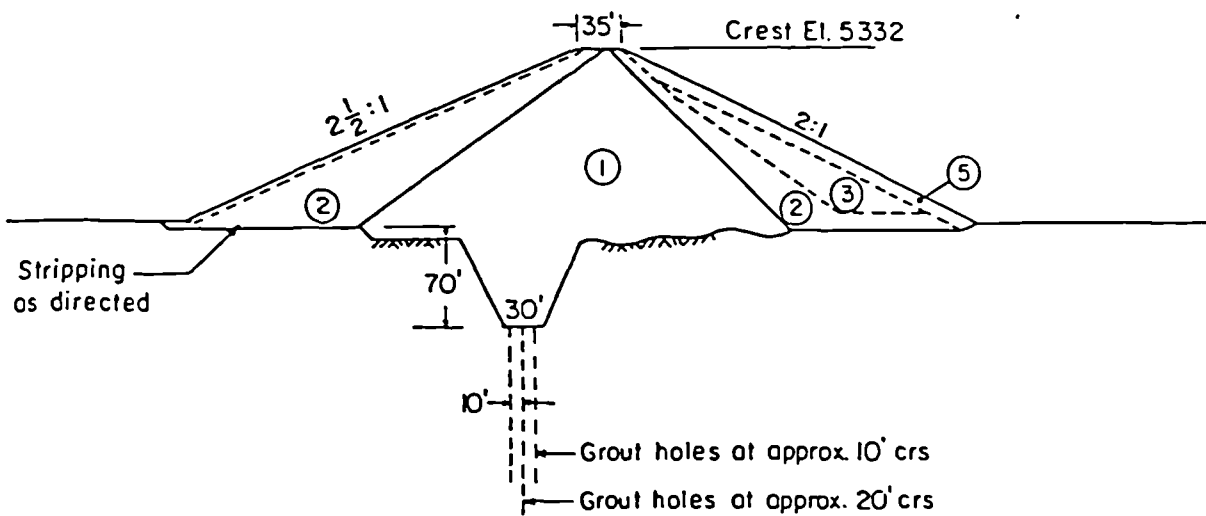
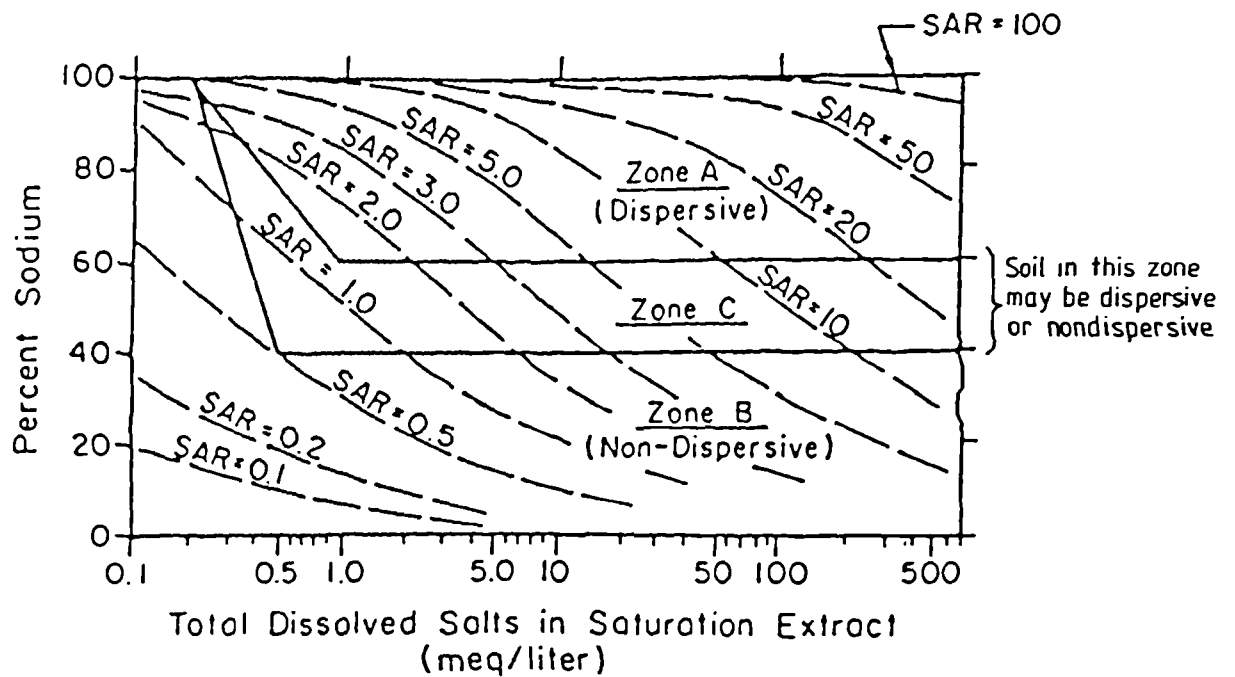
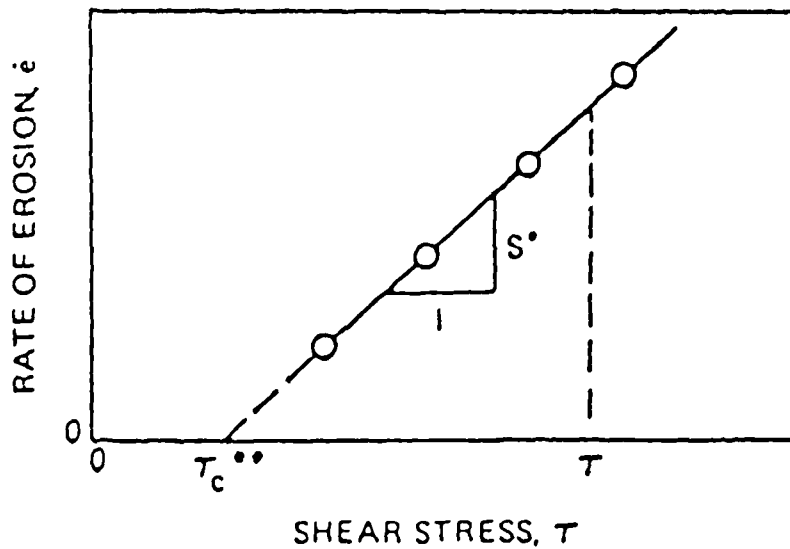


Fig 4.12 TETON DAM : TYPICAL CROSS SECTION OVER ABUTMENT SECTIONS FOUNDED ON JOINTED RHYOLITE (After Seed and Duncan 1981)



NOTE : Relationship shown valid only when eroding water is relatively pure

Fig 5.1 RELATIONSHIP BETWEEN DISPERSIBILITY (SUSCEPTIBILITY TO COLLOIDAL EROSION) AND DISSOLVED PORE-WATER SALTS BASED ON PINHOLE TESTS AND EXPERIENCE WITH EROSION IN NATURE (After Sherard et al, 1976)



*S = RATE OF CHANGE OF EROSION RATE

** τ_c = CRITICAL SHEAR STRESS

$$\dot{e} = S(\tau - \tau_c) \quad \tau > \tau_c$$

Fig 5.2 DEFINITION OF CRITICAL SHEAR STRESS, RATE OF CHANGE OF EROSION RATE AND RATE OF EROSION (After Arulanandan and Perry, 1983)

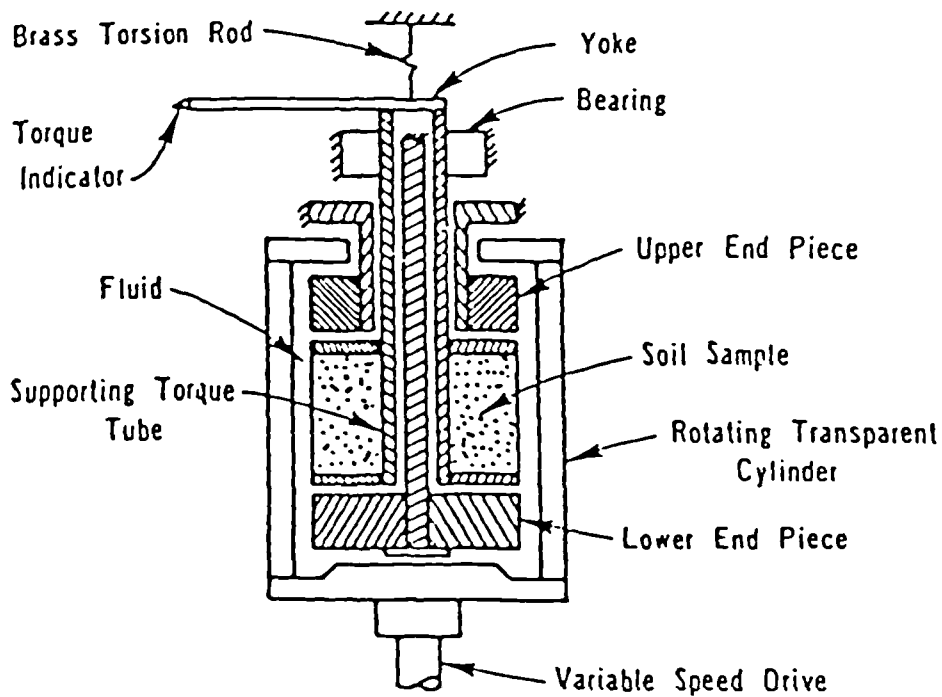


Fig 5.3 CROSS SECTIONAL VIEW OF ROTATING CYLINDER TEST APPARATUS (After Arulanandan et al 1975)

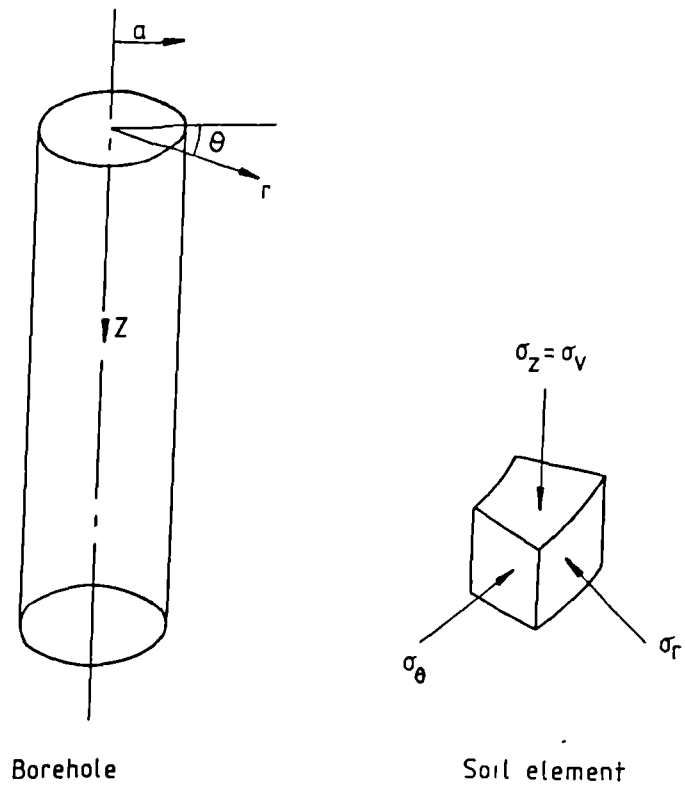


Fig 6.1 THE IDEALIZED MODEL

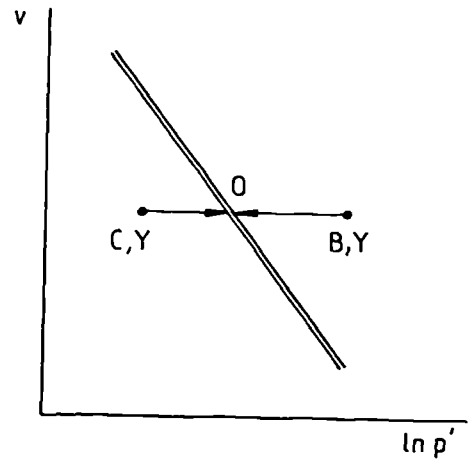
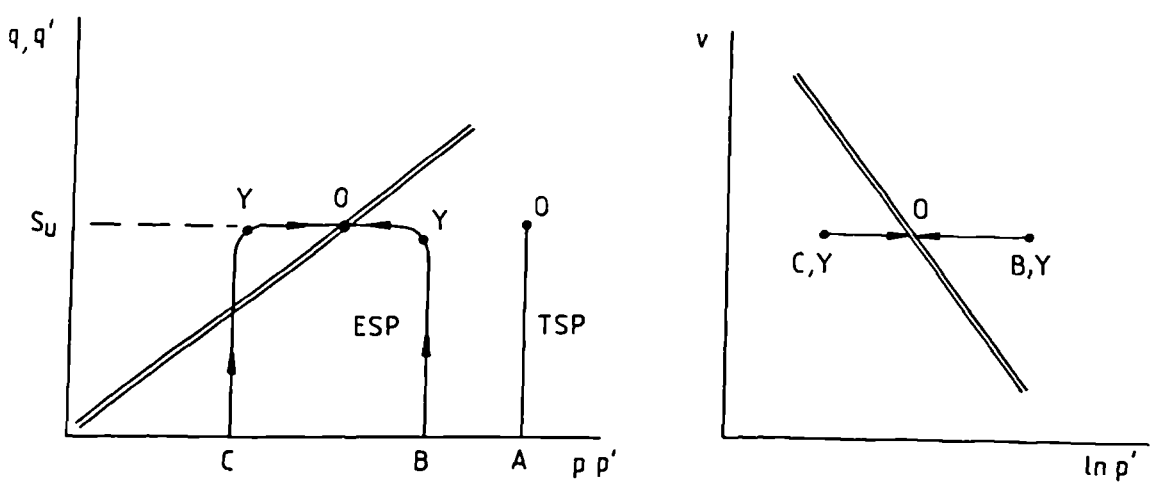


Fig 6.2 STRESS PATH DURING HYDRAULIC FRACTURE TESTS ON IDEAL ELASTIC-PLASTIC SOIL

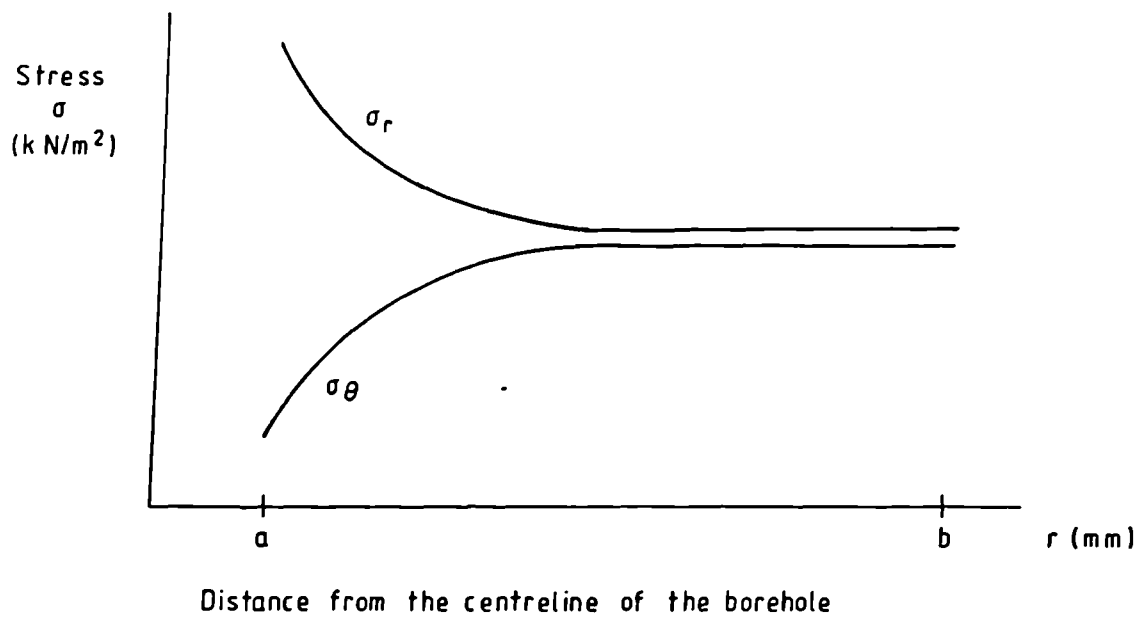


Fig 6.3 DISTRIBUTION OF STRESSES AWAY FROM THE BOREHOLE

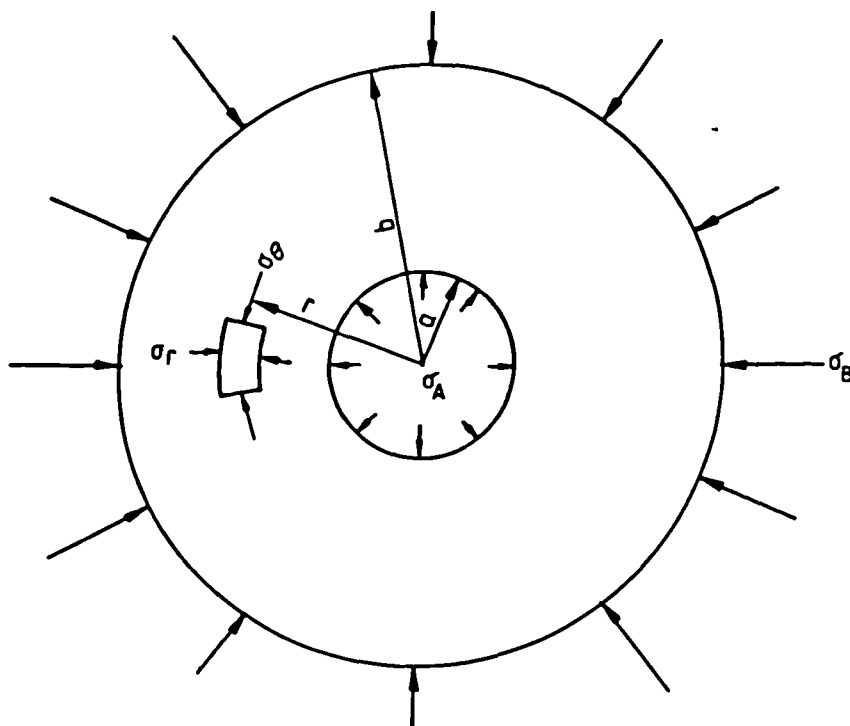


Fig 6.4 PLANE STRAIN ANALYSIS OF A THICK HOLLOW CYLINDER

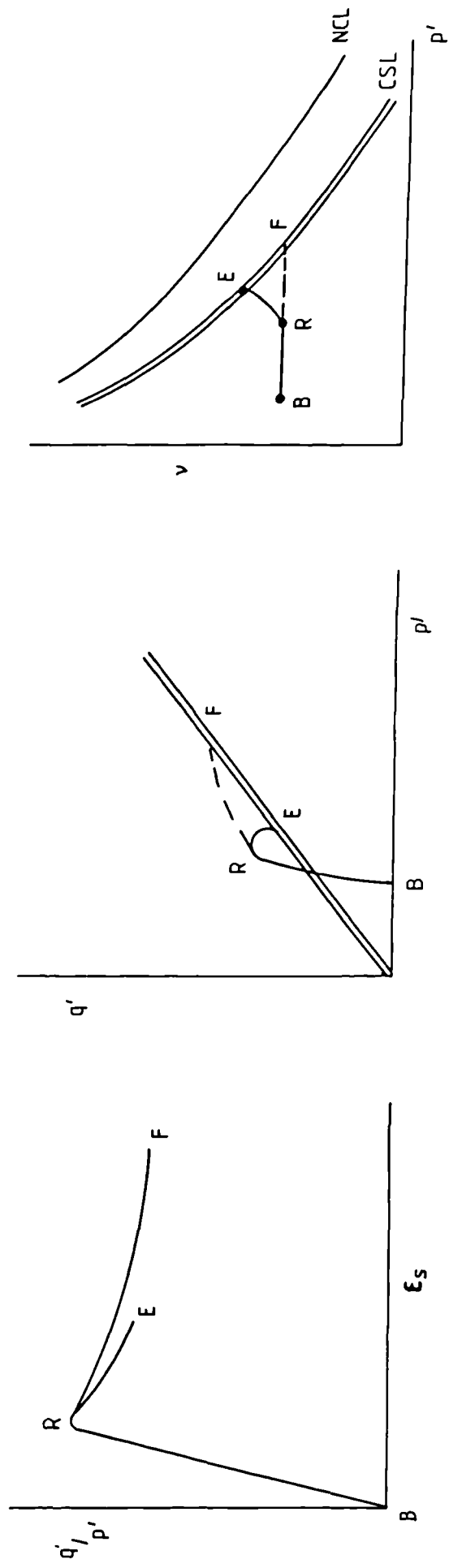


Fig 6.5 POSSIBLE BEHAVIOUR OF OVERCONSOLIDATED SAMPLES DURING FRACTURING TESTS

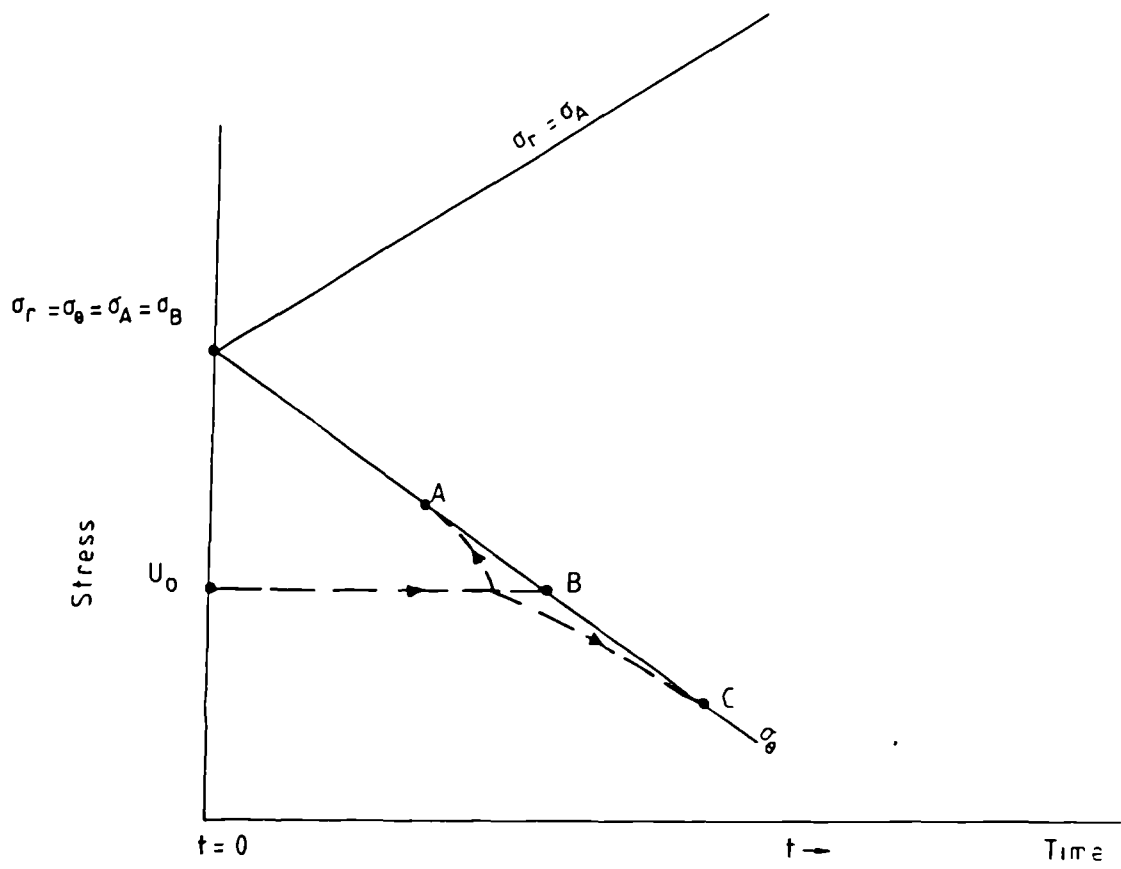
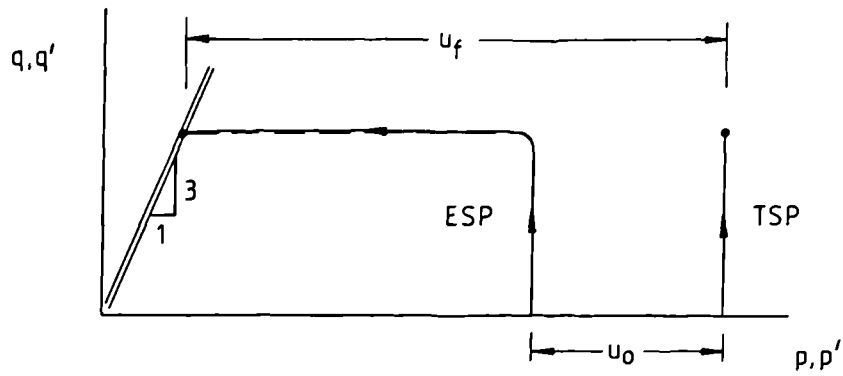
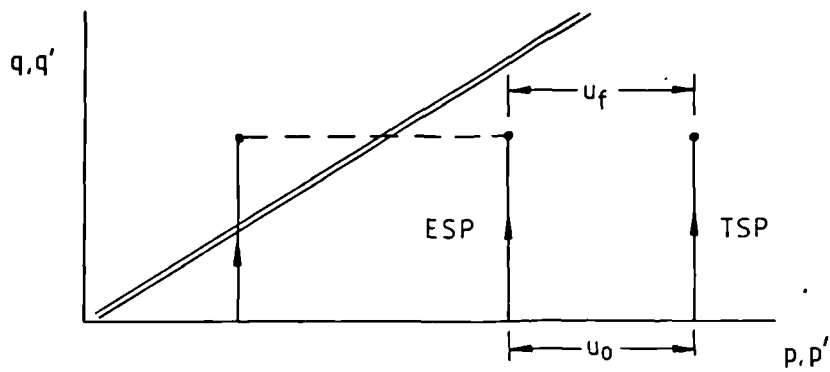


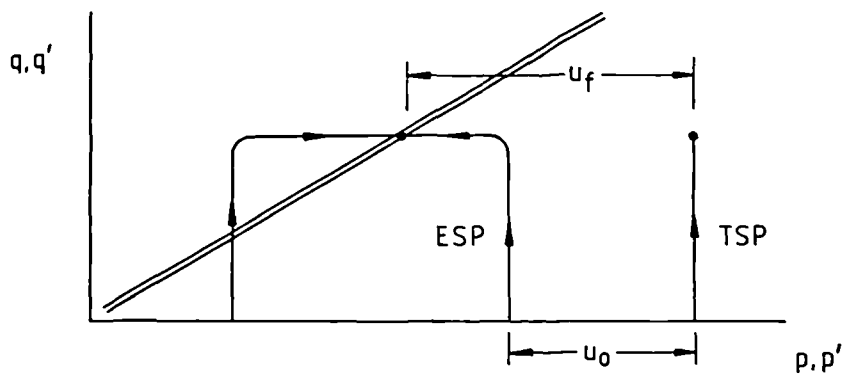
Fig 6.6 POSSIBLE STRESS CHANGES IN A SOIL ELEMENT ADJACENT TO THE CAVITY DURING HYDRAULIC FRACTURING TEST



a) Fracture occurs at $q' = 3p'$ (no-tension cut-off)



b) Fracture occurs at yield $u_f = u_0$



c) Fracture occurs on critical state line

Fig 6.7 PORE PRESSURE AT FAILURE IN A FRACTURING TEST

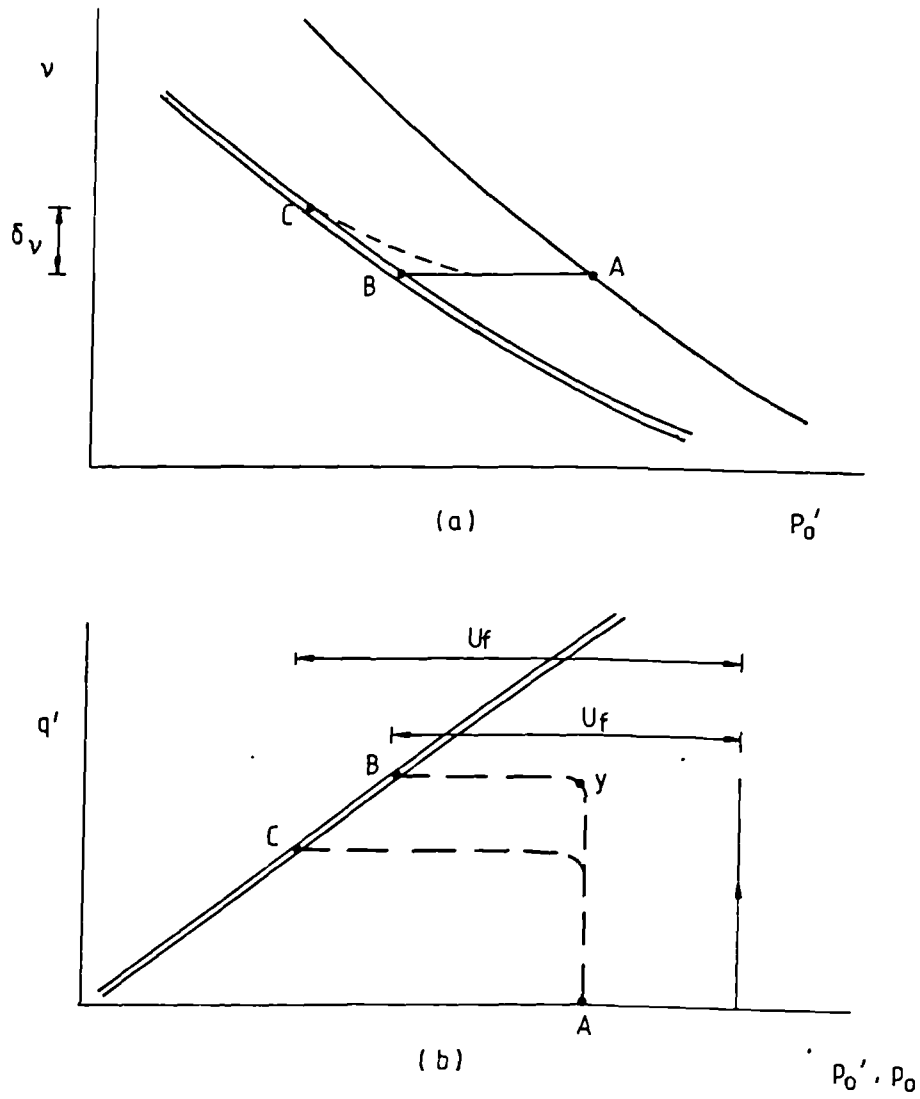


Fig 6.8 THE EFFECT OF PENETRATING FLUID

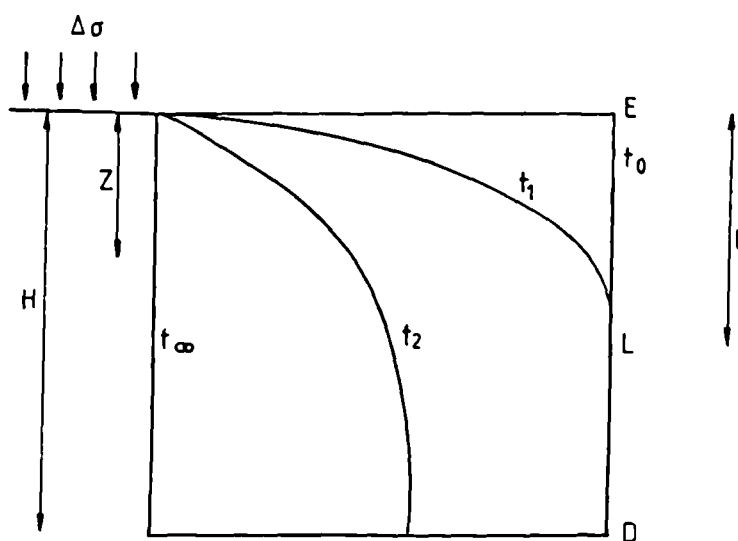


Fig 6.9 ISOCHRONES DURING I-D - CONSOLIDATION

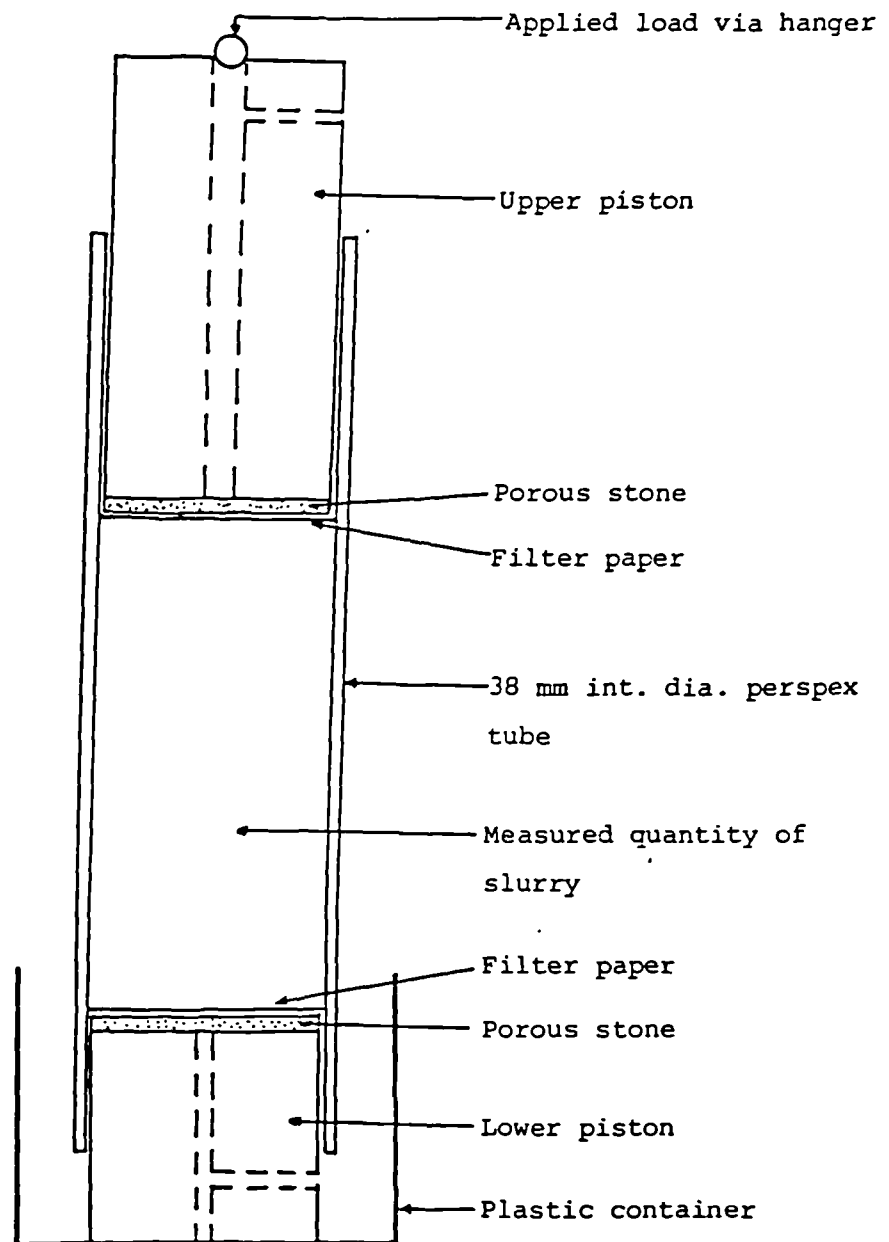


Fig 7.1 SAMPLE PRESS

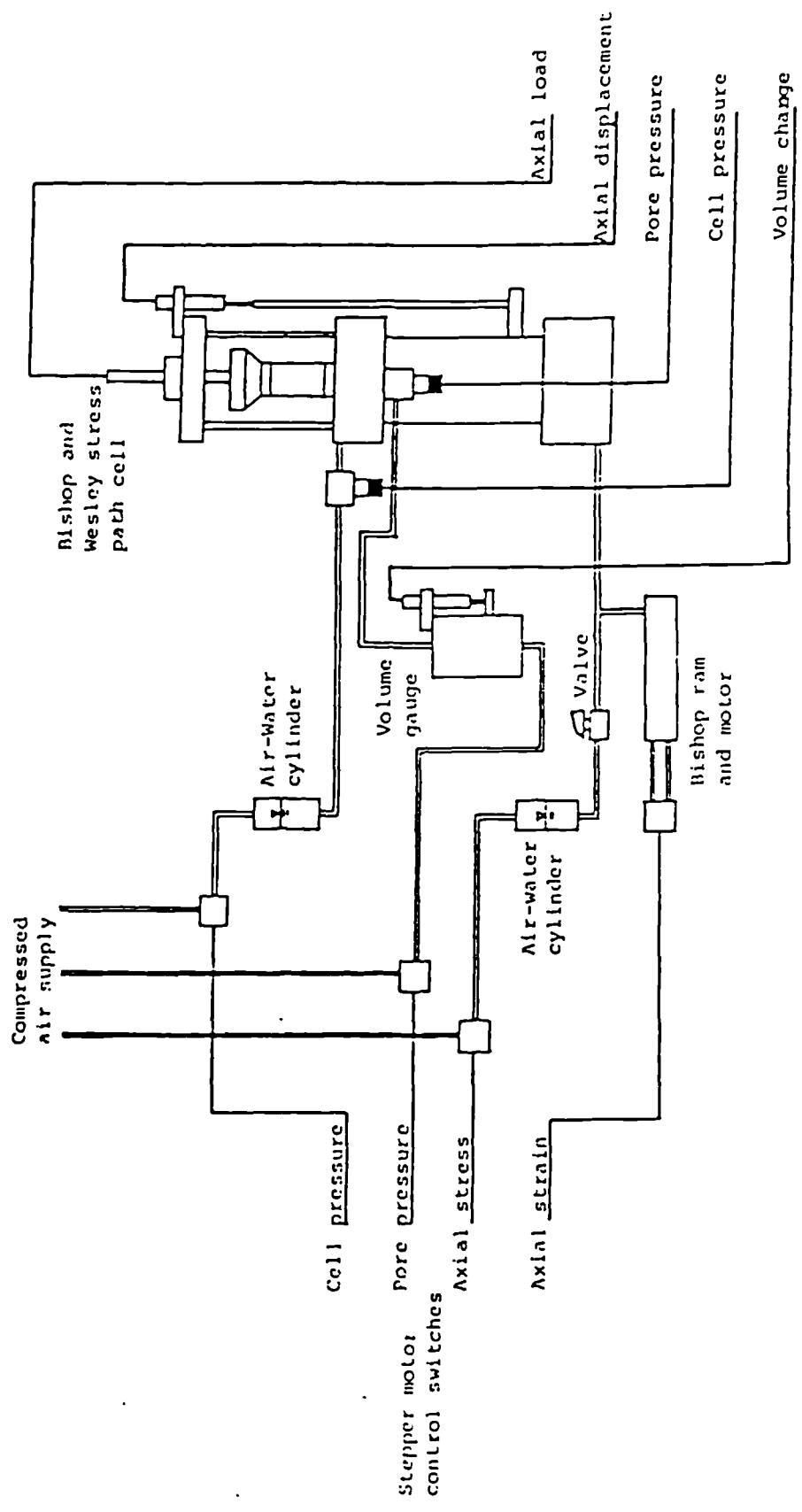


Fig 7.2 LOADING FOR A HYDRAULIC CELL FOR TRIAXIAL STRESS CONTROLLED AND STRAIN CONTROLLED TESTS AND FOR STRESS PATH TESTS

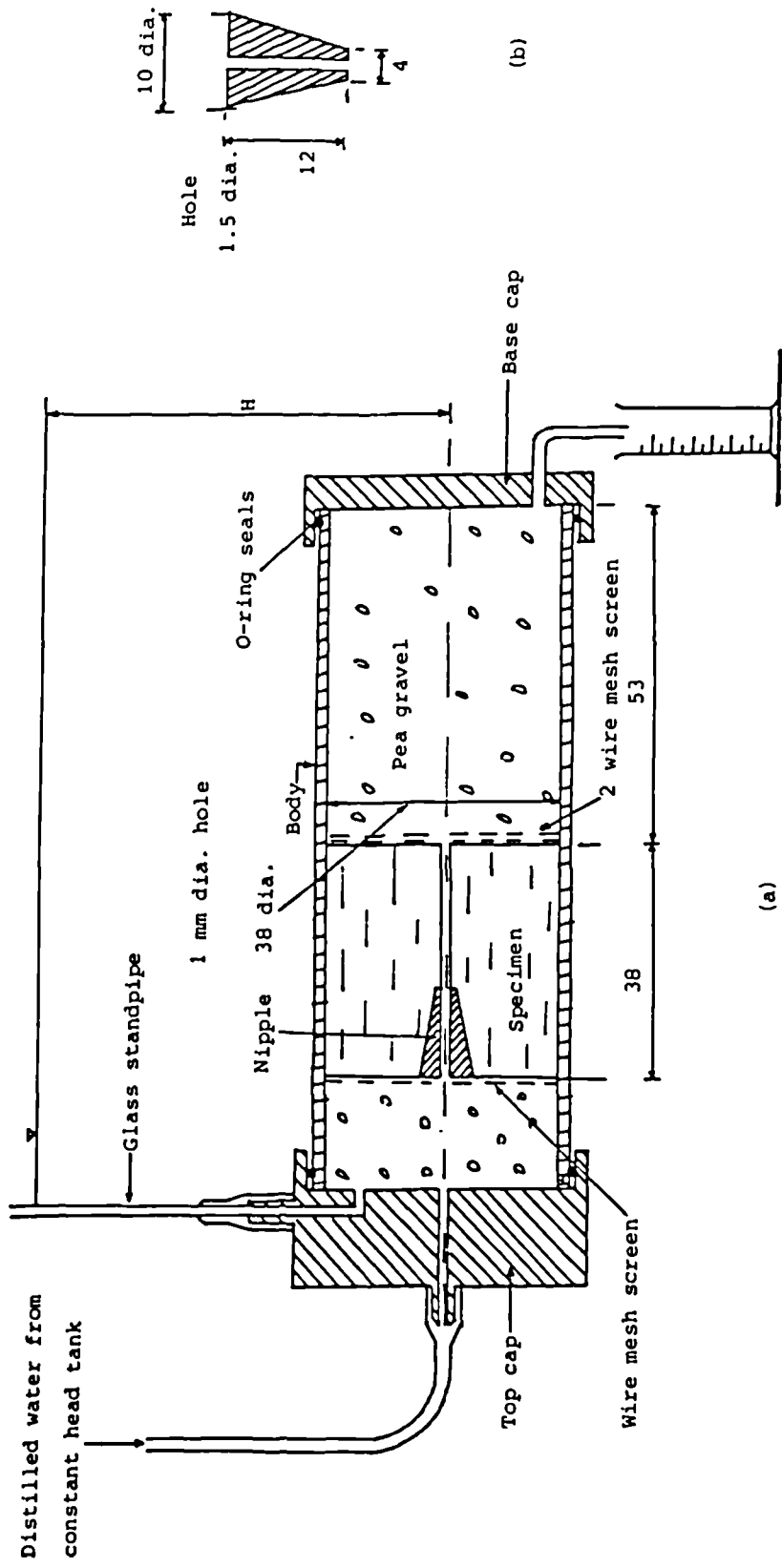


Fig 7.3 APPARATUS FOR PINHOLE TESTS: (a) GENERAL ARRANGEMENT (b) DETAILS OF NIPPLE (dimensions in mm) (After Sherard et al 1976a)

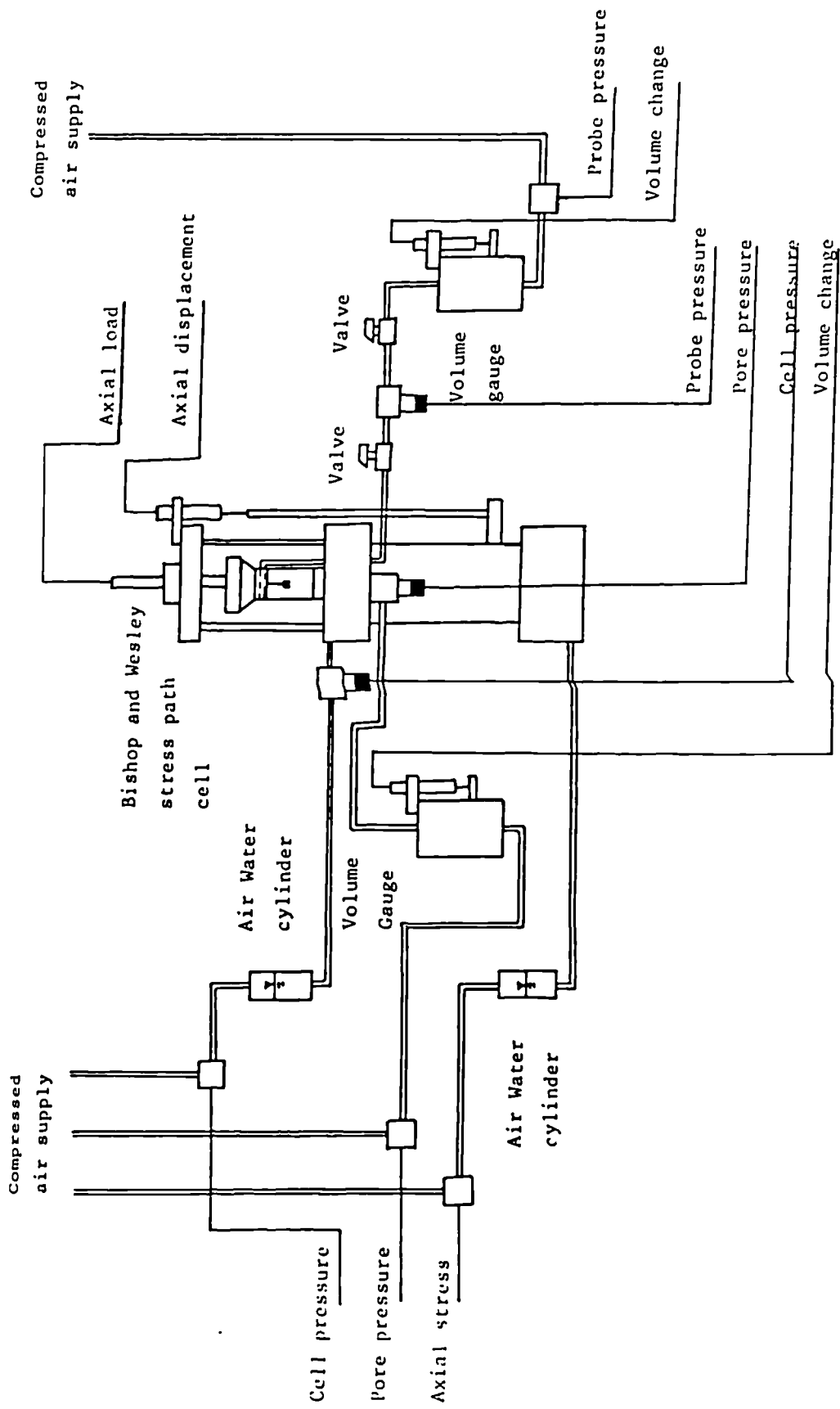


Fig 7.4 LABORATORY HYDRAULIC FRACTURE APPARATUS

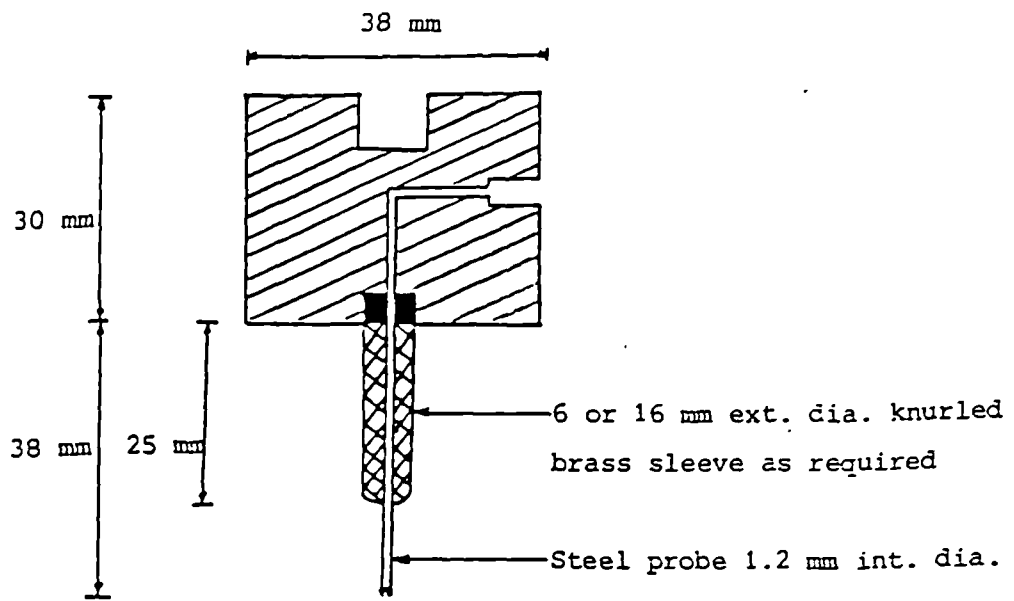


Fig 7.5 SAMPLE'S TOP CAP AND THE PROBE (not to scale)

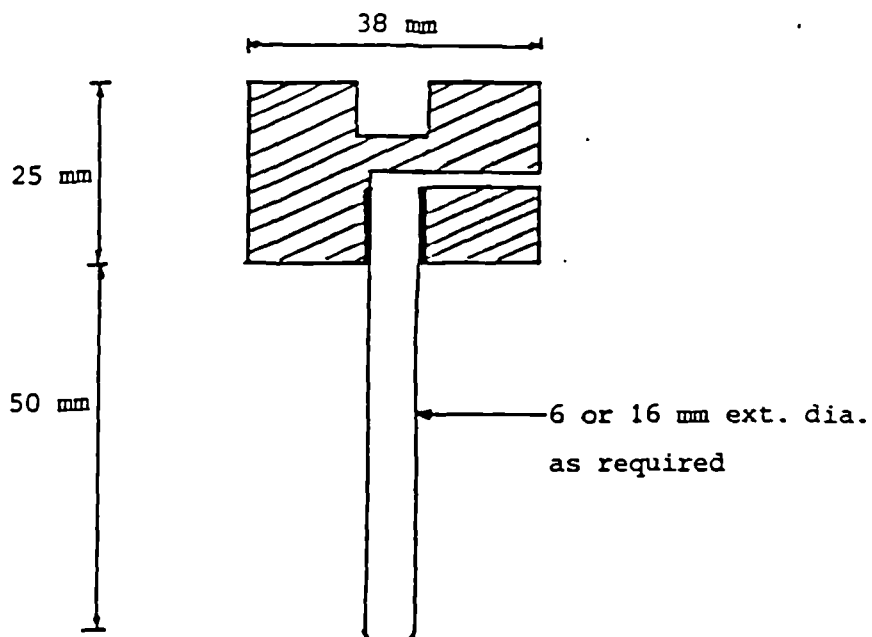


Fig 7.7 SAMPLE BORER (not to scale)

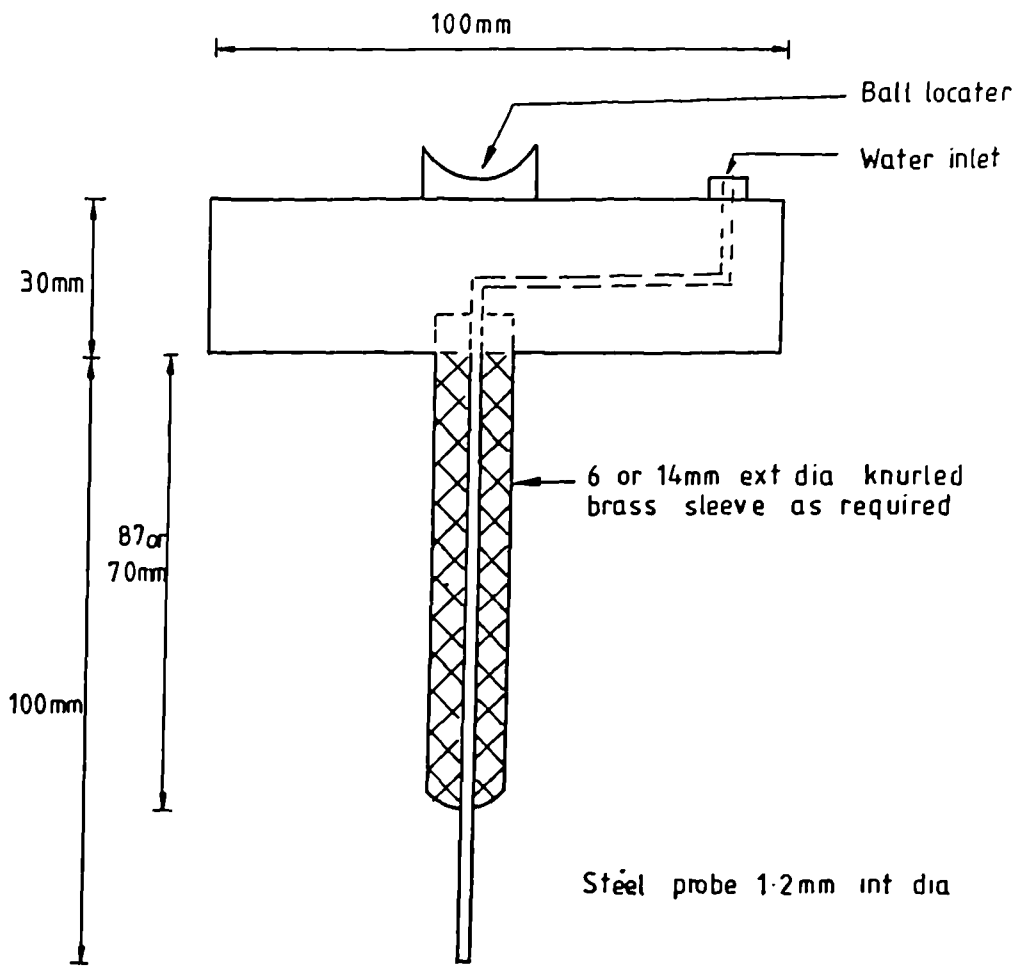


Fig 7.6 100mm SAMPLES TOP CAP AND THE PROBE (not to scale)

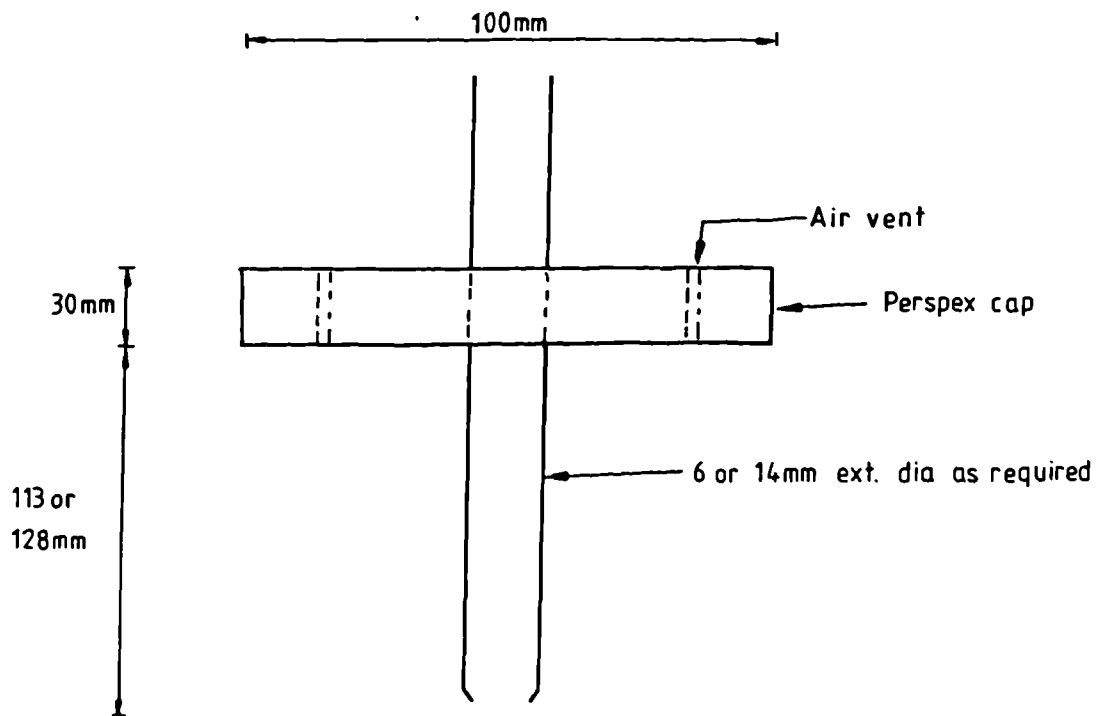


Fig 7.8 100mm SAMPLE BORER (not to scale)

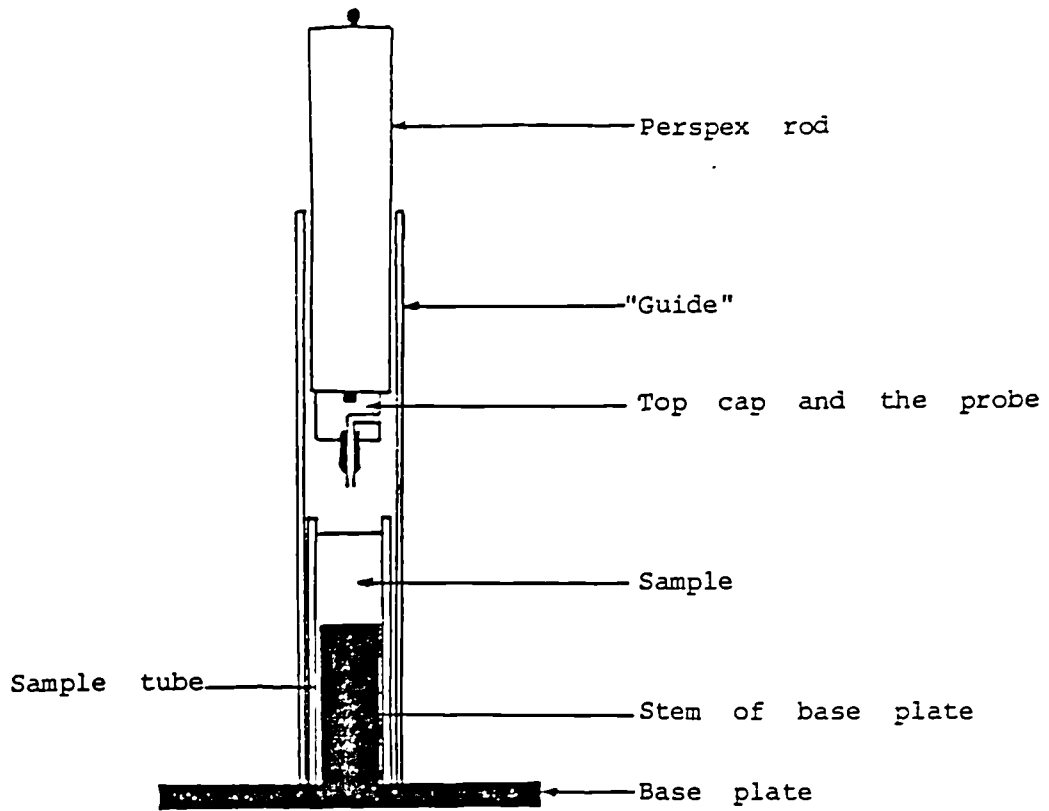


Fig 7.9 'FINAL' SET UP

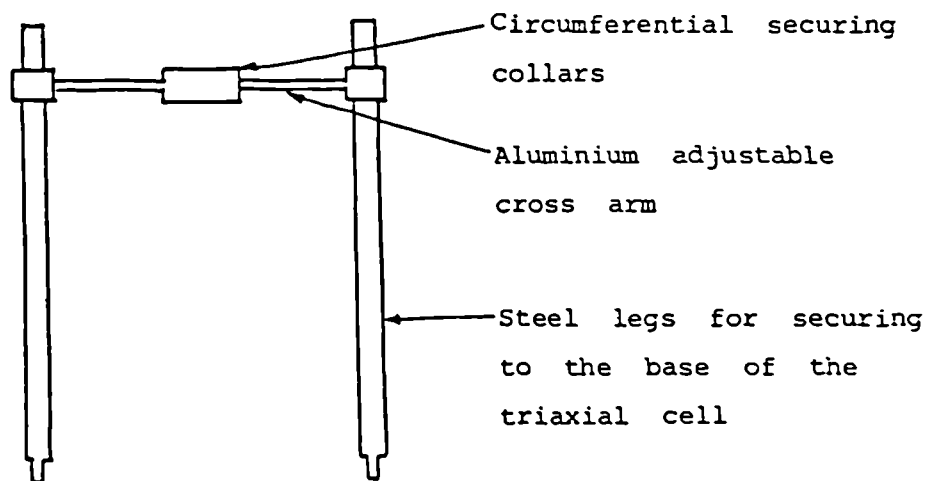


Fig 710 SAMPLE'S TOP CAP HOLDER

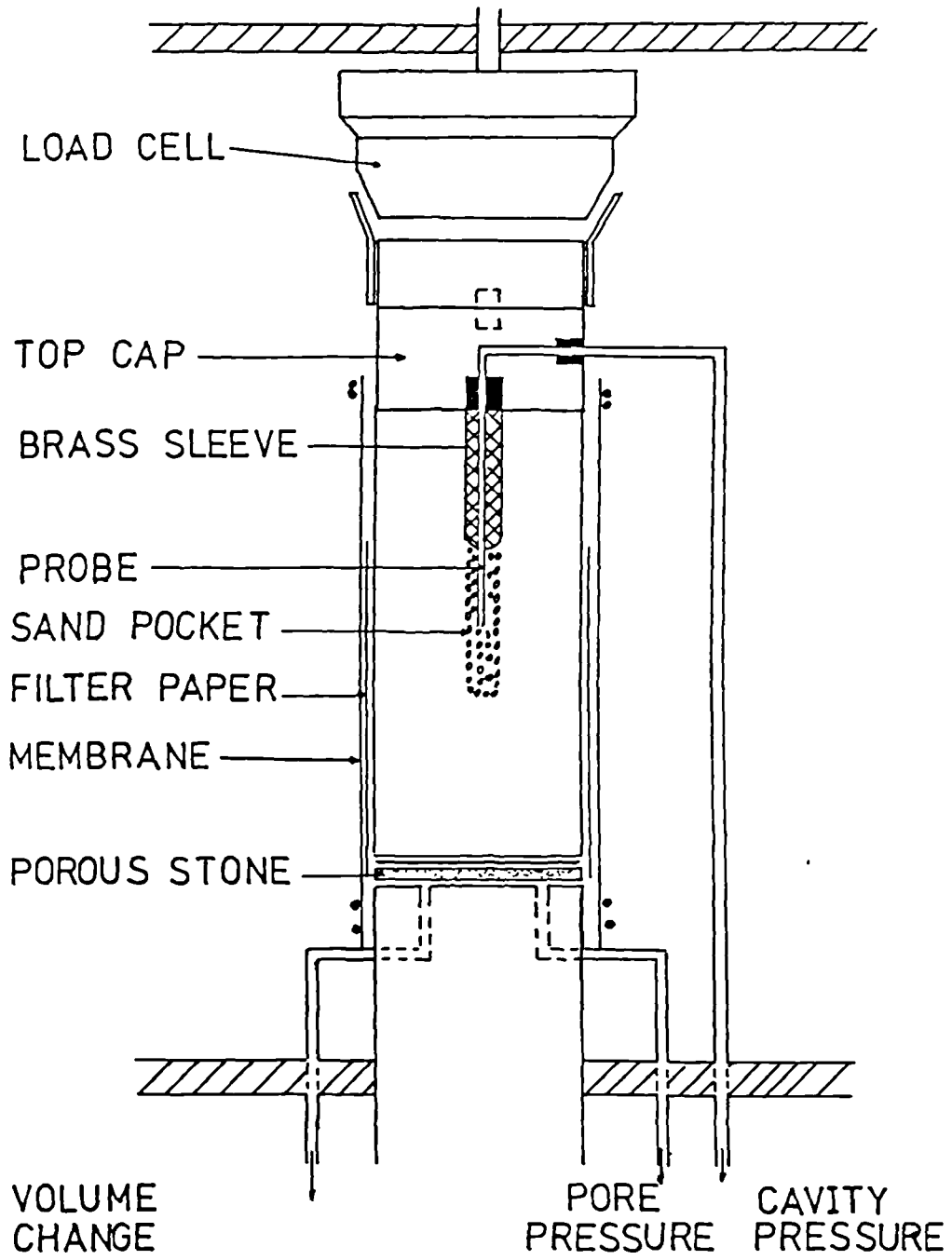


Fig 8.1 SAMPLE SET-UP

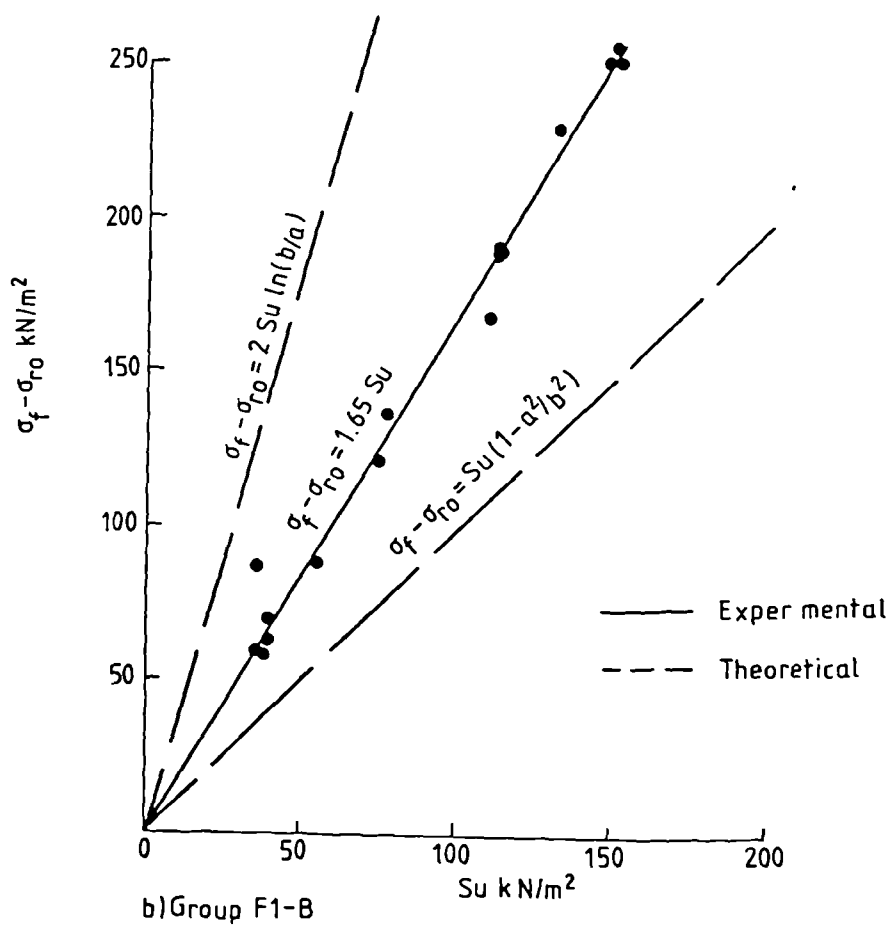
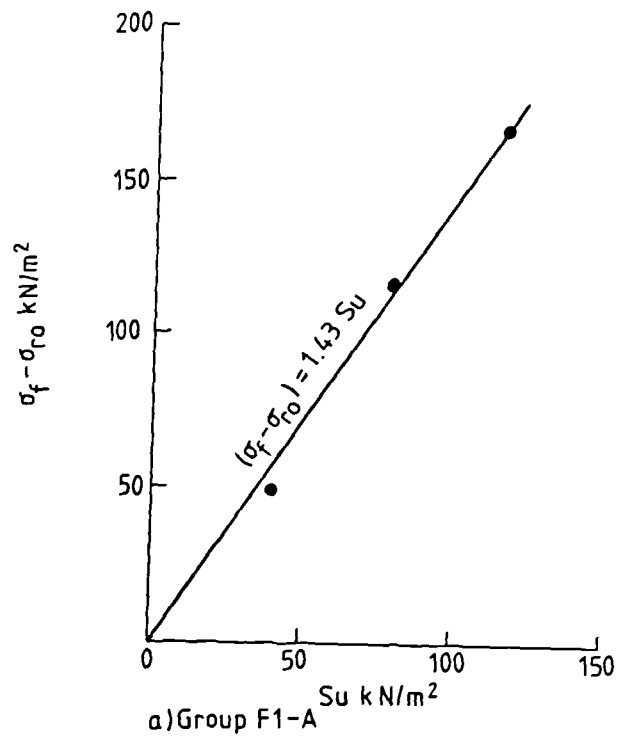


Fig 10.1 PLOT OF $\sigma_f - \sigma_{ro}$ AGAINST S_u : GROUP F1-A AND F1-B (INITIAL FRACTURING TESTS)

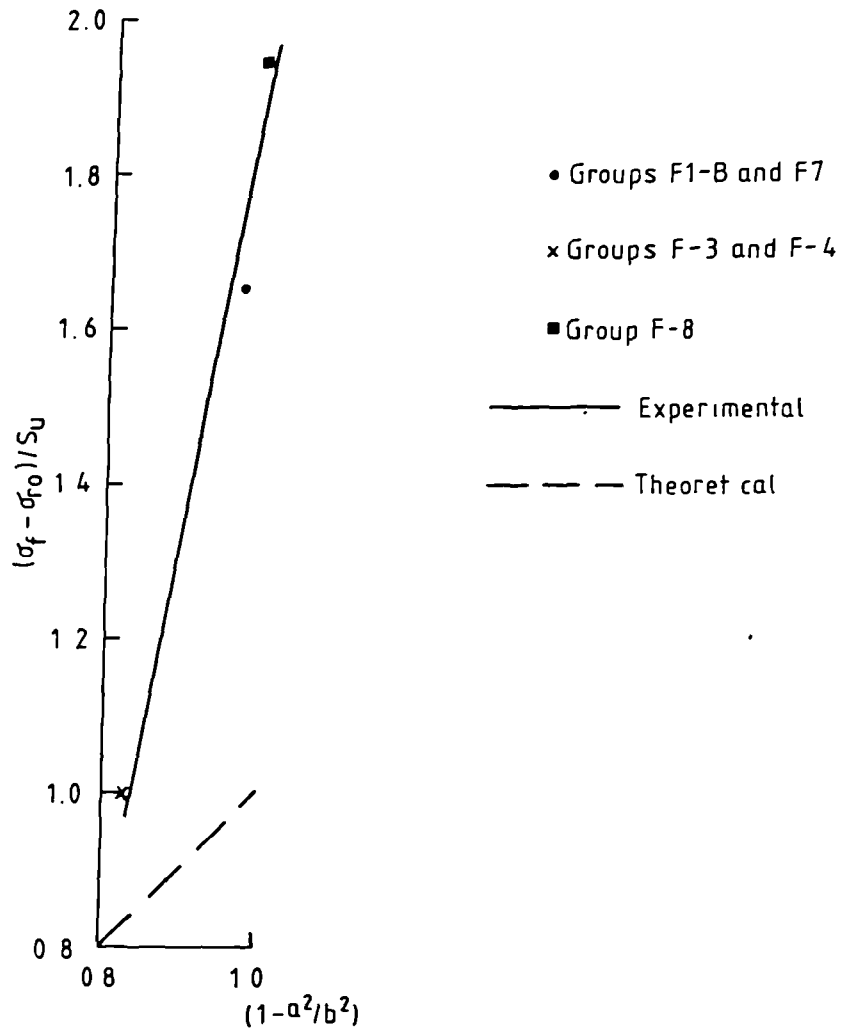


Fig 10.1A PLOT OF $(\sigma_f - \sigma_{r0})$ AGAINST $(1 - a^2/b^2)$
(GROUPS F-1B, F-3, F-4, F-7 and F-8)

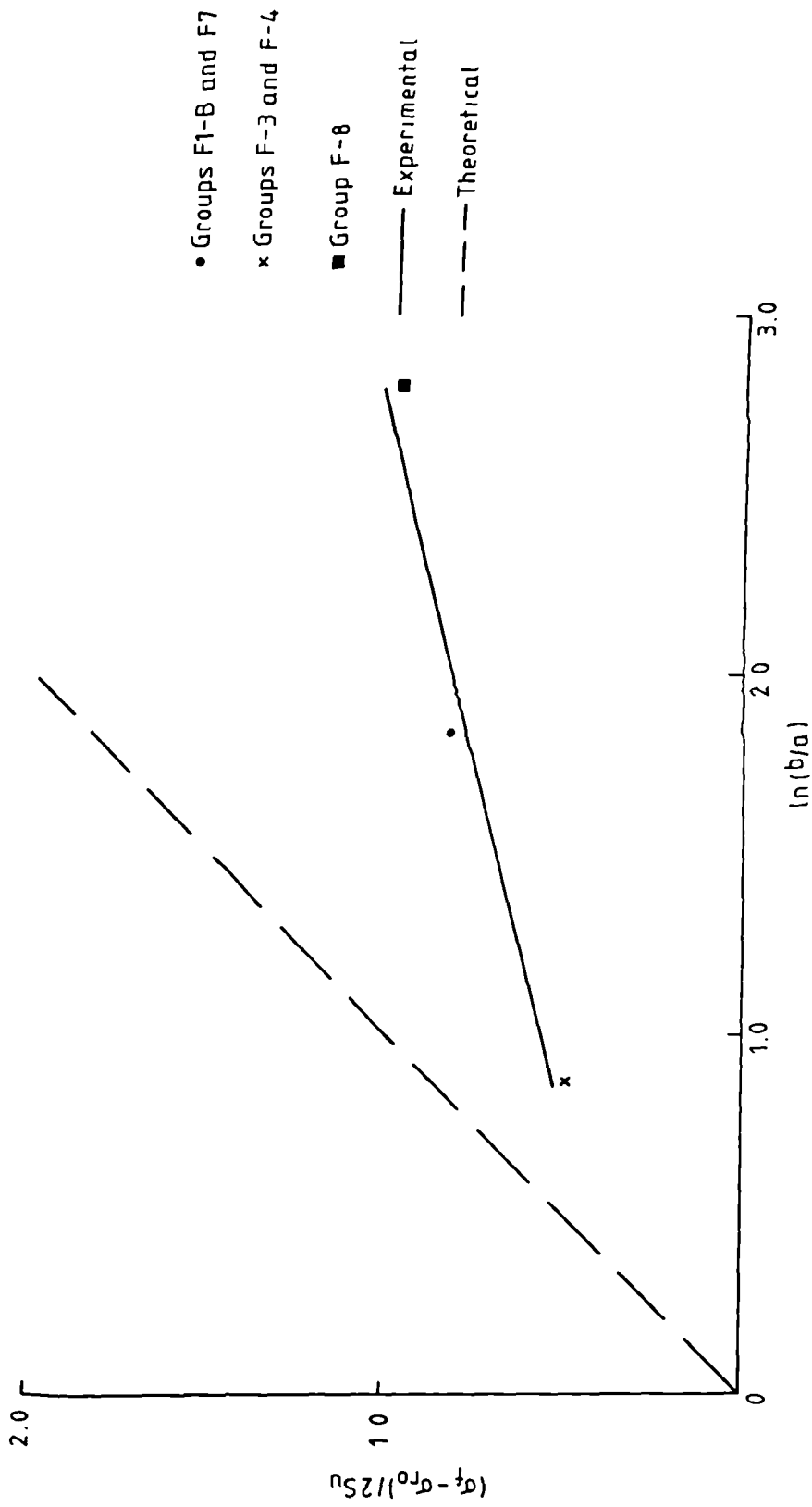


Fig 10.1B PLOT OF $(\sigma_f - \sigma_{f0}) / 2S_u$ AGAINST $\ln(b/a)$
 (GROUPS F1-B, F-3, F-4, F-7 and F-8)

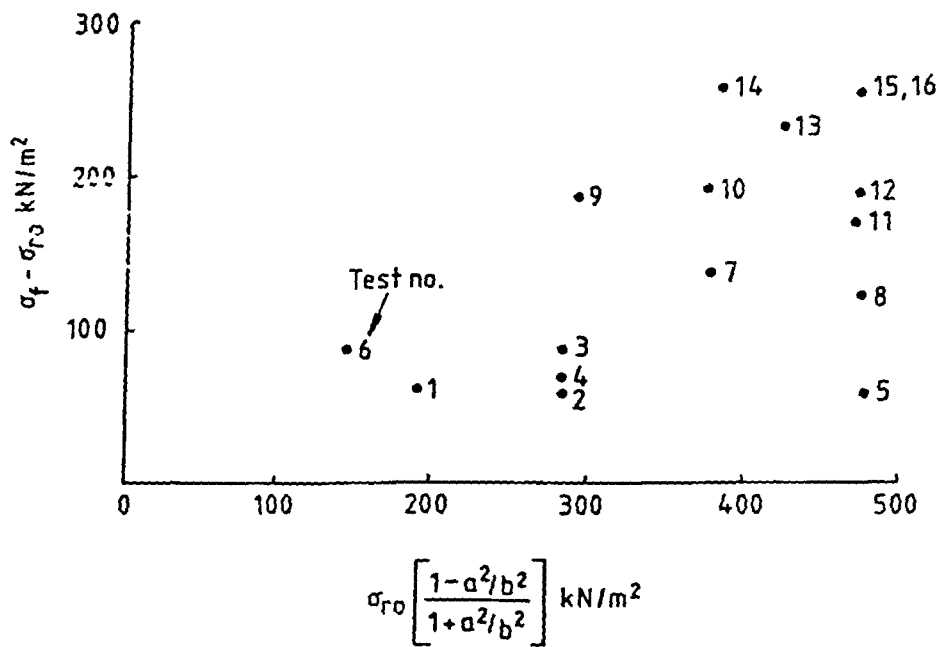


Fig 10.2 PLOT OF $\sigma_f - \sigma_{r0}$ AGAINST $\sigma_{r0} \left[\frac{1 - a^2/b^2}{1 + a^2/b^2} \right]$: GROUP F1-B
(INITIAL FRACTURING TESTS)

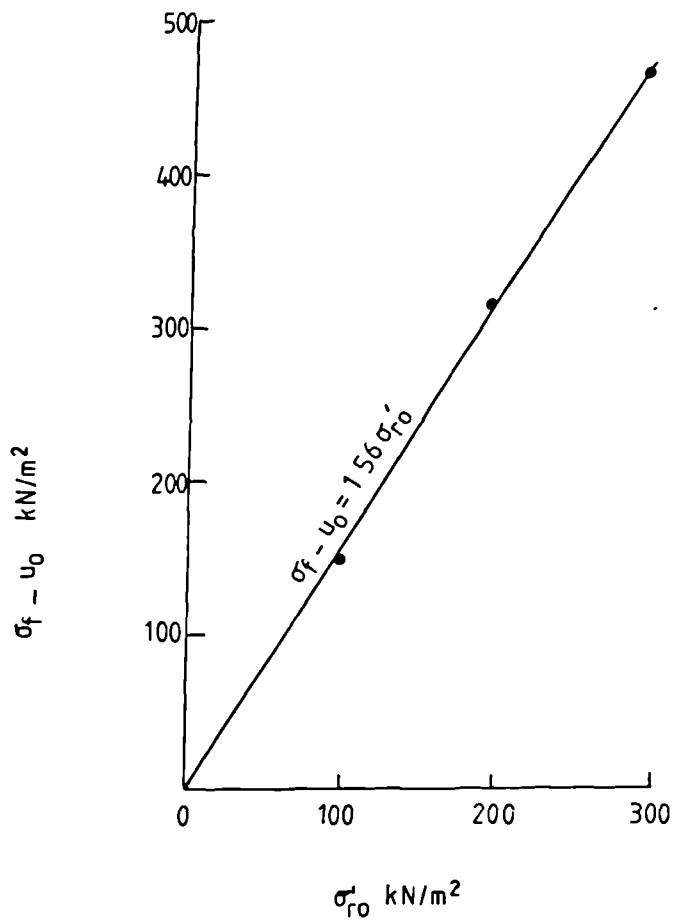


Fig 10.3 PLOT OF $\sigma_f - u_0$ AGAINST σ'_{r0} : GROUP F1-A
(INITIAL FRACTURING TESTS)

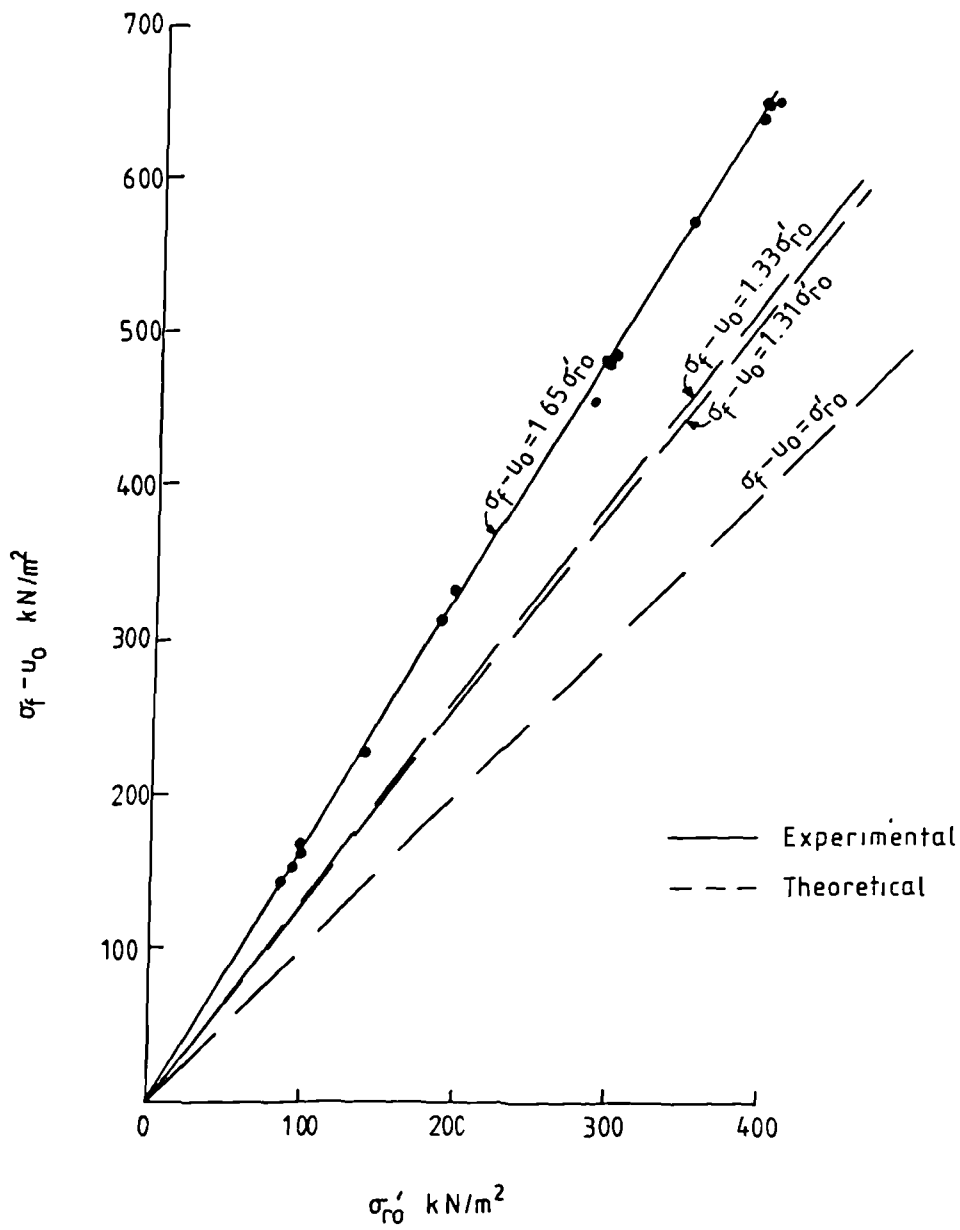


Fig 10.4 PLOT OF $\sigma_f - u_0$ AGAINST σ'_{r0} : GROUP F1-B
(INITIAL FRACTURING TEST)

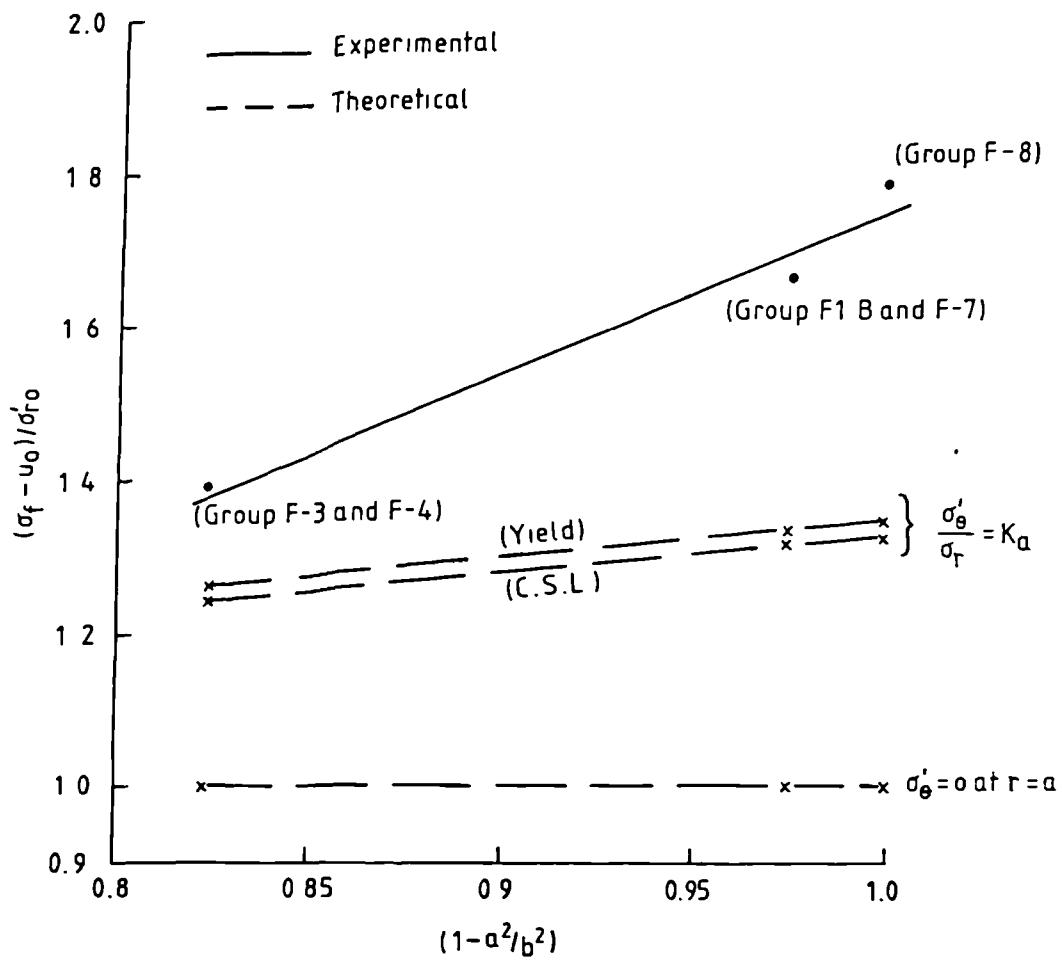


Fig 10.4A PLOT OF $(\sigma_f - u_0) / \sigma'_{r0}$ AGAINST $(1 - a^2/b^2)$

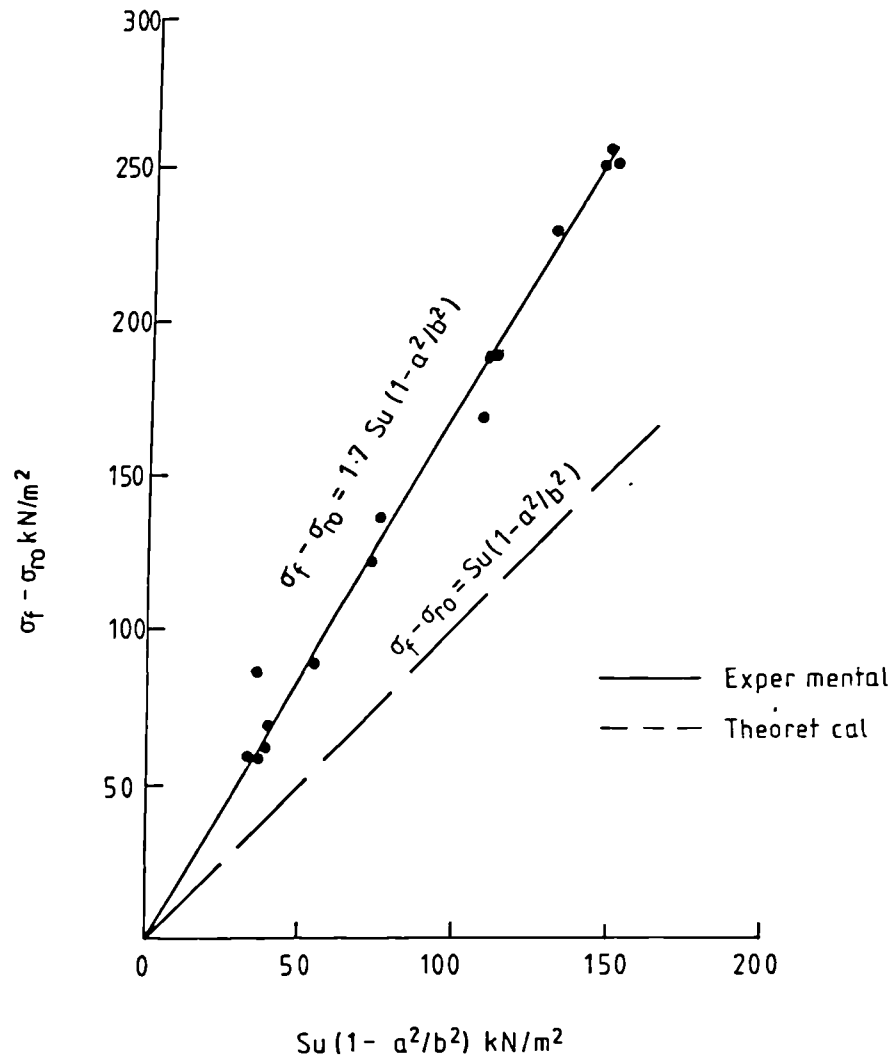


Fig 10.5 PLOT OF $\sigma_f - \sigma_{r0}$ AGAINST $Su(1 - a^2/b^2)$: GROUP F1-B
 (INITIAL FRACTURING TESTS)

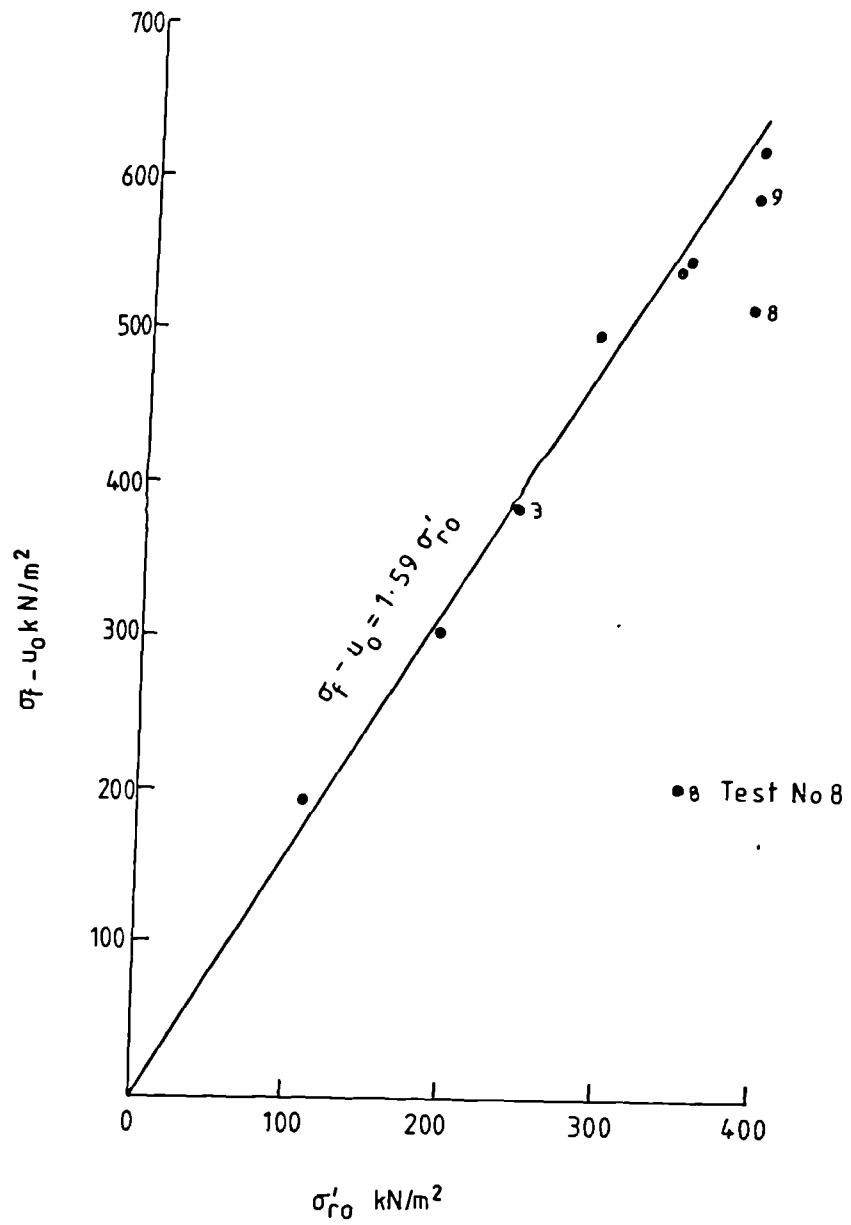


Fig 10.6 PLOT OF $\sigma_f - u_0$ AGAINST σ'_{r0} : GROUP F-2

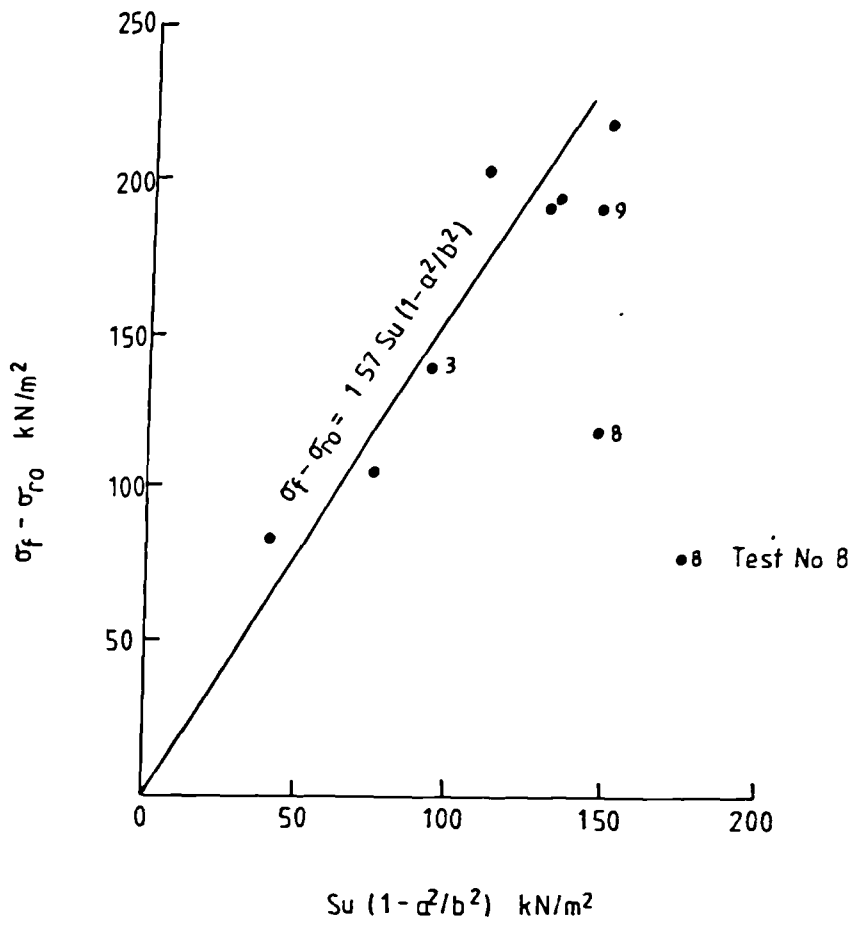


Fig 10.7 PLOT OF $\sigma_f - \sigma_{r0}$ AGAINST $Su(1 - a^2/b^2)$: GROUP F-2

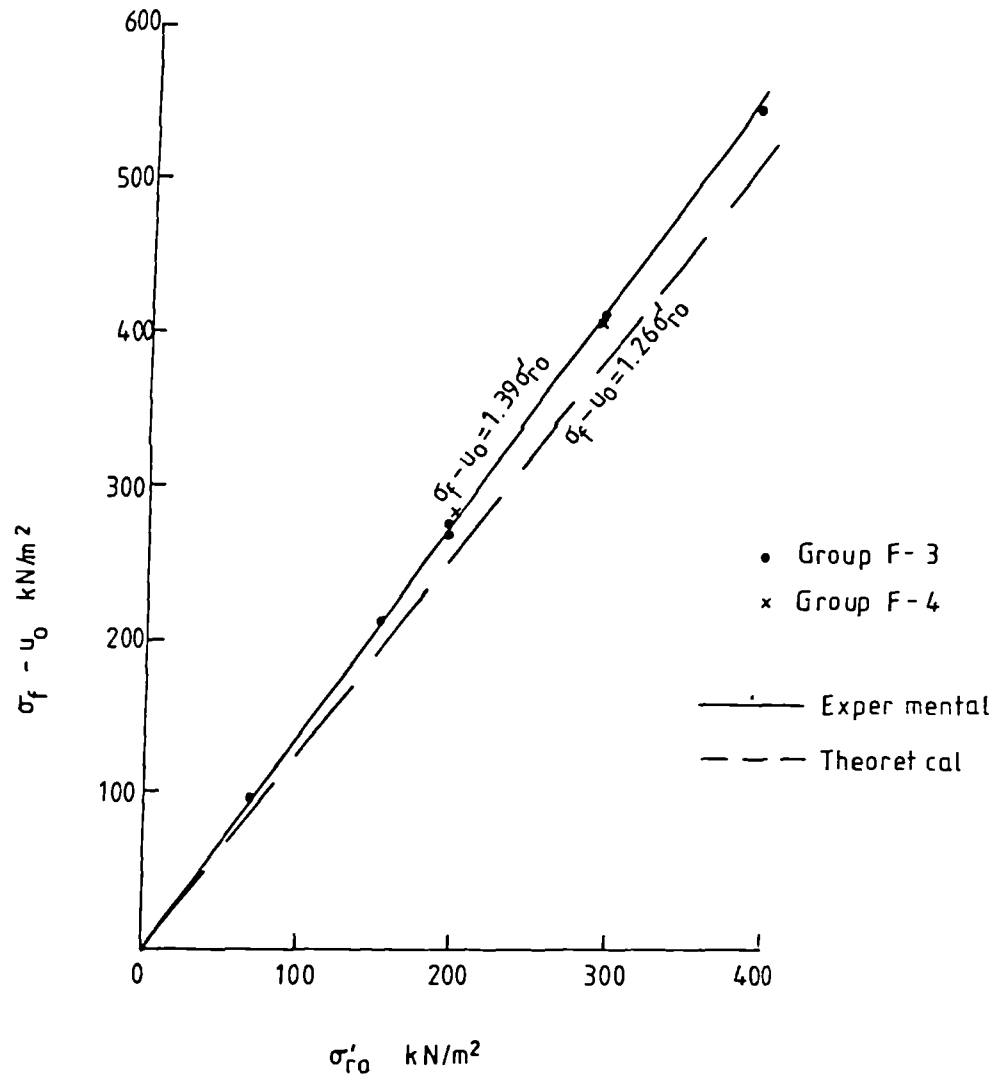


Fig 10.8 PLOT OF $\sigma_f - u_0$ AGAINST σ'_{r0} : GROUP F-3 AND F-4

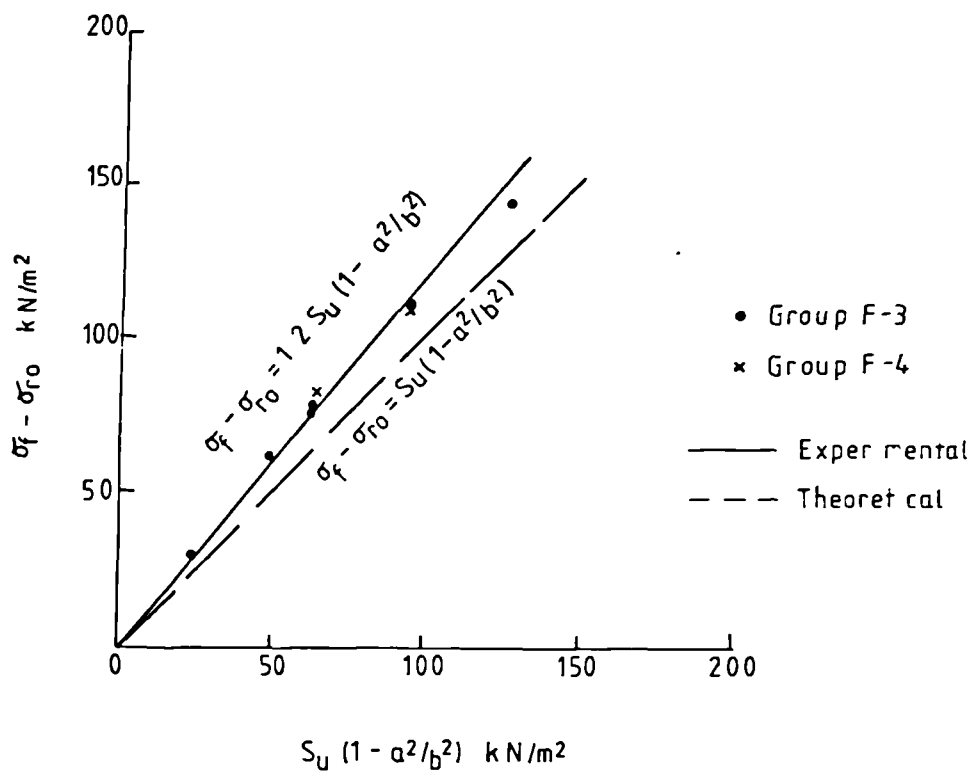


Fig 10.9 PLOT OF $\sigma_f - \sigma_{r0}$ AGAINST $S_u (1 - a^2/b^2)$:
 GROUPS F-3 AND F-4

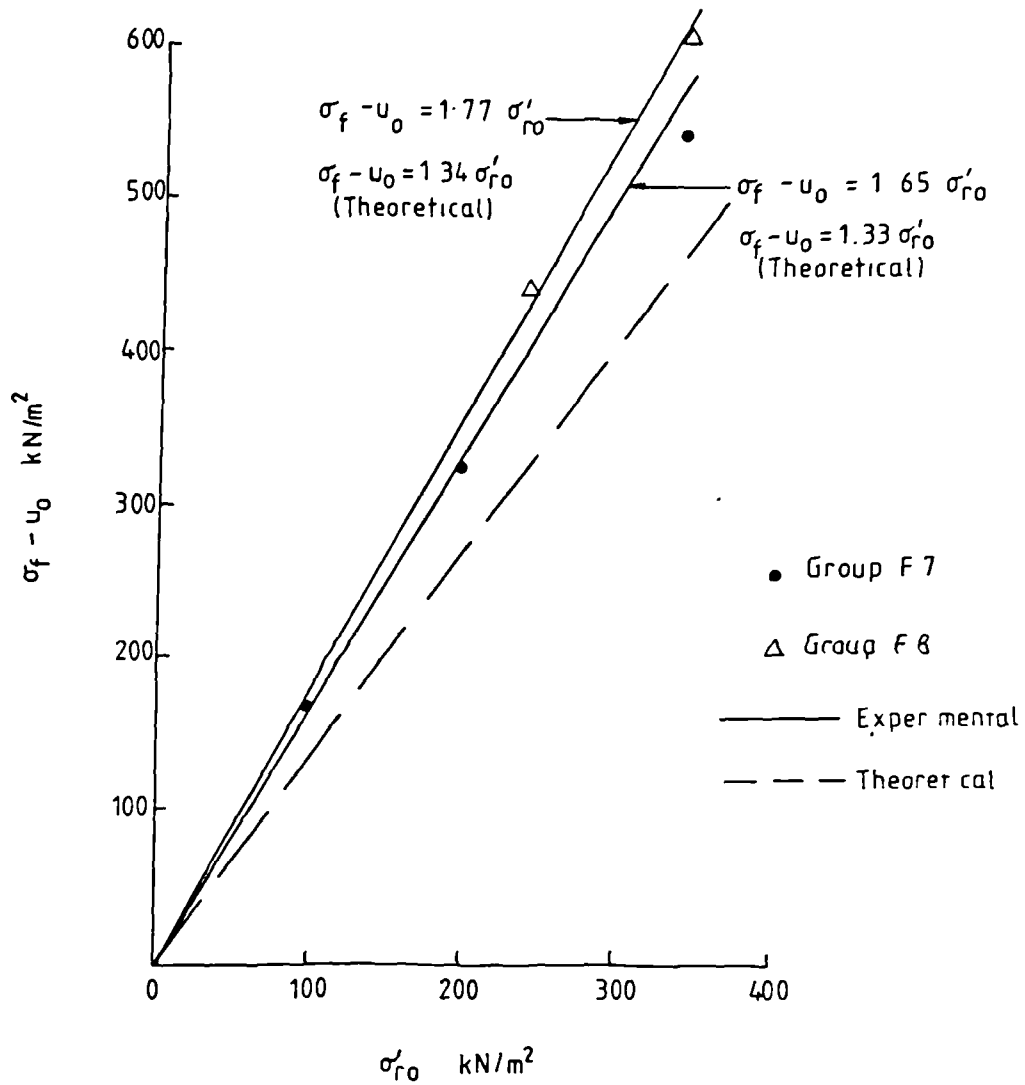


Fig 10.10 PLOT OF $\sigma_f - u_0$ AGAINST σ'_{r0} : GROUPS F-7 AND F-8
(INITIAL FRACTURING TESTS)

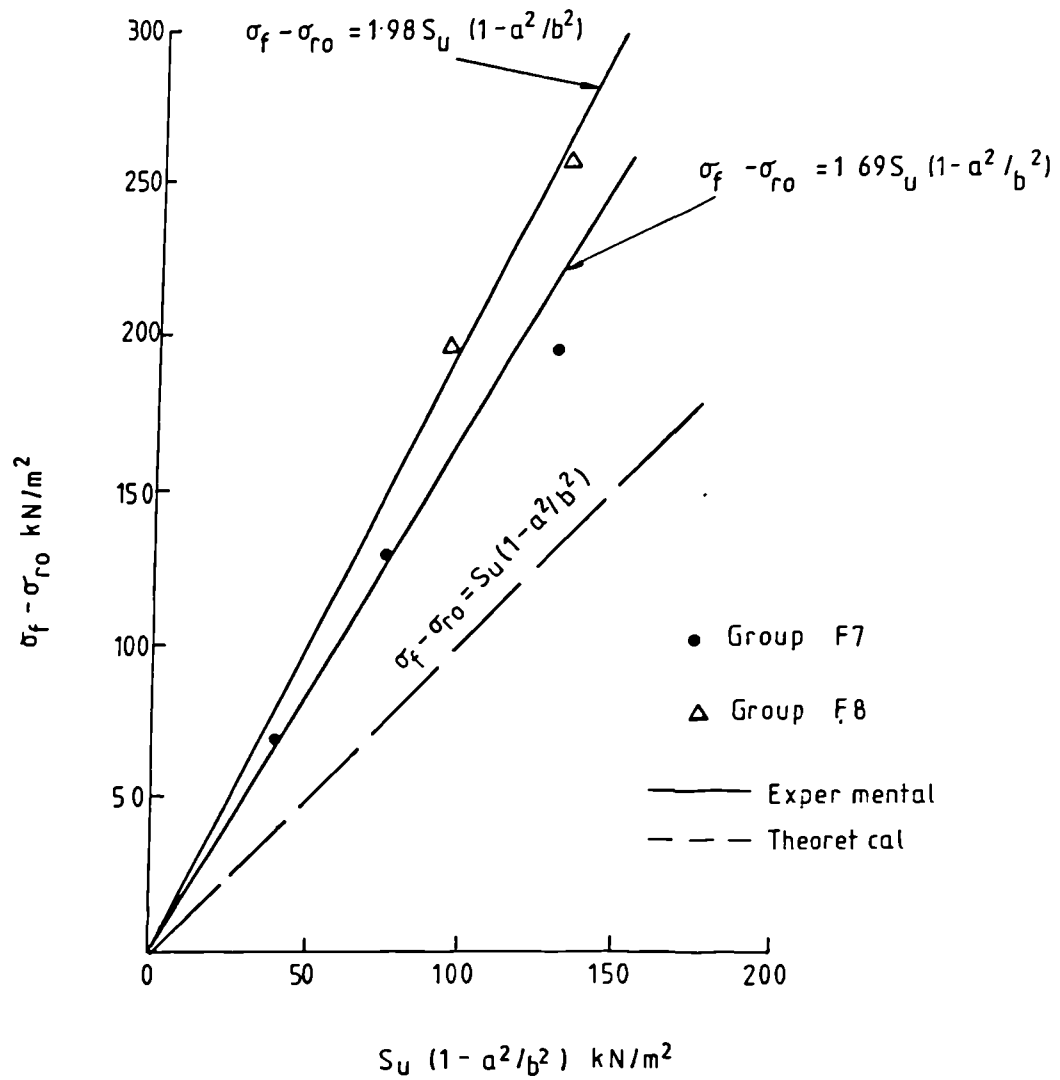


Fig 10.11 PLOT OF $\sigma_f - \sigma_{ro}$ AGAINST $S_u (1 - a^2/b^2)$: GROUPS F-7 AND F-8 (INITIAL FRACTURING TESTS)

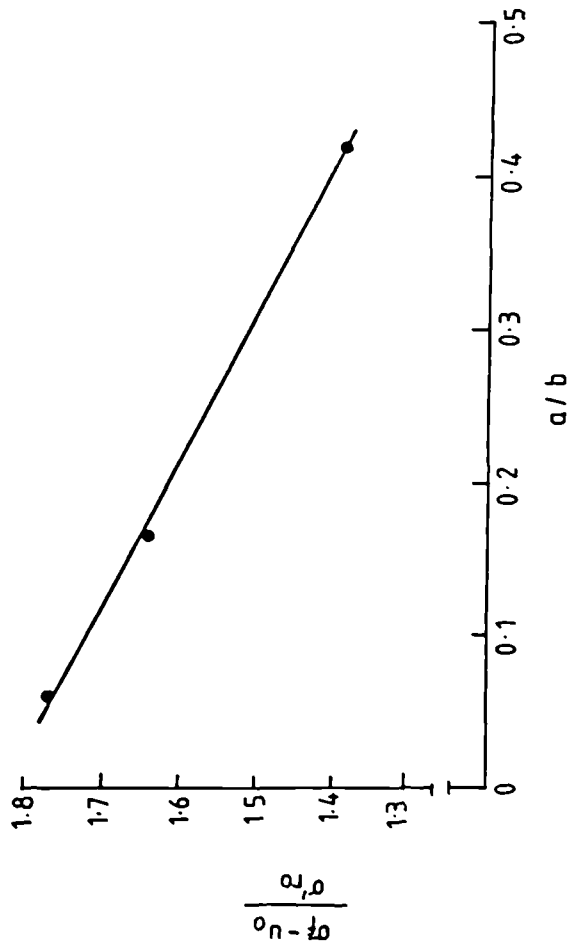


Fig 10.12 EFFECT OF RATIO OF HOLE SIZE TO THE
SAMPLE SIZE ON $\sigma_f - u_0 / \sigma_{f0}$

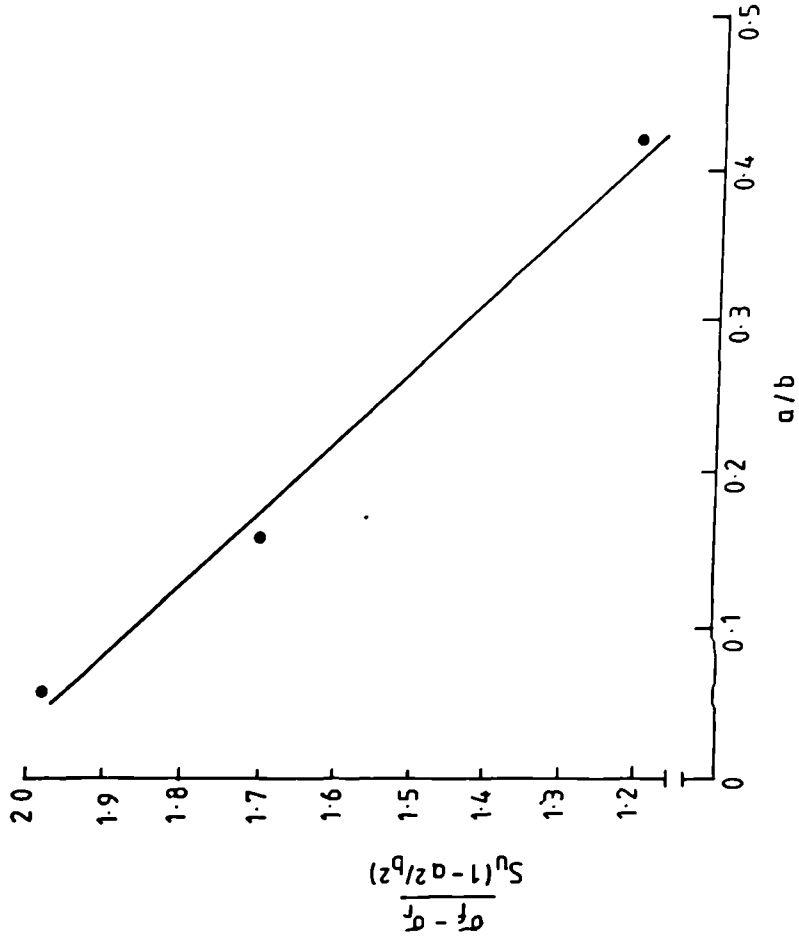


Fig 10.13 EFFECT OF RATIO OF HOLE SIZE TO THE
SAMPLE SIZE ON $\frac{\sigma_f - u_0}{Su(1 - a^2/b^2)}$

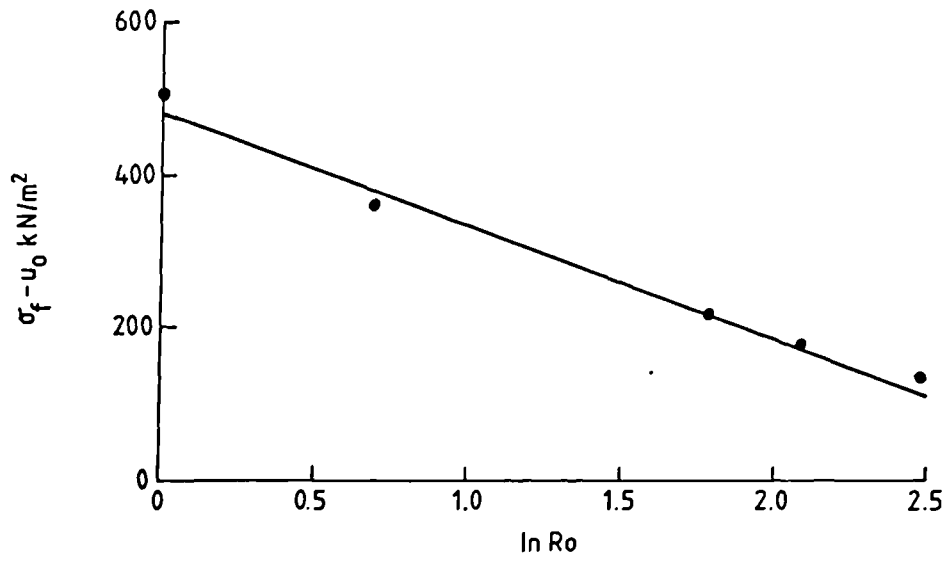


Fig 10.14 PLOT OF $\sigma_f - u_0$ AGAINST $\ln R_0$: GROUP F-5

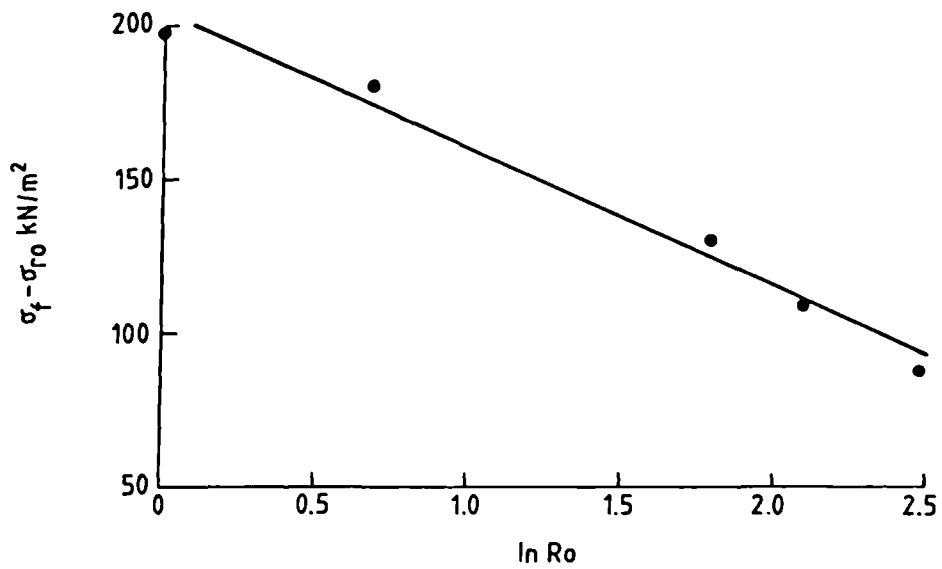


Fig 10.15 PLOT OF $\sigma_f - \sigma_{r0}$ AGAINST $\ln R_0$: GROUP F-5

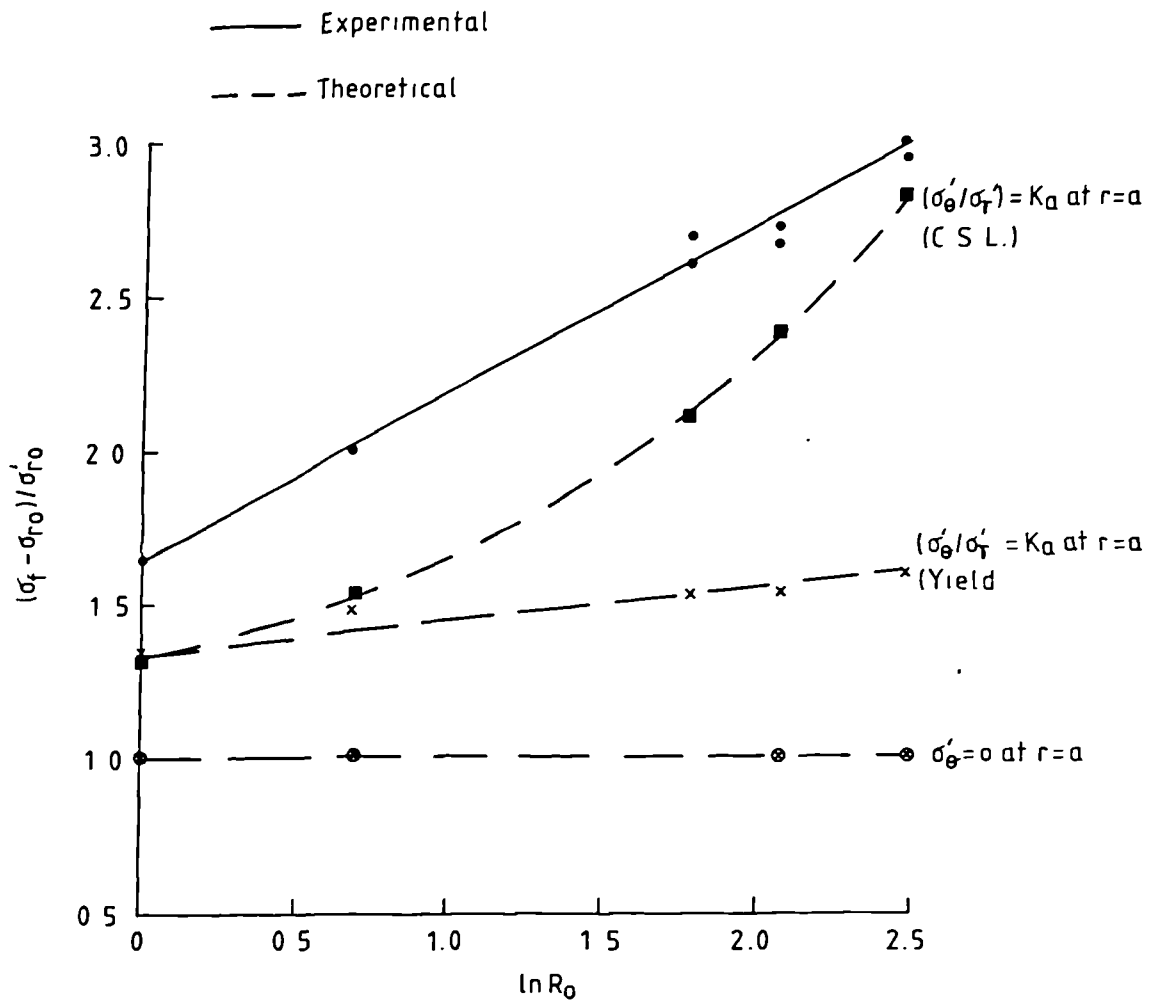


Fig 10.16 PLOT OF $(\sigma_f - \sigma_{r0}) / \sigma'_{r0}$ AGAINST $\ln R_0$
 GROUP F-5

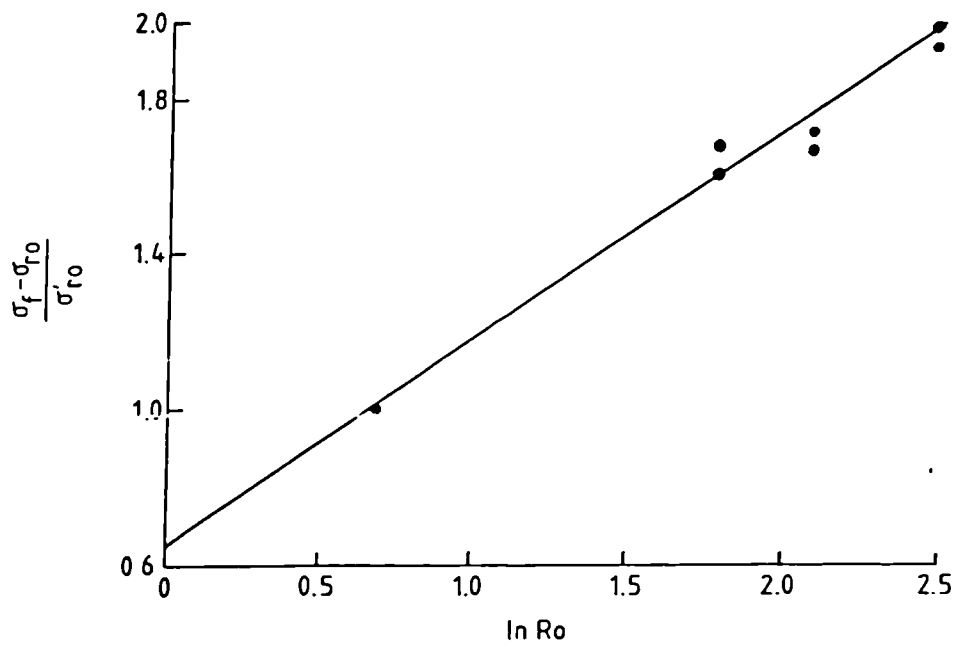


Fig 10.17 PLOT OF $\frac{\sigma_f - \sigma_{r0}}{\sigma'_{r0}}$ AGAINST ln Ro: GROUP F-5

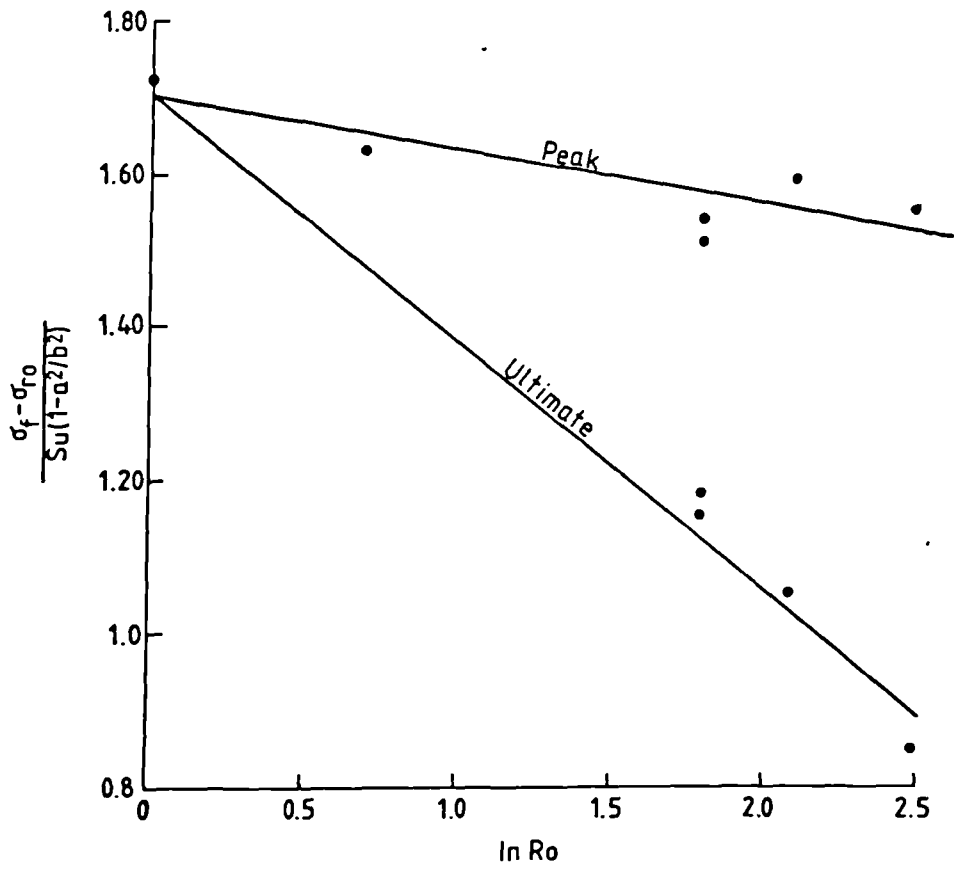


Fig 10.18 PLOT OF $\sigma_f - \sigma_{r0} / Su(1 - a^2/b^2)$ AGAINST $\ln Ro$

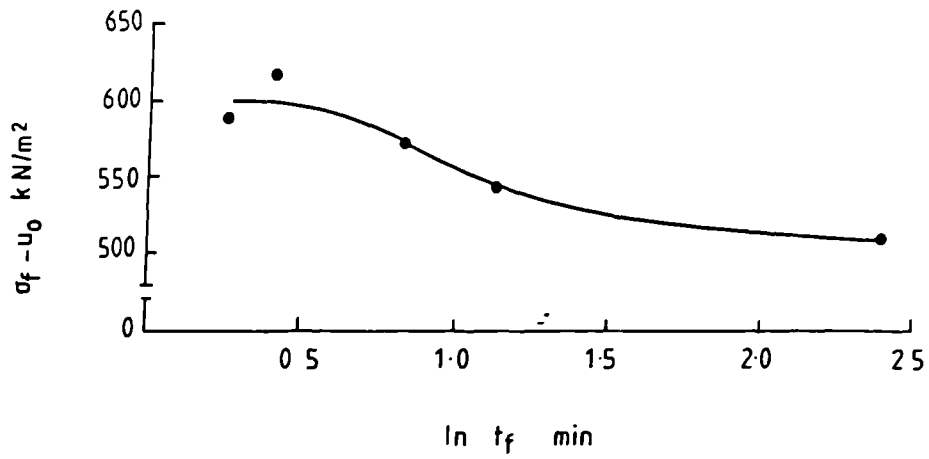


Fig 10.19 EFFECT OF TIME TO FAILURE ON $\sigma_f - \sigma_{u_0}$: GROUP F-3

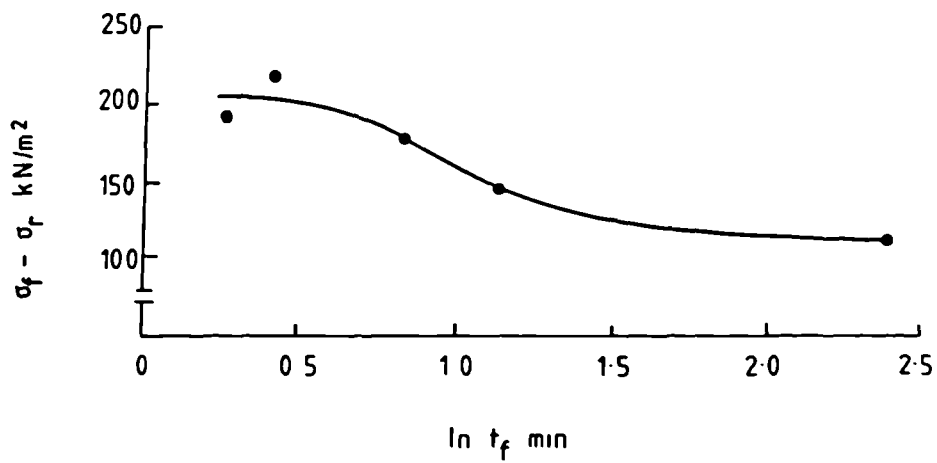


Fig 10.20 EFFECT OF TIME TO FAILURE ON $\sigma_f - \sigma_r$: GROUP F-3

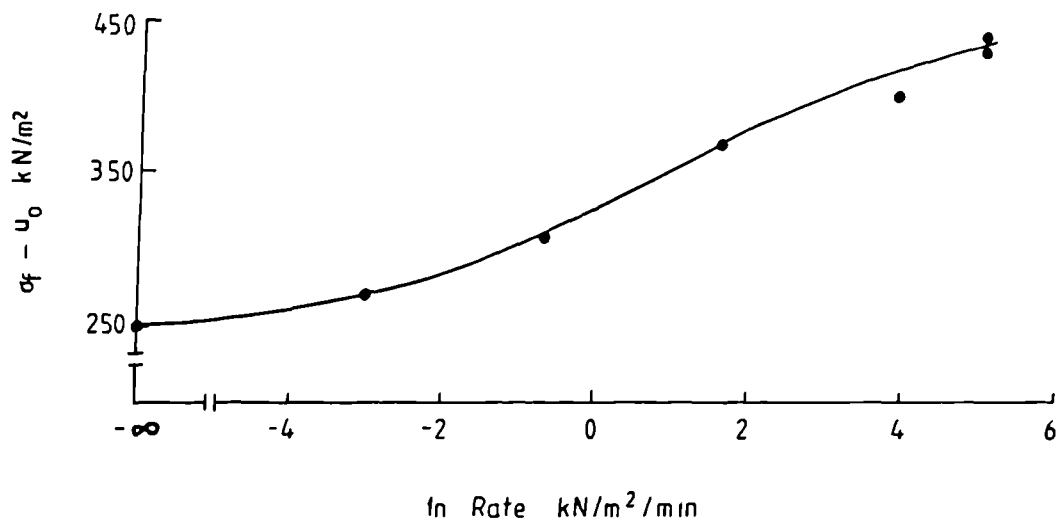


Fig 10.21 EFFECT OF RATE OF LOADING ON $\sigma_f - u_0$:
GROUP F-6

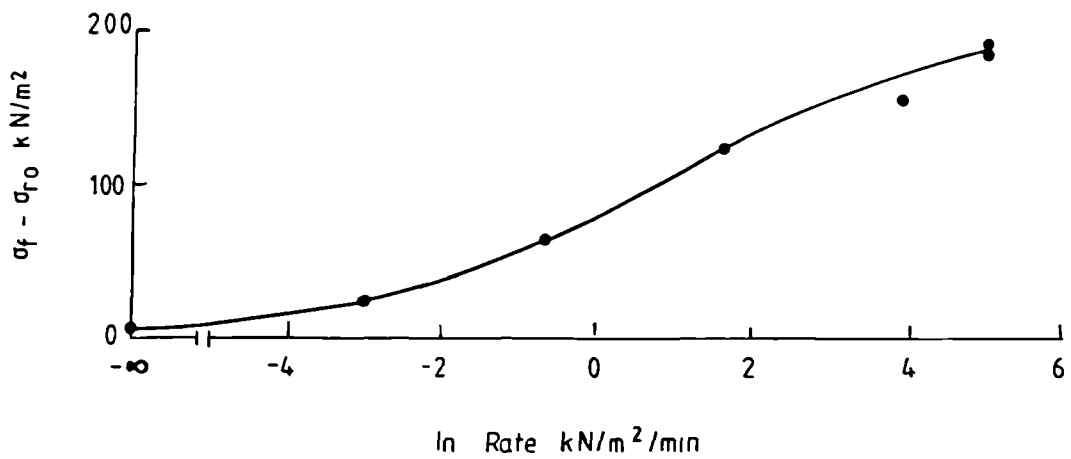


Fig 10.22 EFFECT OF RATE OF LOADING ON $\sigma_f - \sigma_{r0}$:
GROUP F-6

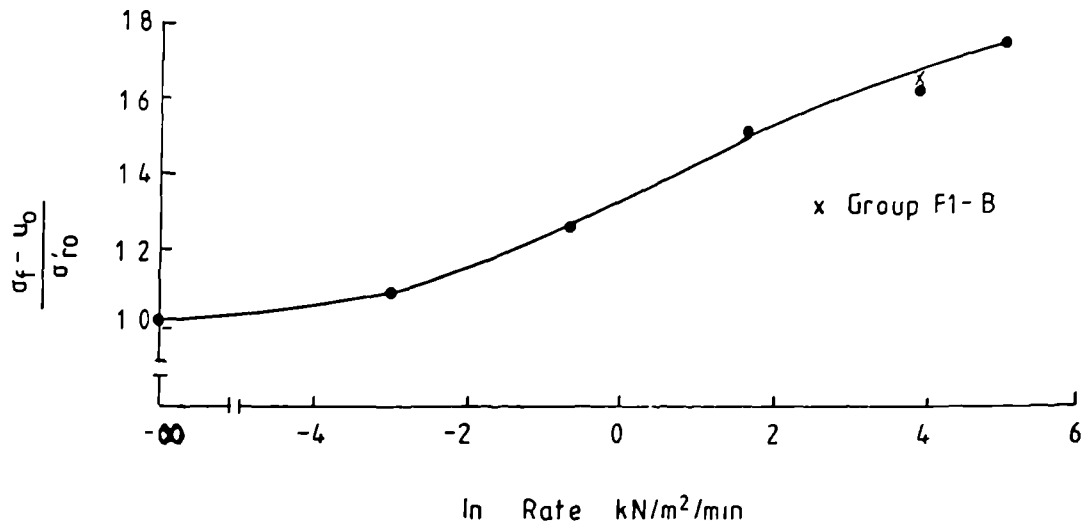


Fig 10.23 EFFECT OF RATE OF LOADING ON $\sigma_f - u_0 / \sigma'_{r0}$
GROUP F-6

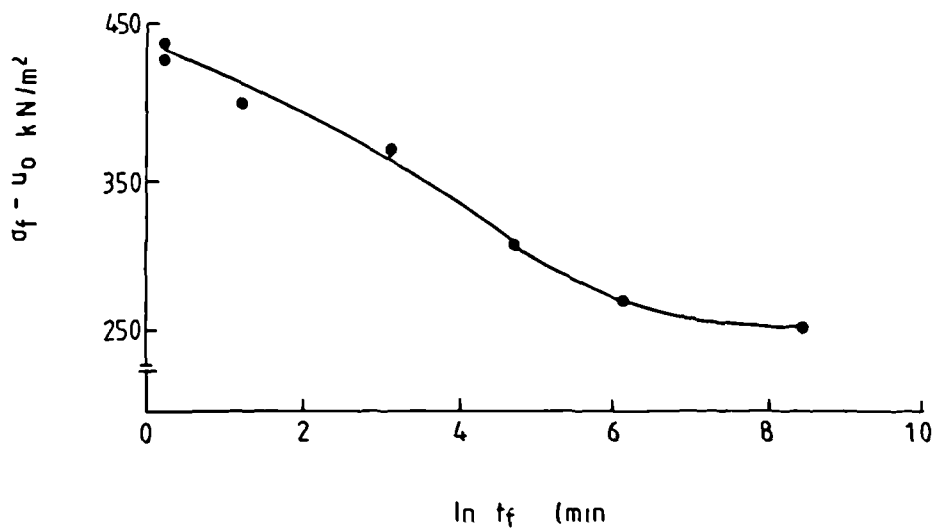


Fig 10.24 EFFECT OF TIME TO FAILURE ON $\sigma_f - u_0$:
GROUP F-6

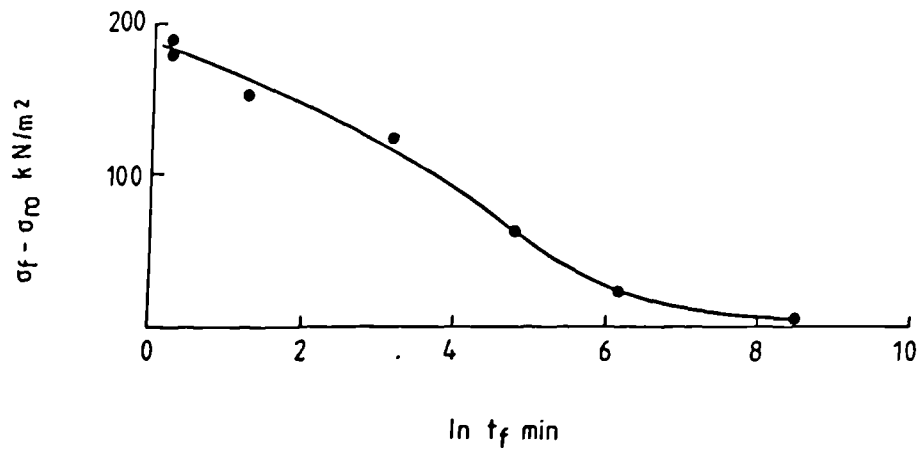


Fig 10.25 EFFECT OF TIME TO FAILURE ON $\sigma_f - \sigma_{r0}$:
GROUP F-6

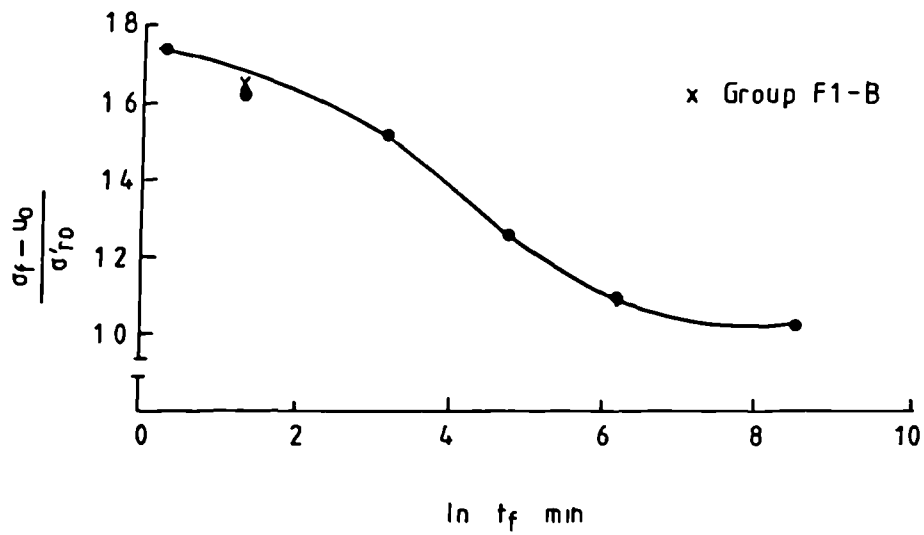


Fig 10.26 EFFECT OF TIME TO FAILURE ON $\frac{\sigma_f - u_0}{\sigma'_{r0}}$:
GROUP F-6

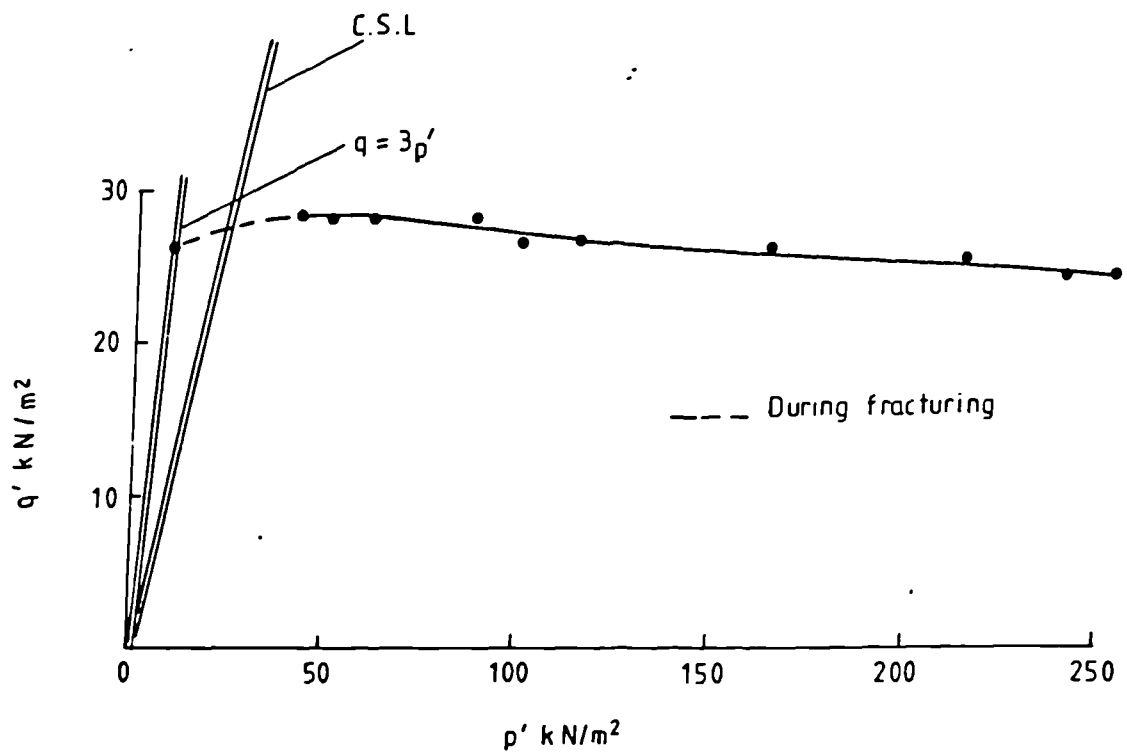


Fig 10.27 "APPARENT" STRESS PATH DURING FRACTURING TEST ON SAMPLE F6-6

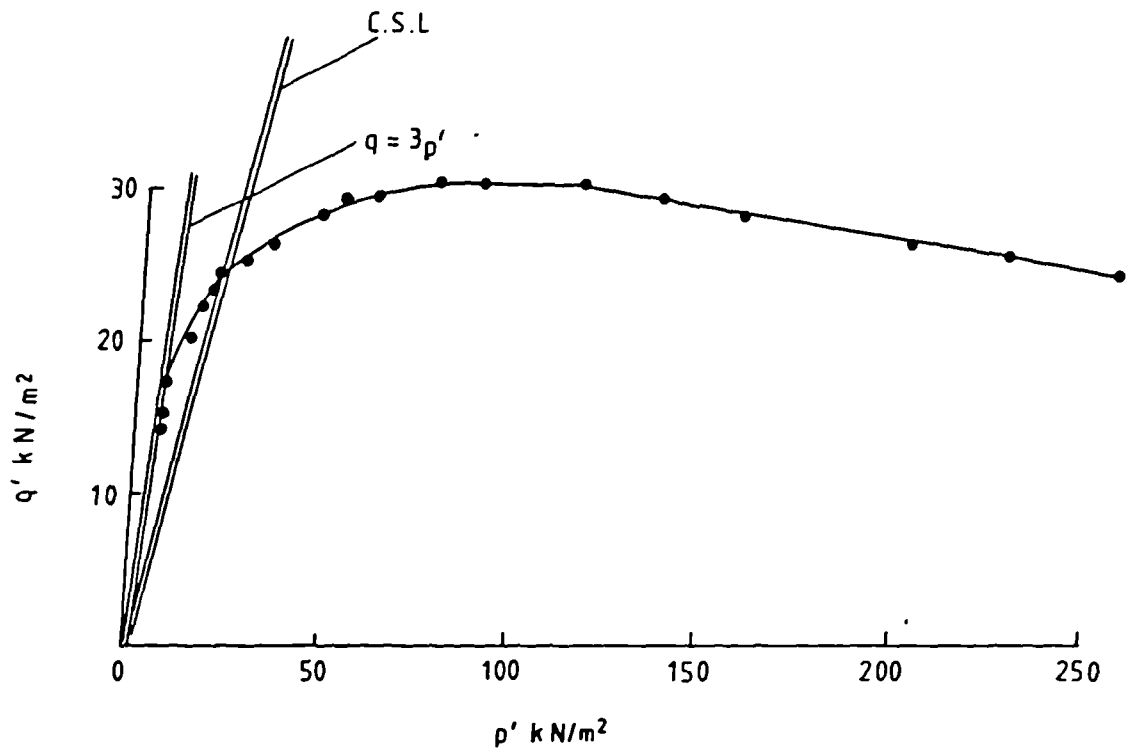


Fig 10.28 "APPARENT" STRESS PATH DURING FRACTURING TEST ON SAMPLE F6-7

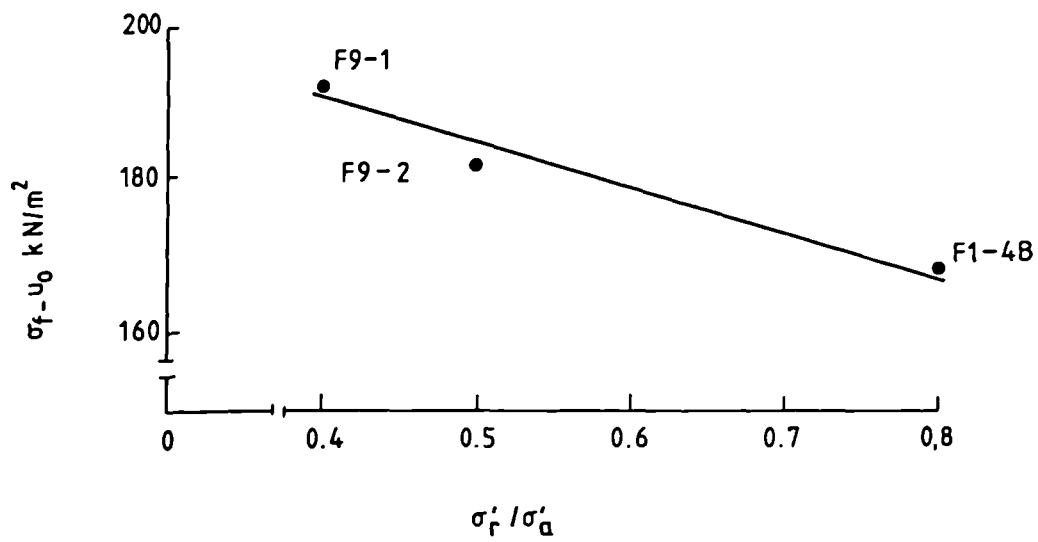


Fig 10.29 EFFECT OF STRESS RATIO σ'_r/σ'_a ON $\sigma_f - u_0$:
GROUP F-9

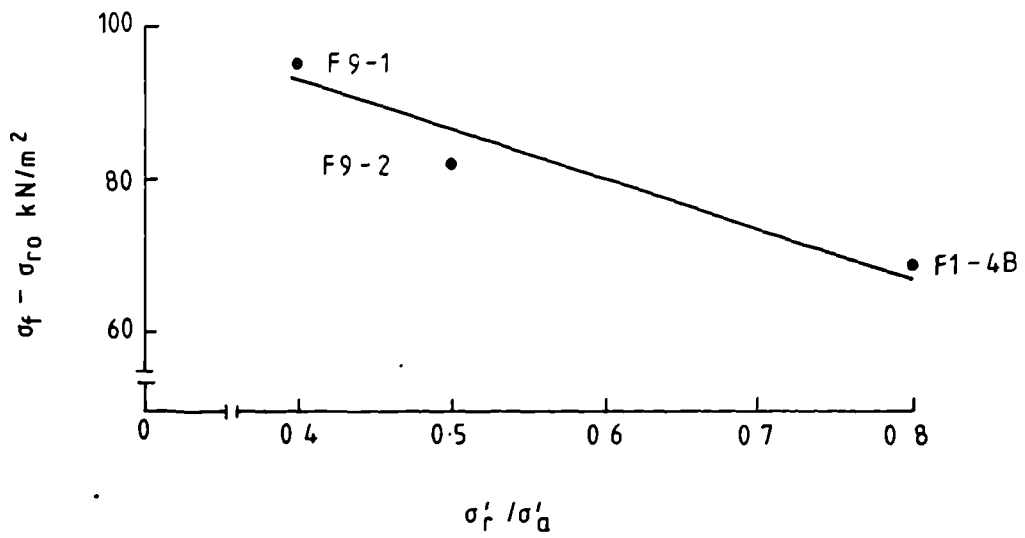


Fig 10.30 EFFECT OF STRESS RATIO σ'_r / σ'_a ON $\sigma_f - \sigma_{ro}$
GROUP F-9

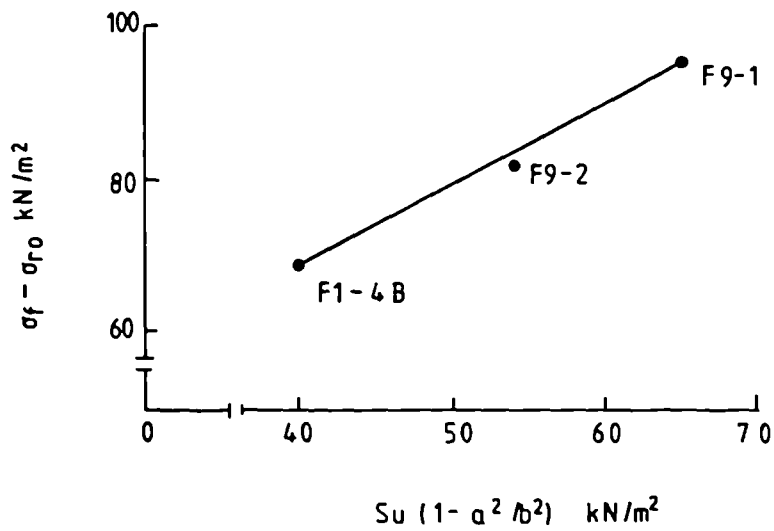


Fig 10.31 EFFECT OF UNDRAINED SHEAR STRENGTH ON $\sigma_f - \sigma_{ro}$
GROUP F-9

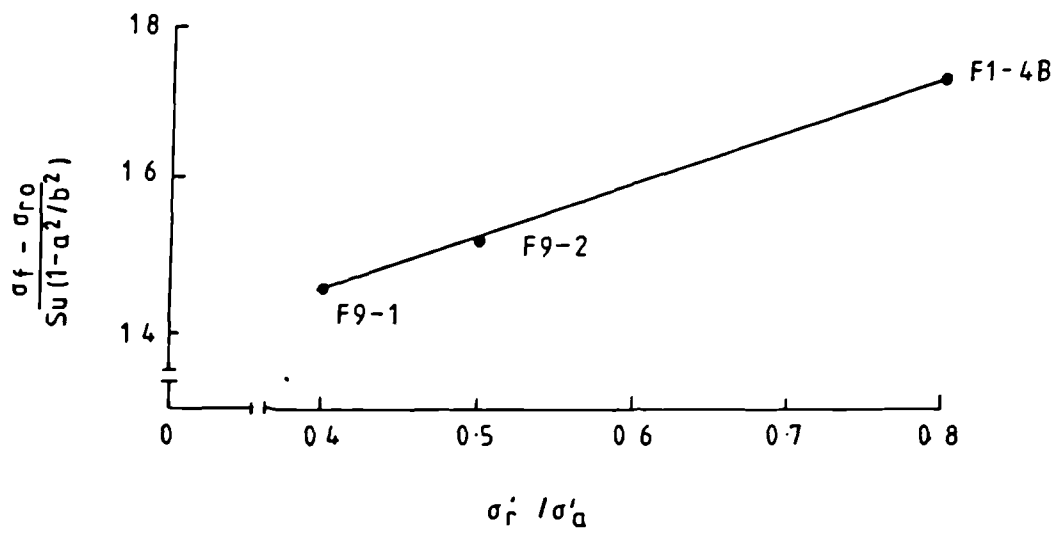


FIG 10.32 EFFECT OF STRESS RATIO σ_r / σ'_a ON $\sigma_f - \sigma_{r0} / Su(1 - a^2/b^2)$: GROUP F-9

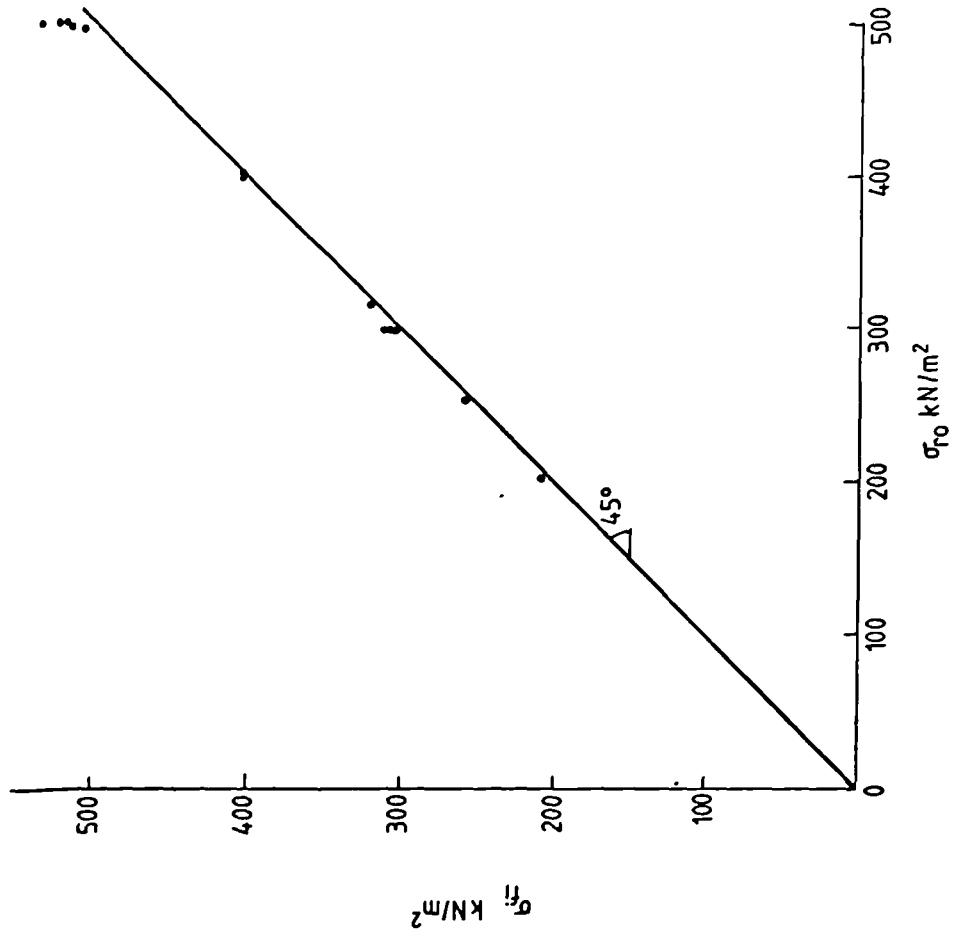


Fig 10.34 PLOT OF σ_{fi} AGAINST σ_{ro}

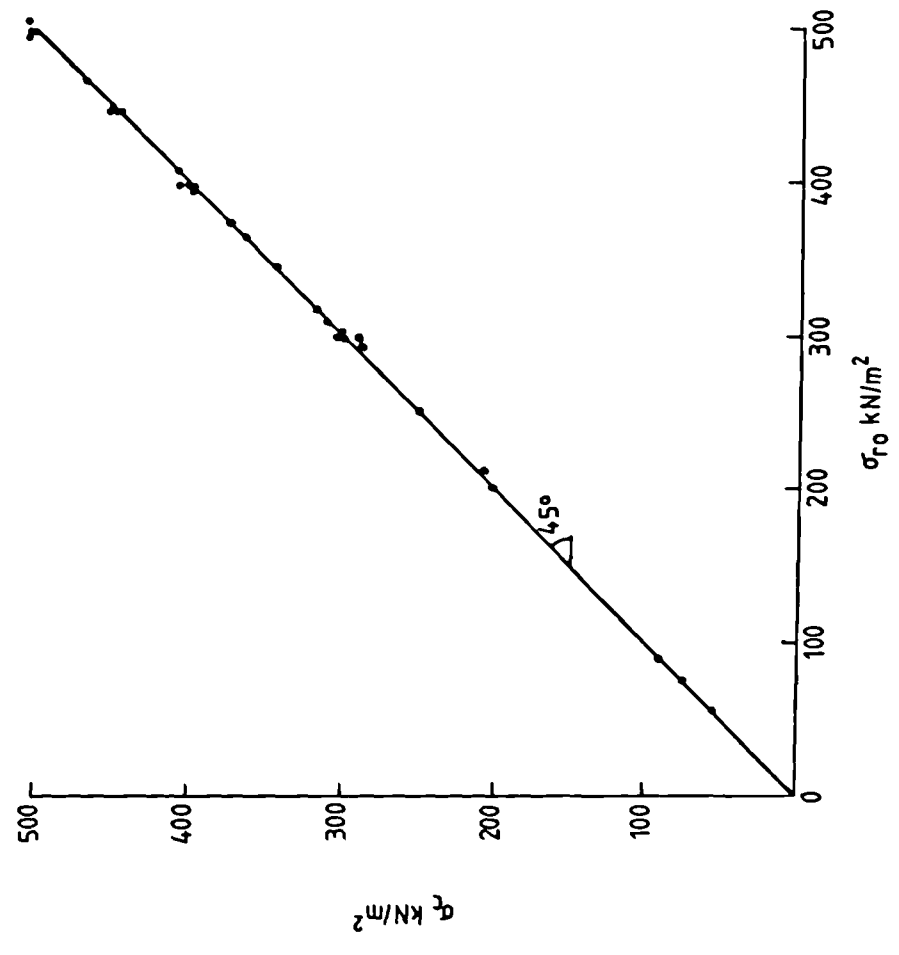


Fig 10.33 PLOT OF σ_c AGAINST σ_{ro}

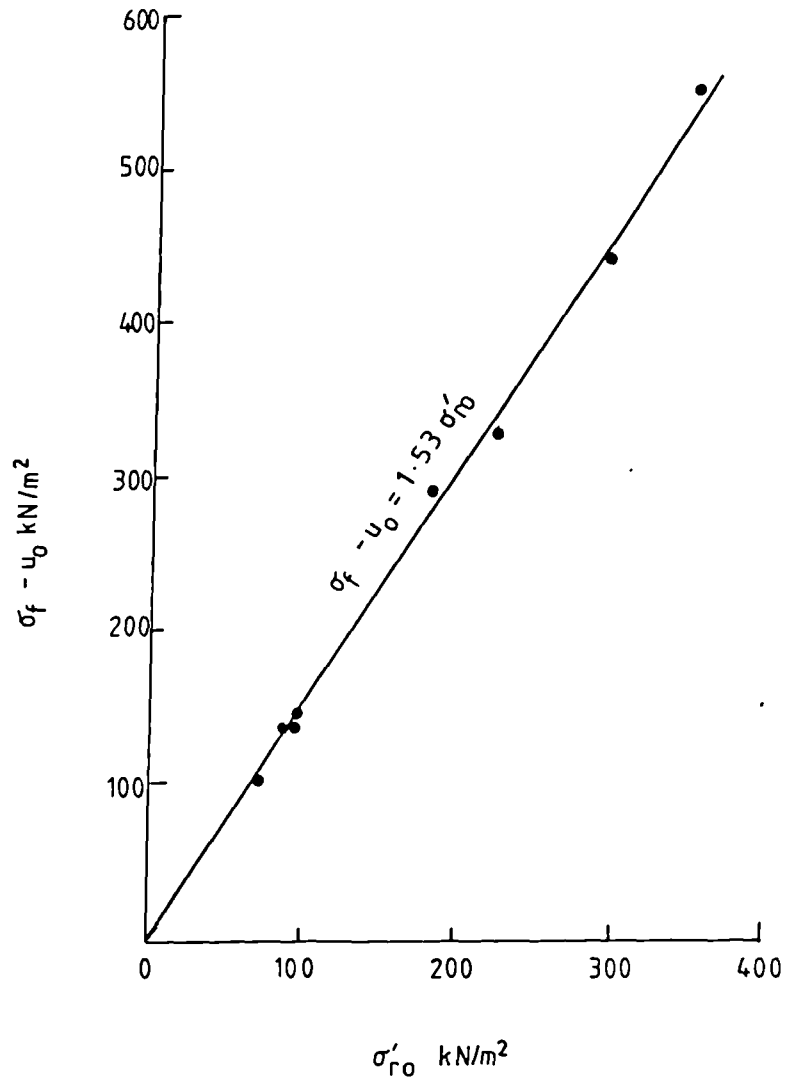


Fig 10.35 PLOT OF $\sigma_f - u_0$ AGAINST σ'_{r0} : GROUP F1-B
(DELAYED FRACTURING TESTS)

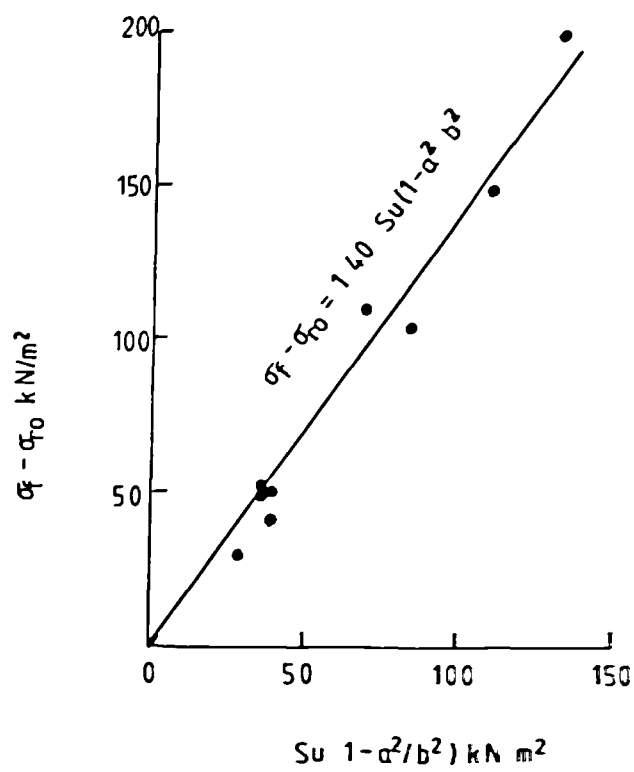


Fig 10.36 PLOT OF $\sigma_f - \sigma_{r0}$ AGAINST $Su(1 - a^2/b^2)$: Group F1-B
(DELAYED FRACTURING TESTS)

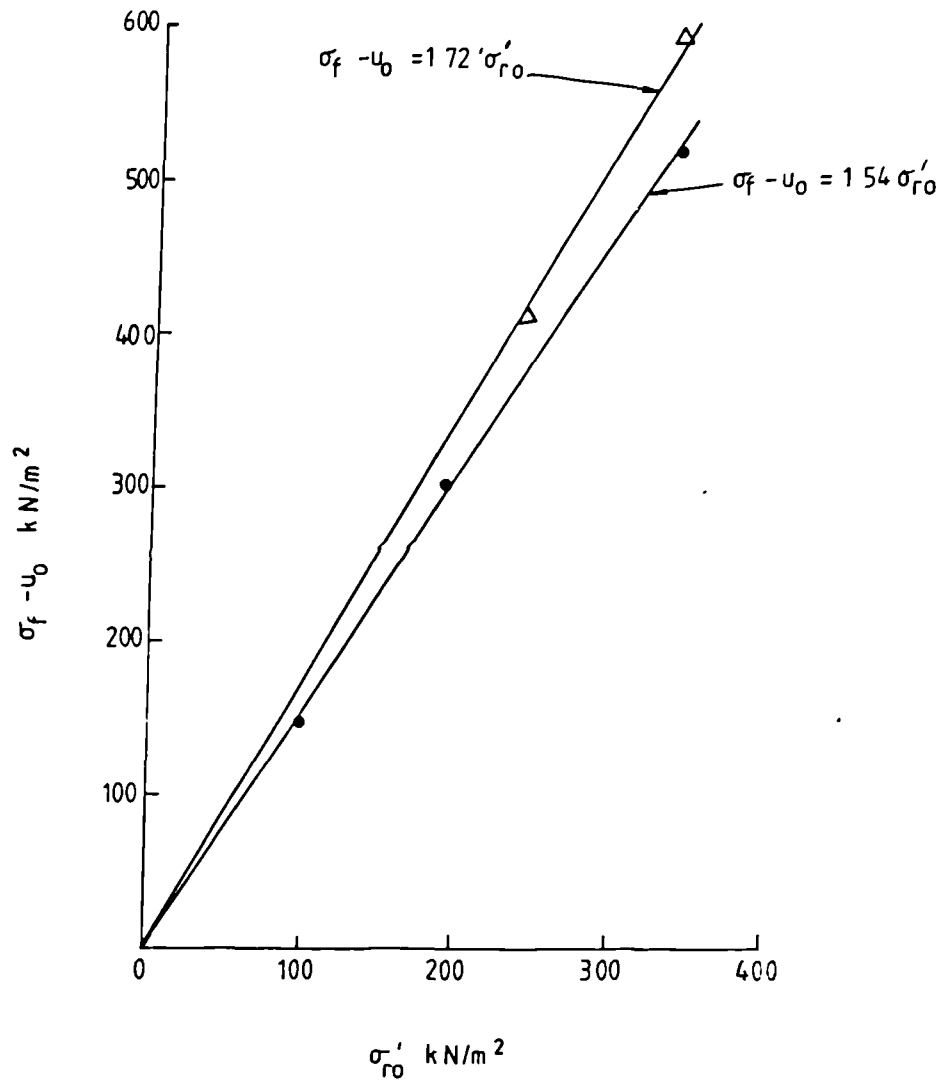


Fig 10.37 PLOT OF $\sigma_f - u_0$ AGAINST σ'_{r0} : GROUPS F-7 AND F-8
(DELAYED FRACTURING TESTS)

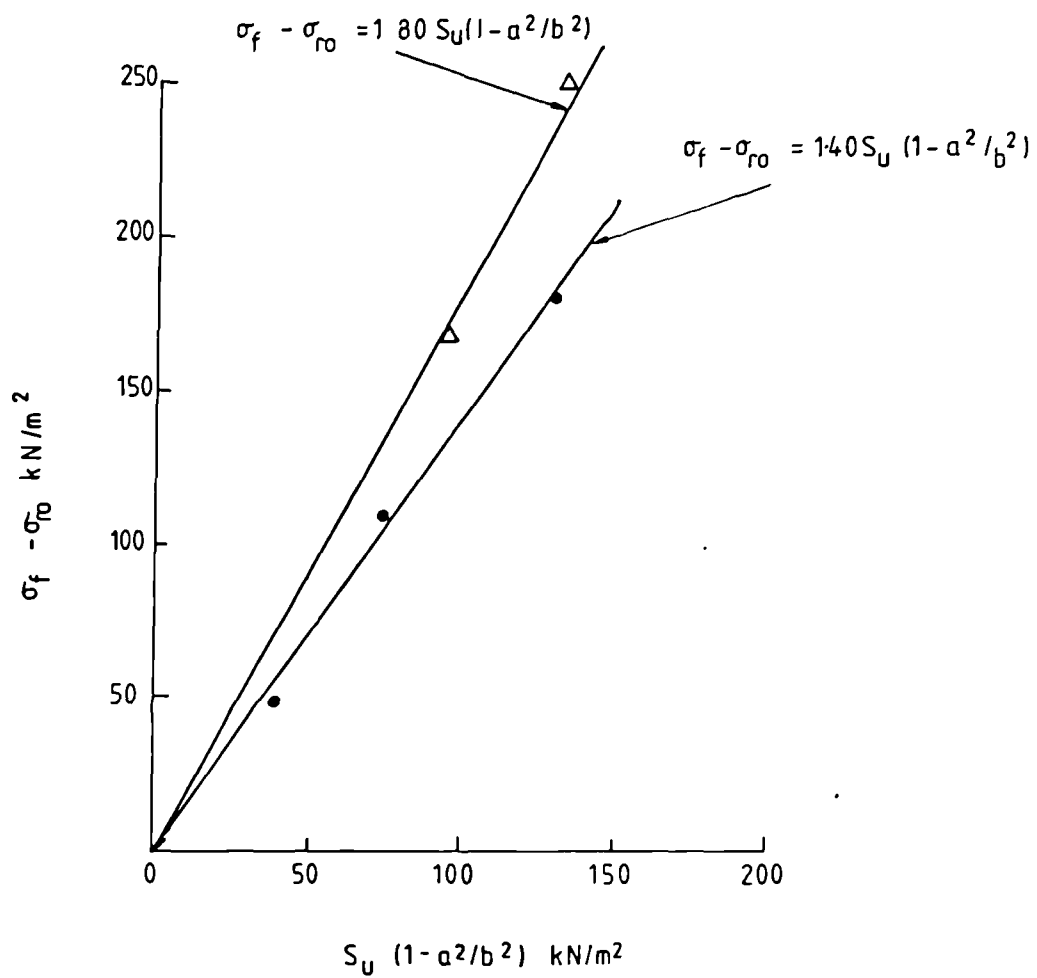


Fig 10.38 PLOT OF $\sigma_f - \sigma_{r0}$ AGAINST $S_u(1 - a^2/b^2)$: GROUP F-7 AND F-8 (DELAYED FRACTURING TESTS)

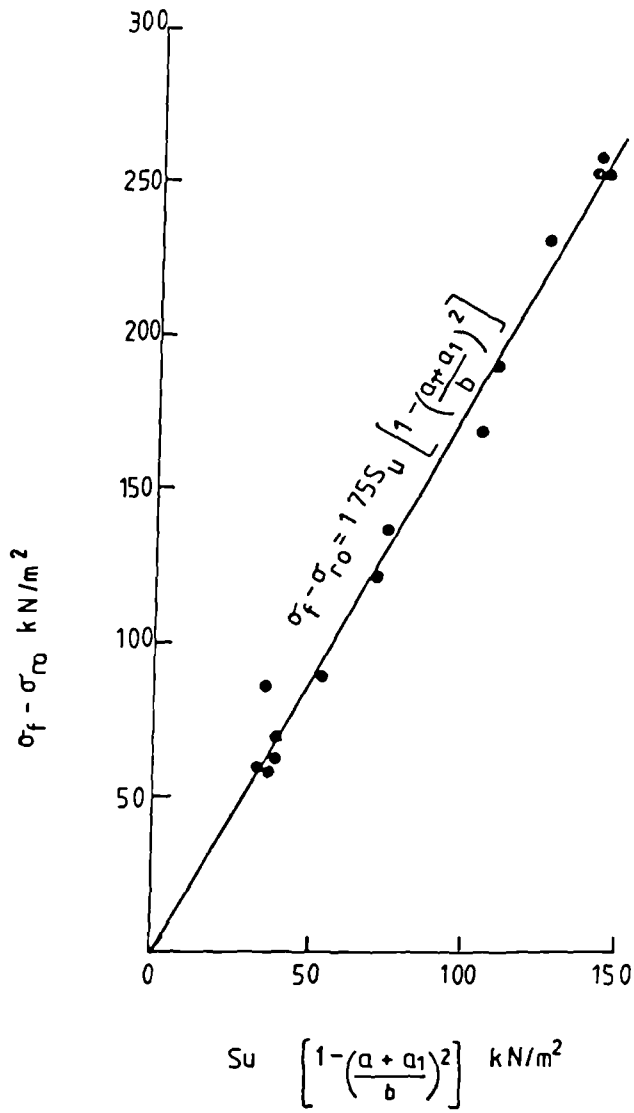


Fig 10.39 PLOT OF $\sigma_f - \sigma_{r0}$ AGAINST $S_u \left[1 - \left(\frac{a+a_1}{b} \right)^2 \right]$:
 GROUP F1-B (after fluid penetration)

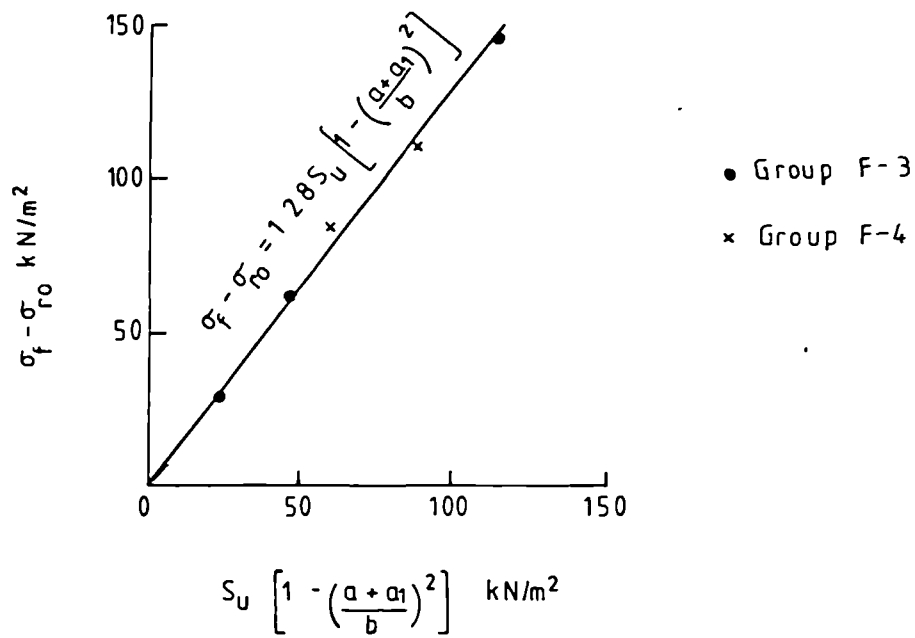


Fig 10.40 PLOT OF $\sigma_f - \sigma_{r0}$ AGAINST $S_u \left[1 - \left(\frac{a+a_1}{b} \right)^2 \right]$:
 GROUPS F-3 AND F-4 (after fluid penetration)

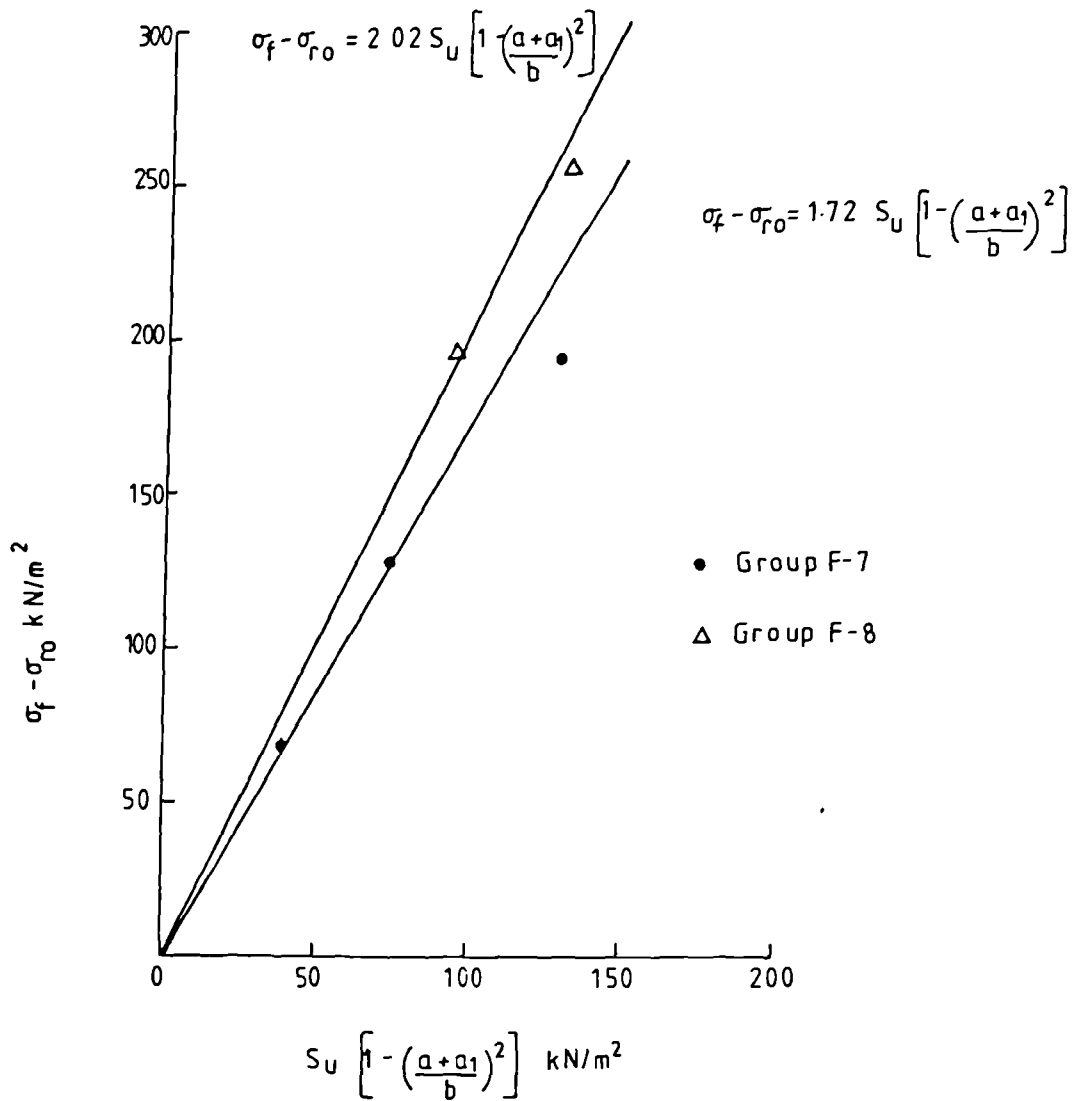


Fig 10.41 PLOT OF $\sigma_f - \sigma_{r0}$ AGAINST $S_u \left[1 - \left(\frac{a+a_1}{b} \right)^2 \right]$:
 GROUPS F-7 AND F-8 (after fluid penetration)

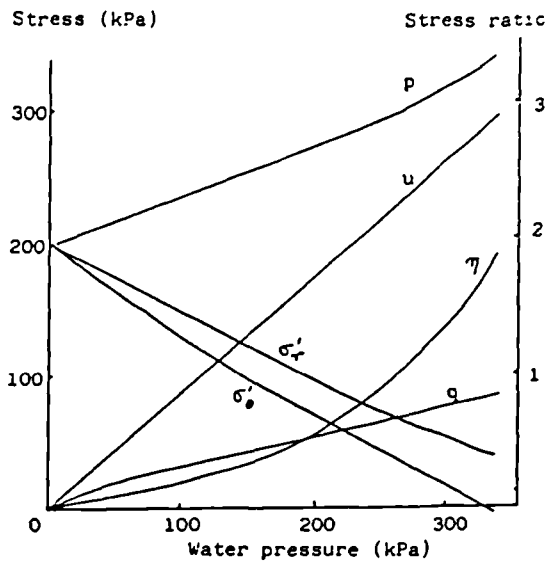


Fig 10.42 VARIATION OF STRESSES WITH CAVITY WATER PRESSURE

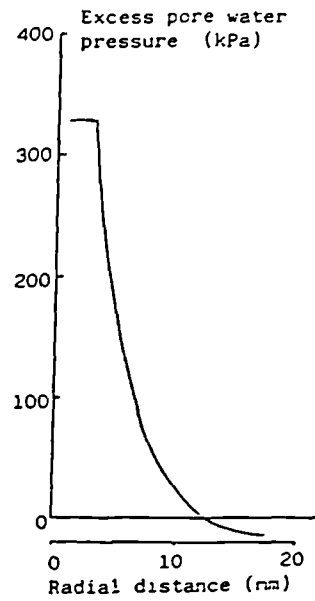


Fig 10.43 RADIAL VARIATION IN PORE PRESSURE AT FRACTURE

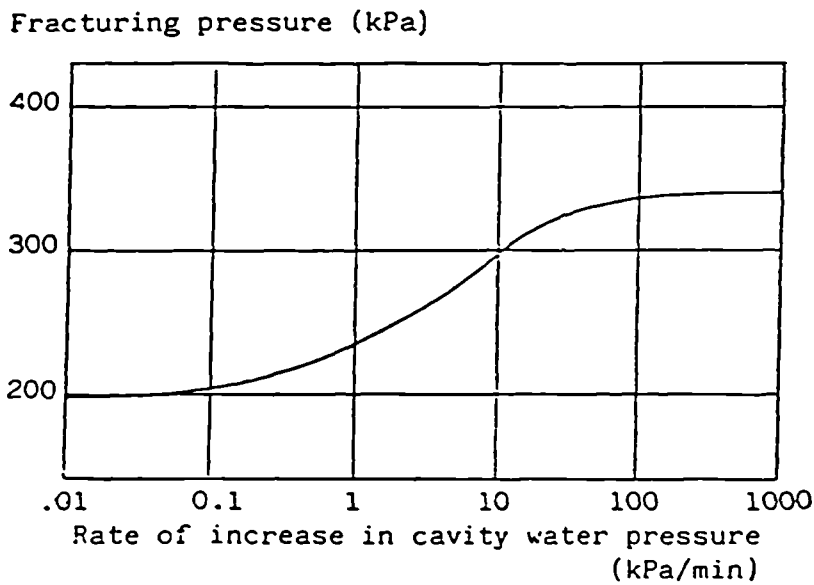
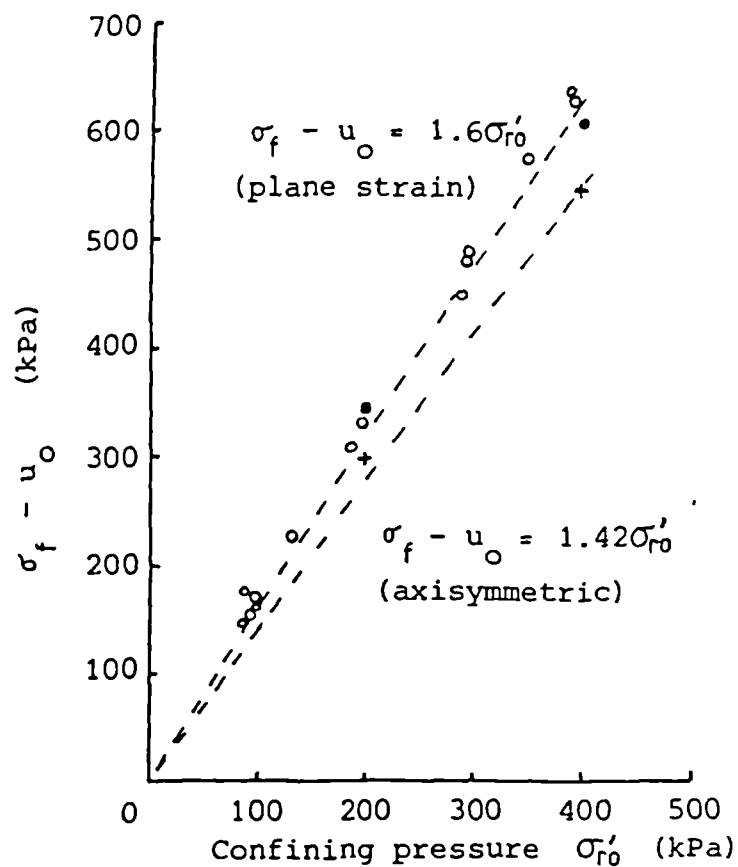


Fig 10.44 INFLUENCE OF RATE ON FRACTURING PRESSURE FOR PLANE STRAIN ANALYSES



Legend

- Plane strain FE analyses
- + Axisymmetric FE analyses
- Experimental data

Fig10.45 VARIATION OF FRACTURING PRESSURE WITH
 CONFINING PRESSURE : RATE 50 kPa/min

Fig10.42 to 10.45 :After Tam, Mhach & Woods (1988)

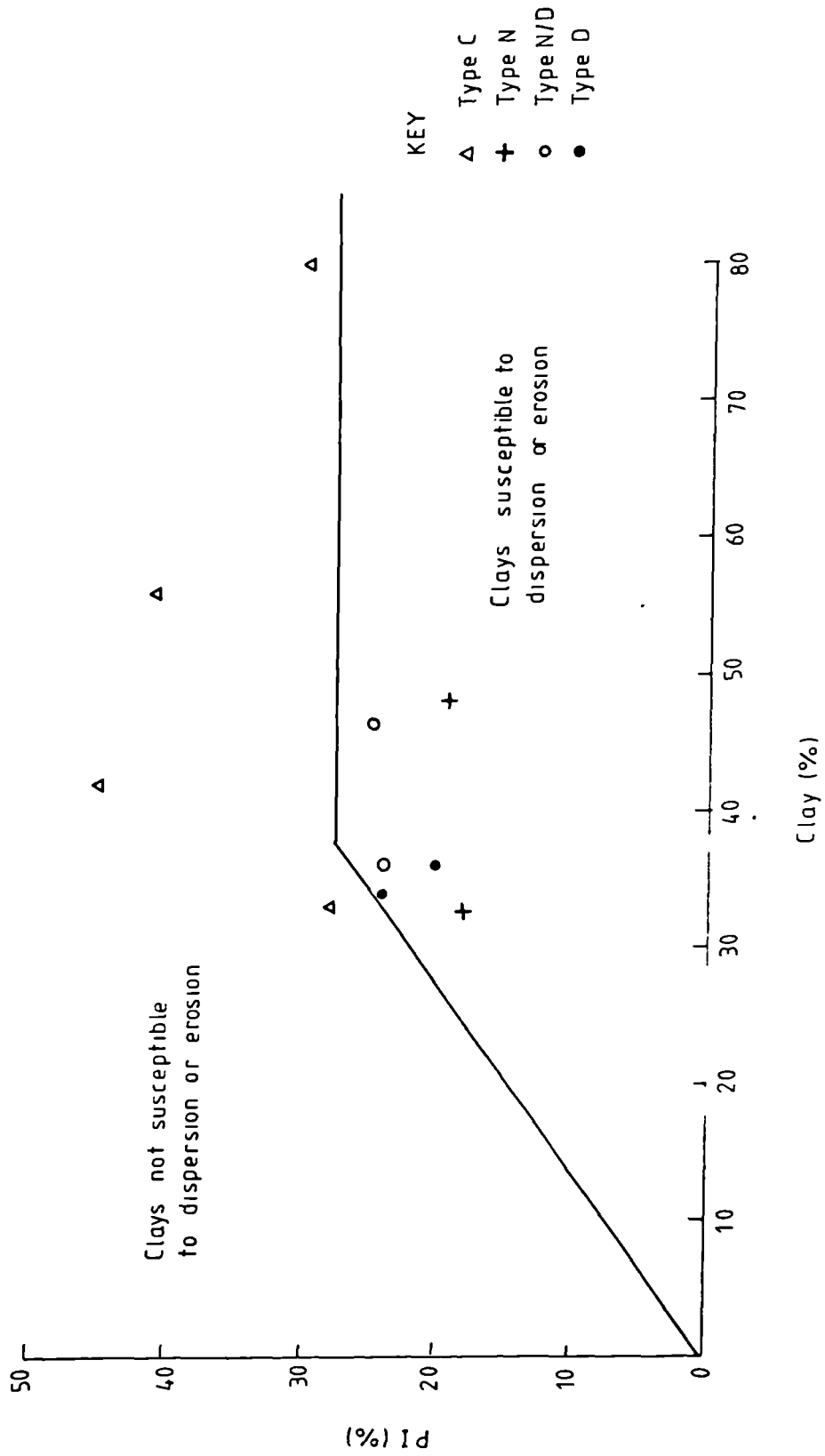


Fig 10.46 ACTIVITY PLOT OF PI(%) VERSUS CLAY CONTENT (%) - GROUP B-1

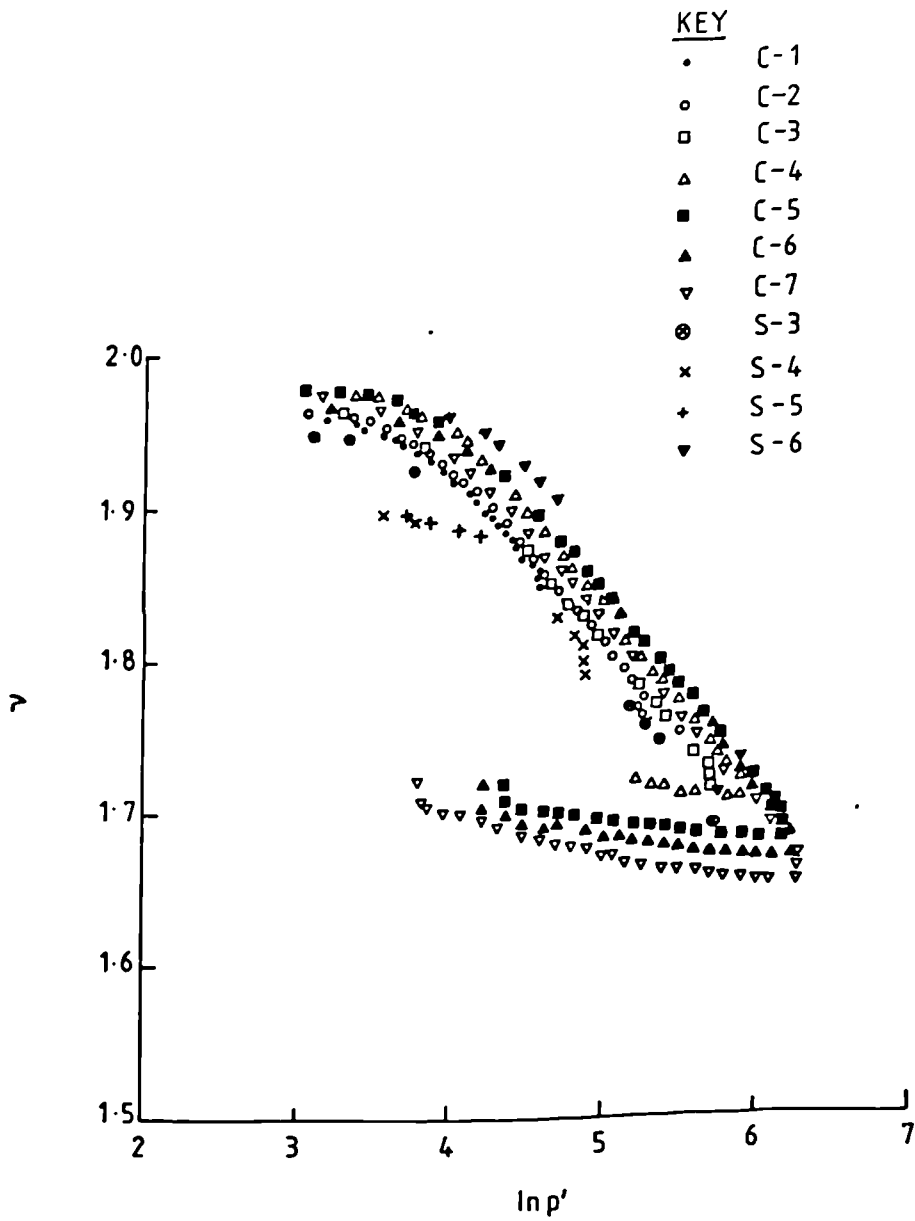


Fig B-1 ISOTROPIC COMPRESSION AND SWELLING RESULTS

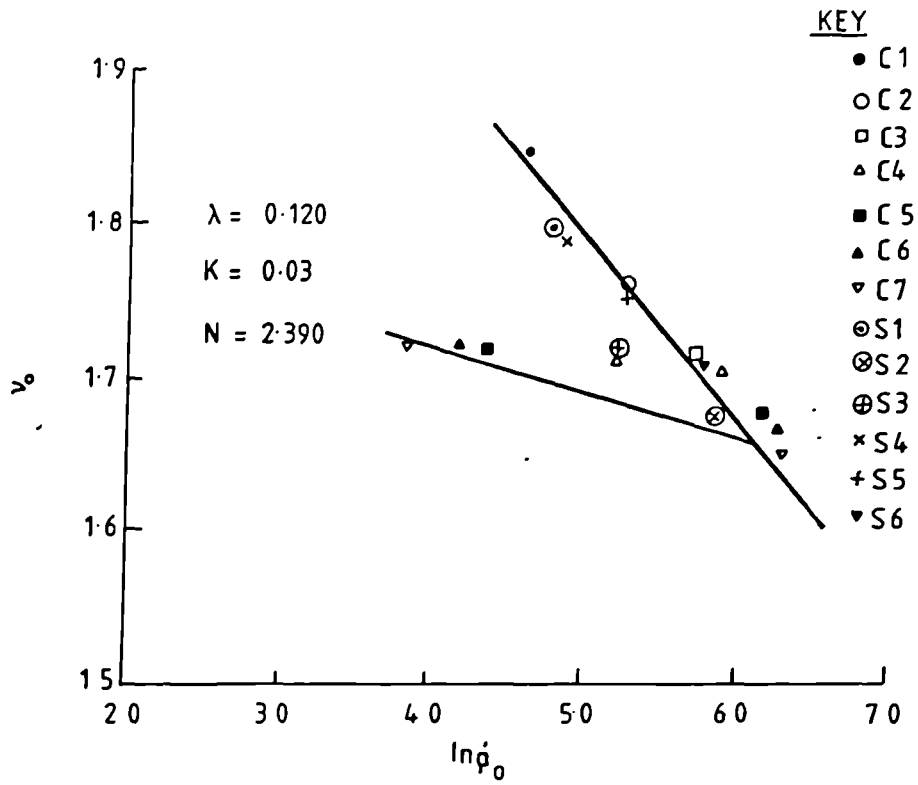


Fig B-2 "CORRECTED" ISOTROPIC COMPRESSION AND SWELLING RESULTS

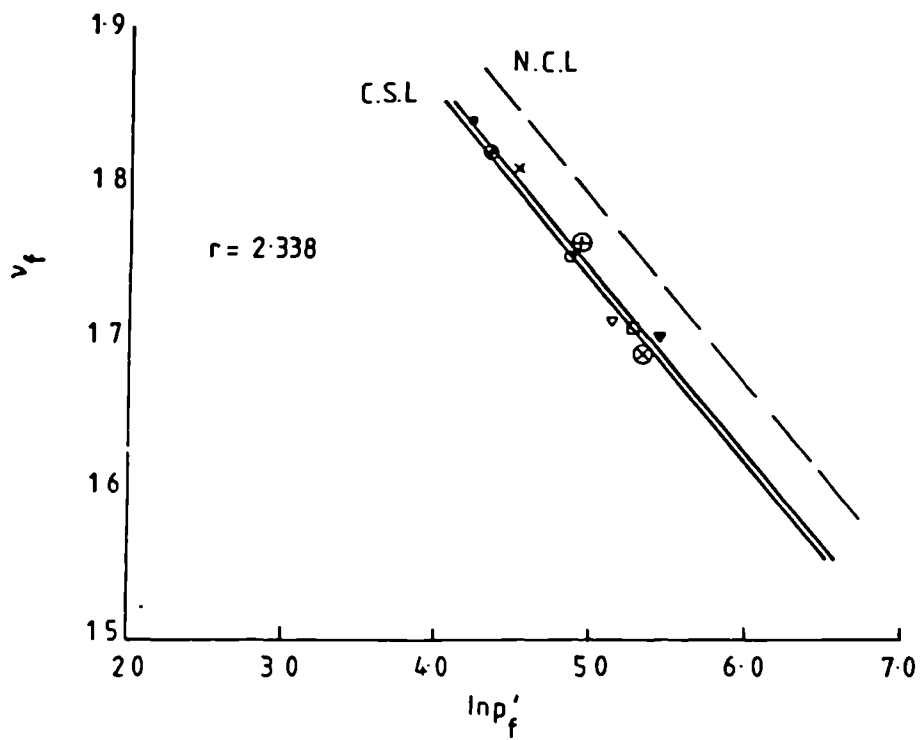


Fig B-3 ULTIMATE STATES

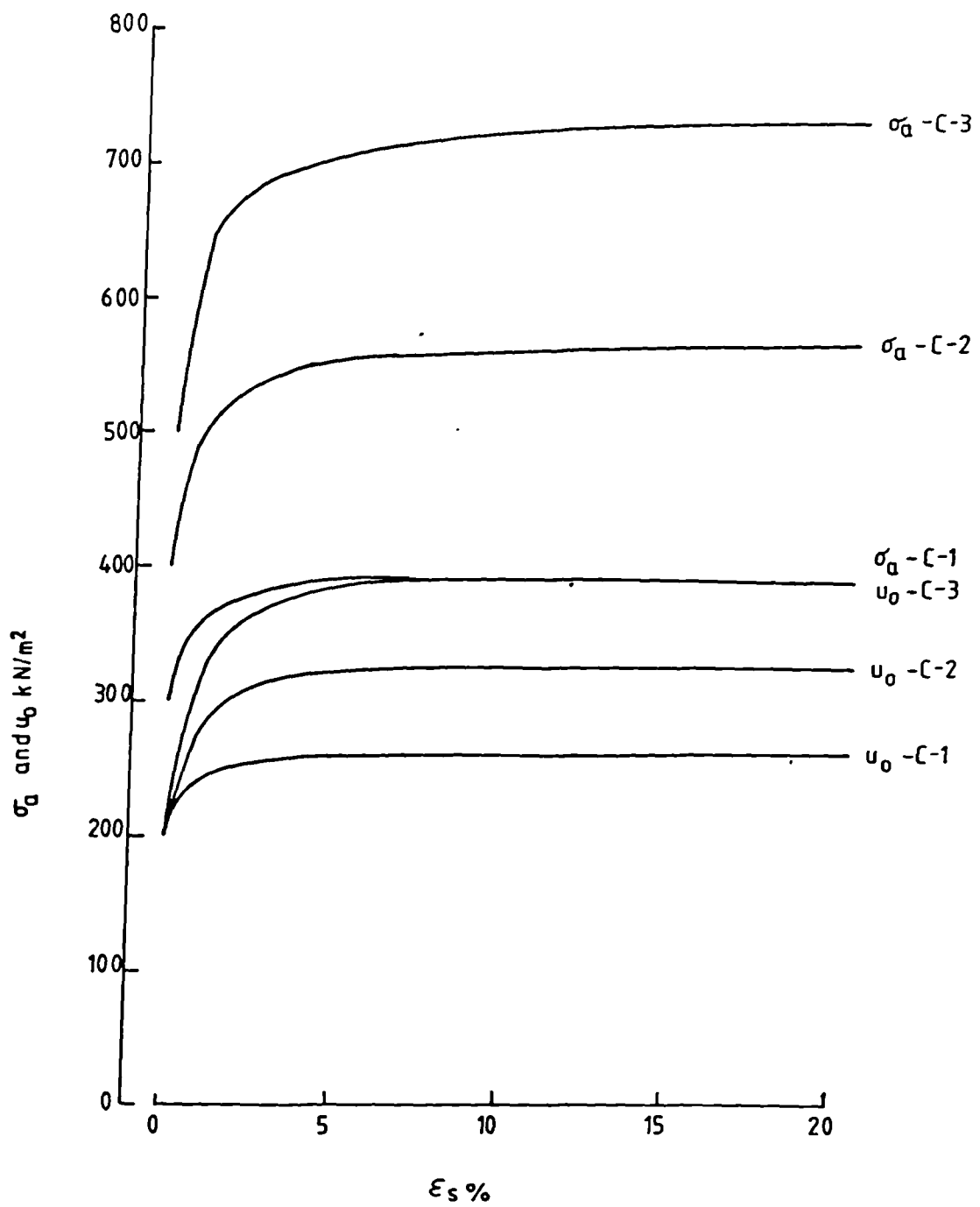


Fig B-4 PLOT OF σ_a AND u_0 AGAINST $\epsilon_s\%$ - NORMALLY CONSOLIDATED SAMPLES (automatic series)

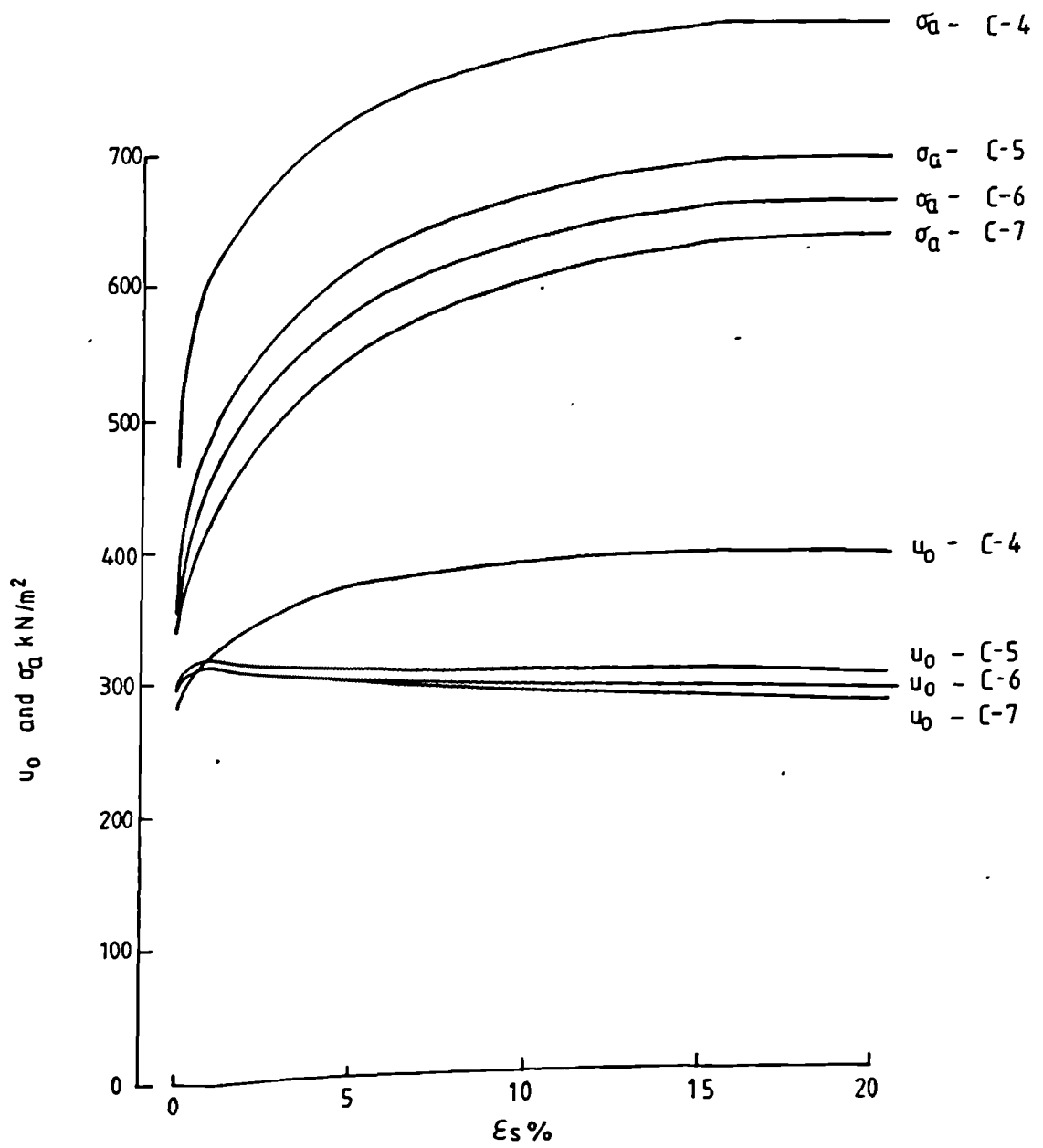


Fig B-5 PLOT OF σ_v AND u_0 AGAINST $\epsilon_s\%$ -
OVERCONSOLIDATED SAMPLES

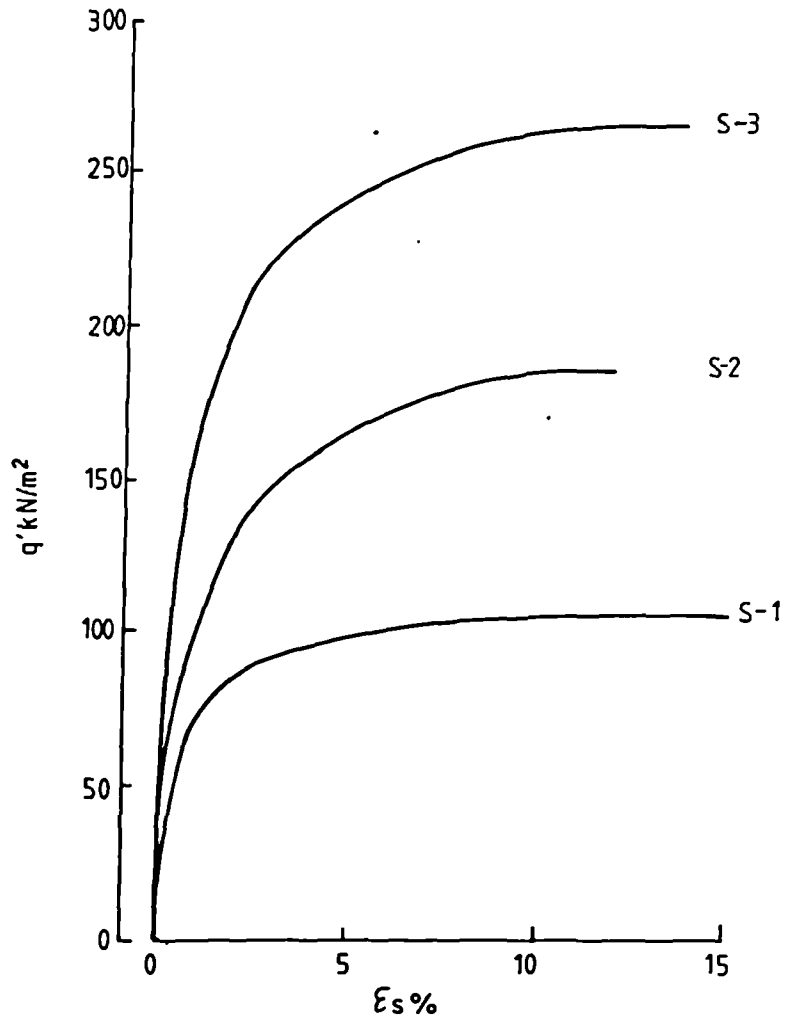


Fig B-6 STRESS - STRAIN BEHAVIOUR OF NORMALLY CONSOLIDATED SAMPLES - COMPRESSION TESTS (semi-automatic series)

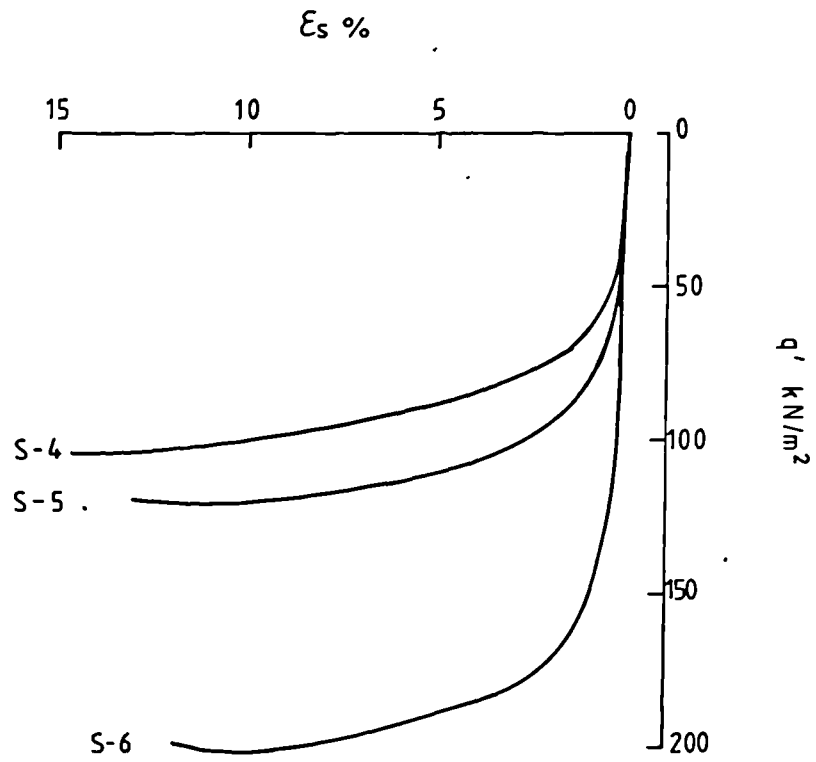


Fig B-7 STRESS -STRAIN BEHAVIOUR OF NORMALLY CONSOLIDATED SAMPLES- EXTENSION TESTS (semi - automatic series)

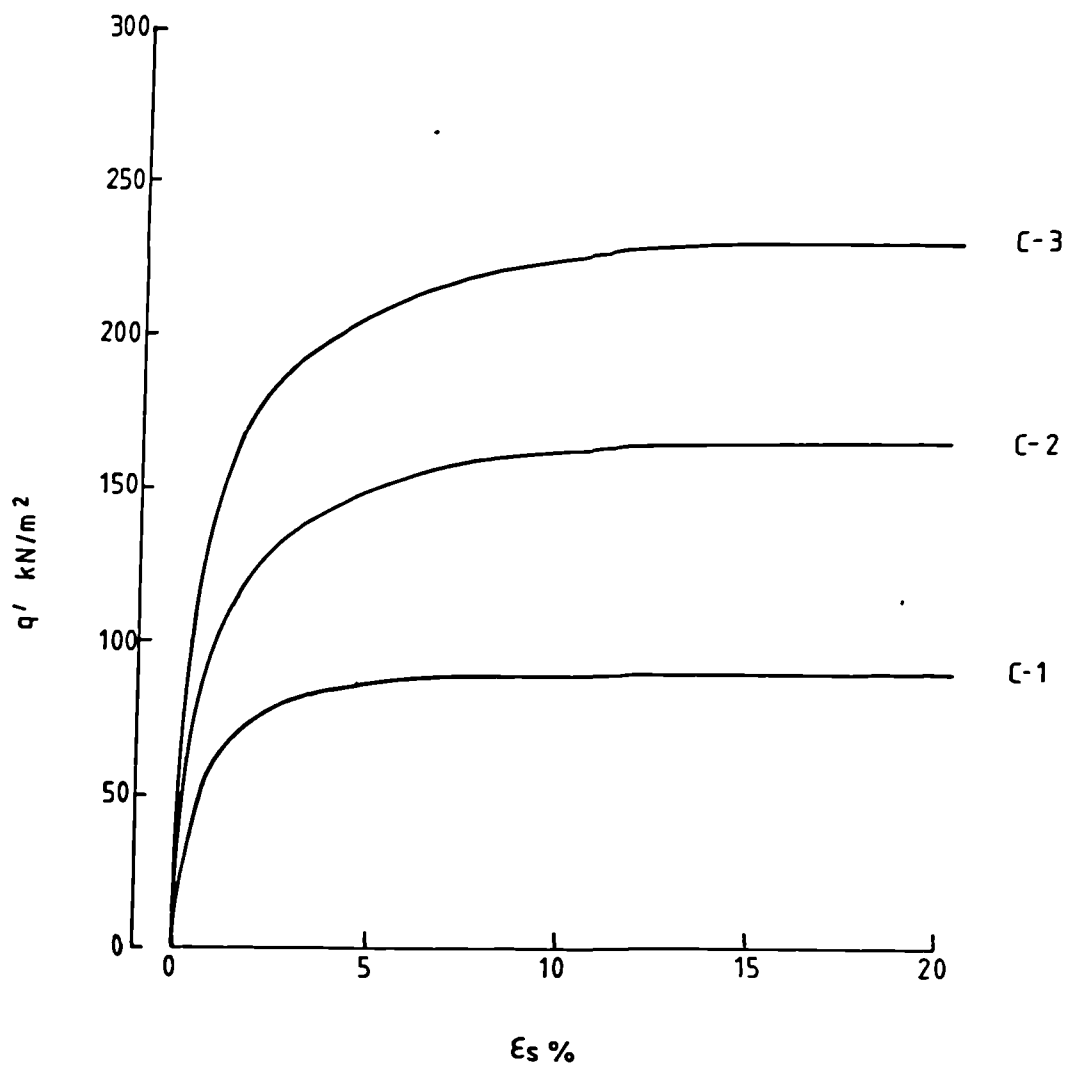


Fig B-8 STRESS-STRAIN BEHAVIOUR OF NORMALLY CONSOLIDATED SAMPLES (automatic series)

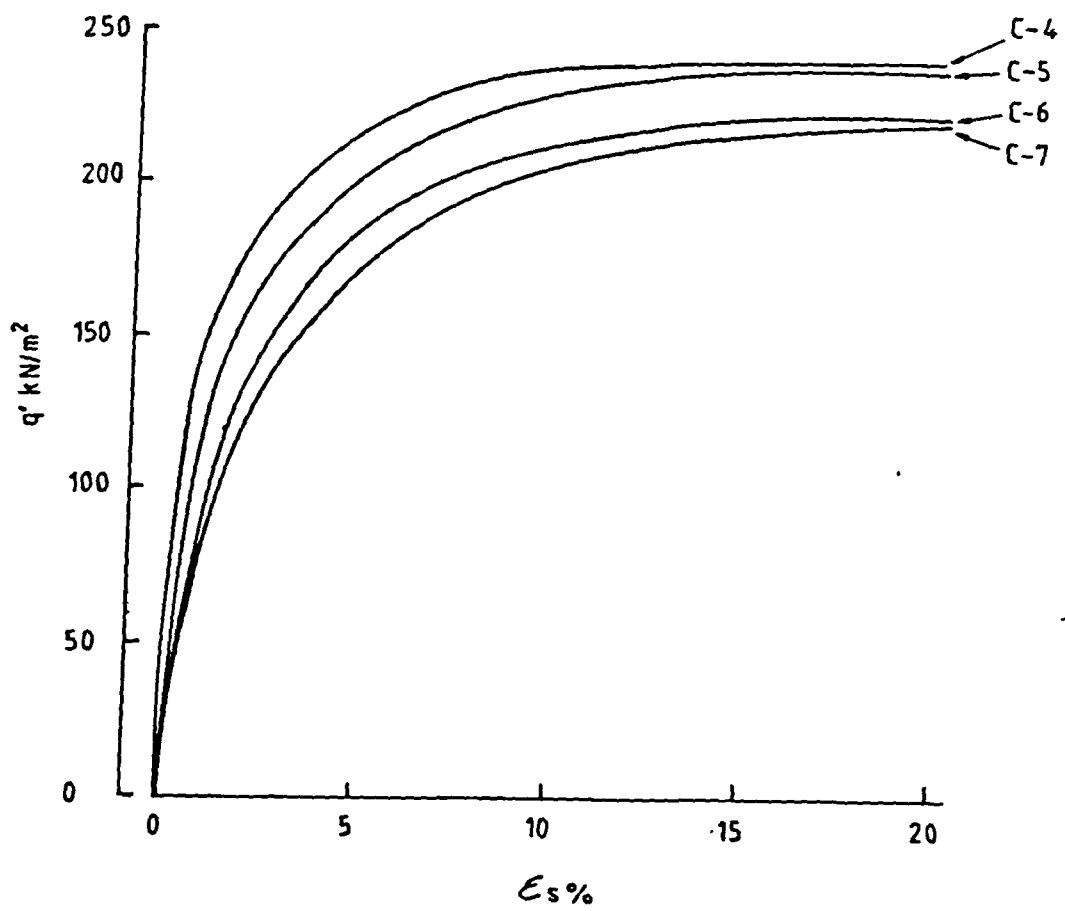


Fig B-9 STRESS STRAIN BEHAVIOUR OF OVERCONSOLIDATED SAMPLES

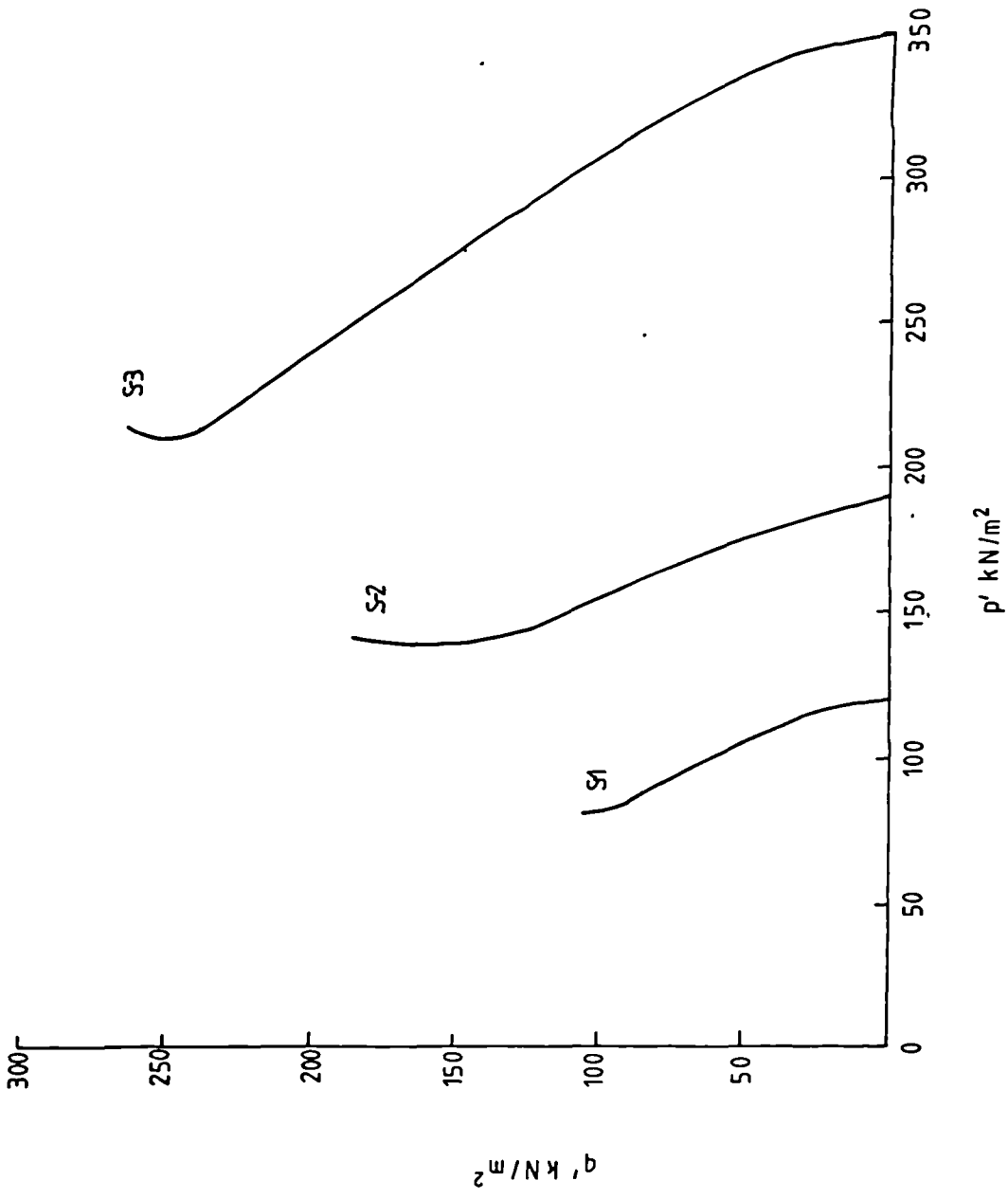


Fig B-10 UNDRAINED EFFECTIVE STRESS PATHS (semi - automatic series)

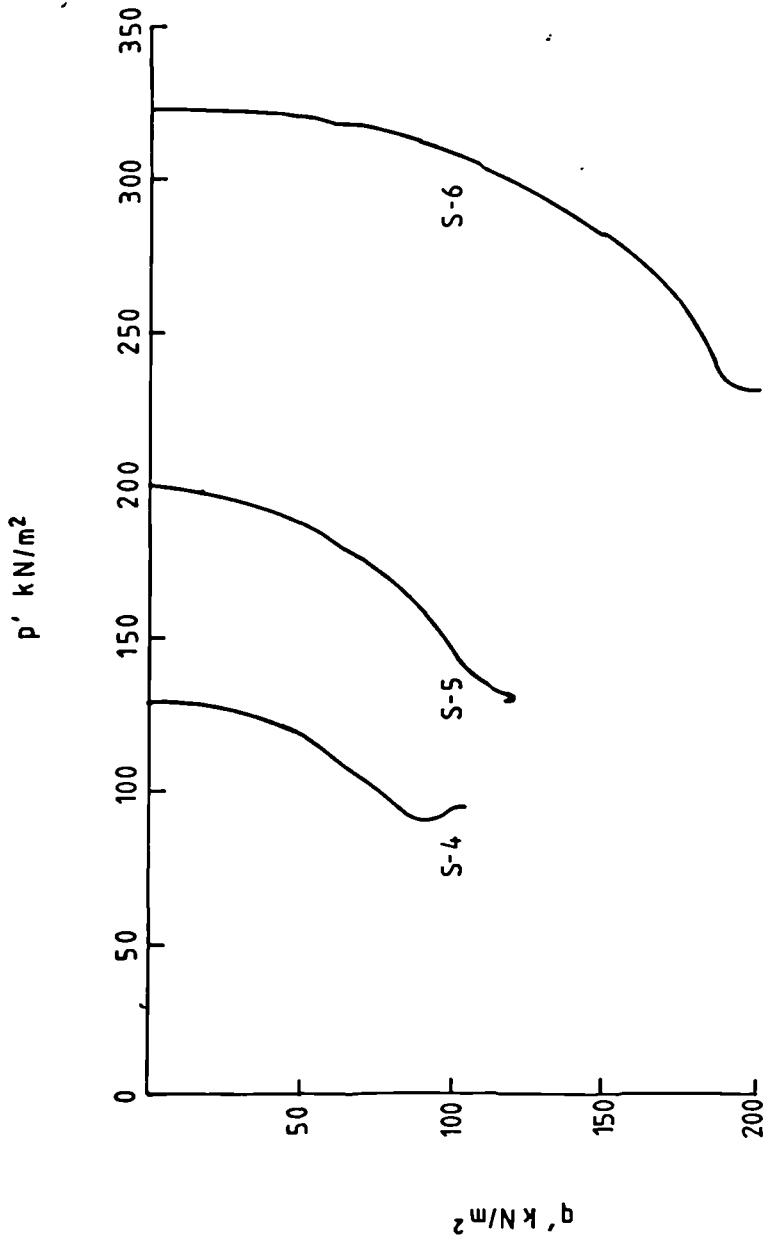


Fig B-11 UNDRAINED EFFECTIVE STRESS PATHS - EXTENSION TESTS (semi-automatic series)

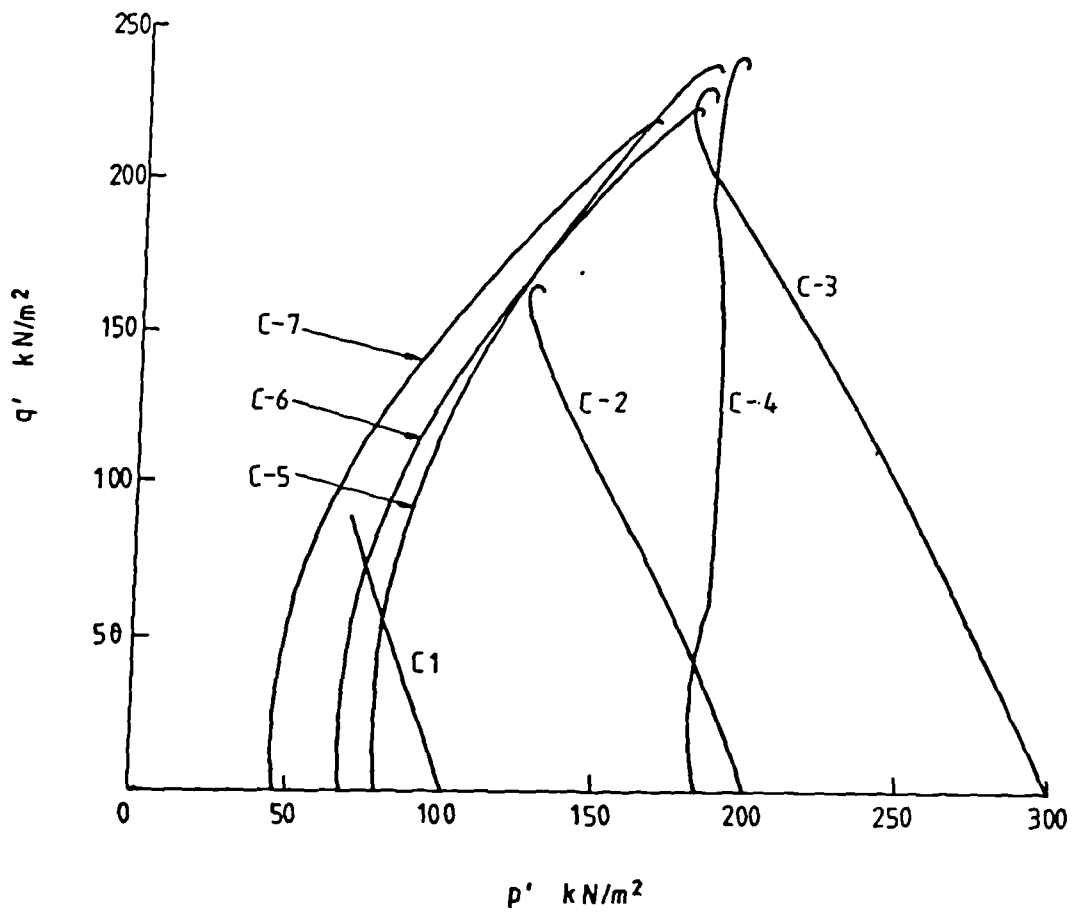
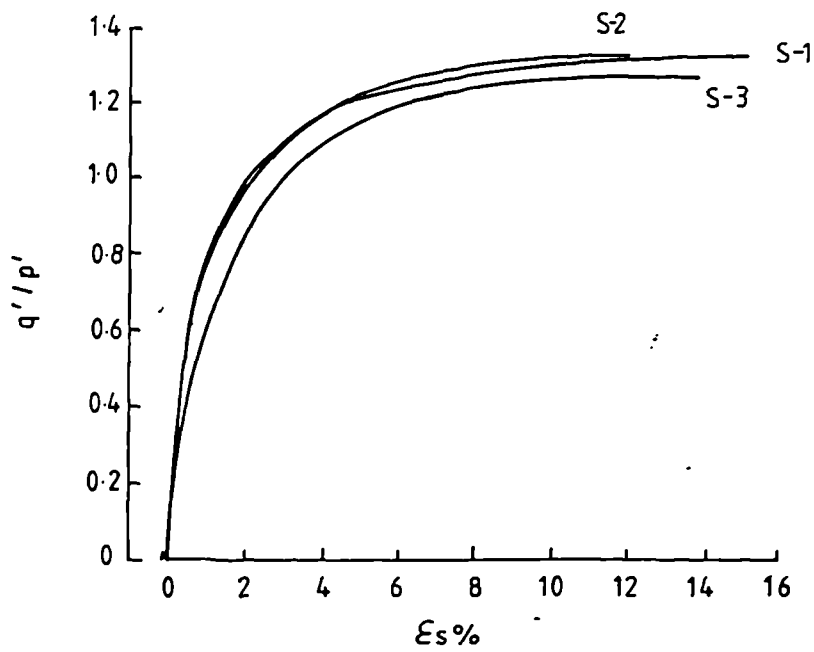
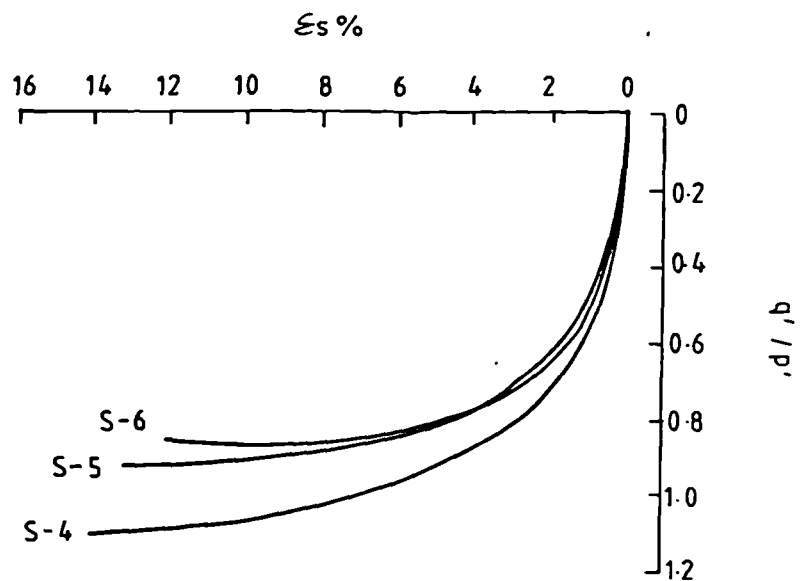


Fig B-12 UNDRAINED EFFECTIVE STRESS PATHS (automatic series)

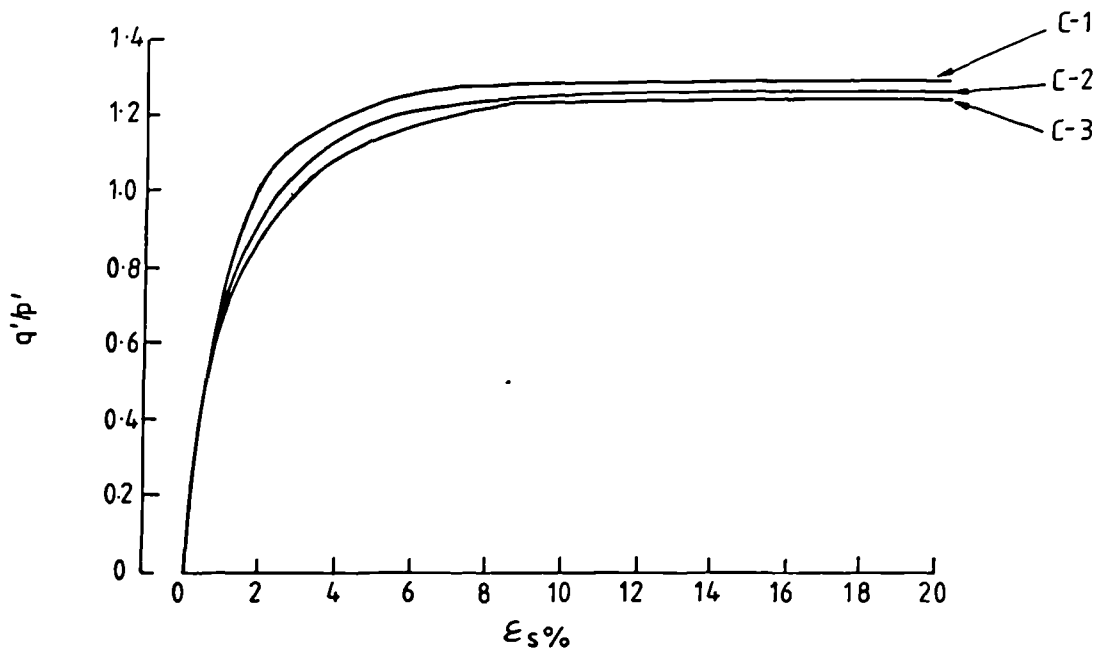


(a) Compression test

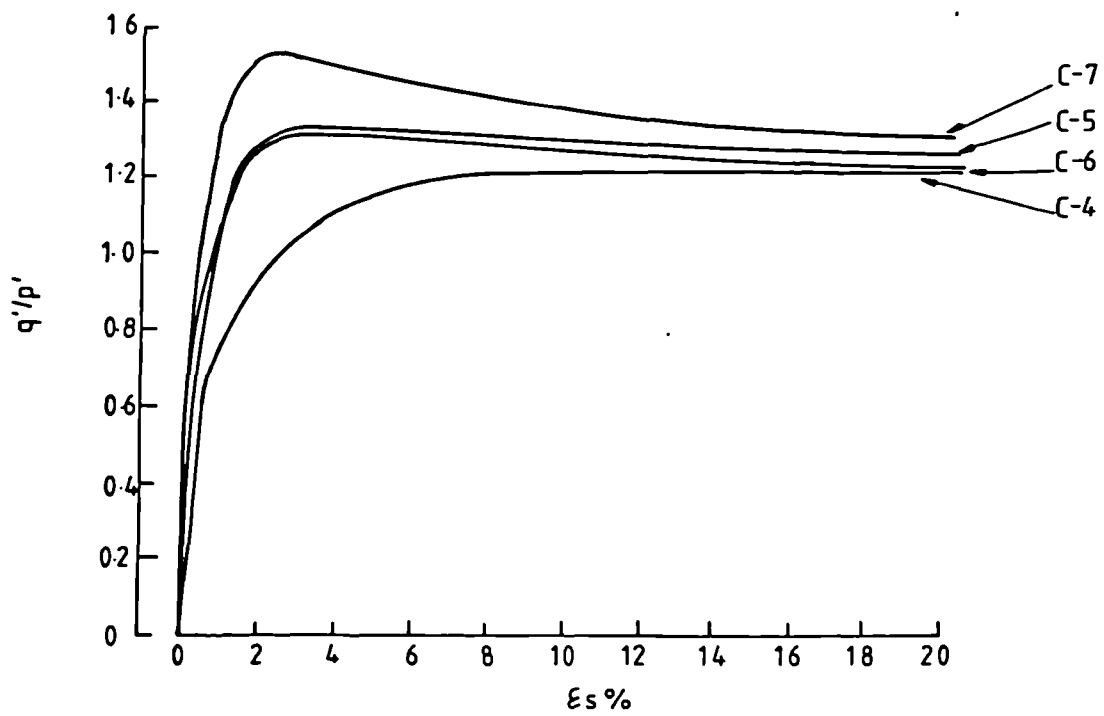


(b) Extension test

Fig B-13 STRESS RATIO - SHEAR STRAIN RELATIONSHIP -
NORMALLY CONSOLIDATED SAMPLES
(semi-automatic series)

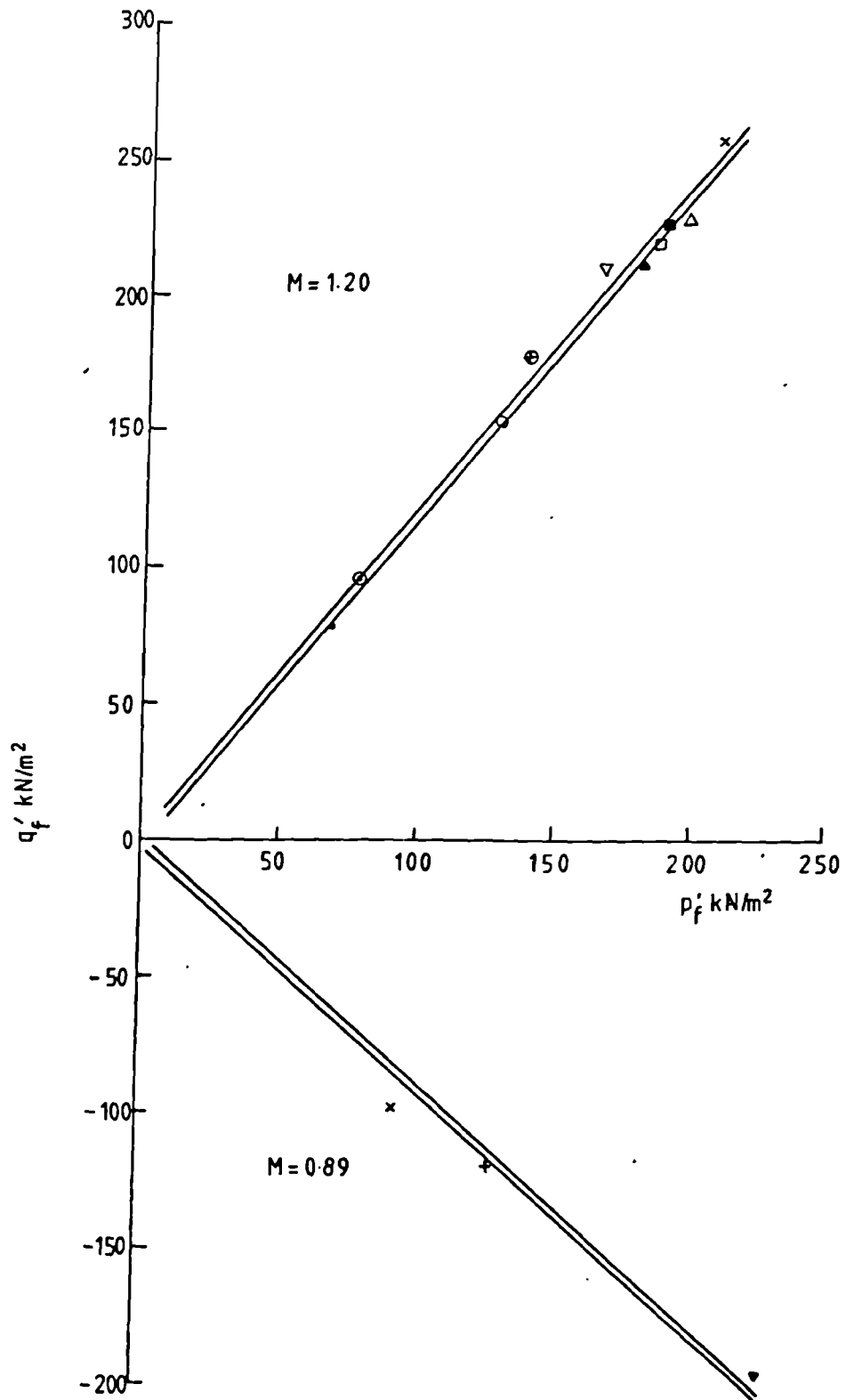


(a) Normally consolidated samples (automatic series)



(b) Overconsolidated samples (automatic series)

Fig B-14 STRESS RATIO - SHEAR STRAIN RELATIONSHIP



NOTE: FOR KEY SEE FIG B-2

Fig B-15 ULTIMATE STATES

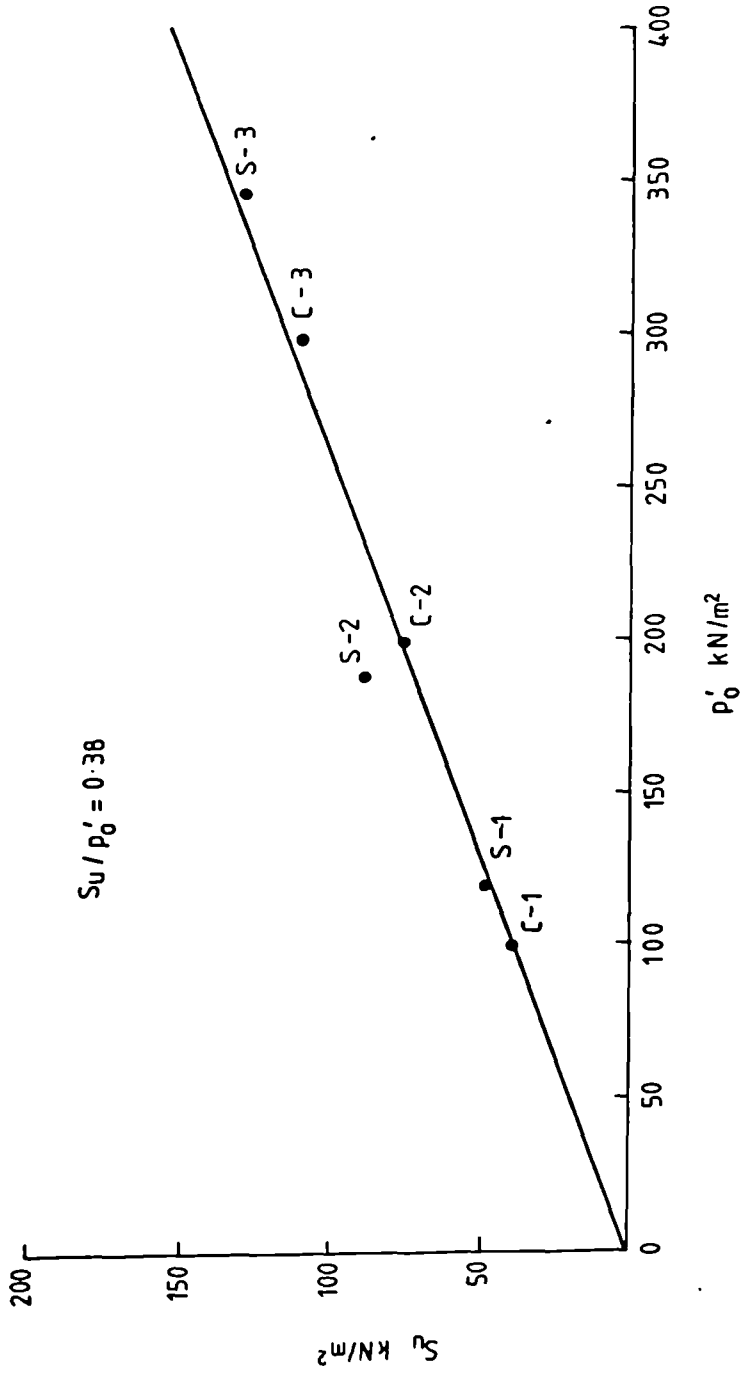


Fig B-16 PLOT OF UNDRAINED SHEAR STRENGTH AGAINST INITIAL EFFECTIVE CONFINING PRESSURE

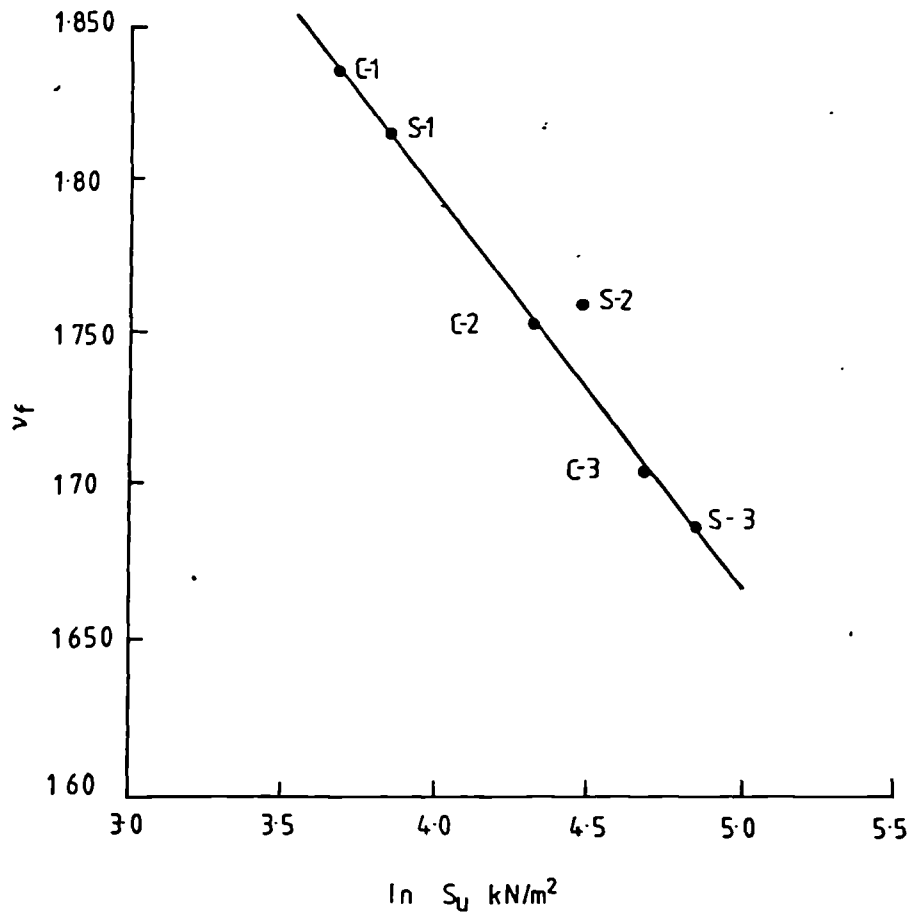


Fig B-17 PLOT OF SPECIFIC VOLUME AT FAILURE AGAINST
UNDRAINED SHEAR STRENGTH

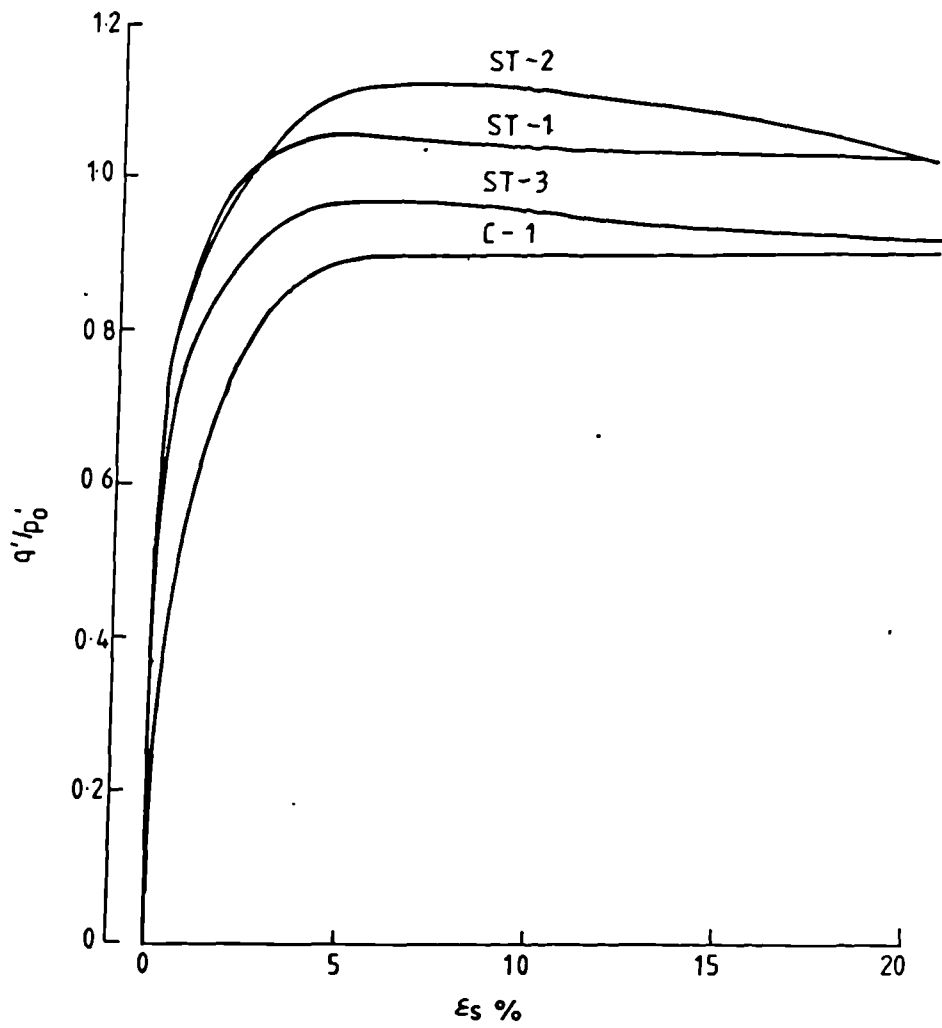


Fig B-18 PLOT OF q/p_0 AGAINST SHEAR STRAIN AT VARIOUS RATES

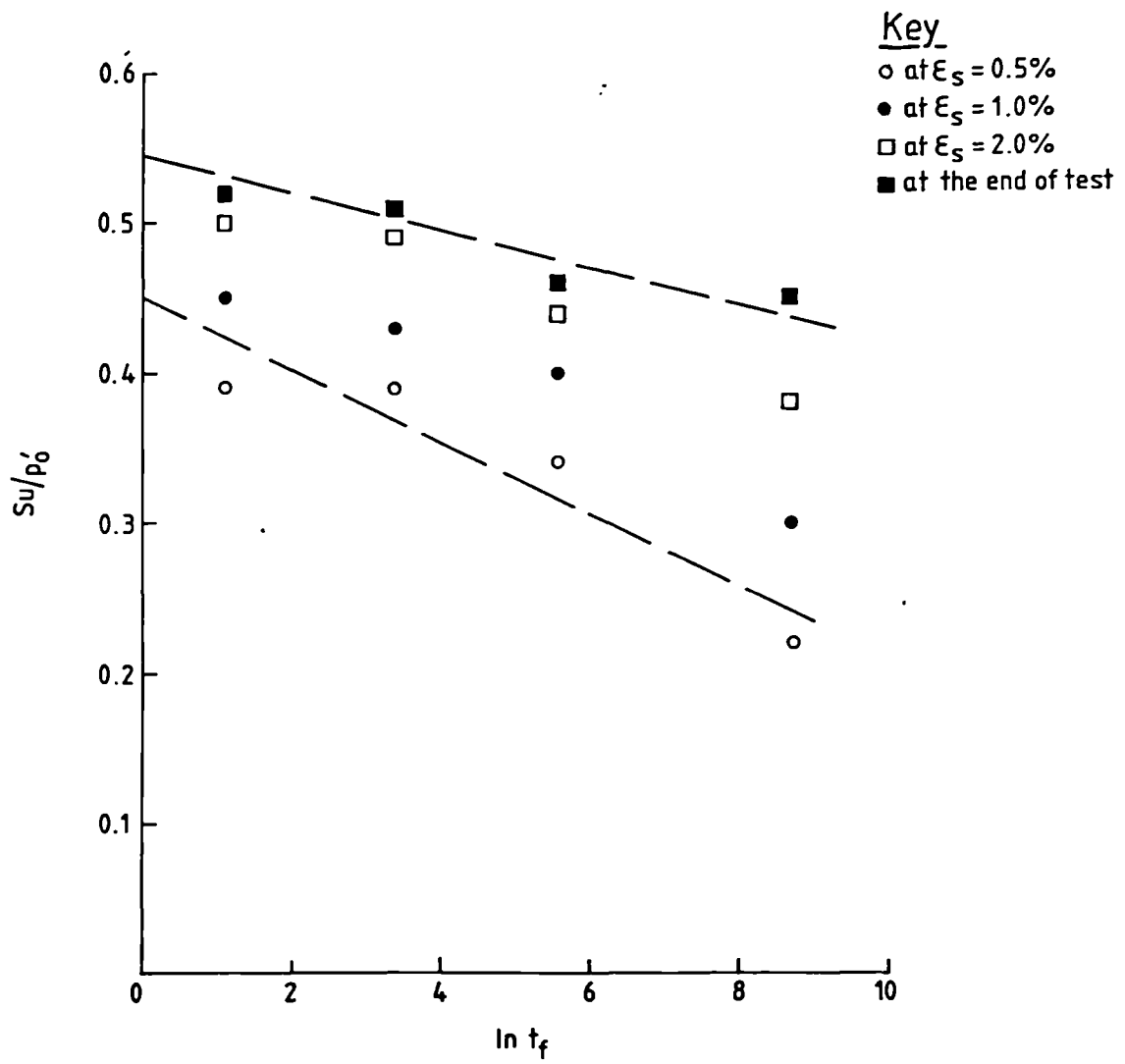


Fig B.19 VARIATION OF S_u/p'_0 WITH TIME

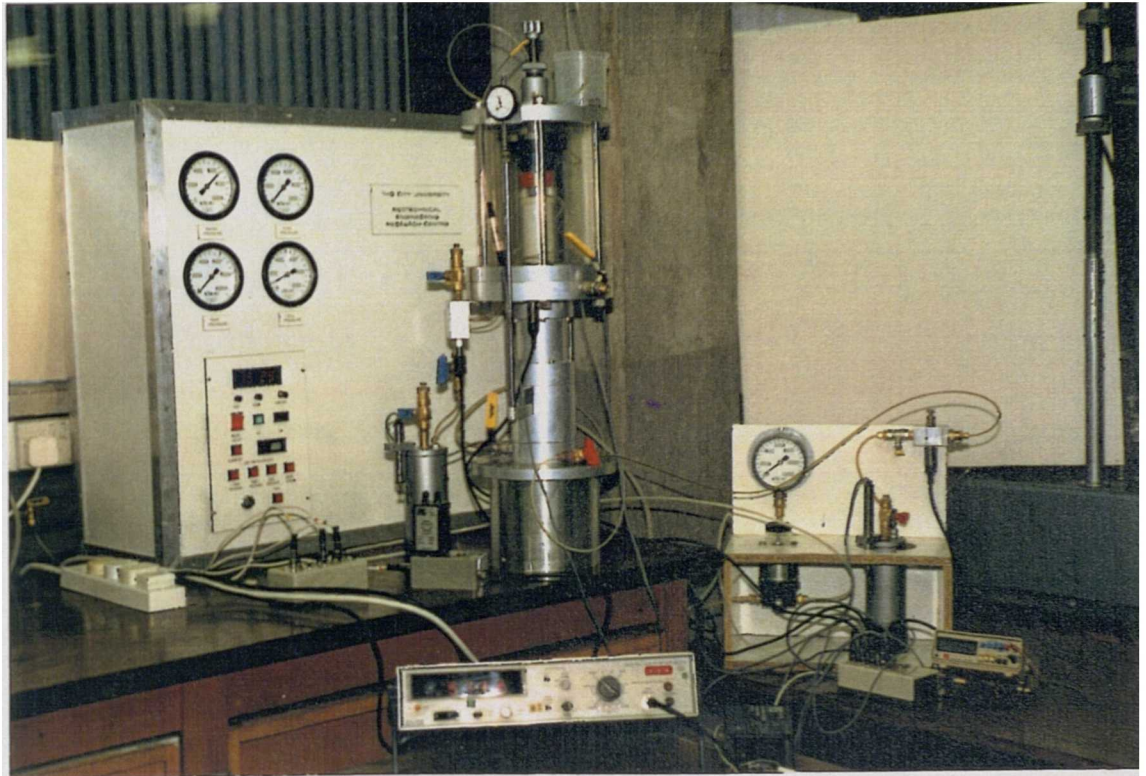


PLATE I Laboratory Hydraulic Fracture Apparatus

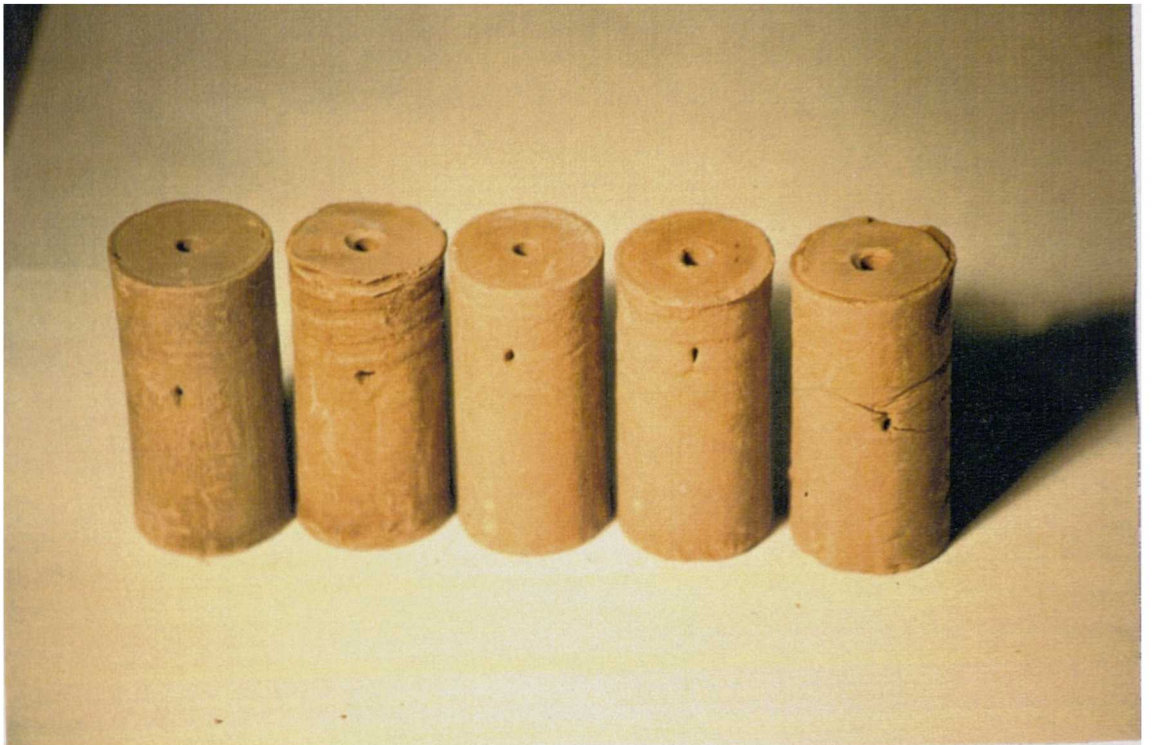


PLATE II Fractured Samples - Group F1

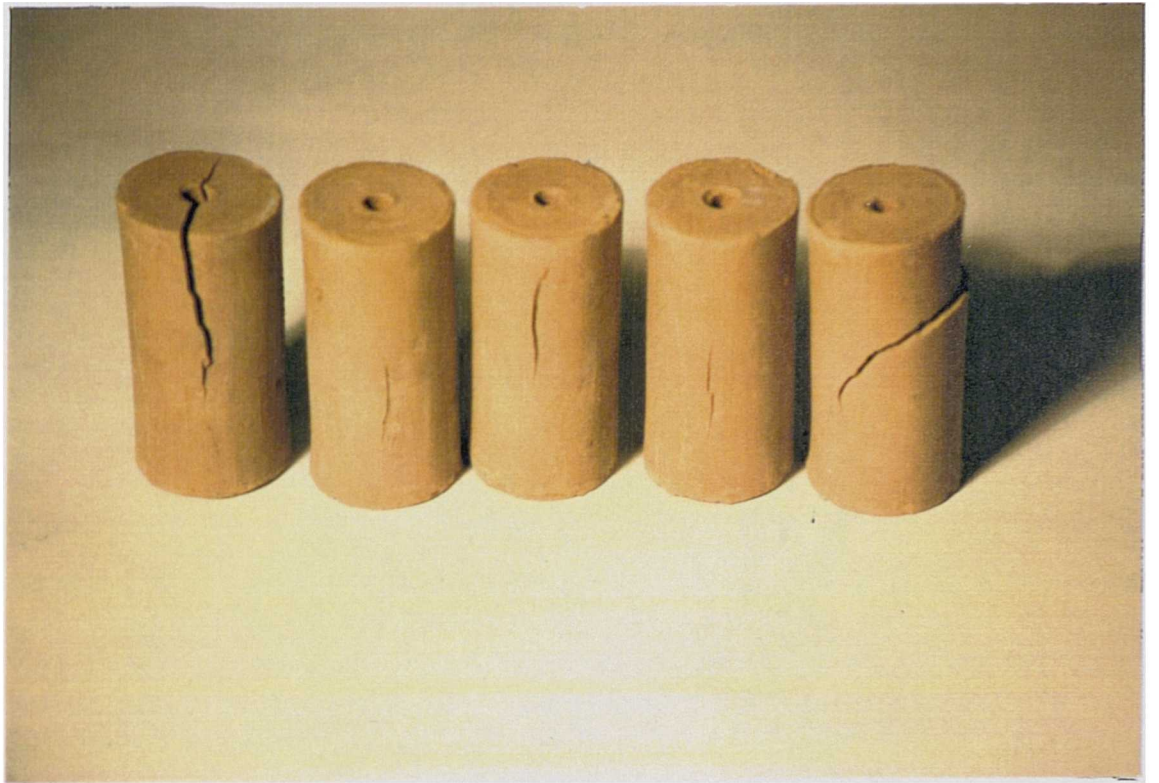


PLATE III Fractured Samples - Group F2

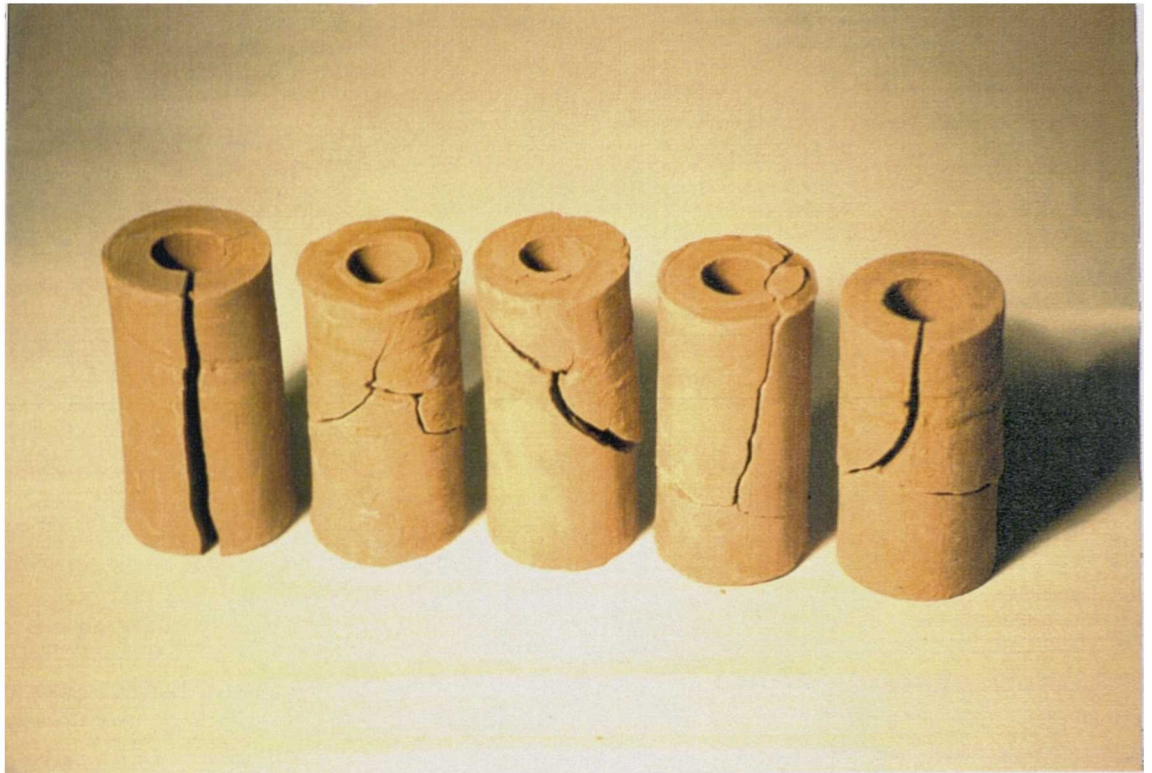


PLATE IV Fractured Samples - Group F3



PLATE V Fractured Samples - Group F7



PLATE VI Fractured Sample - F6 - 7 Sample



PUDDLE CLAY
CWMWERNDEI DAM
O.C.R = 3
TIME INTERVAL 15 mins.

PLATE VII Dispersive - Type D

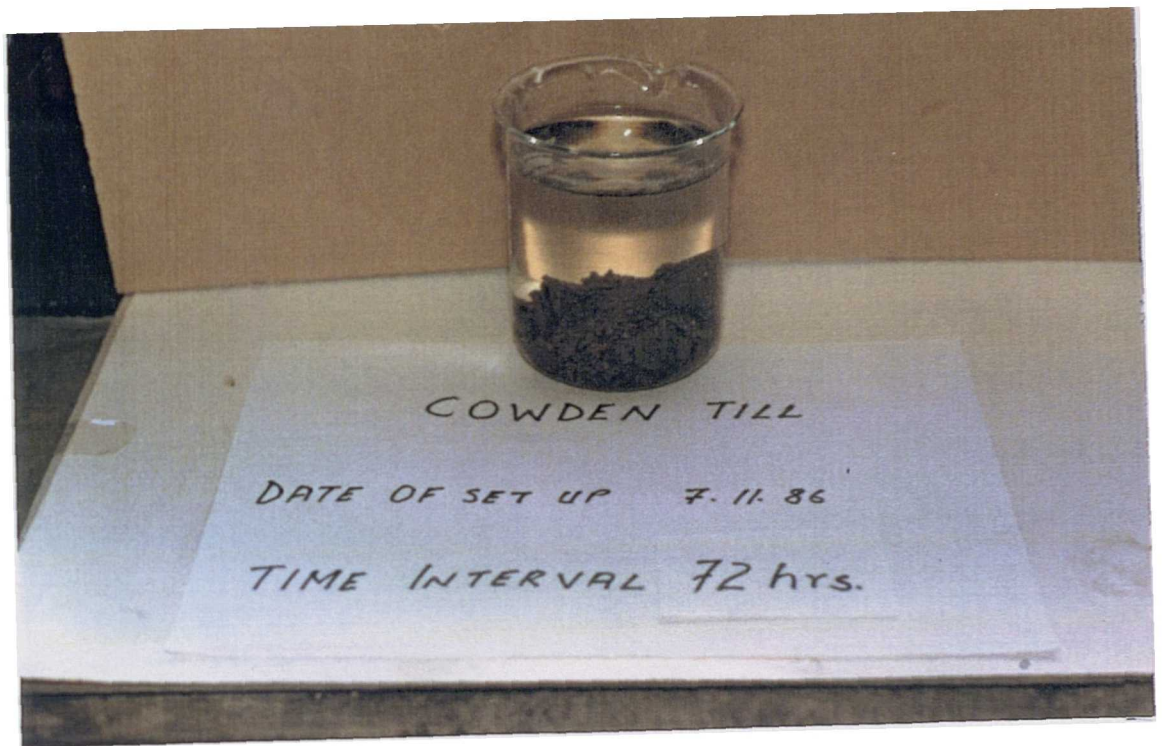


PLATE VIII Non-Dispersive - Type N

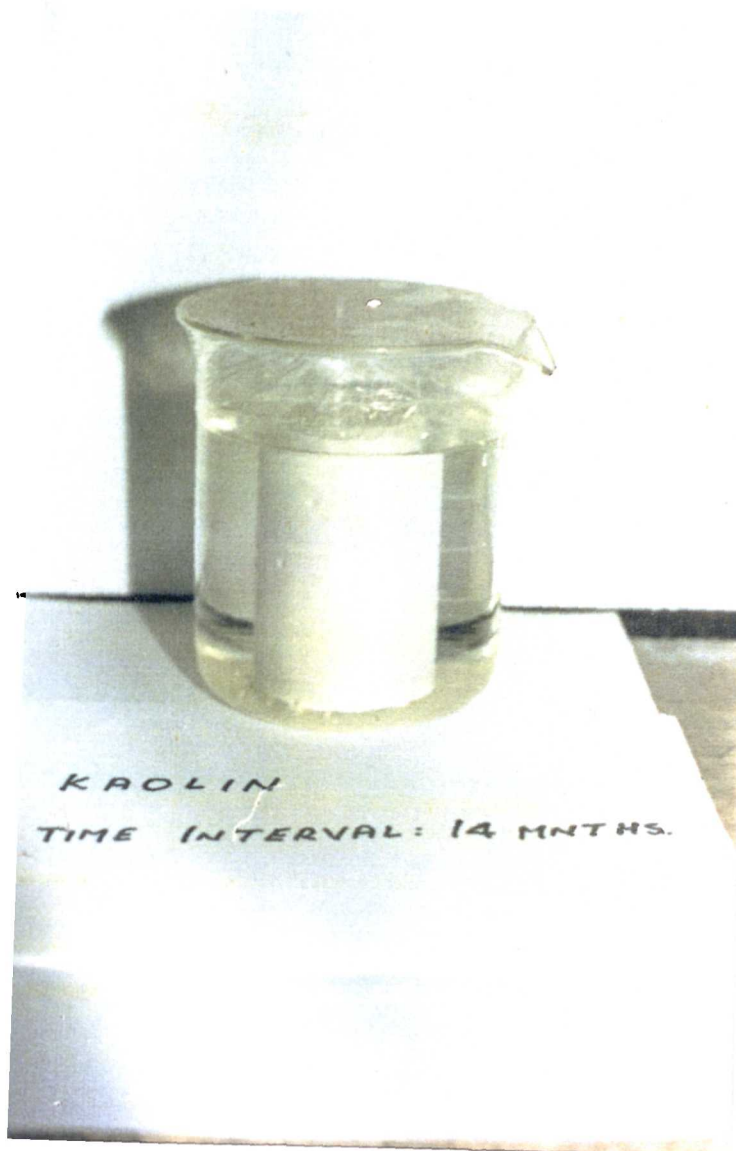


PLATE IX Non-Dispersive - Type C